Supplementary Information

Boosting Quantum Yields and Circularly Polarized Luminescence of Penta- and Hexahelicenes by Doping with Two BN-Groups

Yannik Appiarius,[a,b] Sandra Míguez-Lago,[c] Pim Puylaert,[d] Noah Wolf,[a] Sourabh Kumar,[e] Martin Molkenthin,[a] Delia Miguel,[f] Tim Neudecker,[b,e,g] Michal Juríček,[h] Araceli G. Campaña,[c] and Anne Staubitz[a,b]*

a. University of Bremen, Institute for Organic and Analytical Chemistry, Leobener Strasse 7, 28359 Bremen, Germany; E-mail: staubitz@uni-bremen.de.
b. University of Bremen, MAPEX Center for Materials and Processes, 28359 Bremen, Germany.
c. University of Granada, Unidad de Excelencia de Química, Department of Organic Chemistry, 18071 Granada, Spain.
d. University of Bremen, Institute for Inorganic Chemistry and Crystallography, 28359 Bremen, Germany.
e. University of Bremen, Institute for Physical and Theoretical Chemistry, 28359 Bremen, Germany.
f. University of Granada, Unidad de Excelencia de Química, Department of Physical Chemistry, 18071 Granada, Spain.
g. University of Bremen, Bremen Center for Computational Materials Science, 28359 Bremen, Germany.
h. University of Zurich, Department of Chemistry, 8057 Zurich, Switzerland.

Abstract:

The incorporation of boron–nitrogen (BN) units into polycyclic aromatic hydrocarbons (PAHs) as an isoelectronic replacement of two carbon atoms can significantly improve their optical properties, while the geometries are mostly retained. We report the first non-π-extended penta- and hexahelicenes comprising two aromatic 1,2-azaborinine rings. Comparing them with their all-carbon analogs regarding structural, spectral and (chir)optical properties allowed us to quantify the impact of the heteroatoms. In particular, BN-hexahelicene **BN[6]** exhibited a crystal structure congruent with its analog **CC[6]**, but displayed a fivefold higher fluorescence quantum yield (Φ_{fl} = 0.17) and an outstanding luminescence dissymmetry factor ($|g_{lum}| = 1.33 \times 10^{-2}$). Such an unusual magnification of both properties at the same time makes BN-helicenes suitable candidates as circularly polarized luminescence emitters for applications in materials science.

Abbreviations

app	Apparent (NMR)
aq.	Aqueous
ATR	Attenuated total reflectance
BPin	Boronic acid pinacol ester
br	Broad signal (IR)
calcd.	Calculated
COSY	Correlation spectroscopy (NMR)
CPL	Circularly polarized luminescence
(CSP)-HPLC	Chiral-stationary-phase high-performance liquid chromatography
CPCM	Conductor-like polarizable continuum model
d	Doublet (NMR)
DCM	Dichloromethane
DFT	Density functional theory
DIPA	Di-*iso*propylamine
dtbpy	4,4′-Di-*tert*-butyl-2,2′-dipyridyl
ECD	Electronic circular dichroism
ee	Enantiomeric excess
EI	Electron ionization
λ_{em}	Emission wavelength
equiv.	Equivalent
ESI	Electrospray Ionization
λ_{ex}	Excitation wavelength
FT-IR	Fourier-Transform Infrared spectroscopy
HMBC	Heteronuclear multiple-bond correlation spectroscopy (NMR)
HR-MS	High resolution mass spectrometry
HSQC	Heteronuclear single-quantum correlation spectroscopy (NMR)
J	Coupling constant (NMR)
LED	Light-emitting diode
m	Multiplet (NMR), medium intensity (IR)
m.p.	Melting point
λ_{max}	Wavelength at intensity maximum
Mes	Mesityl group
MTBE	Methyl *tert*-butyl ether
n-BuLi	*n*-Butyllithium
NBS	*N*-Bromosuccinimide
NMR	Nuclear magnetic resonance spectroscopy
NICS	Nucleus-independent chemical shift
PAH	Polycyclic aromatic hydrocarbon
SAEMS	Species-associated emission spectra
TCSPC	Time-correlated single photon counting
TRES	Time-resolved emission spectroscopy

1. General Methods and Materials

Unless stated otherwise, all syntheses were carried out under standard Schlenk conditions under an atmosphere of nitrogen or argon. If necessary, reactions were carried out in a nitrogen flushed glove box from Inert Innovative Technology Inc. or reagents were prepared and stored there. All glassware was heated under a vacuum below 0.1 mbar and flushed with inert gas at least three times prior to use. Syringes were flushed with inert gas at least three times before use. NMR tubes were dried in an oven at 110 °C for at least 2 h before use. If reactions were performed in microwave vials, Biotage® microwave reaction vials (2 – 5 mL or 10 – 20 mL) with aluminum caps and septa were used, withstanding pressures up to 30 bar. If reactions were performed in pressure vials, borosilicate pressure vials from FengTecEx, equipped with PTFE caps were used, withstanding pressures of up to 6 bar. Given yields refer to isolated compounds that were synthesized with a purity of ≥95% as determined by ^{1}H NMR spectroscopy.

1.1. NMR Spectroscopy

NMR spectra were recorded at 297 - 300 K. The respective spectrometers and the measuring frequencies are given in the left table below. The chemical shifts (δ) are given in ppm, relative to the residual solvent signals as denoted in the right table below (^{1}H and ^{13}C{^{1}H} NMR).

Nucleus	Spectrometer frequency
^{1}H	500 MHz (Bruker DRX 500)
	601 MHz (Bruker AVANCE NEO)
^{13}C{^{1}H}	126 MHz (Bruker DRX 500)
	151 MHz (Bruker AVANCE NEO)
^{11}B{^{1}H}	160 MHz (Bruker DRX 500)
	193 MHz (Bruker AVANCE NEO)
^{19}F	565 MHz (Bruker AVANCE NEO)
^{29}Si{^{1}H}	99 MHz (Bruker DRX 500)
	119 MHz (Bruker AVANCE NEO)
^{31}P{^{1}H}	243 MHz (Bruker AVANCE NEO)

Solvent	Reference signal / ppm
$CDCl_3$	7.26 (^{1}H)
	77.16 (^{13}C)
C_6D_6	7.16 (^{1}H)
	128.06 (^{13}C)
CD_2Cl_2	5.32 (^{1}H)
	53.84 (^{13}C)
DMSO-d_6	2.50 (^{1}H)
	39.52 (^{13}C)
$C_2D_2Cl_4$	5.98 (^{1}H)

The signals were identified by using two dimensional methods such as ^{1}H - ^{1}H COSY, ^{1}H - ^{13}C{^{1}H} HSQC and ^{1}H - ^{13}C{^{1}H} HMBC experiments when possible. The positions of hydrogen and carbon atoms are labelled with letters to simplify their assignment.

1.2. IR Spectroscopy

IR spectra were recorded with a Thermo Scientific Nicolet FT-IR Spectrometer System spectrometer with an ATR unit, equipped with a diamond window. The absorption bands are reported in cm^{-1}.

1.3. Melting Points

Melting points were determined with a Büchi Melting Point M-560 apparatus with a heating rate of 5 °C min^{-1}.

1.4. Optical Measurements

All measurements were performed in DCM solutions. Absorption spectra that served for the determination of the extinction coefficients were recorded on a Shimadzu UV-2700 spectrometer. Absorption spectra that served for the determination of the sample concentration for temperature-dependent ECD measurements were recorded on an Agilent 8453 spectrophotometer. Quantum yields are double-corrected and were determined on a Jasco FP-8300 spectrofluorometer, using a Jasco ILF-835 integrating sphere. ECD spectra at increased temperature were recorded on a Jasco J-715 or J-815 spectropolarimeter. All other absorption, emission, ECD and CPL spectra were measured on an Olis DSM172 spectrophotometer, using an LED (λ_{ex} = 300 or 370 nm) as excitation source. Absorption, ECD and fluorescence spectra

were measured with an integration time of 0.01 s and a slit width of 2.00 mm or 3.00 mm. CPL was measured with an integration time of 1 s and a slit width of 1.00 mm. The obtained CPL spectra represent the average of several consecutive scans (**BN[5]**: 75 scans, **CC[5]**: 168 scans, **BN[6]**: 50 scans, **BN[5]-(CN)$_2$**: 52 scans). For all measurements, quartz cuvettes (path length: 1 cm) were used.

1.5. Time-Resolved Fluorescence

Time-resolved fluorescence decay traces were collected via the TCSPC method using a FluoTime 200 fluorometer (PicoQuant GmbH). The excitation source was a 375 nm laser using a 10 MHz excitation frequency (BN-helicenes) or a 320 nm LED (carbohelicenes). The full width at half maximum (fwhm) of the laser pulses was around 40 ps. The fluorescence emission was collected at a 90° geometry, focused at the detector after crossing through a polarizer (set at the magic angle), 2 mm slits, and a 2 nm bandwidth monochromator. TCSPC was achieved by a TimeHarp200 board, set at 36 ps/channel. Fluorescence decay traces were collected for the necessary time to reach 20 000 counts at the peak channel. For the analyzed compounds, decay traces were collected at the maximum of the main peaks of the emission spectra.

The fluorescence decay traces were fitted to a mono- or bi-exponential function (depending on the compound and the wavelength), by using a Levenberg-Marquardt algorithm-based nonlinear least-squares error minimization deconvolution method iterative reconvolution methods (FluoFit 4.4 package, PicoQuant GmbH). For each sample, the decay traces were fitted globally with the decay times linked as shared parameters, whereas the pre-exponential factors were local adjustable parameters. The quality of fittings was assessed by the value of the reduced chi-squared, χ^2, parameter and random distributions of the weighted residuals and the autocorrelation functions.

Time-resolved emission spectroscopy (TRES) was performed with a 325 nm LED as excitation source and operating at 10 MHz excitation frequency during a fixed amount of time (500 s), to maintain the overall intensity information. For **CC[5]** and **CC[6]**, 37 fluorescence decay traces in the 360 - 540 nm emission range ($\Delta\lambda_{fl}$ = 5 nm) while for **BN[6]**, 30 fluorescence decay traces in the 400 - 545 nm emission range were collected.

For the TRES analysis and the estimation of the species-associated emission spectra (SAEMS), the fitting procedure described above was performed. The SAEMS of each species *i* at any given emission wavelength ($SAEMS_i(\lambda_{em})$) is given by the fluorescence intensity emitted by the species *i* ($A_{i,\lambda em} \times \tau_i$), normalized by the total intensity and corrected for the different detection sensitivity using the total intensity of the steady-state spectrum ($I_{ss,\lambda fl}$):

$$SAEMS_i(\lambda_{em}) = \frac{A_{i,\lambda em} \times \tau_i}{\sum_i A_{i,\lambda em} \times \tau_i} \cdot I_{ss,\lambda em}$$

The approximate contribution of each species can be assessed as the area under the SAEMS. This estimation assumes equal excitation rate for all the species, as the initial amount of each form in the excited state (after the pulse excitation) is unknown.

1.6. Mass Spectrometry

GC-MS analyses were performed using an Agilent Technologies 7890 B chromatograph with an Agilent Technologies 5977A mass selective detector and an Agilent Technologies dimethylpolysiloxane column (19091S-931E, nominal length 30 m, 0.25 mm diameter, 0.25 µm grain size). High resolution EI mass spectra were recorded on a double focusing mass spectrometer ThemoQuest MAT 95 XL from Finnigan MAT (EI, 70 eV, R ~ 10 000). High resolution ESI mass spectra were recorded on a Bruker Impact II. All signals were reported with the quotient from mass to charge (*m/z*).

1.7. Photochemical Setup

All photochemical syntheses were performed in a steel reaction vessel (maximum filling volume ~ 140 mL), equipped with two glass windows on each side, a steel screw cap with septum and a gas inlet (see below). Generally, the reaction mixtures were pre-mixed in a round-bottom flask and then poured into the vessel. After sealing, the mixtures were degassed by bubbling argon through them for 5 min while stirring. Two LEDs (Nichia NCSU276A, emission maximum at

365 nm, powered by 3500 mAh batteries) were used as light sources. The respective mixtures were stirred under irradiation for the timeframes as denoted in the experimental procedures. The decay of the radiance is shown below and was determined with an International Light Technologies ILT2400 Optical Meter and is given in mW/cm^2.

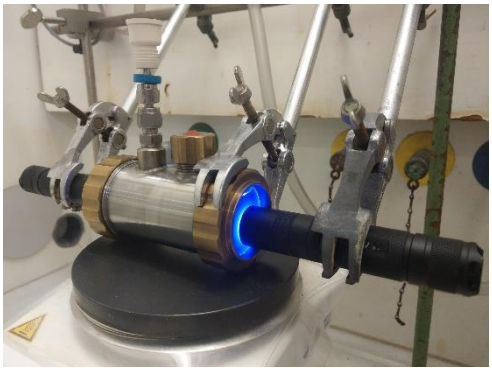

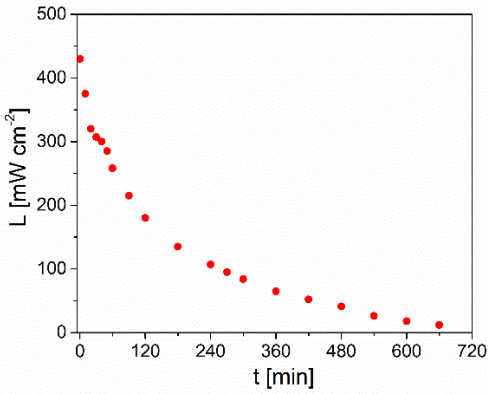

1.8. Chromatography

TLC was performed using silica gel on alumina plates (Macherey-Nagel, ALUGRAM® Xtra SIL G/UV$_{254}$); the individual spots were visualized under a Lamag UV lamp (wavelengths: 254 nm / 365 nm). Manual chromatographic purifications were performed with the aid of silica gel provided by Macherey-Nagel (0.063 – 0.040 mm) and Merck (0.040 – 0.015 mm). Automated purifications were performed utilizing an Interchim Puriflash® 430 system. The cartridges were used depending on the amount of substance (40 g – 120 g; supplied from Interchim GmbH; grain size: 30 or 50 µm).

1.9. Single Crystals

Single crystals were grown as denoted in the section Single Crystal Data. In all cases, a suitable crystal was selected and measured on a Bruker D8 Venture CMOS diffractometer. The crystal was kept at 100.00 K during data collection. Using Olex2[1], the structure was solved with the XT[2] structure solution program using Intrinsic Phasing and refined with the XL[3] refinement package using Least Squares minimization. The Deposition Numbers as denoted in the section Single Crystal Data contain the supplementary crystallographic data for this paper. These data are provided free of charge by the joint Cambridge Crystallographic Data Centre and Fachinformationszentrum Karlsruhe Access Structures service www.ccdc.cam.ac.uk/structures.

1.10. (CSP)-HPLC

Chiral resolutions by (CSP)-HPLC were run either on an Agilent Series 1100 instrument equipped with a ReproSil Chiral-MIA (5 µm, 250 x 4.6 mm, amylose material) column for analytical amounts of sample, using a flow rate of 1.0 mL min^{-1} or on an Agilent Technologies 1260 Infinity II instrument equipped with a Chiralpak IA (5 µm, 250 x 10 mm, amylose material) column for semi-preparative amounts of sample, using a flow rate of 3.8 - 4.0 mL min^{-1}. The eluent mixtures and injection volumes are given for each individual compound in Section 4.

1.11. Chemicals

Unless stated otherwise, chemicals were used without further purification. In case the purity is not denoted in the table, it was not stated by the supplier.

Chemical	Supplier	Purity	Purification / Notes
4,4′-Azobis(4-cyanopentanoic acid)	Sigma Aldrich	98%	
(1,1′-Bis(diphenylphosphino)-ferrocene)dichloropalladium(II)	abcr	99.9%	[B]
Bis(pinacolato)diboron	abcr	98%	
Bis(triphenylphosphine) palladium(II) dichloride	chempur	99%	[B]

Chemical	Supplier	Purity	Purification / Notes
4-Bromobenzaldehyde	BLD Pharm	99%	
(4-Bromobenzyl)-triphenylphosphonium bromide	BLD Pharm	97%	
N-Bromosuccinimide	TCI	98%	
Bromo(triphenylphosphine)gold(I)	Alfa Aesar	99.99%	Premion[B]
1-(*tert*-Butyldimethylsilyl)-2-chloro-1,2-azaborinine	abcr	98%	[B]
n-Butyllithium	Acros	Acroseal	2.5 M solution in hexanes
Celite® 535	Roth		
Copper(I) iodide	Alfa Aesar	99.998%	[B]
(1,5-Cyclooctadiene)-(methoxy)iridium(I) dimer	Sigma Aldrich	>98%	[B]
1,2-Dibromobenzene	Thermo Fisher	98%	
Dichloro(*p*-cymene)ruthenium(II) dimer	Apollo Scientific	98%	[B]
Dichloro(1,3-bis(diphenyl-phosphino)propane)nickel(II)	Sigma Aldrich	97%	[B]
2-Dicyclohexylphosphino-2′,6′-dimethoxybiphenyl (SPhos)	Strem	98%	[B]
2,7-Dihydroxynaphthalene	Thermo Fisher	97%	
Di*iso*propylamine	Sigma Aldrich	99.5%	dist. from CaH_2 [A] [B] [C]
4,4'-Di-*tert*-butyl-2,2'-bipyridyl	Sigma Aldrich	98%	
Gold(III) chloride	abcr	99%	[B]
Iodine	abcr	99%	
Iodine monochloride	Sigma Aldrich	Sure/Seal	1.0 M solution in DCM
Mesitylmagnesium bromide	Sigma Aldrich	Sure/Seal	1.0 M solution in diethyl ether [B]
Methylmagnesium bromide	Thermo Fisher		3.0 M solution in diethyl ether [B]
Piperidine	abcr	99%	
Platinum(II) chloride	chempur	99.9%	[B]
Potassium hydroxide	Sigma Aldrich	85%+	
Potassium phosphate	Sigma Aldrich	98%+	
Propylene oxide	Thermo Fisher	99%+	
Silver hexafluoroantimonate(V)	Alfa Aesar	99%	[B]
Sodium hydrogen carbonate	VWR	100%	
Sodium hydroxide	VWR	98.6%	
Sodium sulfate	Merck	99%+	
Sodium thiosulfate pentahydrate	VWR	99.8%+	
Terephthalaldehyde	BLD Pharm	99.63%	
Triethylamine	Acros	99%	anhydrous [A] [B]
Trifluoromethanesulfonic acid anhydride	abcr	99%	
Trimethylsilyl chloride	Sigma Aldrich	99%	
Trimethylsilylacetylene	abcr / fluorochem	98%	[A] [B]
Triphenylphosphine	Alfa Aesar	99%	
Tris(dibenzylideneacetone)-dipalladium(0)	Sigma Aldrich	97%+	[B]

Purification methods:

[A] Degassed by bubbling argon

[B] Stored under inert conditions in a glove box / in a Schlenk vessel

[C] Stored over molecular sieves (3 or 4 Å)

1.12. Solvents

Unless stated otherwise, solvents were used without further purification. If a dried solvent was required, the additional purification / desiccation steps as denoted in the last column of the subsequent table were performed. Moreover, the use of a dried solvent is mentioned in the regarding experimental procedure, if relevant.

Solvent	Supplier	Purity / Purification	Additional Purifications / Desiccation
Benzene	Sigma Aldrich	99.8%	[B]
Benzene-d_6	Deutero	>99.5%	
Chloroform	Sigma Aldrich	99.0-99.4%	
Chloroform-d_1	Deutero	99.8%	[C]
Cyclohexane	VWR	99.5%	
Dichloromethane	VWR	100%	
Dichloromethane-d_2	Deutero	>99.6%	
Diethyl ether	VWR	distilled by rotary evaporation	[D]
Dimethylformamide	VWR	99.9%	
1,4-Dioxane	Thermo Fisher	99.5%	[B] [C]
Ethyl acetate	VWR	99.9%	
n-Hexane	Sigma Aldrich	99%	
Hydrochloric acid	Merck	37% aq. solution	
Mesitylene	Merck	98%	[A] [B]
Methanol	VWR	100%	
Methyl-*tert*-butyl ether	Acros	Acroseal, 99%	[A] [B]
n-Pentane	VWR	95%, distilled by rotary evaporation	
Pyridine	Sigma Aldrich	99.5%+	
Sulfuric acid	VWR	95%	
Tetrahydrofuran	VWR	100%	[B] [D]
Toluene	VWR	HPLC grade	[B] [D]
Water		Deionized	[A]

Purification methods:

[A] Degassed by bubbling argon

[B] Stored under inert conditions in a glove box / in a Schlenk vessel

[C] Stored over molecular sieves (3 or 4 Å)

[D] Purified via an Inert PS-MD-6 solvent purification system (SPS) (if denoted as “dry”)

2. Experimental Procedures

2.1. Synthetic Route towards BN[5] and BN[5]-(CN)$_2$

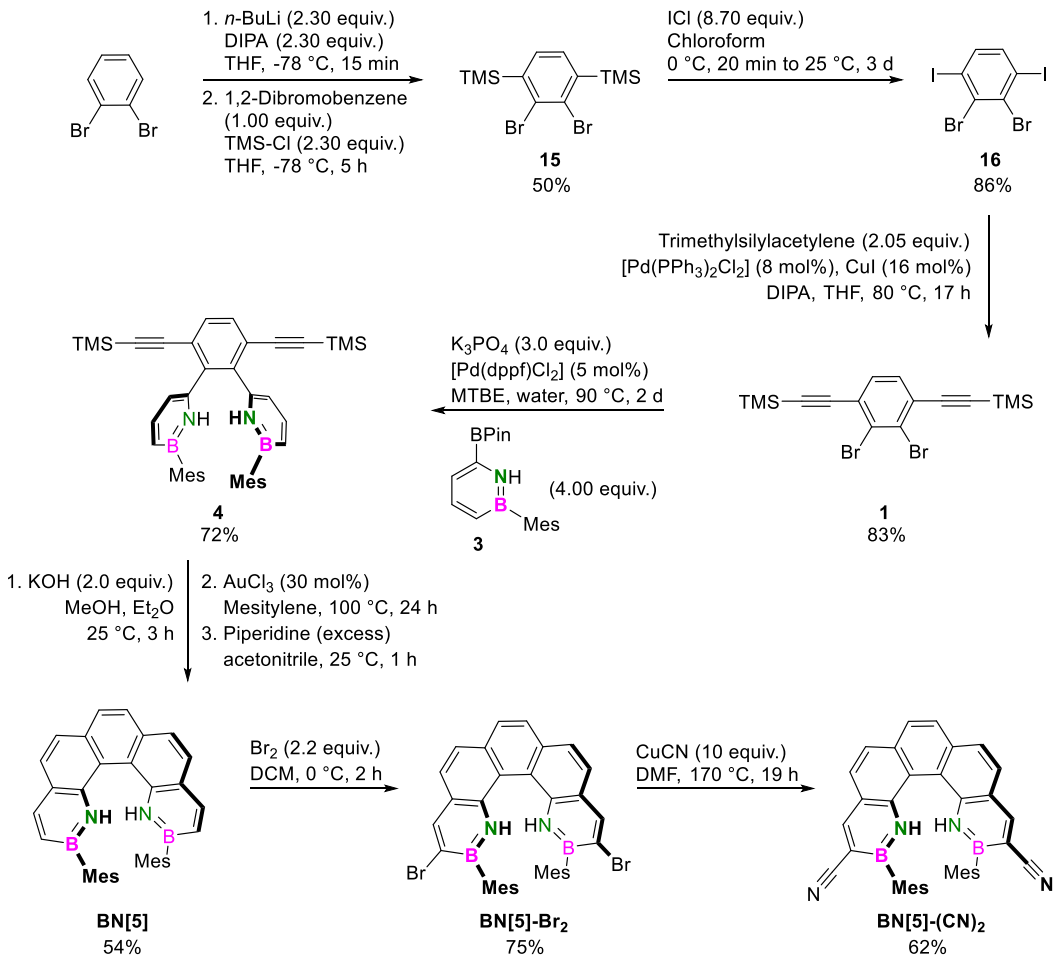

Scheme S1. Overview of the syntheses towards **BN[5]** and subsequent functionalization to obtain **BN[5]-(CN)$_2$**.

2.1.1. 1-Hydro-2-mesityl-1,2-azaborinine (14)

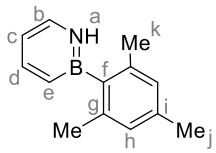

In a glove box, 1-(*tert*-butyldimethylsilyl)-2-chloro-1,2-azaborinine (2.28 g, 10.0 mmol, 1.00 equiv.) was dissolved in dry THF (100 mL). Outside the box on a Schlenk line, the solution was cooled to –78 °C. A solution of mesityllithium (3.15 g, 25.0 mmol, 2.50 equiv.)* in dry THF (15 mL) was added over the course of 5 min while stirring. The cooling bath was removed and stirring was continued for 30 min. *n*-Pentane and water (50 mL, respectively) were added and the phases were separated. The aqueous layer was extracted with *n*-pentane (3 x 50 mL) and the combined organic phases were washed with water (2 x 50 mL). After drying over sodium sulfate, filtration and evaporation of THF and *n*-pentane in vacuo, a yellow oil was obtained. ^{1}H NMR spectroscopy revealed a quantitative conversion. The crude product was dissolved in dry THF (200 mL). At 25 °C, a solution of tetra-*n*-butylammonium fluoride (1.0 M in THF, 12.0 mL, 12.0 mmol, 1.20 equiv.) was added at once. Stirring was continued for 1 h at this temperature. Afterwards, cyclohexane and water (50 mL, respectively) were added and the phases were separated. The aqueous layer was extracted with cyclohexane (3 x 50 mL) and the combined organic phases were washed with water (2 x 50 mL). After drying over sodium sulfate, filtration and evaporation of the solvents in vacuo, a brown oil was obtained. Remaining mesitylene and *tert*-butyldimethylsilylated derivatives were removed by rotary evaporation (5 mbar, 95 °C water bath temperature) until weight constancy (this took ca. 3–4 h). A light brown oil (1.90 g, 96% over two steps, Lit.[4]: 66%) was obtained, that slowly solidified at 5 °C.

^{1}H NMR (500 MHz, $CDCl_3$): δ = 7.89 (app br s, 1H, a),[5] 7.74 (ddd, ^3J = 11.1, 6.5 Hz, ^4J = 1.2 Hz, 1H, d), 7.41 (dd, ^3J = 7.0, 6.5 Hz, 1H, b), 6.93 – 6.87 (m, 3H, e, h), 6.40 (dddd, ^3J = 6.5, 6.5 Hz, ^4J = 1.5, 1.5 Hz, 1H, c), 2.33 (s, 3H, j), 2.19 (s, 6H, k) ppm.

^{13}C{^{1}H} NMR* (126 MHz, $CDCl_3$): δ = 143.9 (d), 140.4 (g), 137.4 (i), 133.9 (b), 127.3 (h), 110.6 (c), 23.2 (k), 21.3 (j) ppm.

^{11}B{^{1}H} NMR (160 MHz, $CDCl_3$): δ = 36.1 ppm.

IR (ATR): $\tilde{\nu}$ [cm^{-1}] = 3372 (m), 3086 (w), 3025 (w), 2956 (w), 2914 (w), 1652 (w), 1597 (m), 1540 (s), 1448 (s), 1339 (m), 1150 (m), 971 (m), 870 (m), 852 (s), 766 (s), 712 (s).

HR-MS (EI, 70 eV, R ~ 10 000): *m/z* (%) calcd. for $C_{13}H_{16}{}^{11}BN$ 197.13703 $[M]^+$, found 197.13732 $[M]^+$ (100).

M.p.: 53 °C.

R_f (silica, eluents: 5% diethyl ether in cyclohexane): 0.43.

* Compound synthesized according to a literature procedure.[6]

** The signals of the carbon atoms e and f were not detected due to the presence of an adjacent boron atom.[7-9]

2.1.2. 1-Hydro-2-mesityl-6-(4,4,5,5-tetramethyl-1,3,2-dioxaborolan-2-yl)-1,2-azaborinine (3)

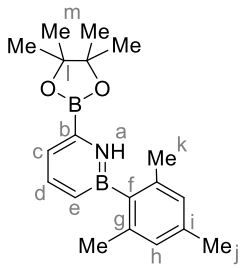

In a glove box, $[Ir(OMe)(cod)]_2$ (99.4 mg, 150 µmol, 1.5 mol%), dtbpy (80.5 mg, 300 µmol, 3 mol%), bis(pinacolato)diboron (2.79 g, 11.0 mmol, 1.10 equiv.) and dry MTBE (40 mL) were mixed. The mixture was added to a stirred solution of 1-hydro-2-mesityl-1,2-azaborinine (**14**, 1.97 g, 10.0 mmol, 1.00 equiv.) in dry MTBE (160 mL) and stirring was continued for 17 h at 25 °C. The solvent was removed in vacuo and the dark brown, crude product was purified by column chromatography (silica, eluents: 5% diethyl ether in *n*-pentane) to yield a colorless solid (2.32 g, 72%, Lit.[4]: 95%).

^{1}H NMR (500 MHz, $CDCl_3$): δ = 8.40 (app br s, 1H, a),[5] 7.72 (dd, ^3J = 11.1, 6.5 Hz, 1H, d), 7.06 (ddd, ^3J = 11.1 Hz, ^4J = 1.7, 1.3 Hz, 1H, e), 6.97 (ddd, ^3J = 6.5 Hz, ^4J = 1.7, 1.3 Hz, 1H, c), 6.89 (s, 2H, h), 2.32 (s, 3H, j), 2.17 (s, 6H, k), 1.33 (s, 12H, m) ppm.

^{13}C{^{1}H} NMR* (126 MHz, $CDCl_3$): δ = 142.6 (d), 140.4 (g), 137.3 (i), 127.2 (h), 119.8 (c), 84.8 (l), 25.0 (m), 23.3 (k), 21.3 (j) ppm.

^{11}B{^{1}H} NMR (160 MHz, $CDCl_3$): δ = 35.9 (azaborinine), 29.5 (BPin) ppm.

IR (ATR): $\tilde{\nu}$ [cm^{-1}] = 3394 (m), 3020 (w), 2972 (m), 2921 (m), 2854 (w), 1705 (w), 1609 (m), 1543 (m), 1446 (w), 1413 (m), 1370 (s), 1325 (s), 1142 (s), 960 (m), 847 (s).

HR-MS (EI, 70 eV, R ~ 10 000): *m/z* (%) calcd. for $C_{19}H_{27}{}^{10}B_2NO_2$ 321.22950 $[M]^+$, found 321.23008 $[M]^+$ (100).

M.p.: 141 °C.

R_f (silica, eluents: 5% diethyl ether in *n*-pentane): 0.33.

* The signals of the carbon atoms b, e and f were not detected due to the presence of an adjacent boron atom.[7-9]

2.1.3. 1,4-bis(Trimethylsilyl)-2,3-dibromobenzene (15)

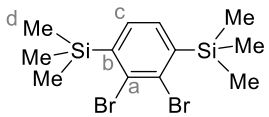

Dry THF (50 mL) was cooled to –78 °C in a 500 mL Schlenk flask. At this temperature, *n*-BuLi (9.20 mL, 23.0 mmol, 2.30 equiv.) and DIPA (2.33 g, 23.0 mmol, 2.30 equiv.) were added. After 15 min of stirring, the resulting solution was added to a solution of 1,2-dibromobenzene (2.36 g, 10.0 mmol, 1.00 equiv.) and trimethylsilyl chloride (2.50 g, 23.0 mmol, 2.30 equiv.) in dry THF (50 mL) at –78 °C over the course of 3 min. The reaction mixture was stirred at this temperature for 5 h and quenched with diluted sulfuric acid (2 M, 50 mL). The resulting mixture was diluted with water (100 mL) and extracted with diethyl ether (3 x 40 mL). The combined organic layers were dried over sodium sulfate and the solvent was removed in vacuo. The product was allowed to crystallize (14 d, –20 °C) and washed with methanol (5 mL) to obtain colorless, rhomboid crystals (1.90 g, 50%, Lit.[10]: 55%).

^{1}H NMR (500 MHz, $CDCl_3$): δ = 7.33 (s, 2H, c), 0.39 (s, 18H, d) ppm.

^{13}C{^{1}H} NMR (126 MHz, $CDCl_3$): δ = 145.9 (b), 134.1 (c), 133.5 (a), -0.3 (d) ppm.

^{29}Si{^{1}H} NMR (99 MHz, $CDCl_3$): δ = 0.4 ppm.

IR (ATR): $\tilde{\nu}$ [cm^{-1}] = 3057 (w), 2953 (m), 2897 (w), 1405 (w), 1371 (w), 1319 (s), 1248 (s), 1189 (s), 1159 (s), 1034 (s), 837 (s), 756 (s), 710 (m), 659 (m), 660 (w).

HR-MS (EI, 70 eV, R ~ 10 000): *m/z* (%) calc. for $C_{12}H_{20}{}^{79}Br_2Si_2$ 377.94648 [M]$^+$, found 377.94596 [M]$^+$ (5), 365.0 (100).

M.p.: 70 °C (Lit.[11]: 71 – 73 °C).

R$_f$ (silica, eluent: cyclohexane): 0.79.

2.1.4. 2,3-Dibromo-1,4-diiodobenzene (16)

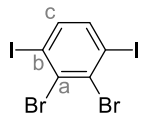

Iodine monochloride (1.0 M in DCM, 110 mL, 110 mmol, 8.70 equiv.) was added to a solution of 1,4-bis(trimethylsilyl)-2,3-dibromobenzene (**15**, 4.82 g, 12.7 mmol, 1.00 equiv.) in chloroform (200 mL) at 0 °C over the course of 20 min. The mixture was stirred for 3 d at 25 °C. The solvent was removed in vacuo. Using a rotary evaporator (5 mbar, 80 °C water bath temperature), the remaining iodine and iodine monochloride were sublimed to the edge of the reaction flask until the remaining solid had a pale-yellow color. The latter was crystallized from methanol (–20 °C, ca. 100 mL) to yield colorless flakes (5.35 g, 86%, Lit.[12]: 91%).

^{1}H NMR (500 MHz, $CDCl_3$): δ = 7.47 (s, 2H, c) ppm.

^{13}C{^{1}H} NMR (126 MHz, $CDCl_3$): δ = 139.9 (c), 132.0 (a), 101.6 (b) ppm.

IR (ATR): $\tilde{\nu}$ [cm^{-1}] = 3078 (w), 3024 (w), 2963 (w), 1399 (s), 1318 (s), 1310 (s), 1152 (s), 1005 (s), 943 (w), 798 (s), 748 (w), 731 (s), 708 (s).

HR-MS (EI, 70 eV, R ~ 10 000): *m/z* (%) calc. for $C_6H_2{}^{79}Br_2I_2$ 485.66072 [M]$^+$, found 485.66098 [M]$^+$ (43), 487.7 (100).

M.p.: 130 °C (Lit.[12]: 125 – 126 °C).

R$_f$ (silica, eluent: cyclohexane): 0.74.

2.1.5. 2,3-Dibromo-1,4-bis((trimethylsilyl)ethynyl)benzene (1)

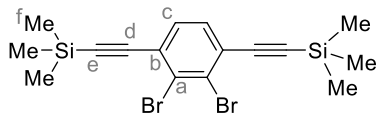

In a glove box, 2,3-dibromo-1,4-diiodobenzene (**16**, 4.88 g, 10.0 mmol, 1.00 equiv.), copper(I) iodide (305 mg, 1.60 mmol, 16 mol%), [Pd(PPh$_3$)$_2$Cl$_2$] (491 mg, 0.70 mmol, 7.0 mol%), DIPA (40 mL) and dry THF (200 mL) were placed in a Schlenk flask. While stirring, trimethylsilylacetylene (2.01 g, 20.5 mmol, 2.05 equiv.) was added dropwise to the mixture, which subsequently was heated to 80 °C for 17 h. After cooling, DCM and water (200 mL, respectively) were added. The phases were separated and the aqueous layer was extracted with DCM (3 x 50 mL). The organic layer was then washed with water (2 x 100 mL). The combined organic layers were dried over sodium sulfate, filtered and concentrated in vacuo. The crude product was filtered over silica (eluent: cyclohexane). Removing the solvent in vacuo furnished a yellow oil (3.56 g, 83%), that slowly crystallized at 25 °C.

^{1}H NMR (601 MHz, $CDCl_3$): δ = 7.35 (s, 2H, c), 0.27 (s, 18H, f) ppm.

^{13}C{^{1}H} NMR (151 MHz, $CDCl_3$): δ = 131.5 (c), 128.9 (b), 127.1 (a), 103.2 (e), 102.4 (d), -0.1 (f) ppm.

^{29}Si{^{1}H} NMR (99 MHz, $CDCl_3$): δ = –16.5 ppm.

IR (ATR): $\tilde{\nu}$ [cm^{-1}] = 2953 (w), 2925 (w), 2896 (w), 2171 (w), 2152 (w), 1436 (m), 1408 (w), 1350 (m), 1247 (s), 1095 (w), 912 (w), 839 (s), 824 (s), 757 (s), 698 (m), 656 (m).

HR-MS (EI, 70 eV, R ~ 10 000): *m/z* (%) calc. for $C_{16}H_{20}{}^{79}Br_2Si_2$ 425.94648 [M]$^+$, found 425.94696 [M]$^+$ (22), 413.1 (100).

M.p.: 79 °C.

R$_f$ (silica, eluent: cyclohexane): 0.50.

2.1.6. 1,2-bis(6-(1-Hydro-2-mesityl)-1,2-azaborinyl)-3,6-bis((trimethylsilyl)ethynyl)benzene (4)

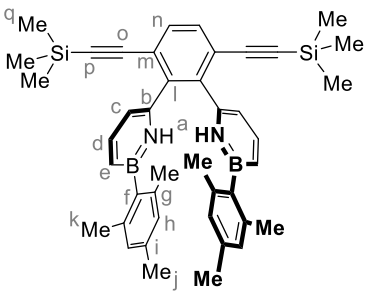

A pressure vial was charged with 2,3-dibromo-1,4-bis(trimethylsilylethynyl)-benzene (**1**, 428 mg, 1.00 mmol, 1.00 equiv.), 2-mesityl-6-(4,4,5,5-tetramethyl-1,3,2-dioxa-borolan-2-yl)-1,2-azaborinine (**3**, 1.29 g, 4.00 mmol, 4.00 equiv.) and potassium phosphate (637 mg, 3.00 mmol, 3.00 equiv.). In a glove box, $[Pd(dppf)Cl_2]$ (36.6 mg, 50.0 µmol, 5 mol%) and dry MTBE (45 mL) were added. Outside the box on a Schlenk line, degassed water (5 mL) was added and the reaction mixture was further degassed by bubbling Ar through it for 5 min. The reaction mixture was heated at 90 °C for 2 d. Water (40 mL) was added and the mixture was extracted with diethyl ether (3 × 40 mL). The combined organic phases were concentrated in vacuo. The crude product was purified by column chromatography (silica, eluents: 1% diethyl ether in cyclohexane) to remove the excess of BPin-azaborinine **3**. Recrystallization from methanol (200 mL) yielded a colorless solid (476 mg, 72%).

^{1}H NMR (600 MHz, $CDCl_3$): δ = 7.57 (dd, ^3J = 11.2, 6.7 Hz, 2H, d), 7.56 (app br s, 2H, a),[5] 7.52 (s, 2H, n), 6.80 (s, 4H, h), 6.71 (dt, ^3J = 11.2 Hz, ^4J = 1.5 Hz, 2H, e), 6.27 (ddd, ^3J = 6.7 Hz, ^4J = 2.0, 1.2 Hz, 2H, c), 2.27 (s, 6H, j), 2.00 (s, 12H, k), 0.07 (s, 18H, q) ppm.

^{13}C{^{1}H} NMR (151 MHz, $CDCl_3$): δ = 143.4 (d), 141.4 (b), 141.1 (l), 140.3 (g), 137.2 (i), 132.7 (n), 130.2 (e), 127.0 (h), 123.9 (m), 112.9 (c), 102.4 (p), 100.9 (o), 23.4 (k), 21.3 (j), –0.2 (q) ppm.

^{11}B{^{1}H} NMR (193 MHz, $CDCl_3$): δ = 37.4 ppm.

^{29}Si{^{1}H} NMR (99 MHz, $CDCl_3$): δ = –17.3 ppm.

IR (ATR): $\tilde{\nu}$ [cm^{-1}] = 3395 (w), 3354 (w), 3019 (w), 2958 (m), 2915 (w), 2856 (w), 2152 (w), 1609 (m), 1544 (s), 1447 (s), 1373 (m), 1249 (s), 1153 (w), 1118 (w), 1087 (w), 885 (s), 840 (s), 761 (s), 730 (m), 701 (w).

HR-MS (ESI positive): *m/z* calc. for $C_{42}H_{50}{}^{11}B_2N_2NaSi_2$ 683.35908 $[M+Na]^+$, found 683.35888 $[M+Na]^+$.

M.p.: 250 °C.

R_f (silica, eluents: 1% diethyl ether in cyclohexane): 0.29.

The signal of the carbon atom f was not detected due to the presence of an adjacent boron atom.[7-9]

2.1.7. 1,14-Dihydro-2,13-dimesityl-1,14-diaza-2,13-diborapentahelicene (BN[5])

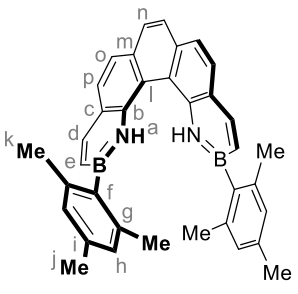

1,2-bis(6-(1-Hydro-2-mesityl)-1,2-azaborinyl)-3,6-bis((trimethylsilyl)ethynyl)benzene (**4**, 266 mg, 403 µmol, 1.00 equiv.) was dissolved in methanol and diethyl ether (100 mL, respectively). Potassium hydroxide (45.2 mg, 806 µmol, 2.00 equiv.) was added and the mixture was stirred for 3 h at 25 °C, when a quantitative deprotection was determined by TLC. Diethyl ether and brine (50 mL, respectively) were added, the phases were separated and the aqueous layer was extracted with diethyl ether (3 x 50 mL). The combined organic layers were washed with water (2 x 50 mL), dried over sodium sulfate, filtered, and the solvents were removed in vacuo. The crude product was placed in a pressure vial. In a glove box, gold(III) chloride (37.1 mg, 121 µmol, 30 mol%) and dry mesitylene (20 mL) were added. The mixture was heated at 100 °C for 24 h. After cooling, it was filtered over Celite and rinsed with toluene (50 mL) to remove the catalyst. The solvents were removed in vacuo the crude product was redissolved in acetonitrile (50 mL). Piperidine (3.0 mL) was added and the mixture was stirred for 1 h at 25 °C to derivatize the *endo*/*exo* side-product **8** (ratio <5%). The volatiles were removed in vacuo and the crude product was filtered over silica (eluents: 1% diethyl ether in cyclohexane). Subsequently, it was dissolved in methanol (100 mL). At a rotary evaporator (water bath temperature: 60 °C), the methanol was slowly evaporated until the product precipitated. This sequence was repeated until no more product was present in solution. Filtration via a glass frit gave a yellow solid (112 mg, 54%).

Deprotected Alkyne (6):

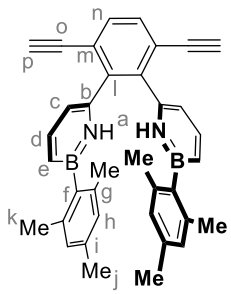

^{1}H NMR (600 MHz, $CDCl_3$): δ = 7.80 (app br s, 2H, a),[5] 7.58 (s, 2H, n), 7.53 (dd, ^3J = 11.1, 6.7 Hz, 2H, d), 6.84 (s, 4H, h), 6.74 (ddd, ^3J = 11.1 Hz, ^4J = 2.0, 1.2 Hz, 2H, e), 6.07 (ddd, ^3J = 6.7 Hz, ^4J = 2.0, 1.2 Hz, 2H, c), 3.14 (s, 2H, p), 2.29 (s, 6H, j), 2.11 (s, 12H, k) ppm.

R_f (silica, eluents: 1% diethyl ether in cyclohexane): 0.06.

Helicene (BN[5]):

^{1}H NMR (600 MHz, $CDCl_3$): δ = 8.31 (br s, 2H, a), 8.23 (d, ^3J = 11.3 Hz, 2H, d), 7.92 (d, ^3J = 8.1 Hz, 2H, p), 7.86 (s, 2H, n), 7.79 (d, ^3J = 8.1 Hz, 2H, o), 7.02 (dd, ^3J = 11.3, ^4J = 1.6 Hz, 2H, e), 6.76 (s, 4H, h), 2.26 (s, 6H, j), 1.81 (s, 12H, k) ppm.

^{13}C{^{1}H} NMR (151 MHz, $CDCl_3$): δ = 145.0 (d), 140.8 (g), 137.7 (i), 136.1 (f), 135.7 (b), 134.5 (m), 132.6 (e), 129.1 (p), 128.0 (n), 127.8 (h), 123.6 (c), 121.5 (o), 117.8 (l), 23.4 (k), 21.3 (j) ppm.

^{11}B{^{1}H} NMR (193 MHz, $CDCl_3$): δ = 37.7 ppm.

IR (ATR): $\tilde{\nu}$ [cm^{-1}] = 3409 (w), 3019 (w), 2959 (m), 2919 (m), 2853 (w), 2360 (w), 2342 (w), 1608 (m), 1571 (s), 1538 (m), 1440 (s), 1344 (m), 1261 (m), 1261 (m), 1068 (m), 1026 (m), 845 (s), 815 (m), 802 (m), 691 (m), 660 (w).

HR-MS (EI, 70 eV, R ~ 10 000): *m/z* (%) calc. for $C_{36}H_{34}{}^{11}B_2N_2$ 514.29752 $[M]^+$, found 514.29664 $[M]^+$ (100).

M.p.: 220 °C.

R_f (silica, eluents: 1% diethyl ether in cyclohexane): 0.12.

UV/Vis (DCM): λ_{max} (ε) = 283 nm (48 213 mol^{-1} dm^3 cm^{-1}).

Fluorescence (DCM): λ_{ex} = 370 nm, λ_{em} = 407, **428** nm.

2.1.8. 3,12-Dibromo-1,14-dihydro-2,13-dimesityl-1,14-diaza-2,13-diborapentahelicene (BN[5]-Br_2)

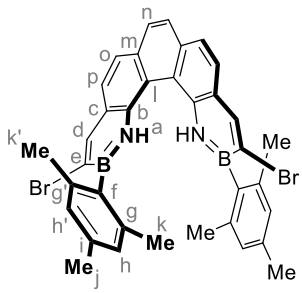

1,14-Dihydro-2,13-dimesityl-1,14-diaza-2,13-diborapentahelicene (**BN[5]**, 51.6 mg, 100 µmol, 1.00 equiv.) was dissolved in DCM (10 mL) and cooled to 0 °C. A solution of bromine (35.2 mg, 220 µmol, 2.20 equiv.) in DCM (1.0 mL) was added over the course of 10 min and the solution was stirred at the same temperature for 2 h. Sodium thiosulfate (300 mg) was added and the mixture was stirred for 15 min at 25 °C. Afterwards, the mixture was filtered and the crude product was subjected to column chromatography (silica, eluents: cyclohexane → 5% diethyl ether in cyclohexane) to yield a yellow solid (50.7 mg, 75%).

^{1}H NMR (601 MHz, $CDCl_3$): δ = 8.55 (s, 2H, d), 8.28 (br s, 2H, a), 7.87 (d, ^3J = 8.2 Hz, 2H, p), 7.84 (s, 2H, n), 7.81 (d, ^3J = 8.2 Hz, 2H, o), 6.92 (d, ^4J = 1.6 Hz, 2H, h), 6.70 (d, ^4J = 1.6 Hz, 2H, h'), 2.29 (s, 6H, j), 2.10 (s, 6H, k), 1.67 (s, 6H, k') ppm.

^{13}C{^{1}H} NMR (151 MHz, $CDCl_3$): δ = 147.2 (d), 142.0 (g), 139.1 (g'), 138.2 (i), 135.2 (b), 134.9 (m), 134.5 (f), 130.4 (e), 128.7 (p), 128.3 (n), 127.8 (h), 127.3 (h'), 123.9 (c), 122.6 (o), 117.6 (l), 23.6 (k), 22.9 (k'), 21.4 (j) ppm.

^{11}B{^{1}H} NMR (193 MHz, $CDCl_3$): δ = 36.4 ppm.

IR (ATR): $\tilde{\nu}$ [cm^{-1}] = 3400 (m), 2964 (w), 2945 (w), 2917 (w), 1610 (s), 1578 (m), 1563 (s), 1452 (m), 1417 (s), 1346 (m), 1218 (w), 1157 (w), 1018 (m), 914 (m), 841 (s), 815 (m), 690 (m).

HR-MS (ESI negative): *m/z* calc. for $C_{36}H_{31}{}^{11}B_2{}^{79}Br_2N_2$ 671.10612 $[M\text{-}H]^-$, found 671.10626 $[M\text{-}H]^-$.

M.p.: Decomposed at T > 310 °C.

R_f (silica, eluents: 2% diethyl ether in cyclohexane): 0.29.

2.1.9. 3,12-Dicyano-1,14-dihydro-2,13-dimesityl-1,14-diaza-2,13-diborapentahelicene (BN[5]-(CN)$_2$)

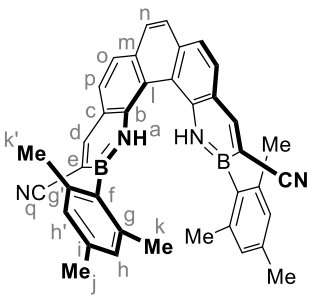

3,12-Dibromo-1,14-dihydro-2,13-dimesityl-1,14-diaza-2,13-diborapentahelicene (**BN[5]-Br$_2$**, 10.1 mg, 15.0 µmol, 1.00 equiv.) and copper(I) cyanide (13.4 mg, 150 µmol, 10.0 equiv.) were placed in a 2 – 5 mL microwave vial. In a glove box, dry DMF (1 mL) was added. The solution was stirred for 19 h at 170 °C in an oil bath. After cooling, water (10 mL) and DCM (10 mL) were added and the phases were separated. The organic layer was washed with water (3 x 10 mL), dried over sodium sulfate, filtered and the solvent was removed in vacuo. The crude product was subjected to column chromatography (silica, eluent: DCM) to yield a yellow solid (5.2 mg, 62%).

^{1}H NMR (601 MHz, $CDCl_3$): δ = 8.69 (s, 2H, d), 8.35 (br s, 2H, a), 8.00 (d, ^3J = 8.3 Hz, 2H, p), 7.97 (s, 2H, n), 7.91 (d, ^3J = 8.3 Hz, 2H, o), 6.92 (s, 2H, h), 6.68 (s, 2H, h'), 2.28 (s, 6H, j), 2.07 (s, 6H, k), 1.66 (s, 6H, k') ppm.

^{13}C{^{1}H} NMR (151 MHz, $CDCl_3$): δ = 154.4 (d), 142.0 (g), 139.1 (g'), 139.0 (i), 137.0 (b), 136.9 (m), 132.1 (f), 130.0 (p), 129.8 (n), 128.5 (h), 127.8 (h'), 123.3 (o), 122.2 (c), 121.2 (q), 117.3 (l), 113.1 (e), 23.4 (k), 23.0 (k'), 21.4 (j) ppm.

^{11}B{^{1}H} NMR (193 MHz, $CDCl_3$): δ = 36.8 ppm.

IR (ATR): $\tilde{\nu}$ [cm^{-1}] = 3436 (w), 3423 (w), 3292 (w), 2962 (w), 2922 (w), 2853 (w), 2214 (m), 1608 (m), 1575 (s), 1540 (m), 1432 (m), 1377 (w), 1354 (w), 1233 (w), 1217 (w), 1159 (w), 963 (w), 844 (m), 740 (w), 687 (m).

HR-MS (ESI negative): *m/z* calc. for $C_{38}H_{31}{}^{11}B_2N_4$ 565.27528 [M-H]$^-$, found 565.27481 [M-H]$^-$.

M.p.: Decomposed at T > 345 °C.

R$_f$ (silica, eluent: DCM): 0.61.

UV/Vis (DCM): λ_{max} (ε) = 313 nm (27 991 mol^{-1} dm^3 cm^{-1}).

Fluorescence (DCM): λ_{ex} = 370 nm, λ_{em} = **424**, 446 nm.

2.2. Synthetic Route towards BN[6]

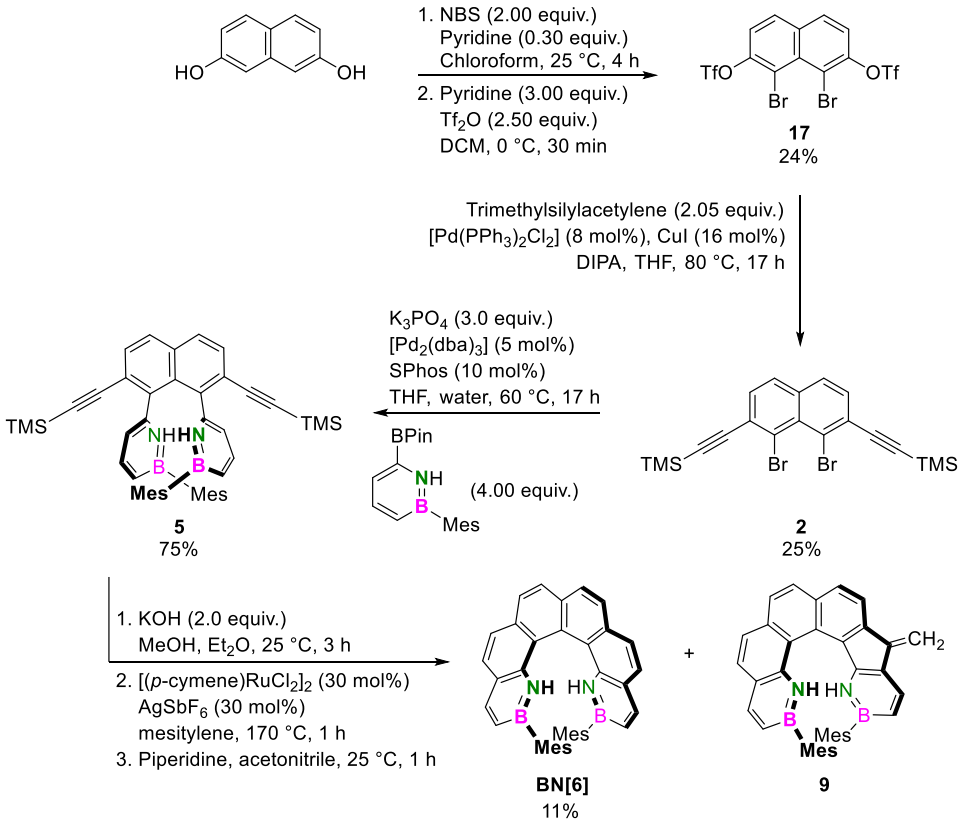

Scheme S2. Overview of the syntheses towards **BN[6]**.

2.2.1. 1,8-Dibromo-2,7-bis(trifluoromethylsulfonyl)naphthalene (17)

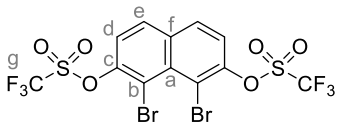

2,7-Dihydroxynaphthalene (12.8 g, 80.0 mmol, 1.00 equiv.), NBS (28.4 g, 160 mmol, 2.00 equiv.) and pyridine (1.88 g, 24.0 mmol, 0.30 equiv.) were dissolved in chloroform (500 mL). The solution was stirred for 4 h at 25 °C. It was washed with HCl (1 M, 3 x 150 mL) and water (3 x 100 mL). The combined organic layers were dried over sodium sulfate and the solvent was removed in vacuo. The obtained yellow solid (13.7 g, 43.1 mmol, 1.00 equiv. under the assumption that solely species with two bromo substituents were present) was dissolved in DCM (200 mL). It was cooled to 0 °C, then pyridine (10.3 g, 129 mmol, 3.00 equiv.) was added at once and trifluoromethanesulfonic acid anhydride (30.4 g, 108 mmol, 2.50 equiv.) was added dropwise over the course of 10 min. The reaction was allowed to stir at 0 °C for 30 min. The mixture was washed with a sat. aq. sol. of $NaHCO_3$ (3 x 150 mL) and extracted with DCM (3 x 80 mL). The organic layer was washed with an aq. sol. of HCl (10%, 3 x 100 mL), dried over sodium sulfate and the solvent was removed in vacuo. The crude product was recrystallized from methanol twice (90 mL used, respectively) to yield colorless needles (6.00 g, 24%, Lit.[13]: 27%).

^{1}H NMR (601 MHz, $CDCl_3$): δ = 7.97 (d, ^3J = 9.0 Hz, 2H, e), 7.56 (d, ^3J = 9.0 Hz, 2H, d) ppm.

^{13}C{^{1}H} NMR: (151 MHz, $CDCl_3$): δ = 148.5 (c), 134.1 (f), 131.3 (a), 131.0 (e), 122.0 (d), 118.8 (q, $^1J_{C\text{-}F}$ = 320.7 Hz, g), 116.0 (b) ppm.

^{19}F NMR: (565 MHz, $CDCl_3$): δ = –73.2 ppm.

IR (ATR): $\tilde{\nu}$ [cm^{-1}] = 3112 (w), 3082 (w), 2852 (w), 2359 (w), 1590 (w), 1494 (w), 1428 (s), 1412 (m), 1322 (m), 1246 (m), 1233 (m), 1201 (s), 1178 (s), 1147 (s), 1131 (s), 991 (m), 873 (s), 844 (s), 832 (s), 775 (m), 770 (m), 727 (s), 696 (m).

HR-MS (EI, 70 eV, R ~ 10 000): *m/z* (%) calc. for $C_{12}H_4{}^{79}Br_2F_6O_6S_2$ 579.77147 $[M]^+$, found 579.77205 $[M]^+$ (25), 287.9 (100).

M.p.: 123 °C.

R_f (silica, eluents: 7% diethyl ether in cyclohexane): 0.17.

2.2.2. 1,8-Dibromo-2,7-bis(trimethylsilylethynyl)naphthalene (2)

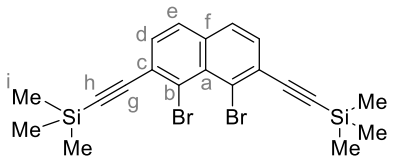

In a glove box, 1,8-dibromo-2,7-bis(trifluoromethylsulfonyl)naphthalene (**17**, 232 mg, 400 µmol, 1.00 eq), trimethylsilylacetylene (314 mg, 3.20 mmol, 8.00 equiv.), $[Pd(dppf)Cl_2]$ (14.6 mg, 20.0 µmol, 5 mol%), CuI (14.6 mg, 40.0 µmol, 10 mol%) were mixed and suspended in dry DMF and TEA (4.0 mL, respectively). The mixture was stirred for 17 h at 25 °C. The mixture was diluted with DCM (50 mL) and washed with water (3 x 30 mL). The solvent was removed in vacuo and the residue was purified by column chromatography (silica, eluent: cyclohexane). Crystallization from methanol (2 mL) yielded a yellow solid (75.3 mg, 39%). The reaction was repeated on a 10.0 mmol scale, directly performing a crystallization from methanol (40 mL) without prior column chromatography (1.17 g, 25%).

^{1}H NMR (600 MHz, $CDCl_3$): δ = 7.65 (d, ^3J = 8.4 Hz, 2H, e), 7.51 (d, ^3J = 8.4 Hz, 2H, d), 0.31 (s, 18H, i) ppm.

^{13}C{^{1}H} NMR (151 MHz, $CDCl_3$): δ = 135.5 (f), 130.6 (d), 130.4 (a), 128.4 (c), 128.3 (e), 123.9 (b), 105.0 (g), 102.6 (h), -0.1 (i) ppm.

^{29}Si{^{1}H} NMR (99 MHz, $CDCl_3$): δ = –16.7 ppm.

IR (ATR): $\tilde{\nu}$ [cm^{-1}] = 2958 (w), 2898 (w), 2359 (w), 2342 (w), 2151 (w), 1494 (w), 1331 (w), 1244 (m), 1193 (m), 1182 (m), 1141 (m), 834 (s), 758 (s), 697 (s).

HR-MS (EI, 70 eV, R ~ 10 000): *m/z* (%) calc. for $C_{20}H_{22}{}^{79}Br_2Si_2$ 475.96213 $[M]^+$, found 475.96264 $[M]^+$ (43), 477.7 (100).

M.p.: 164 °C.

R_f (silica, eluent: cyclohexane): 0.13.

2.2.3. 1,8-bis(6-(1-Hydro-2-mesityl)-1,2-azaborinyl)-2,7-bis((trimethylsilyl)ethynyl)naphthalene (5)

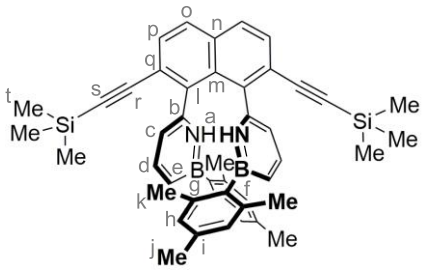

A pressure vial was charged with 1,8-dibromo-2,7-bis(trimethylsilylethynyl)-naphthalene (**2**, 163 mg, 340 µmol, 1.00 equiv.), 2-mesityl-6-(4,4,5,5-tetramethyl-1,3,2-dioxaborolan-2-yl)-1,2-azaborinine (**3**, 439 mg, 1.36 mmol, 4.00 equiv.) and potassium phosphate (217 mg, 1.02 mmol, 3.00 mmol). In a glove box, $[Pd_2(dba)_3]$ (15.6 mg, 17.0 µmol, 5 mol%), SPhos (14.0 mg, 34.1 µmol, 10 mol%) and dry THF (15.3 mL) were added. Outside the glove box on a Schlenk line, degassed water (1.7 mL) was added and the reaction mixture was degassed by bubbling Ar through it for 5 min. The reaction mixture was heated at 60 °C for 17 h. Water (10 mL) was added and the mixture was extracted with DCM (3 x 10 mL). The combined organic phases were concentrated in vacuo. The crude product was purified via column chromatography (silica, eluents: 1% diethyl ether in cyclohexane) to yield a yellow solid (182 mg, 75%).

^{1}H NMR (600 MHz, $CDCl_3$): δ = 7.82 (d, ^3J = 8.5 Hz, 2H, o), 7.60 (d, ^3J = 8.5 Hz, 2H, p), 7.42 (dd, ^3J = 11.2, 6.7 Hz, 2H, d), 7.20 (app br s, 2H, a),[5] 6.84 (s, 4H, h), 6.66 (ddd, ^3J = 11.2 Hz, ^4J = 2.1, 1.2 Hz, 2H, e), 6.16 (ddd, ^3J = 6.7 Hz, ^4J = 2.1, 1.1 Hz, 2H, c), 2.30 (s, 12H, k), 2.27 (s, 6H, j), 0.05 (s, 18H, t) ppm.

^{13}C{^{1}H} NMR (151 MHz, $CDCl_3$): δ = 143.4 (d), 142.9 (b), 140.5 (g), 139.6 (l), 138.4 (f), 137.1 (i), 133.6 (n), 129.9 (p), 129.8 (m), 129.3 (o), 129.3 (e), 127.3 (h), 125.4 (q), 113.2 (c), 103.1 (r), 100.5 (s), 23.7 (k), 21.2 (j), –0.1 (t) ppm.

^{11}B{^{1}H} NMR (193 MHz, $CDCl_3$): δ = 36.8 ppm.

^{29}Si{^{1}H} NMR (99 MHz, $CDCl_3$): δ = –17.6 ppm.

IR (ATR): $\tilde{\nu}$ [cm^{-1}] = 3393 (w), 3349 (w), 3018 (w), 2958 (m), 2917 (w), 2856 (w), 2359 (w), 2342 (w), 2154 (m), 1610 (m), 1539 (s), 1447 (s), 1364 (w), 1250 (s), 1153 (w), 980 (w), 910 (w), 872 (s), 844 (s), 760 (s), 719 (m), 670 (w).

HR-MS (EI, 70 eV, R ~ 10 000): *m/z* (%) calc. for $C_{46}H_{52}{}^{11}B_2N_2Si_2$ 710.38654 $[M]^+$, found 710.38710 $[M]^+$ (100).

M.p.: Decomposed at T > 250 °C.

R_f (silica, eluents: 1% diethyl ether in cyclohexane): 0.14.

2.2.4. 1,16-Dihydro-2,15-dimesityl-1,16-diaza-2,15-diborahexahelicene (BN[6])

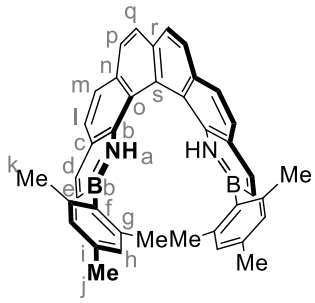

1,8-bis(6-(1-Hydro-2-mesityl)-1,2-azaborinyl)-2,7-bis((trimethylsilyl)ethynyl)naphthalene (**5**, 142 mg, 200 µmol, 1.00 equiv.) was dissolved in methanol (50 mL) and diethyl ether (50 mL). Potassium hydroxide (22.4 mg, 400 µmol, 2.00 equiv.) was added and the mixture was stirred for 3 h at 25 °C, when a quantitative deprotection was determined by TLC. Diethyl ether (50 mL) and brine (50 mL) were added, the phases were separated and the aqueous layer was extracted with diethyl ether (3 x 50 mL). The combined organic layers were washed with water (2 x 50 mL), dried over sodium sulfate, filtered, and the solvents were removed in vacuo. The crude product was placed in a pressure vial. In a glove box, $[(p\text{-cymene})RuCl_2]_2$ (36.7 mg, 60.0 µmol, 30 mol%), $AgSbF_6$ (20.6 mg, 60.0 µmol, 30 mol%) and dry mesitylene (10 mL) were added. The mixture was heated at 170 °C for 1 h. After cooling, the mixture was filtered over silica and rinsed with toluene (100 mL) to remove the catalyst. The solvents were removed in vacuo the crude product was redissolved in acetonitrile (50 mL). Piperidine (3.0 mL) was added and the mixture was stirred for 1 h at 25 °C to derivatize the *endo*/*exo* side-product **9** (ratio <20%). The volatiles were removed in vacuo and the crude product was filtered over silica (eluents: 1% diethyl ether in cyclohexane) to yield a light brown solid (12.2 mg, 11%).

Deprotected Alkyne (7):

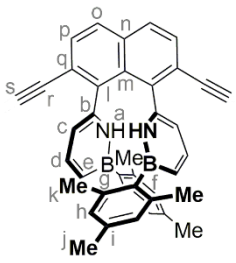

^{1}H NMR (600 MHz, $CDCl_3$): δ = 7.87 (d, ^3J = 8.5 Hz, 2H, o), 7.65 (d, ^3J = 8.5 Hz, 2H, p), 7.51 (app br s, 2H, a),[5] 7.42 (dd, ^3J = 11.2, 6.7 Hz, 2H, d), 6.85 (s, 4H, h), 6.64 (ddd, ^3J = 11.2 Hz, ^4J = 1.6, 1.6 Hz, 2H, e), 6.07 (ddd, ^3J = 6.7 Hz, ^4J = 1.6, 1.6 Hz, 2H, c), 3.04 (s, 2H, s), 2.29 (s, 12H, k), 2.28 (s, 6H, j) ppm.

R_f (silica, eluents: 1% diethyl ether in cyclohexane) = 0.07. **R_f** (silica, eluents: 5% diethyl ether in cyclohexane) = 0.36.

Helicene (BN[6]):

^{1}H NMR (600 MHz, $CDCl_3$): δ = 8.70 (br s, 2H, a), 8.04 (d, ^3J = 11.3 Hz, 2H, d), 7.95 (d, ^3J = 8.3 Hz, 2H, p), 7.92 (d, ^3J = 8.3 Hz, 2H, q), 7.73 (d, ^3J = 8.4 Hz, 2H, l), 7.71 (d, ^3J = 8.4 Hz, 2H, m), 6.87 (dd, ^3J = 11.3 Hz, ^4J = 1.7 Hz, 2H, e), 6.65 (s, 4H, h), 2.23 (s, 6H, j), 1.68 (s, 12H, k) ppm.

^{13}C{^{1}H} NMR* (151 MHz, $CDCl_3$): δ = 144.8 (d), 139.9 (g), 136.9 (i), 136.6 (b), 133.1 (n), 132.7 (r), 132.2 (e), 129.0 (l), 127.6 (p), 126.9 (q), 126.8 (h), 122.3 (c), 120.8 (m), 120.1 (s), 119.2 (o), 23.1 (k), 21.1 (j) ppm.

^{11}B{^{1}H} NMR (193 MHz, $CDCl_3$): δ = 37.4 ppm.

IR (ATR): $\tilde{\nu}$ [cm^{-1}] = 3382 (w), 3018 (w), 2956 (m), 2922 (m), 2852 (m), 2359 (w), 1735 (w), 1609 (m), 1597 (m), 1581 (m), 1560 (m), 1540 (m), 1439 (s), 1349 (m), 1259 (m), 1153 (m), 1027 (m), 845 (s), 737 (m), 725 (m), 677 (w).

HR-MS (ESI positive): *m/z* calc. for $C_{40}H_{37}{}^{11}B_2N_2$ 567.31374 $[M+H]^+$, found 567.31476 $[M+H]^+$.

M.p.: Decomposed at T > 300 °C.

R_f (silica, eluents: 1% diethyl ether in cyclohexane): 0.26.

UV/Vis (DCM): λ_{max} (ε) = 280 nm (52 178 mol^{-1} dm^3 cm^{-1}).

Fluorescence (DCM): λ_{ex} = 370 nm, λ_{em} = **434**, 459 nm.

* The signal of the carbon atom f was not detected due to the presence of an adjacent boron atom.[7-9]

2.3. Synthetic Route towards CC[5]

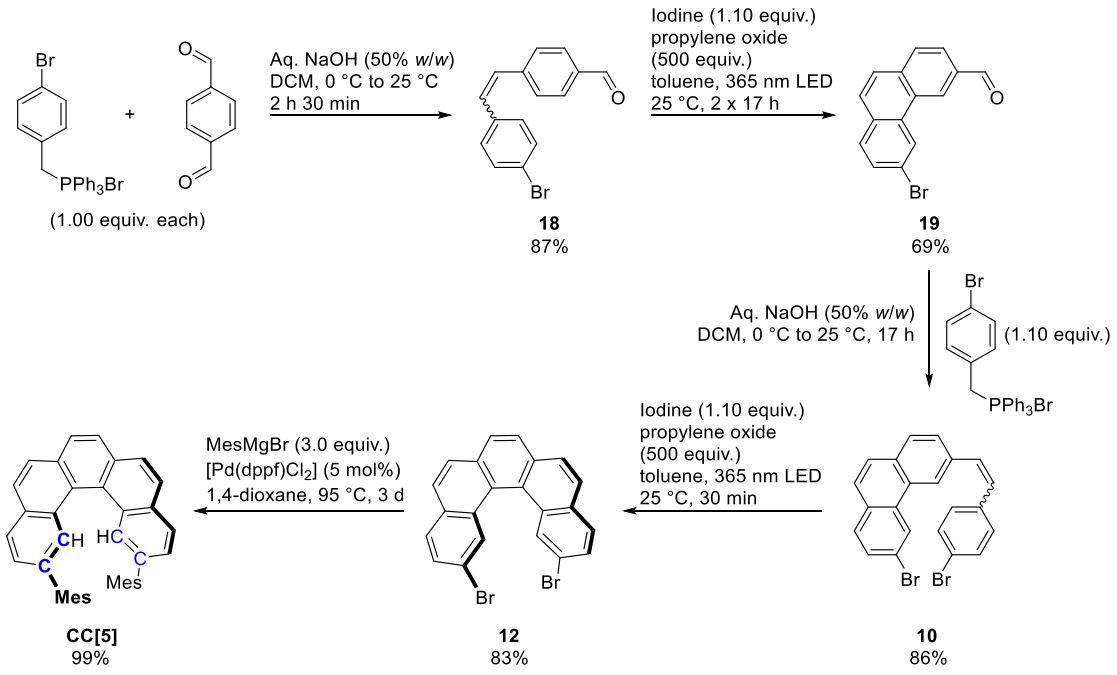

Scheme S3. Overview of the syntheses towards **CC[5]**.

2.3.1. (*E*)/(*Z*)-4-Bromo-4'-formylstilbene (18)

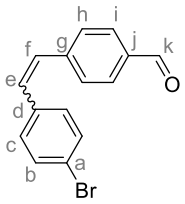

Terephthalaldehyde (804 mg, 6.00 mmol, 1.00 equiv.) and (4-bromobenzyl)triphenylphosphonium bromide (3.07 g, 6.00 mmol, 1.00 equiv.) were dissolved in DCM (100 mL) and cooled to 0 °C in an ice bath. An aqueous solution of sodium hydroxide (4.0 mL, 50% *w/w*) was added dropwise over the course of 5 min. After removal of the ice bath, the reaction was allowed to warm to 25 °C and stirring was continued for 2 h 30 min. Water (100 mL) was added and the phases were separated. The aqueous layer was extracted with DCM (3 x 30 mL). The combined organic layers were washed with water (2 x 50 mL), dried over sodium sulfate, filtered and the solvent was removed in vacuo. The crude product was filtered over silica (eluent: DCM) to remove triphenylphosphine oxide and further purified by column chromatography (silica, eluents: 50% DCM in *n*-hexane) to yield a slightly yellow solid/oil (1.49 g, 87%). The isomeric ratio of the crude product (*E*/*Z*) was 0.26/0.74. If desired, the *Z*-isomer (yellow oil at ambient conditions) can be collected isomerically pure as the first fraction.

(*Z*)-Isomer:

^{1}H NMR (601 MHz, $CDCl_3$): δ = 9.96 (s, 1H, k), 7.75 (d, ^3J = 8.2 Hz, 2H, i), 7.39 – 7.34 (m, 4H, h+b), 7.08 (d, ^3J = 8.5 Hz, 2H, c), 6.68 – 6.63 (m, 2H, f+e) ppm.

^{13}C{^{1}H} NMR (151 MHz, $CDCl_3$): δ = 191.8 (k), 143.4 (g), 135.5 (d), 135.3 (j), 131.7 (b), 131.7 (e), 130.6 (c), 129.9 (i), 129.9 (f), 129.6 (h), 121.8 (a) ppm.

IR (ATR): $\tilde{\nu}$ [cm^{-1}] = 3046 (w), 3016 (w), 2824 (w), 2732 (w), 1694 (s), 1600 (s), 1581 (m), 1484 (s), 1304 (m), 1210 (s), 1166 (s), 1070 (s), 1008 (s), 970 (s), 884 (m), 824 (s), 796 (s), 670 (m).

HR-MS (EI, 70 eV, R ~ 10 000): *m/z* (%) calc. for $C_{15}H_{11}{}^{79}BrO$ 285.99878 $[M]^+$, found 285.99844 $[M]^+$ (40), 178.0 (100).

R_f (silica, eluents: 50% DCM in *n*-hexane): 0.39.

(*E*)-Isomer:*

^{1}H NMR (600 MHz, $CDCl_3$): δ = 10.00 (s, 1H), 7.87 (d, ^3J = 8.3 Hz, 2H), 7.64 (d, ^3J = 8.3 Hz, 2H), 7.51 (d, ^3J = 8.5 Hz, 2H), 7.40 (d, ^3J = 8.5 Hz, 2H), 7.19 (d, ^3J = 16.3 Hz, 1H), 7.12 (d, ^3J = 16.3 Hz, 1H) ppm.

R_f (silica, eluents: 50% DCM in *n*-hexane): 0.46.

* Because the *(E)*-isomer was not isolated, only the ^{1}H NMR shifts from the isomeric mixture could be analyzed.

2.3.2. 6-Bromo-3-formylphenanthrene (19)

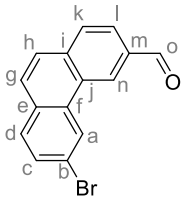

4-Bromo-4'-formylstilbene (**18**, 57.4 mg, 200 µmol, 1.00 equiv., isomeric mixture) was dissolved in toluene (120 mL). Iodine (55.8 mg, 220 µmol, 1.10 equiv.) and propylene oxide (7.00 mL, 100 mmol, 500 equiv.) were added and the mixture was degassed by bubbling Ar through it for 5 min. At 25 °C and under vigorous stirring, the mixture was irradiated for 2 x 17 h (see Section 1 for the photochemical setup). Four equal approaches were run and combined for the subsequent purification procedure. The volatiles were removed in vacuo and the crude product was subjected to filtration over silica (eluents: 50% DCM in *n*-hexane → DCM) to yield a colorless solid (185 mg, 69%).

^{1}H NMR (600 MHz, $CDCl_3$): δ = 10.26 (s, 1H, o), 9.05 (d, ^4J = 1.5 Hz, 1H, n), 8.87 (d, ^4J = 1.8 Hz, 1H, a), 8.09 (dd, ^3J = 8.2 Hz, ^4J = 1.5 Hz, 1H, l), 7.99 (d, ^3J = 8.2 Hz, 1H, k), 7.84 (d, ^3J = 8.8 Hz, 1H, g), 7.79 (app d, 2H, d+h), 7.75 (dd, ^3J = 8.5 Hz, ^4J = 1.8 Hz, 1H, c) ppm.

^{13}C{^{1}H} NMR (151 MHz, $CDCl_3$): δ = 192.3 (o), 136.3 (i), 134.6 (m), 132.0 (f), 130.9 (e), 130.8 (c), 130.5 (d), 129.8 (g), 129.8 (k), 129.2 (j), 127.2 (n), 127.0 (h), 125.9 (l), 125.8 (a), 122.1 (b) ppm.

IR (ATR): $\tilde{\nu}$ [cm^{-1}] = 3064 (w), 2956 (w), 2925 (w), 2851 (w), 2810 (w), 2702 (w), 1698 (m), 1682 (s), 1608 (m), 1590 (m), 1497 (m), 1233 (m), 1198 (m), 1183 (m), 1075 (m), 906 (m), 843 (s), 786 (s), 705 (m).

HR-MS (EI, 70 eV, R ~ 10 000): *m/z* (%) calc. for $C_{15}H_9{}^{79}BrO$ 283.98313 $[M]^+$, found 283.98287 $[M]^+$ (65), 176.0 (100).

M.p.: 200 °C.

R_f (silica, eluents: 50% DCM in *n*-hexane): 0.38.

2.3.3. (*E*)/(*Z*)-6-Bromo-3-(2-(4-bromophenyl)ethenyl)phenanthrene (10)

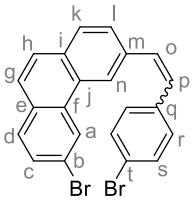

6-Bromo-3-formylphenanthrene (**19**, 114 mg, 400 µmol, 1.00 equiv.) and (4-bromobenzyl)-triphenylphosphonium bromide (225 mg, 440 µmol, 1.10 equiv.) were dissolved in DCM (40 mL) and cooled to 0 °C in an ice bath. An aqueous solution of sodium hydroxide (2.0 mL, 50% *w/w*) was added dropwise over the course of 5 min. After removal of the ice bath, the reaction was allowed to warm to 25 °C and stirring was continued for 17 h. Water (50 mL) was added and the phases were separated. The aqueous layer was extracted with DCM (3 x 30 mL). The combined organic layers were dried over sodium sulfate, filtered and the solvent was removed in vacuo. The isomeric ratio of the crude product (*E*/*Z*) was 0.29/0.71. The crude mixture was filtered over silica (eluents: 10% DCM in *n*-hexane) to furnish a colorless solid (151 mg, 86%). If desired, the *Z*-isomer (colorless oil that slowly solidifies) can be collected isomerically pure by column chromatography as the first fraction, using an eluent mixture of 5% DCM in *n*-hexane.

(*Z*)-Isomer:

^{1}H NMR (600 MHz, $CDCl_3$): δ = 8.54 (d, ^4J = 1.9 Hz, 1H, a), 8.46 (d, ^4J = 1.7 Hz, 1H, n), 7.73 (d, ^3J = 8.5 Hz, 1H, d), 7.71 (d, ^3J = 8.2 Hz, 1H, k), 7.69 (d, ^3J = 8.8 Hz, 1H, h), 7.68 – 7.63 (m, 2H, c+g), 7.46 (dd, ^3J = 8.2 Hz, ^4J = 1.7 Hz, 1H, l), 7.38 (d, ^3J = 8.4 Hz, 2H, s), 7.17 (d, ^3J = 8.4 Hz, 2H, r), 6.87 (d, ^3J = 12.1 Hz, 1H, o), 6.68 (d, ^3J = 12.1 Hz, 1H, p) ppm.

^{13}C{^{1}H} NMR (151 MHz, $CDCl_3$): δ = 136.3 (q), 135.5 (m), 131.8 (e), 131.7 (s), 131.5 (i), 131.1 (o), 130.8 (f), 130.7 (r), 130.2 (d), 130.0 (c), 130.0 (p), 129.3 (j), 128.6 (k), 128.1 (l), 127.2 (h), 126.6 (g), 125.6 (a), 123.3 (n), 121.4 (t), 121.1 (b) ppm.

IR (ATR): $\tilde{\nu}$ [cm^{-1}] = 3056 (w), 3012 (w), 2920 (w), 2849 (w), 1591 (m), 1483 (m), 1419 (m), 1068 (m), 1010 (m), 908 (m), 847 (s), 808 (m), 763 (m), 667 (m).

HR-MS (EI, 70 eV, R ~ 10 000): *m/z* (%) calc. for $C_{22}H_{14}{}^{79}Br_2$ 435.94568 $[M]^+$, found 435.94577 $[M]^+$ (45), 437.9 (100).

M.p.: 132 °C.

R_f (silica, eluents: 10% DCM in *n*-hexane): 0.49.

(*E*)-Isomer:*

^{1}H NMR (600 MHz, $CDCl_3$): δ = 8.85 (d, ^4J = 1.5 Hz, 1H), 8.63 (s, 1H), 7.88 (d, ^3J = 8.3 Hz, 1H), 7.84 (dd, ^3J = 8.3 Hz, ^4J = 1.6 Hz, 1H), 7.76 (d, ^3J = 8.5 Hz, 1H), 7.73 – 7.64 (m, 2H), 7.53 (d, ^3J = 8.5 Hz, 2H), 7.48 (d, ^3J = 8.5 Hz, 2H), 7.37 (d, ^3J = 16.3 Hz, 1H), 7.26 (d, ^3J = 16.3 Hz, 1H), 7.17 (d, ^3J = 8.4 Hz, 1H) ppm.

R_f (silica, eluents: 10% DCM in *n*-hexane): 0.58.

* Because the *(E)*-isomer was not isolated, only the ^{1}H NMR shifts from the isomeric mixture could be analyzed.

2.3.4. 2,13-Dibromopentahelicene (12)

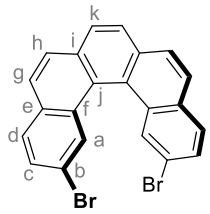

6-Bromo-3-(2-(4-bromophenyl)ethenyl)phenanthrene (**10**, 87.6 mg, 200 µmol, 1.00 equiv.) was dissolved in toluene (120 mL). Iodine (55.8 mg, 220 µmol, 1.10 equiv.) and propylene oxide (7.00 mL, 100 mmol, 500 equiv.) were added and the mixture was degassed by bubbling Ar thought the reaction mixture for 5 min. At 25 °C and under vigorous stirring, the mixture was irradiated for 30 min (see Section 1 for the photochemical setup). After removing the solvents in vacuo, the crude product was washed with *n*-pentane (3 x 5 mL) via a frit to furnish a slightly yellow solid (72.4 mg, 83%).

^{1}H NMR (600 MHz, $CDCl_3$): δ = 8.69 (d, ^4J = 1.9 Hz, 1H, a), 7.91 – 7.87 (m, 3H, g+h+k), 7.83 (d, ^3J = 8.5 Hz, 1H, d), 7.65 (dd, ^3J = 8.5 Hz, ^4J = 1.9 Hz, 1H, c) ppm.

^{13}C{^{1}H} NMR (151 MHz, $CDCl_3$): δ = 132.9 (i), 131.6 (f), 131.3 (e), 131.1 (a), 129.8 (c), 129.7 (d), 127.9 (k), 127.4 (g), 127.0 (h), 125.9 (j), 119.1 (b) ppm.

^{1}H NMR (601 MHz, C_6D_6): δ = 8.78 (d, ^4J = 1.8 Hz, 2H, a), 7.50 (s, 2H, k), 7.49 (d, ^3J = 8.5 Hz, 2H, h), 7.44 (d, ^3J = 8.5 Hz, 2H, g), 7.37 (dd, ^3J = 8.5 Hz, ^4J = 1.9 Hz, 2H, c), 7.26 (d, ^3J = 8.5 Hz, 2H, d) ppm.

^{13}C{^{1}H} NMR (151 MHz, C_6D_6): δ = 133.2 (i), 131.9 (f), 131.5 (a), 131.5 (e), 129.9 (c), 129.8 (d), 128.0 (k), 127.6 (g), 126.9 (h), 126.2 (j), 119.4 (b) ppm.

IR (ATR): $\tilde{\nu}$ [cm^{-1}] = 3040 (w), 2953 (w), 2921 (w), 2851 (w), 1589 (m), 1474 (m), 1424 (m), 1294 (m), 1084 (m), 936 (m), 905 (m), 842 (s), 833 (s), 819 (s), 762 (m), 679 (m).

HR-MS (EI, 70 eV, R ~ 10 000): *m/z* (%) calc. for $C_{22}H_{12}{}^{79}Br_2$ 433.93003 $[M]^+$, found 433.93059 $[M]^+$ (15), 276.0 (100).
M.p.: 259 °C (Lit.[14]: 227 °C).
R_f (silica, eluents: 5% DCM in *n*-hexane) = 0.36.

2.3.5. 2,13-Dimesitylpentahelicene (CC[5])

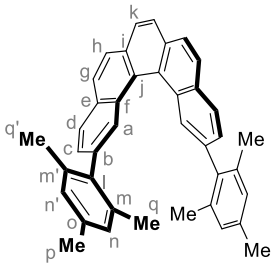

In a glove box, 2,13-dibromopentahelicene (**12**, 43.6 mg, 200 µmol, 1.00 equiv.) and $[Pd(dppf)Cl_2]$ (4.1 mg, 5.0 µmol, 5 mol%) were suspended in dry 1,4-dioxane (12 mL) in a 10 – 20 mL microwave vial. Outside the glove box, a solution of mesitylmagnesium bromide (1 M in diethyl ether, 0.30 mL, 300 µmol, 3.00 equiv.) was added while stirring. The mixture was heated at 95 °C for 3 d in an oil bath. After cooling, water (50 mL) and DCM (200 mL) were added, the phases were separated and the aqueous layer was extracted with DCM (3 x 50 mL). The combined organic phases were dried over sodium sulfate, filtered and the solvents were removed in vacuo. The crude product was filtered over silica (eluent: DCM) to yield a slightly yellow solid (51.0 mg, 99%).

^{1}H NMR (601 MHz, DCM-d_2): δ = 8.50 (d, ^4J = 1.5 Hz, 2H, a), 7.94 (d, ^3J = 8.5 Hz, 2H, g), 7.92 (d, ^3J = 8.1 Hz, 2H, d), 7.90 (s, 2H, k), 7.89 (d, ^3J = 8.5 Hz, 2H, h), 7.21 (dd, ^3J = 8.1 Hz, ^4J = 1.5 Hz, 2H, c), 6.95 (s, 2H, n), 6.74 (s, 2H, n'), 2.29 (s, 6H, p), 1.73 (s, 6H, q), 1.56 (s, 6H, q') ppm.
^{13}C{^{1}H} NMR (151 MHz, DCM-d_2): δ = 138.7 (l), 137.8 (b), 137.0 (m), 136.7 (o), 135.4 (m'), 133.2 (i), 131.8 (e), 131.5 (f), 129.1 (c), 129.0 (n), 128.6 (a), 128.4 (d), 128.3 (n'), 128.0 (g), 127.9 (k), 127.6 (j), 126.7 (h), 22.1 (q), 21.1 (p), 20.6 (q') ppm.
IR (ATR): $\tilde{\nu}$ [cm^{-1}] = 3045 (w), 3008 (w), 2950 (w), 2916 (w), 2854 (w), 1612 (m), 1474 (m), 1437 (m), 1376 (w), 1250 (w), 1031 (w), 907 (m), 847 (s), 819 (w), 737 (w), 683 (w).
HR-MS (EI, 70 eV, R ~ 10 000): *m/z* (%) calc. for $C_{40}H_{34}$ 514.26550 $[M]^+$, found 514.26535 $[M]^+$ (100).
M.p.: 282 °C.
R_f (silica, eluents: 10% DCM in *n*-hexane) = 0.24.
UV/Vis (DCM): λ_{max} (ε) = 275 nm (34 207 mol^{-1} dm^3 cm^{-1}).
Fluorescence (DCM): λ_{ex} = 300 nm, λ_{em} = **409**, 425 nm.

2.4. Synthetic Route towards CC[6]

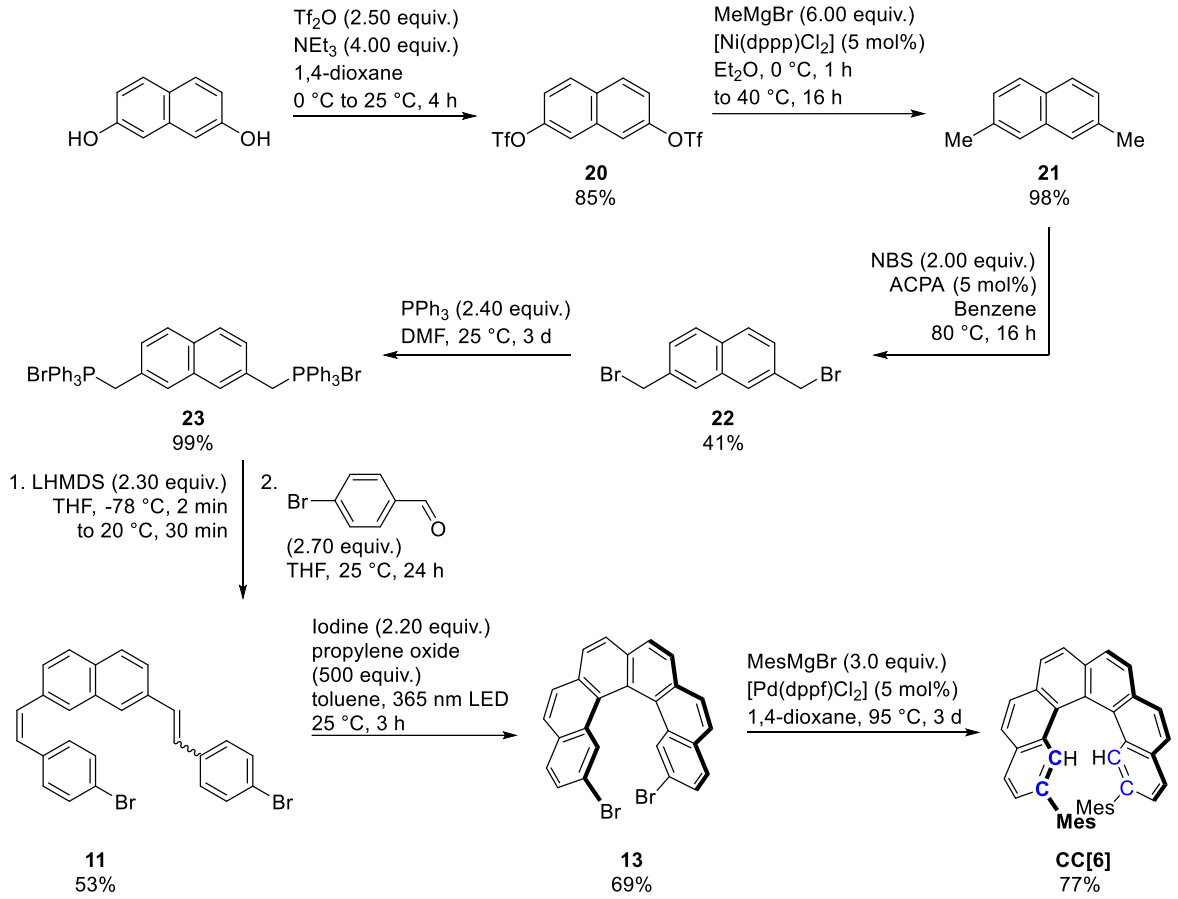

Scheme S4. Overview of the syntheses towards **CC[6]**.

2.4.1. 2,7-bis(trifluoromethylsulfonyl)naphthalene (20)

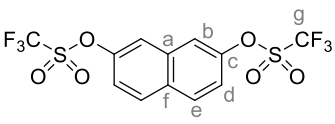

2,7-Dihydroxynaphthalene (3.20 g, 20.0 mmol, 1.00 equiv.) and triethylamine (11.0 mL, 80.0 mmol, 4.00 equiv.) were dissolved in 1,4-dioxane (100 mL). The solution was cooled to 0 °C. *Via* an addition funnel, trifluoromethanesulfonic acid anhydride (8.41 mL, 50.0 mmol, 2.50 equiv.) was added over the course of 20 min. The dark solution was allowed to warm to 25 °C and stirred for 4 h at this temperature. Subsequently, it was poured into 1 M aqueous HCl (50 mL). The resulting phases were separated and the aqueous phase was extracted with DCM (3 x 20 mL). The combined organic layers were washed with brine (30 mL), dried over sodium sulfate and filtered. The solvents were removed in vacuo and the crude product was purified by column chromatography (silica, eluents: 5% ethyl acetate in cyclohexane) to yield a colorless solid (7.13 g, 85%, Lit.[15]: 75%).

^{1}H NMR (600 MHz, $CDCl_3$): δ = 8.01 (d, ^3J = 9.0 Hz, 2H, e), 7.81 (d, ^4J = 2.4 Hz, 2H, b), 7.48 (dd, ^3J = 9.0 Hz, ^4J = 2.4 Hz, 2H, d) ppm.

^{13}C{^{1}H} NMR (151 MHz, $CDCl_3$): δ = 148.4 (c), 133.8 (a), 131.4 (f), 131.0 (e), 121.3 (d), 119.6 (b), 118.9 (q, ^1J = 320.8 Hz, g) ppm.

^{19}F NMR (565 MHz, $CDCl_3$): δ = –72.7 ppm.

IR (ATR): $\tilde{\nu}$ [cm^{-1}] = 3096 (w), 1633 (w), 1511 (w), 1412 (s), 1204 (s), 1186 (s), 1133 (s), 1109 (s), 957 (s), 894 (s), 882 (s), 849 (s), 840 (s), 774 (m), 768 (m), 751 (m), 726 (s), 690 (m).

HR-MS (EI, 70 eV, R ~ 10 000): *m/z* (%) calc. for $C_{12}H_6F_6O_6S_2$ 423.95045 $[M]^+$, found 423.95105 $[M]^+$ (46), 129.9 (100).

M.p.: 61 °C (Lit.[15]: 63 – 64 °C).

R_f (silica, eluents: 5% ethyl acetate in cyclohexane): 0.27.

2.4.2. 2,7-Dimethylnaphthalene (21)

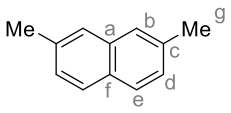

In a glove box, 2,7-bis(trifluoromethylsulfonyl)naphthalene (**20**, 5.94 g, 14.0 mmol, 1.00 equiv.) and [Ni(dppp)Cl_2] (379 mg, 0.70 mmol, 5 mol%) were dissolved in dry diethyl ether (120 mL). Outside the box on a Schlenk line, the red solution was cooled to 0 °C and treated with a solution of methylmagnesium bromide (3 M in diethyl ether, 28.0 mL, 84.0 mmol, 6.00 equiv.) dropwise over the course of 60 min. The solution was heated at 40 °C for 16 h. Afterwards, it was cooled to 0 °C and water (25 mL) was added dropwise. After the addition of an aqueous solution of HCl (1 M, 50 mL), the phases were separated and the aqueous phase was extracted with diethyl ether (3 x 50 mL). The combined organic layers were washed with a sat. aq. sol. of sodium hydrogen carbonate (50 mL), dried over sodium sulfate and filtered. Evaporation of the solvent in vacuo gave a slightly yellow solid (2.15 g, 98%, Lit.[15]: 99%).

^{1}H NMR (600 MHz, $CDCl_3$): δ = 7.70 (d, ^3J = 8.3 Hz, 2H, e), 7.53 (s, 2H, b), 7.25 (d, ^3J = 8.3 Hz, 2H, d), 2.50 (s, 6H, g) ppm.

^{13}C{^{1}H} NMR (151 MHz, $CDCl_3$): δ = 135.6 (c), 134.0 (a), 130.1 (f), 127.5 (e), 127.4 (d), 126.4 (b), 21.9 (g) ppm.

IR (ATR): $\tilde{\nu}$ [cm^{-1}] = 3047 (w), 3011 (w), 2909 (m), 2851 (w), 2721 (w), 1636 (w), 1615 (w), 1436 (m), 1375 (s), 1274 (m), 1178 (m), 1037 (m), 965 (m), 911 (s), 832 (s), 769 (m), 720 (m), 694 (m).

HR-MS (EI, 70 eV, R ~ 10 000): *m/z* (%) calc. for $C_{12}H_{12}$ 156.09335 $[M]^+$, found 156.09326 $[M]^+$ (100).

M.p.: 96 °C (Lit.[15]: 96 – 97 °C).

2.4.3. 2,7-bis(Bromomethyl)naphthalene (22)

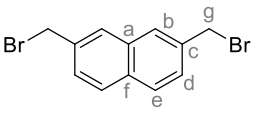

2,7-Dimethylnaphthalene (**21**, 1.80 g, 11.5 mmol, 1.00 equiv.), NBS (4.09 g, 23.0 mmol, 2.00 equiv.) and 4,4′-azobis(4-cyanopentanoic acid) (161 mg, 575 µmol, 5 mol%) were dissolved in benzene (10 mL) in a 10 – 20 mL microwave vial. The vial was capped and flushed with nitrogen for 5 min, before the mixture was heated at 80 °C for 16 h in an oil bath. After cooling, it was filtered over Celite (eluent: DCM) to remove precipitated succinimide. The solvents were removed in vacuo and the crude product was purified by column chromatography (silica, eluent: cyclohexane). Mixed fractions were recrystallized from methanol (24 mL). Combining clean fractions and removing the solvents in vacuo furnished a colorless solid (1.47 g, 41%).

^{1}H NMR (600 MHz, $CDCl_3$): δ = 7.82 (d, ^3J = 8.5 Hz, 2H, e), 7.82 – 7.79 (m, 2H, b), 7.52 (dd, ^3J = 8.5 Hz, ^4J = 1.8 Hz, 2H, d), 4.65 (s, 4H, g) ppm.

^{13}C{^{1}H} NMR (151 MHz, $CDCl_3$): δ = 136.0 (c), 133.1 (a), 132.8 (f), 128.7 (e), 128.0 (b), 127.7 (d), 33.9 (g) ppm.

IR (ATR): $\tilde{\nu}$ [cm^{-1}] = 3022 (w), 2969 (w), 2853 (w), 1925 (w), 1814 (w), 1439 (m), 1345 (m), 1212 (s), 1183 (m), 1134 (m), 908 (s), 851 (s), 784 (m), 770 (m), 697 (m), 667 (m).

HR-MS (EI, 70 eV, R ~ 10 000): *m/z* (%) calc. for $C_{12}H_{10}{}^{79}Br_2$ 311.91438 $[M]^+$, found 311.91433 $[M]^+$ (7), 154.0 (100).

M.p.: 150 °C (Lit.[16]: 146 – 147 °C).

R_f (silica, eluent: cyclohexane): 0.24.

2.4.4. Naphthalene-2,7-bis(methylenetriphenylphosphonium) dibromide (23)

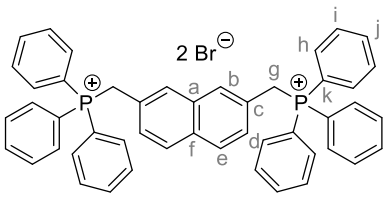

2,7-bis(Bromomethyl)naphthalene (**22**, 1.10 g, 3.50 mmol, 1.00 equiv.) and triphenyl phosphine (2.20 g, 8.40 mmol, 2.40 equiv.) were dissolved in DMF (11.0 mL) and stirred at 25 °C for 3 d. Toluene (33 mL) was added and the solution was stirred for 30 min. The colorless precipitation was filtered, washed with toluene (20 mL) and dried in a high vacuum (120 °C, 0.02 mbar). After 18 h, more precipitate was present in the mother liquor. It was filtered, washed with toluene (10 mL) and dried under the same conditions. A colorless solid (2.92 g, 99%, Lit.[17]: 99%) was obtained.

^{1}H NMR (601 MHz, DMSO-d_6): δ = 7.94 – 7.89 (m, 6H, j), 7.76 – 7.65 (m, 26H, e+h+i), 7.27 – 7.18 (m, 2H, b), 7.08 (ddd, ^3J = 8.6 Hz, ^4J = 1.6, 1.6 Hz, 2H, d), 5.36 (d, $^2J_{H\text{-}P}$ = 16.1 Hz, 4H, g) ppm.

$^{13}C\{^1H\}$ NMR (151 MHz, DMSO-d_6): δ = 135.2 (j), 134.0 (d, $^3J_{C\text{-}P}$ = 10.4 Hz, h), 132.0 (a), 131.4 (f), 130.1 (d, $^2J_{C\text{-}P}$ = 12.5 Hz, i), 129.8 (d, $^3J_{C\text{-}P}$ = 8.2 Hz, b), 128.8 (d), 128.3 (e), 126.6 (d, $^2J_{C\text{-}P}$ = 9.3 Hz, c), 117.7 (d, $^1J_{C\text{-}P}$ = 85.6 Hz, k), 28.1 (d, $^1J_{C\text{-}P}$ = 46.9 Hz, g) ppm.

$^{31}P\{^1H\}$ NMR (243 MHz, DMSO-d_6): δ = 23.1 ppm.

IR (ATR): $\tilde{\nu}$ [cm^{-1}] = 3040 (w), 3007 (w), 2987 (w), 2846 (w), 2777 (w), 1660 (w), 1586 (w), 1435 (m), 1110 (s), 995 (m), 841 (m), 744 (s), 717 (s), 688 (s).

HR-MS (ESI positive): *m/z* calc. for $C_{48}H_{40}P_2^{2+}$ 339.12971 $[M\text{-}2Br]^{2+}$; found 339.12947 $[M\text{-}2Br]^{2+}$.

M.p.: (348 °C, Lit.[18]: 364 – 367 °C).

2.4.5. (*Z,Z*)/(*E,Z*)-2,7-bis(2-(4-Bromophenyl)ethenyl)naphthalene (11)

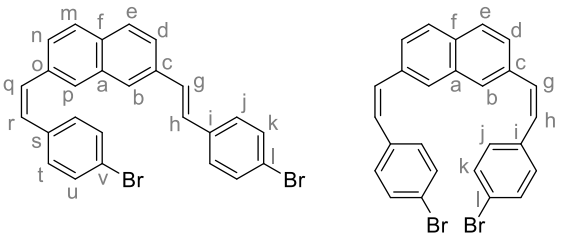

Naphthalene-2,7-bis(methylenetriphenylphosphonium) dibromide (**23**, 500 mg, 0.60 mmol, 1.00 equiv.) was suspended in dry THF (10 mL). An LHMDS solution (1.0 M in THF, 1.37 mL, 2.30 equiv.) was added at –78 °C over the course of 2 min. The mixture was allowed to warm to 25 °C over 30 min, turning red. A solution of 4-bromobenzaldehyde (298 mg, 1.61 mmol, 2.70 equiv.) in dry THF (1.0 mL) was added and the color changed to yellow/brown. The mixture was stirred for 24 h at 25 °C. The solvents were removed in vacuo and the crude solid was filtered over silica (eluent: DCM) to remove triphenylphosphine oxide. The solvents were removed in vacuo and remaining aldehyde was removed by Kugelrohr distillation (66 °C, 0.12 mbar). The isomeric ratio (*E,Z*/*Z,Z*) of crude product was 0.61/0.39. The crude product was purified by column chromatography (silica, eluents: 5% ethyl acetate in cyclohexane) to yield an off-white solid (155 mg, 53%, Lit.[17]: 65%). If desired, the (*Z,Z*)-isomer (off-white solid) can be collected isomerically pure as the first fraction.

(*Z,Z*)-Isomer:

^{1}H NMR (601 MHz, $CDCl_3$): δ = 7.60 (m, 4H, b+e), 7.34 (d, ^3J = 8.5 Hz, 4H, k), 7.28 (dd, ^3J = 8.4 Hz, ^4J = 1.7 Hz, 2H, d), 7.14 (d, ^3J = 8.5 Hz, 4H, j), 6.76 (d, ^3J = 12.2 Hz, 2H, g), 6.59 (d, ^3J = 12.2 Hz, 2H, h) ppm.

$^{13}C\{^1H\}$ NMR (151 MHz, $CDCl_3$): δ = 136.2 (i), 134.9 (c), 133.6 (a), 131.9 (f), 131.5 (k), 130.9 (g), 130.7 (j), 129.5 (h), 128.2 (b), 127.6 (e), 127.1 (d), 121.3 (l) ppm.

IR (ATR): $\tilde{\nu}$ [cm^{-1}] = 3044 (w), 3010 (w), 2963 (w), 1904 (w), 1704 (w), 1623 (w), 1483 (s), 1069 (m), 1009 (s), 959 (m), 909 (s), 822 (s), 811 (s), 745 (s).

HR-MS (EI, 70 eV, R ~ 10 000): *m/z* (%) calc. for $C_{26}H_{18}{}^{79}Br_2$ 487.97698 $[M]^+$, found 487.97751 $[M]^+$ (46), 489.9 (100).

M.p.: 134 °C.

R_f (silica, eluents: 5% ethyl acetate in cyclohexane): 0.55.

(*E,Z*)-Isomer:

^{1}H NMR (601 MHz, $CDCl_3$): δ = 7.76 (d, ^3J = 8.5 Hz, 1H), 7.73 (d, ^4J = 1.5 Hz, 1H), 7.71 – 7.68 (m, 2H), 7.65 (d, ^3J = 8.4 Hz, 1H), 7.50 (d, ^3J = 8.4 Hz, 2H), 7.42 (d, ^3J = 8.4 Hz, 2H), 7.34 (d, ^3J = 8.4 Hz, 2H), 7.29 (dd, ^3J = 8.5 Hz, ^4J = 1.6 Hz, 1H), 7.23 (d, ^3J = 16.3 Hz, 1H), 7.16 – 7.12 (m, 3H), 6.78 (d, ^3J = 12.2 Hz, 1H), 6.60 (d, ^3J = 12.2 Hz, 1H) ppm.

R_f (silica, eluents: 5% ethyl acetate in cyclohexane): 0.64.

* Because the *(E,Z)*-isomer was not isolated, only the ^{1}H NMR shifts from the isomeric mixture could be analyzed.

2.4.6. 2,15-Dibromohexahelicene (13)

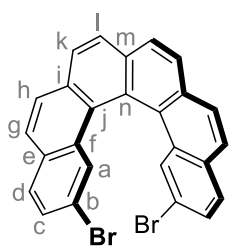

2,7-bis(2-(4-Bromophenyl)ethenyl)naphthalene (**11**, 98.0 mg, 200 µmol, 1.00 equiv., isomeric mixture) was dissolved in toluene (120 mL). Iodine (112 mg, 440 µmol, 2.20 equiv.) and propylene oxide (7.00 mL, 100 mmol, 500 equiv.) were added and the mixture was degassed by bubbling Ar through it for 5 min. At 25 °C and under vigorous stirring, the mixture was irradiated for 3 h (see Section 1 for the photochemical setup). After removing the solvents in vacuo, the crude product was washed with *n*-pentane and acetonitrile (3 x 5 mL, respectively) to furnish a colorless solid (66.8 mg, 69%).

^{1}H NMR (601 MHz, $CDCl_3$): δ = 8.04 (d, ^{3}J = 8.2 Hz, 2H, l), 8.00 (d, ^{3}J = 8.2 Hz, 2H, k), 7.96 (d, ^{3}J = 8.5 Hz, 2H, h), 7.92 (d, ^{3}J = 8.5 Hz, 2H, g), 7.74 (d, ^{3}J = 8.5 Hz, 2H, d), 7.71 (d, ^{4}J = 1.9 Hz, 2H, a), 7.39 (dd, ^{3}J = 8.5 Hz, ^{4}J = 1.9 Hz, 2H, c) ppm.

^{13}C{^{1}H} NMR (151 MHz, $CDCl_3$): δ = 133.3 (m), 132.0 (i), 130.9 (g), 130.8 (f), 130.1 (a), 129.4 (d), 129.1 (c), 127.8 (l), 127.7 (g), 127.5 (k), 126.9 (h), 126.5 (j), 123.9 (n), 119.4 (b) ppm.

IR (ATR): $\tilde{\nu}$ [cm^{-1}] = 3041 (w), 2953 (w), 2922 (w), 2852 (w), 1589 (m), 1494 (m), 1468 (m), 1422 (m), 1276 (m), 1119 (m), 1077 (m), 994 (m), 914 (m), 901 (m), 844 (s), 840 (s), 826 (s), 812 (s), 768 (s), 700 (m), 663 (m).

HR-MS (EI, 70 eV, R ~ 10 000): *m/z* (%) calc. for $C_{26}H_{14}{}^{79}Br_2$ 483.94568 $[M]^+$, found 483.94571 $[M]^+$ (45), 486.0 (100).

M.p.: 346 °C (Lit.[19]: 293 °C under decomposition).

R_f (silica, eluent: cyclohexane) = 0.26.

2.4.7. 2,15-Dimesitylhexahelicene (CC[6])

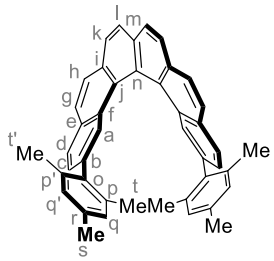

In a glove box, 2,15-dibromohexahelicene (**13**, 48.6 mg, 100 µmol, 1.00 equiv.) and $[Pd(dppf)Cl_2]$ (4.1 mg, 5.0 µmol, 5 mol%) were suspended in 1,4-dioxane (12 mL) in a 10 – 20 mL microwave vial. Outside the box on a Schlenk line, a solution of mesitylmagnesium bromide (1 M in diethyl ether, 0.30 mL, 300 µmol, 3.00 equiv.) was added while stirring. The mixture was heated at 95 °C for 3 d in an oil bath. After cooling, water (50 mL) and DCM (200 mL) were added, the phases were separated and the aqueous layer was extracted with DCM (3 x 50 mL). The combined organic phases were dried over sodium sulfate, filtered and the solvents were removed in vacuo. The crude product was filtered over silica (eluent: DCM) and washed with *n*-pentane and acetonitrile (50 mL, respectively) via a frit to yield a slightly yellow solid (43.4 mg, 77%).

^{1}H NMR (601 MHz, $CDCl_3$): δ = 7.91 (d, ^{3}J = 8.2 Hz, 2H, l), 7.89 (d, ^{3}J = 8.2 Hz, 2H, k), 7.85 – 7.80 (m, 6H, d+g+h), 7.56 (d, ^{4}J = 1.5 Hz, 2H, a), 6.99 (dd, ^{3}J = 8.1 Hz, ^{4}J = 1.5 Hz, 2H, c), 6.76 (s, 2H, q), 6.65 (s, 2H, q‘), 2.22 (s, 6H, s), 1.43 (s, 6H, t), 1.33 (s, 6H, t‘) ppm.

^{13}C{^{1}H} NMR (151 MHz, $CDCl_3$): δ = 139.0 (o), 138.9 (b), 136.2 (r), 136.2 (p), 136.0 (p’), 132.9 (m), 131.3 (e), 131.2 (f), 130.7 (i), 128.7 (j), 128.3 (d/g)*, 127.9 (c), 127.9 (d/g)*, 127.7 (q’), 127.7 (a), 127.6 (q), 127.3 (k), 126.5 (l), 126.0 (h), 124.0 (n), 21.2 (t), 21.1 (s), 20.5 (t‘) ppm.

^{1}H NMR (600 MHz, C_6D_6): δ = 8.01 (s, 2H, a), 7.67 (d, ^{3}J = 8.1 Hz, 2H), 7.60 (d, ^{3}J = 8.1 Hz, 2H), 7.57 – 7.53 (m, 4H), 7.44 (d, ^{3}J = 8.6 Hz, 2H), 6.98 (d, ^{3}J = 8.1 Hz, 2H), 6.84 (s, 2H, q), 6.50 (s, 2H, q’), 2.08 (s, 6H, s), 1.76 (s, 6H, t), 1.21 (s, 6H, t’) ppm.

IR (ATR): $\tilde{\nu}$ [cm^{-1}] = 3015 (w), 2969 (w), 2851 (w), 1609 (w), 1469 (m), 1435 (m), 1375 (m), 1245 (w), 1118 (w), 1034 (w), 848 (s), 841 (s), 818 (m), 769 (m), 735 (m), 703 (m), 669 (m).

HR-MS (EI, 70 eV, R ~ 10 000): *m/z* (%) calc. for $C_{44}H_{36}$ 564.28115 $[M]^+$, found 564.28077 $[M]^+$ (100).

M.p.: > 400 °C.

R_f (silica, eluents: 2% diethyl ether in cyclohexane) = 0.41. Note: Due to the poor solubility of this compound in most organic solvents, column chromatography is not suitable for purification of amounts larger than analytical scale.

UV/Vis (DCM): λ_{max} (ε) = 266 nm (44 672 mol^{-1} dm^3 cm^{-1}).

Fluorescence (DCM): λ_{ex} = 300 nm, λ_{em} = **423**, 444 nm.

2.5. Optimization of the Ring Closure towards BN[5]

In a glove box, the deprotected alkyne (**6**, 1.00 equiv.) was mixed with the respective catalyst and co-catalyst (30 mol%, respectively) and dry mesitylene (1 mL) in a 2 – 5 mL microwave vial and heated at the below indicated temperature / time protocol in an oil bath. After cooling, most of the solvent was removed in vacuo. A solution of trimethoxybenzene (1.00 equiv.) in $CDCl_3$ was added and the conversions were determined by integrating and referencing the N*H*-signals of the formed species in the ^{1}H NMR spectra. The broad singlet at δ = 8.32 ppm represents **BN[5]** (*endo/endo*), while the signals at δ = 8.77 and 8.67 ppm represent the *endo/exo* derivative **8**. The *exo/exo* derivative was not found. The singlet at δ = 6.80 ppm is due to remaining mesitylene.

Table S1. Optimization scheme and ^{1}H NMR spectra of the crude mixtures from the electrophilic ring closure towards **BN[5]**.

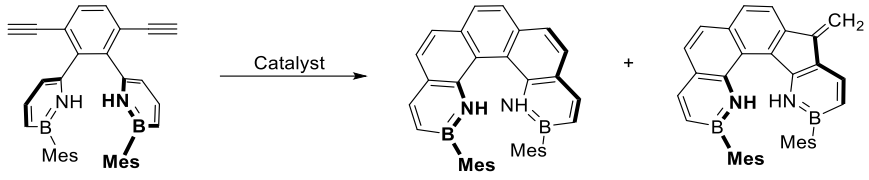

Entry	Catalyst System	Time, temperature	*endo/endo*	*endo/exo*
a)	$AuBrPPh_3$ / $AgSbF_6$	17 h, 100 °C	41%	<5%
b)	$AuCl_3$	17 h, 100 °C	66%	<5%
c)	$PtCl_2$	17 h, 100 °C	33%	28%
d)	[(*p*-Cymene)RuCl]$_2$ / $AgSbF_6$	17 h, 100 °C	44%	18%

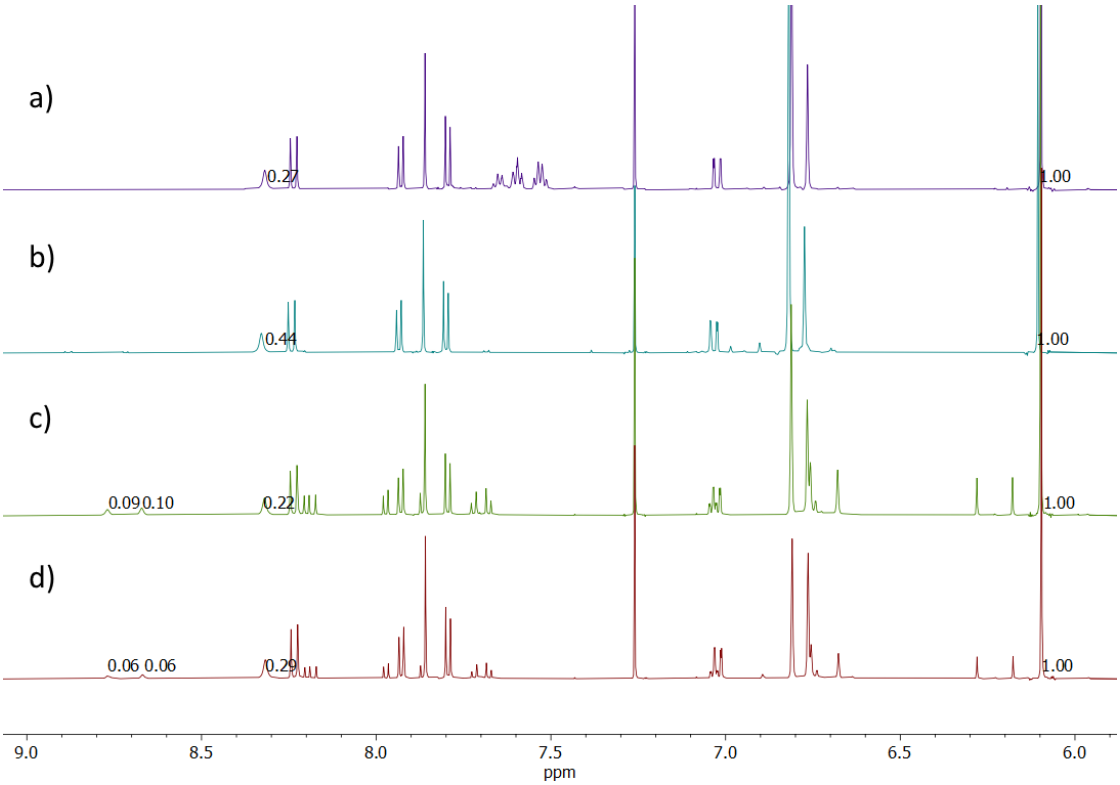

2.6. Optimization of the Ring Closure towards BN[6]

In a glove box, deprotected alkyne (**7**, 1.00 equiv.) was mixed with the respective catalyst and co-catalyst (30 mol%, respectively) and dry mesitylene (1 mL) in a 2 – 5 mL microwave vial and heated at the below indicated temperature / time protocol in an oil bath. After cooling, most of the solvent was removed in vacuo. A solution of trimethoxybenzene (1.00 equiv.) in $CDCl_3$ was added and the conversions were determined by integrating and referencing the N*H*-signals of

the formed species in the ^{1}H NMR spectra. The broad singlet at δ = 8.71 ppm represents **BN[6]** (*endo/endo*), while the signal at δ = 8.95 ppm represents the *endo/exo* derivative **9**. The *exo/exo* derivative was not found. The singlet at δ = 6.80 ppm is due to remaining mesitylene. The broadened baselines and the throughout reduced conversions into ring-closed products indicate that decomposition occurs rapidly with all catalysts and temperature / time protocols.

Table S2. Optimization scheme and ^{1}H NMR spectra of the crude mixtures from the electrophilic ring closure towards **BN[6]**.

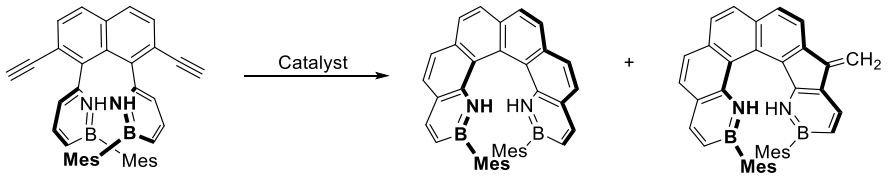

7 **BN[6]** **9**

Entry	Catalyst System	Time, temperature	*reactant*	*endo/endo*	*endo/exo*
a)	$AuBrPPh_3$ / $AgSbF_6$	17 h, 140 °C	-	<2%	32%
b)	$AuCl_3$	17 h, 140 °C	-	8%	30%
c)	$PtCl_2$	17 h, 140 °C	-	5%	10%
d)	$[(p\text{-Cymene})RuCl]_2$ / $AgSbF_6$	17 h, 140 °C	-	12%	<2%
e)	$[(p\text{-Cymene})RuCl]_2$ / $AgSbF_6$	17 h, 100 °C	17%	<2%	<2%
f)	$[(p\text{-Cymene})RuCl]_2$ / $AgSbF_6$	17 h, 170 °C	-	10%	<2%
g)	$[(p\text{-Cymene})RuCl]_2$ / $AgSbF_6$	1 h, 170 °C	-	15%	<2%

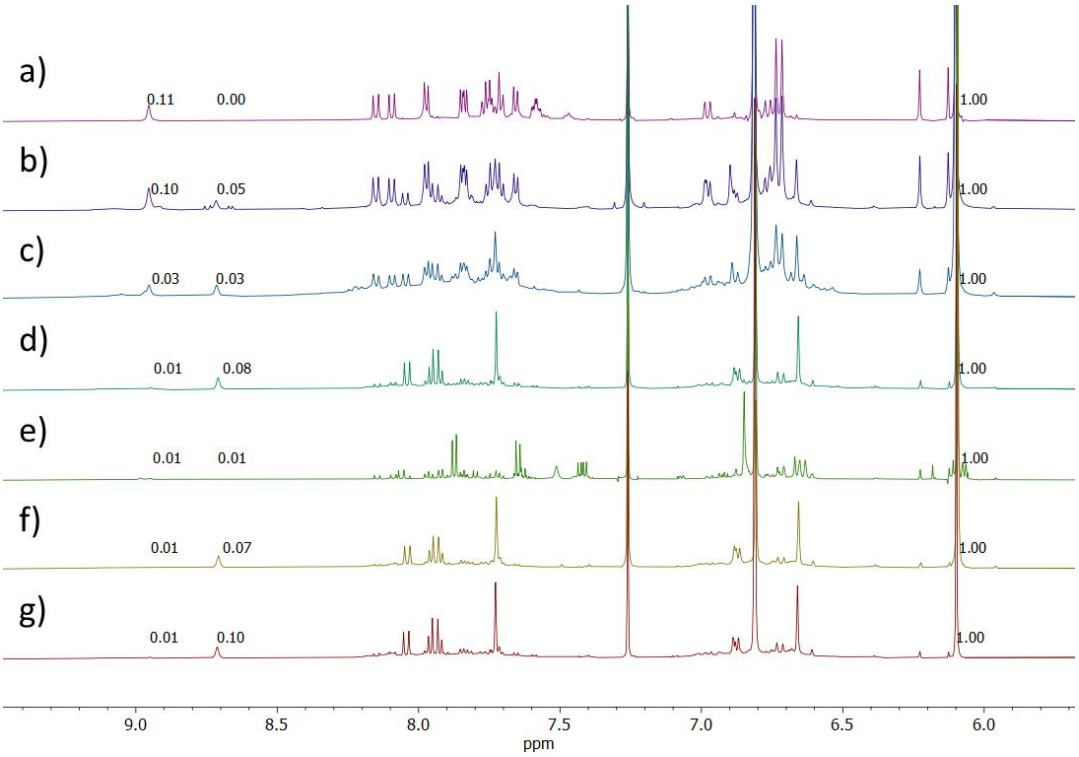

2.7. Isolation of *endolexo* Hexahelicene (9)

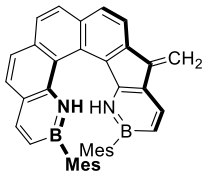

In a glove box, deprotected alkyne **7** (11.3 mg, 20.0 µmol, 1.00 equiv.) was mixed with $AuBrPPh_3$ (3.2 mg, 6.0 µmol, 30 mol%), $AgSbF_6$ (2.1 mg, 6.0 µmol, 30 mol%) and dry mesitylene (1 mL) in a 2 – 5 mL microwave vial. The mixture was heated to 140 °C for 17 h in an oil bath. After cooling, the solvent was removed in vacuo. Subsequently, it was filtered over silica (eluent: cyclohexane) to obtain a bright, yellow solid (3.9 mg, 34%).

^{1}H NMR (600 MHz, $CDCl_3$): δ = 8.94 (br s, 1H), 8.14 (d, ^3J = 11.4 Hz, 1H), 8.09 (d, ^3J = 11.2 Hz, 1H), 7.99 – 7.94 (m, 2H), 7.85 – 7.81 (m, 2H), 7.75 (d, ^3J = 8.5 Hz, 1H), 7.70 (d, ^3J = 8.5 Hz, 1H), 7.65 (d, ^3J = 8.2 Hz, 1H), 6.97 (dd, ^3J = 11.4 Hz, ^4J = 1.8 Hz, 1H), 6.75 (dd, ^3J = 11.2 Hz, ^4J = 1.7 Hz, 1H), 6.73 (s, 2H), 6.71 (s, 2H), 6.22 (s, 1H), 6.12 (s, 1H), 2.22 (s, 3H), 2.22 (s, 3H), 1.88 (s, 6H), 1.82 (s, 6H) ppm.

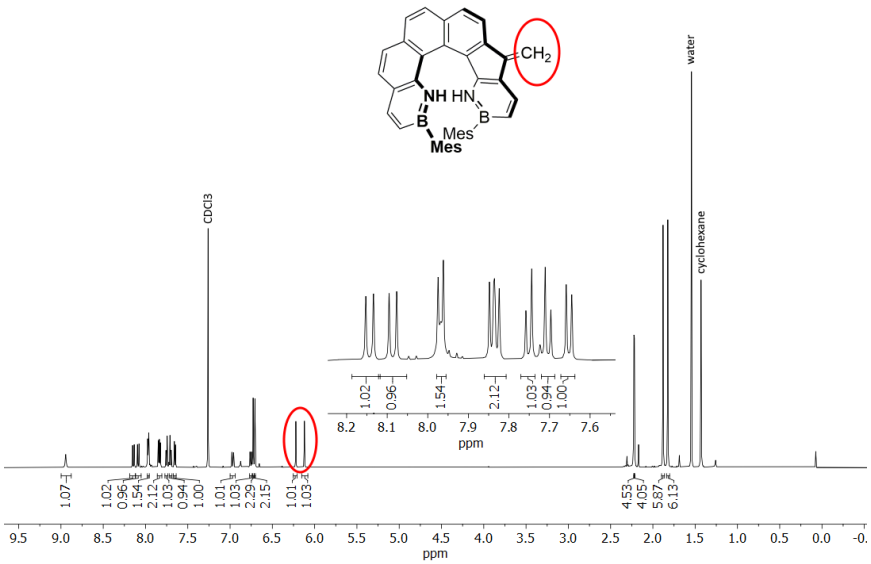

Fig. S1. ^{1}H NMR spectrum of the endo/exo derivative **9**, revealing two separate resonances for the exocyclic CH_2-group.

2.8. Investigation of the Electrophilic Bromination of CC[5]

The reactivity of the carbohelicenes under electrophilic bromination conditions was tested by dissolving **CC[5]** (40 µmol, 1.0 equiv.) in DCM (5 mL) at 0 °C and adding bromine (84 µmol, 2.1 equiv.) dropwise. After stirring for 1 h at this temperature, the volatiles were removed *in vacuo* and the relatively pure 5,6-dibrominated addition product was detected by ^{1}H NMR spectroscopy, with few impurities in the aromatic region. These signals intensified after leaving the crude product in air for 7 d and heating it to 75 °C for 6 h in boiling chloroform. However, the characteristic aliphatic resonances of the Br_2-adduct at δ ~ 5.8 ppm were still present. After additional heating of the crude product to 130 °C for 6 h in boiling toluene, the adduct signals had vanished and the mixture consisted of 5-brominated helicene as the major component, as well as the dehalogenated reactant **CC[5]**. Fig. S2 shows the respective ^{1}H NMR spectra of reactant, dibrominated adduct and mixture of reactant and 5-brominated product after heating.

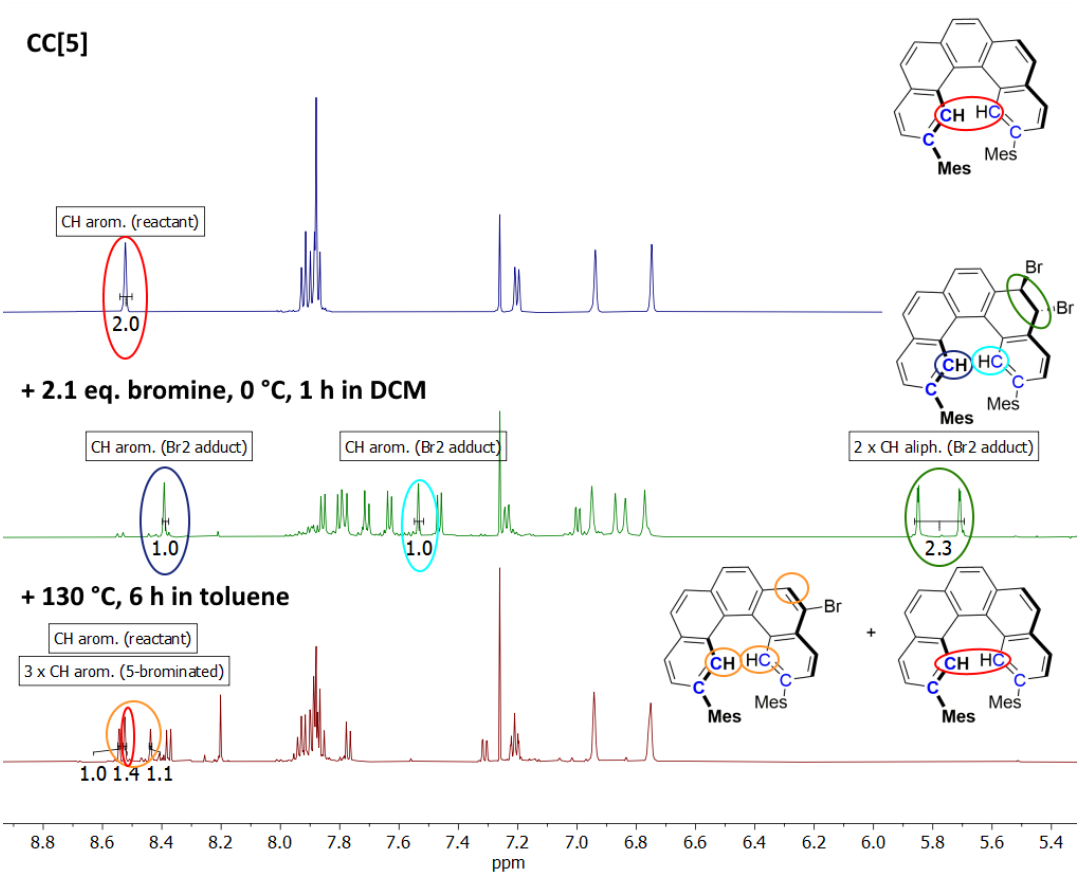

Fig. S2. Comparison of the ^{1}H NMR spectra before and after the electrophilic bromination of **CC[5]**.

3. Crystallography

3.1. 1,14-Dihydro-2,13-dimesityl-1,14-diaza-2,13-diborapentahelicene (BN[5])

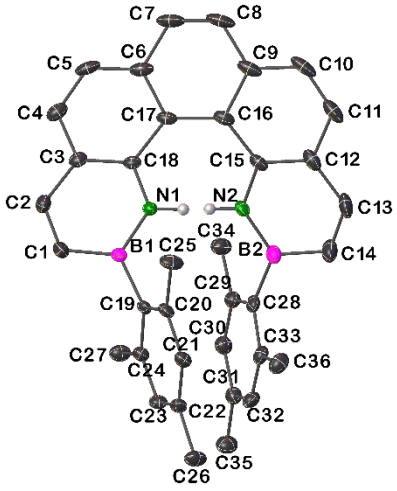

Colorless single crystals of $C_{36}H_{34}B_2N_2$ (**BN[5]**) were grown by dissolving a small amount (ca. 5 mg) of the compound in DCM (ca. 1 mL) in a sample vial. Acetonitrile (ca. 5 mL) was added to a second, larger vial. The small vial was placed in the larger vial, which was capped. DCM was allowed to evaporate slowly at 25 °C, while letting the acetonitrile diffuse into the small vial over the course of 10 d. CCDC Deposition Number: 2192802.

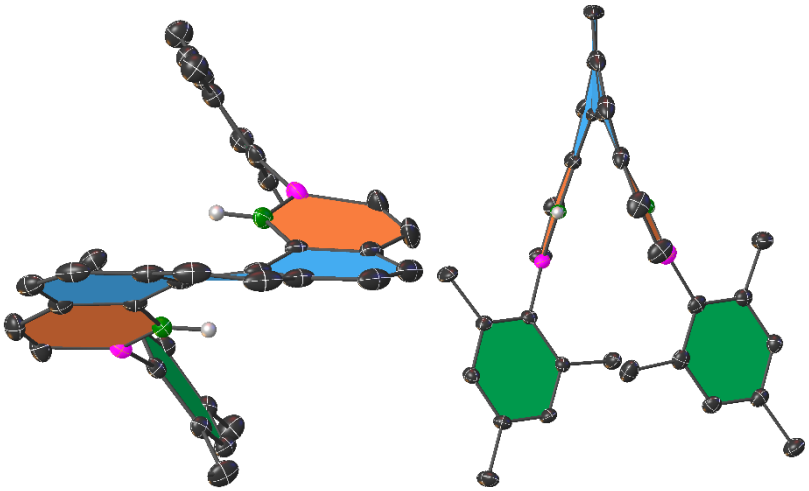

Fig. S3. Top view and view along the central phenyl-unit of **BN[5]**.

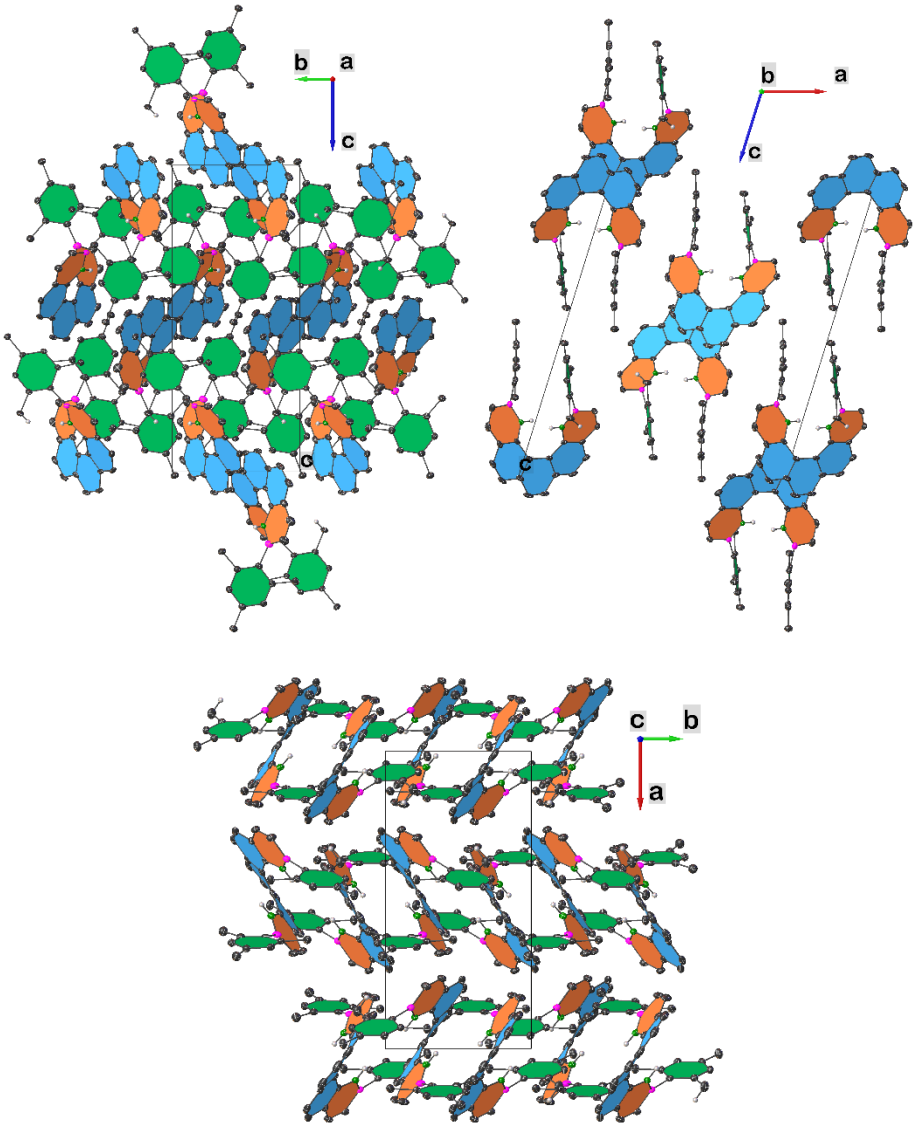

Fig. S4. Unit cell packing view of a **BN[5]** crystal along the a, b and c-axes.

Table S3. Crystal data and structure refinement for **BN[5]**.

Empirical formula	$C_{36}H_{34}B_2N_2$
Formula weight	516.27
Temperature/K	100.0
Crystal system	monoclinic
Space group	$P2_1/n$
a/Å	17.5703(6)
b/Å	8.2181(3)
c/Å	20.6544(8)
α/°	90
β/°	107.2030(10)
γ/°	90
Volume/Å^3	2848.96(18)
Z	4
ρ_{calc}g/cm^3	1.204
μ/mm^{-1}	0.068
F(000)	1096.0
Crystal size/mm^3	0.4 × 0.2 × 0.15
Radiation	MoKα (λ = 0.71073)
2Θ range for data collection/°	4.854 to 56.564
Index ranges	-23 ≤ h ≤ 23, -10 ≤ k ≤ 10, -27 ≤ l ≤ 27
Reflections collected	87140
Independent reflections	7059 [R_{int} = 0.0894, R_{sigma} = 0.0396]
Data/restraints/parameters	7059/0/367
Goodness-of-fit on F^2	1.041
Final R indexes [I>=2σ (I)]	R_1 = 0.0509, wR_2 = 0.1188
Final R indexes [all data]	R_1 = 0.0714, wR_2 = 0.1283
Largest diff. peak/hole / e Å^{-3}	0.33/-0.25

Table S4. Fractional Atomic Coordinates (×10^4) and Equivalent Isotropic Displacement Parameters (Å^2×10^3) for **BN[5]**. U_{eq} is defined as 1/3 of the trace of the orthogonalized U_{IJ} tensor.

Atom	*x*	*y*	*z*	$U_{(eq)}$
N1	3938.9(7)	2968.0(14)	6598.7(5)	15.0(2)
N2	5533.2(7)	2190.9(15)	6768.9(6)	17.6(2)
C18	3683.6(8)	1786.1(17)	6101.5(6)	15.6(3)
C24	4289.0(8)	3950.1(17)	8400.6(7)	17.1(3)
C19	4001.3(8)	4517.2(17)	7725.1(6)	15.5(3)
C22	4557.3(8)	6723.9(18)	8818.4(7)	18.3(3)
C20	4020.7(8)	6200.3(18)	7609.7(7)	17.3(3)
C23	4558.1(8)	5052.8(18)	8929.1(7)	19.0(3)
C3	3011.9(8)	863.6(18)	6110.3(7)	18.8(3)
C17	4060.1(8)	1553.4(17)	5574.9(6)	17.7(3)
C21	4294.0(8)	7275.5(18)	8154.5(7)	18.4(3)
C16	4796.7(9)	2318.7(17)	5546.6(7)	19.3(3)

C15	5453.5(8)	2781.8(18)	6118.5(7)	18.7(3)
C33	6390.8(8)	2817.2(19)	8652.6(7)	20.8(3)
C31	6631.2(8)	482.2(19)	9410.1(7)	21.2(3)
C29	6238.6(8)	94.6(19)	8185.9(7)	20.3(3)
C4	2688.3(9)	-270.6(18)	5583.1(7)	23.4(3)
C28	6235.8(8)	1788.3(19)	8078.9(7)	19.5(3)
C6	3631.0(9)	592.8(18)	5012.0(7)	22.3(3)
C2	2631.2(8)	1106(2)	6631.9(7)	23.1(3)
C27	4321.4(10)	2150.7(18)	8561.2(7)	23.4(3)
C5	2978.6(9)	-371.4(19)	5044.7(7)	25.1(3)
C30	6439.4(9)	-529.5(19)	8845.8(7)	21.3(3)
C32	6584.7(8)	2155.8(19)	9303.1(7)	21.3(3)
C7	3832.0(10)	692(2)	4388.2(7)	29.2(4)
C1	2902.4(9)	2199(2)	7137.8(7)	24.4(3)
C12	6077.8(9)	3749(2)	6033.4(8)	24.5(3)
C9	4917.6(10)	2522.7(19)	4897.8(7)	24.6(3)
C36	6339.9(9)	4650.3(19)	8581.8(8)	27.1(3)
C8	4404.3(11)	1710(2)	4325.4(7)	30.7(4)
C34	6051.6(10)	-1103(2)	7603.5(8)	26.9(3)
C26	4833.5(10)	7882.3(19)	9407.9(7)	25.9(3)
C25	3731.2(10)	6901(2)	6901.5(7)	26.7(3)
C10	5562.4(11)	3459(2)	4825.0(8)	30.3(4)
C35	6893.6(10)	-195(2)	10121.7(7)	27.3(3)
C11	6100.4(10)	4128(2)	5369.7(8)	29.2(4)
C13	6715.7(9)	4264(2)	6610.0(9)	31.9(4)
C14	6780.3(9)	3759(2)	7245.7(8)	32.5(4)
B1	3619.8(9)	3248(2)	7148.6(7)	16.6(3)
B2	6165.0(10)	2573(2)	7365.1(9)	22.4(3)

Table S5. Anisotropic Displacement Parameters ($Å^2×10^3$) for **BN[5]**. The Anisotropic displacement factor exponent takes the form: $-2π^2[h^2a^{*2}U_{11}+2hka^*b^*U_{12}+…]$.

Atom	U_{11}	U_{22}	U_{33}	U_{23}	U_{13}	U_{12}
N1	14.9(5)	17.3(6)	13.0(5)	-0.7(4)	4.1(4)	0.1(4)
N2	16.8(5)	21.5(6)	16.3(5)	4.6(5)	7.5(4)	1.9(5)
C18	18.8(6)	15.6(7)	10.4(6)	1.1(5)	1.3(5)	5.0(5)
C24	19.1(6)	17.7(7)	15.5(6)	0.3(5)	6.9(5)	1.2(5)
C19	14.2(6)	20.4(7)	13.6(6)	-1.0(5)	7.0(5)	1.3(5)
C22	21.1(7)	19.2(7)	15.5(6)	-3.6(5)	6.9(5)	-1.2(6)
C20	18.2(6)	22.4(7)	13.3(6)	2.5(5)	7.7(5)	2.1(6)
C23	22.7(7)	21.0(7)	12.2(6)	1.4(5)	3.4(5)	1.0(6)
C3	19.0(6)	18.9(7)	15.1(6)	1.1(5)	-0.2(5)	2.3(6)
C17	24.2(7)	16.8(7)	11.1(6)	1.7(5)	3.5(5)	9.2(6)
C21	22.9(7)	16.5(7)	17.9(7)	0.4(5)	9.3(5)	0.8(6)
C16	27.7(7)	17.4(7)	15.0(6)	3.1(5)	9.6(6)	10.3(6)
C15	22.3(7)	20.1(7)	17.4(6)	5.3(5)	11.4(5)	7.9(6)
C33	14.3(6)	22.1(7)	23.3(7)	1.9(6)	1.5(5)	-1.9(6)
C31	18.2(6)	25.5(8)	19.0(7)	2.9(6)	4.3(5)	-0.2(6)
C29	16.5(6)	24.9(8)	19.3(7)	-0.5(6)	4.9(5)	-0.3(6)
C4	23.6(7)	18.5(7)	21.5(7)	-0.4(6)	-3.6(6)	1.5(6)
C28	11.1(6)	27.3(8)	18.7(7)	2.9(6)	2.1(5)	-1.0(6)
C6	30.7(8)	19.0(7)	13.4(6)	-1.3(5)	0.6(6)	11.1(6)
C2	17.0(7)	28.5(8)	23.0(7)	-0.5(6)	4.6(5)	-5.2(6)
C27	32.0(8)	18.6(7)	18.2(7)	1.0(6)	5.2(6)	1.0(6)
C5	31.6(8)	19.0(7)	15.8(7)	-5.9(6)	-6.7(6)	7.6(6)
C30	22.4(7)	20.1(7)	21.8(7)	2.3(6)	7.2(6)	0.0(6)
C32	19.0(7)	23.5(8)	18.4(7)	-2.0(6)	0.7(5)	-3.0(6)
C7	44.0(9)	27.4(8)	12.9(7)	-3.5(6)	3.4(6)	16.1(7)
C1	21.1(7)	35.0(9)	19.6(7)	-3.2(6)	10.0(6)	-4.4(6)
C12	23.3(7)	27.0(8)	28.5(8)	9.3(6)	15.8(6)	8.0(6)
C9	37.9(9)	23.2(8)	16.8(7)	6.3(6)	14.6(6)	15.7(7)
C36	24.6(8)	23.3(8)	28.2(8)	3.4(6)	0.0(6)	-1.3(6)
C8	51.3(10)	30.2(9)	13.2(7)	3.9(6)	13.6(7)	20.9(8)
C34	31.1(8)	29.3(8)	20.4(7)	-1.4(6)	7.6(6)	-1.1(7)
C26	37.9(9)	21.3(8)	18.6(7)	-4.3(6)	8.4(6)	-3.5(7)
C25	41.3(9)	24.9(8)	14.0(7)	4.1(6)	8.4(6)	2.8(7)
C10	44.8(10)	30.0(9)	26.1(8)	12.1(7)	25.9(7)	18.4(7)
C35	31.2(8)	29.4(8)	19.7(7)	4.0(6)	5.1(6)	0.3(7)
C11	33.1(8)	29.6(9)	34.1(9)	13.4(7)	24.2(7)	11.7(7)
C13	19.5(7)	40.0(10)	40.2(9)	10.1(8)	15.0(7)	-3.5(7)
C14	18.4(7)	46.2(11)	31.4(9)	8.1(8)	5.2(6)	-6.0(7)
B1	16.1(7)	20.2(8)	13.0(7)	0.0(6)	3.8(5)	2.5(6)
B2	15.0(7)	29.8(9)	22.3(8)	3.9(7)	5.5(6)	1.3(7)

Table S6. Bond Lengths for **BN[5]**.

Atom	Atom	Length/Å	Atom	Atom	Length/Å
N1	C18	1.3880(17)	C33	C28	1.415(2)
N1	B1	1.4261(18)	C33	C32	1.395(2)
N2	C15	1.3960(17)	C33	C36	1.514(2)
N2	B2	1.428(2)	C31	C30	1.390(2)
C18	C3	1.407(2)	C31	C32	1.392(2)
C18	C17	1.4432(18)	C31	C35	1.511(2)
C24	C19	1.4149(18)	C29	C28	1.409(2)
C24	C23	1.3897(19)	C29	C30	1.400(2)
C24	C27	1.513(2)	C29	C34	1.513(2)
C19	C20	1.406(2)	C4	C5	1.356(2)
C19	B1	1.576(2)	C28	B2	1.580(2)
C22	C23	1.392(2)	C6	C5	1.411(2)
C22	C21	1.3873(19)	C6	C7	1.435(2)
C22	C26	1.5082(19)	C2	C1	1.353(2)
C20	C21	1.3993(19)	C7	C8	1.344(3)
C20	C25	1.5132(19)	C1	B1	1.521(2)
C3	C4	1.418(2)	C12	C11	1.418(2)
C3	C2	1.440(2)	C12	C13	1.437(2)
C17	C16	1.456(2)	C9	C8	1.424(2)
C17	C6	1.423(2)	C9	C10	1.414(2)
C16	C15	1.437(2)	C10	C11	1.354(3)
C16	C9	1.4274(19)	C13	C14	1.349(2)
C15	C12	1.407(2)	C14	B2	1.529(2)

Table S7. Bond Angles for **BN[5]**.

Atom	Atom	Atom	Angle/°	Atom	Atom	Atom	Angle/°
C18	N1	B1	125.79(12)	C30	C31	C35	121.60(14)
C15	N2	B2	125.79(13)	C32	C31	C35	120.37(14)
N1	C18	C3	117.14(12)	C28	C29	C34	121.86(13)
N1	C18	C17	122.04(13)	C30	C29	C28	120.17(13)
C3	C18	C17	120.76(12)	C30	C29	C34	117.95(14)
C19	C24	C27	121.17(12)	C5	C4	C3	120.47(15)
C23	C24	C19	119.94(13)	C33	C28	B2	118.70(14)
C23	C24	C27	118.89(12)	C29	C28	C33	117.91(13)
C24	C19	B1	118.36(12)	C29	C28	B2	123.02(13)
C20	C19	C24	118.15(12)	C17	C6	C7	119.36(15)
C20	C19	B1	123.34(12)	C5	C6	C17	120.92(13)
C23	C22	C26	120.37(13)	C5	C6	C7	119.59(14)
C21	C22	C23	117.94(13)	C1	C2	C3	122.27(13)
C21	C22	C26	121.69(13)	C4	C5	C6	120.85(13)
C19	C20	C25	121.35(13)	C31	C30	C29	121.74(14)
C21	C20	C19	120.32(12)	C31	C32	C33	121.62(14)
C21	C20	C25	118.32(13)	C8	C7	C6	120.78(15)
C24	C23	C22	122.05(13)	C2	C1	B1	119.23(13)
C18	C3	C4	119.43(13)	C15	C12	C11	119.40(15)
C18	C3	C2	120.80(13)	C15	C12	C13	120.58(13)
C4	C3	C2	119.72(13)	C11	C12	C13	119.90(14)
C18	C17	C16	125.74(12)	C8	C9	C16	119.40(15)
C6	C17	C18	116.05(13)	C10	C9	C16	120.68(15)
C6	C17	C16	118.00(12)	C10	C9	C8	119.85(14)
C22	C21	C20	121.56(13)	C7	C8	C9	121.36(14)
C15	C16	C17	126.08(12)	C11	C10	C9	121.15(14)
C9	C16	C17	117.99(13)	C10	C11	C12	120.11(15)
C9	C16	C15	115.74(14)	C14	C13	C12	122.45(15)
N2	C15	C16	121.76(13)	C13	C14	B2	119.53(15)
N2	C15	C12	117.17(13)	N1	B1	C19	121.93(12)
C12	C15	C16	120.87(13)	N1	B1	C1	114.59(13)
C28	C33	C36	121.51(13)	C1	B1	C19	123.46(12)
C32	C33	C28	120.35(14)	N2	B2	C28	122.81(13)
C32	C33	C36	118.13(14)	N2	B2	C14	114.04(13)
C30	C31	C32	118.02(13)	C14	B2	C28	123.12(13)

Table S8. Torsion Angles for **BN[5]**.

A	B	C	D	Angle/°	A	B	C	D	Angle/°
N1	C18	C3	C4	175.07(12)	C33	C28	B2	C14	49.3(2)

A	B	C	D	Angle/°	A	B	C	D	Angle/°
N1	C18	C3	C2	-2.36(19)	C29	C28	B2	N2	54.3(2)
N1	C18	C17	C16	9.2(2)	C29	C28	B2	C14	-123.51(18)
N1	C18	C17	C6	-165.38(12)	C4	C3	C2	C1	-178.39(15)
N2	C15	C12	C11	168.39(13)	C28	C33	C32	C31	-0.1(2)
N2	C15	C12	C13	-7.6(2)	C28	C29	C30	C31	0.7(2)
C18	N1	B1	C19	174.38(12)	C6	C17	C16	C15	-154.58(14)
C18	N1	B1	C1	-4.3(2)	C6	C17	C16	C9	20.08(19)
C18	C3	C4	C5	-5.6(2)	C6	C7	C8	C9	10.4(2)
C18	C3	C2	C1	-1.0(2)	C2	C3	C4	C5	171.88(14)
C18	C17	C16	C15	30.9(2)	C2	C1	B1	N1	0.6(2)
C18	C17	C16	C9	-154.43(13)	C2	C1	B1	C19	-178.00(14)
C18	C17	C6	C5	-14.2(2)	C27	C24	C19	C20	-177.22(13)
C18	C17	C6	C7	161.58(13)	C27	C24	C19	B1	7.10(19)
C24	C19	C20	C21	-2.1(2)	C27	C24	C23	C22	179.01(13)
C24	C19	C20	C25	179.42(13)	C5	C6	C7	C8	174.09(14)
C24	C19	B1	N1	-119.79(15)	C30	C31	C32	C33	-3.1(2)
C24	C19	B1	C1	58.73(19)	C30	C29	C28	C33	-3.9(2)
C19	C24	C23	C22	-0.1(2)	C30	C29	C28	B2	168.97(13)
C19	C20	C21	C22	0.5(2)	C32	C33	C28	C29	3.6(2)
C20	C19	B1	N1	64.77(19)	C32	C33	C28	B2	-169.60(13)
C20	C19	B1	C1	-116.71(16)	C32	C31	C30	C29	2.8(2)
C23	C24	C19	C20	1.90(19)	C7	C6	C5	C4	-168.42(14)
C23	C24	C19	B1	-173.78(12)	C12	C13	C14	B2	1.1(3)
C23	C22	C21	C20	1.3(2)	C9	C16	C15	N2	-159.06(13)
C3	C18	C17	C16	-173.89(13)	C9	C16	C15	C12	15.7(2)
C3	C18	C17	C6	11.51(19)	C9	C10	C11	C12	7.2(2)
C3	C4	C5	C6	3.0(2)	C36	C33	C28	C29	-175.43(13)
C3	C2	C1	B1	1.8(2)	C36	C33	C28	B2	11.3(2)
C17	C18	C3	C4	-2.0(2)	C36	C33	C32	C31	178.99(14)
C17	C18	C3	C2	-179.40(13)	C8	C9	C10	C11	-174.21(15)
C17	C16	C15	N2	15.7(2)	C34	C29	C28	C33	177.84(13)
C17	C16	C15	C12	-169.54(14)	C34	C29	C28	B2	-9.2(2)
C17	C16	C9	C8	-12.1(2)	C34	C29	C30	C31	179.03(13)
C17	C16	C9	C10	170.93(13)	C26	C22	C23	C24	178.32(13)
C17	C6	C5	C4	7.4(2)	C26	C22	C21	C20	-178.49(13)
C17	C6	C7	C8	-1.8(2)	C25	C20	C21	C22	179.04(13)
C21	C22	C23	C24	-1.5(2)	C10	C9	C8	C7	173.78(15)
C16	C17	C6	C5	170.74(13)	C35	C31	C30	C29	-176.40(14)
C16	C17	C6	C7	-13.5(2)	C35	C31	C32	C33	176.08(13)
C16	C15	C12	C11	-6.6(2)	C11	C12	C13	C14	-171.04(17)
C16	C15	C12	C13	177.39(14)	C13	C12	C11	C10	170.80(15)
C16	C9	C8	C7	-3.3(2)	C13	C14	B2	N2	-3.9(2)
C16	C9	C10	C11	2.8(2)	C13	C14	B2	C28	174.10(16)
C15	N2	B2	C28	-177.01(13)	B1	N1	C18	C3	5.15(19)
C15	N2	B2	C14	1.0(2)	B1	N1	C18	C17	-177.86(13)

A	B	C	D	Angle/°	A	B	C	D	Angle/°
C15	C16	C9	C8	163.16(13)	B1	C19	C20	C21	173.38(12)
C15	C16	C9	C10	-13.9(2)	B1	C19	C20	C25	-5.1(2)
C15	C12	C11	C10	-5.2(2)	B2	N2	C15	C16	179.61(14)
C15	C12	C13	C14	5.0(3)	B2	N2	C15	C12	4.7(2)
C33	C28	B2	N2	-132.84(16)					

Table S9. Hydrogen Atom Coordinates (Å×10^4) and Isotropic Displacement Parameters (Å^2×10^3) for **BN[5]**.

Atom	*x*	*y*	*z*	U(eq)
H1	4332.6	3600.92	6572.22	18
H2	5161.08	1524.13	6815.51	21
H23	4748.52	4653.88	9380.02	23
H21	4299.37	8410.01	8067.68	22
H4	2265.2	-964.67	5607.28	28
H2A	2173.83	476.56	6620.46	28
H27A	3780.5	1743.63	8500.38	35
H27B	4644.88	1976.57	9031.49	35
H27C	4559.95	1566.42	8255.84	35
H5	2739.8	-1100.21	4684.99	30
H30	6444.66	-1674.78	8909.38	26
H32	6687.64	2865.29	9682.41	26
H7	3557.08	29.65	4015.36	35
H1A	2647.88	2310.79	7482.12	29
H36A	6831.42	5067.56	8510.36	41
H36B	6270.63	5127.89	8995.44	41
H36C	5884.84	4942.38	8193.67	41
H8	4467.71	1891.33	3890.04	37
H34A	5472.78	-1220.78	7416.86	40
H34B	6288.61	-2160.87	7766.7	40
H34C	6272.21	-701.58	7249.71	40
H26A	4458.11	7855.43	9676.65	39
H26B	4858.48	8987.99	9237.55	39
H26C	5363.43	7556.3	9692.41	39
H25A	4161.23	6851.47	6689.31	40
H25B	3570.62	8036.03	6925.23	40
H25C	3274.39	6269.07	6631.35	40
H10	5619.17	3620.45	4386.23	36
H35A	6429.77	-622.18	10237.78	41
H35B	7142.43	670.17	10440.5	41
H35C	7278.99	-1073.7	10148.4	41
H11	6493.77	4853.42	5307.11	35
H13	7106.62	4986.49	6541.16	38
H14	7204.95	4138.81	7616.49	39

3.2. 3,12-Dibromo-1,14-dihydro-2,13-dimesityl-1,14-diaza-2,13-diborapentahelicene (BN[5]-Br_2)

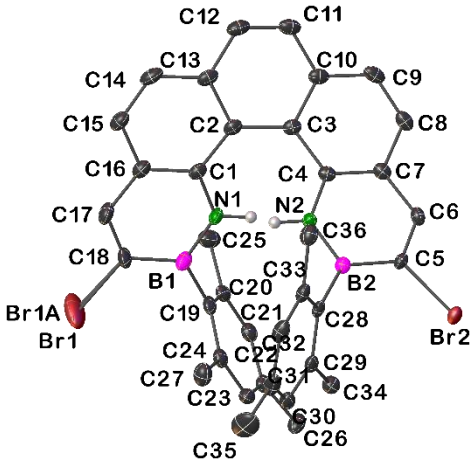

Colorless single crystals of $C_{36}H_{32}B_2Br_2N_2$ (**BN[5]-Br_2**) were grown by dissolving a small amount (ca. 5 mg) of the compound in DCM (ca. 1 mL) in a sample vial. Ethanol (ca. 5 mL) was added to a second, larger vial. The small vial was

placed in the larger vial, which was capped. DCM was allowed to evaporate slowly at 25 °C, while letting the ethanol diffuse into the small vial over the course of 5 d. CCDC Deposition Number: 2212001. Disorder for atom Br1 was modelled over two positions.

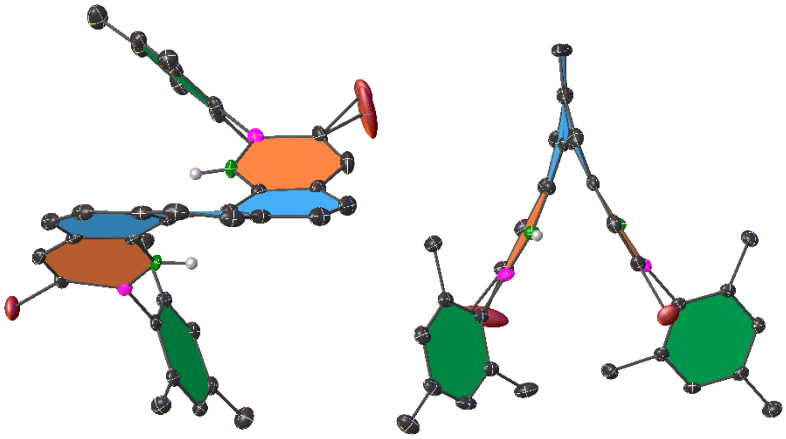

Fig. S5. Top view and view along the central phenyl-unit of **BN[5]-Br$_2$**.

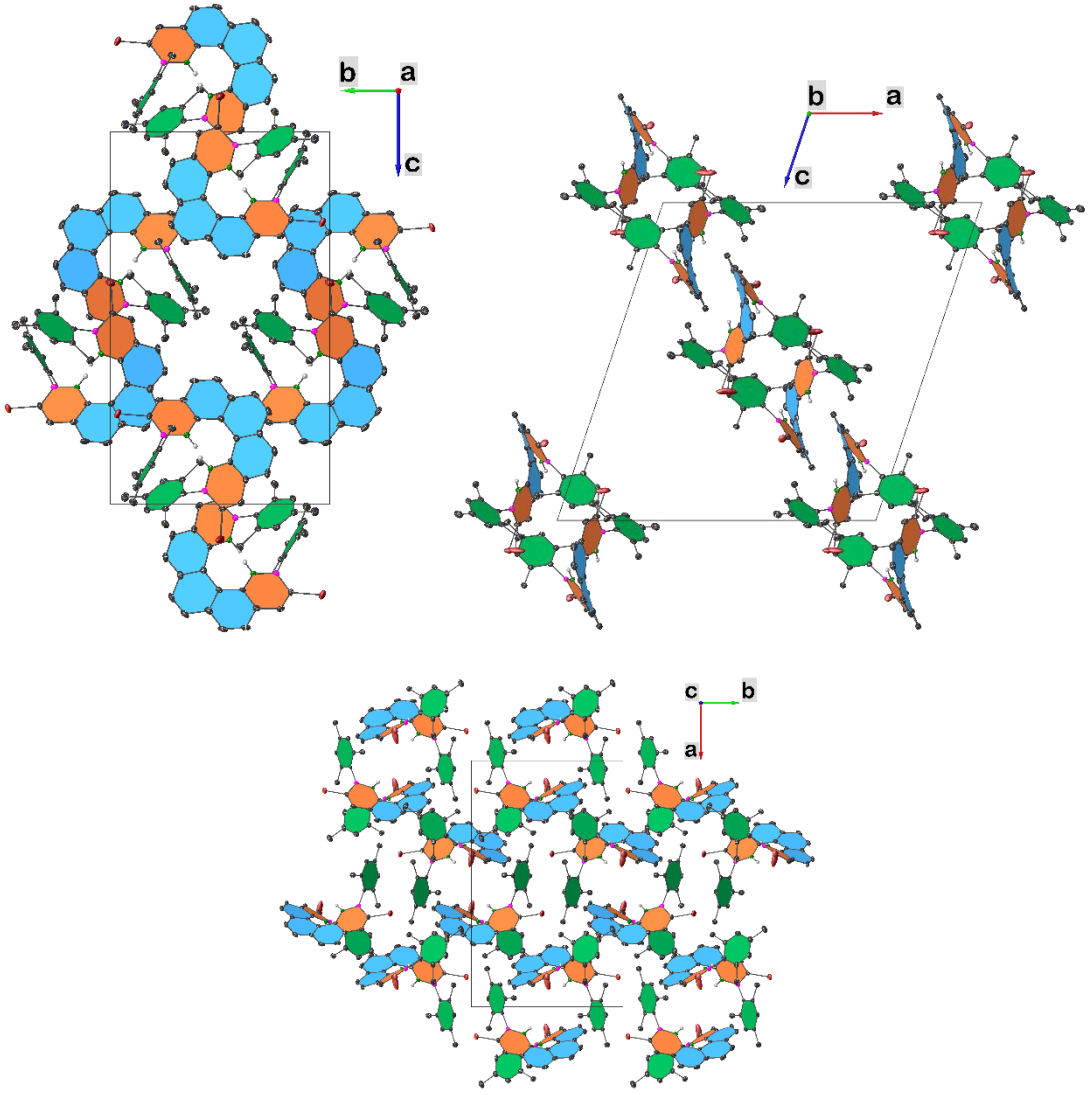

Fig. S6. Unit cell packing view of a **BN[5]-Br$_2$** crystal along the a, b and c-axes.

Table S10. Crystal data and structure refinement for **BN[5]-Br_2**.

Empirical formula	$C_{36}H_{32}B_2Br_2N_2$
Formula weight	674.07
Temperature/K	100.00
Crystal system	monoclinic
Space group	$P2_1/n$
a/Å	21.8649(9)
b/Å	12.8104(8)
c/Å	22.9768(11)
α/°	90
β/°	108.440(2)
γ/°	90
Volume/$Å^3$	6105.3(5)
Z	8
$\rho_{calc}g/cm^3$	1.467
μ/mm^{-1}	2.684
F(000)	2736.0
Crystal size/mm^3	0.505 × 0.449 × 0.108
Radiation	MoKα (λ = 0.71073)
2Θ range for data collection/°	4.448 to 56.648
Index ranges	-29 ≤ h ≤ 29, -17 ≤ k ≤ 17, -30 ≤ l ≤ 30
Reflections collected	108189
Independent reflections	15165 [R_{int} = 0.0782, R_{sigma} = 0.0532]
Data/restraints/parameters	15165/0/804
Goodness-of-fit on F^2	1.031
Final R indexes [I>=2σ (I)]	R_1 = 0.0423, wR_2 = 0.0853
Final R indexes [all data]	R_1 = 0.0696, wR_2 = 0.0957
Largest diff. peak/hole / e $Å^{-3}$	1.73/-0.91

Table S11. Fractional Atomic Coordinates (×10^4) and Equivalent Isotropic Displacement Parameters ($Å^2$×10^3) for **BN[5]-Br_2**. U_{eq} is defined as 1/3 of the trace of the orthogonalized U_{IJ} tensor.

Atom	*x*	*y*	*z*	$U_{(eq)}$
Br2	2684.7(2)	4636.8(2)	6515.2(2)	21.79(7)
Br3	3791.0(2)	5327.8(2)	2570.3(2)	26.97(8)
N2	2133.8(11)	1437.9(16)	6294.0(10)	14.9(4)
N4	3467.3(11)	9562.2(16)	4039.6(10)	15.1(4)
N3	3903.9(10)	8483.2(17)	3141.7(10)	13.8(4)
N1	1156.6(11)	164.9(16)	6551.6(11)	17.9(5)
C55	4745.8(12)	7039.3(18)	3623.4(11)	13.4(5)
C60	4746.6(13)	6446.1(19)	4137.1(12)	16.2(5)
C5	2592.0(12)	3172.5(19)	6619.0(11)	15.4(5)
C54	3638.5(13)	6778.0(19)	2633.3(12)	17.0(5)
C37	3391.9(12)	8959.5(19)	2700.1(11)	14.0(5)
C6	2997.3(12)	2730(2)	7129.9(11)	16.7(5)
C38	3276.1(12)	10053(2)	2706.4(11)	15.4(5)
C56	5334.4(13)	7243.9(18)	3524.2(11)	15.1(5)
C28	1701.6(13)	2846.4(18)	5457.0(11)	15.6(5)
C7	3007.9(12)	1629(2)	7226.3(11)	16.3(5)
C52	3029.1(12)	8335(2)	2208.0(11)	16.7(5)
C58	5917.0(13)	6343.6(19)	4467.0(12)	16.8(5)
C53	3146.7(12)	7232(2)	2197.7(11)	18.5(5)
C10	3184.7(13)	-538(2)	7293.0(12)	18.7(5)
C65	3293.1(14)	7511(2)	5123.8(11)	20.0(6)
C57	5910.5(12)	6894.8(19)	3944.7(11)	16.1(5)
C4	2559.3(12)	975(2)	6813.6(11)	15.4(5)
C8	3528.9(13)	1176(2)	7696.0(12)	19.4(5)
C59	5327.3(13)	6117.7(19)	4551.0(12)	17.0(5)
C19	262.6(12)	1344(2)	6719.1(13)	19.8(6)
C40	3701.1(12)	10470.1(19)	3862.7(11)	15.1(5)
C33	1843.5(13)	2444(2)	4940.6(12)	19.0(5)
C2	2107.3(13)	-880.8(19)	6553.6(11)	17.0(5)
C24	9.7(13)	2248(2)	6380.1(12)	20.2(6)
C13	2314.3(14)	-1905(2)	6475.5(12)	20.1(6)
C39	3562.7(12)	10751(2)	3229.7(12)	16.0(5)
C49	2908.7(13)	10513(2)	2143.1(12)	20.2(6)
C11	3341.7(14)	-1609(2)	7251.0(13)	22.8(6)
C1	1429.2(13)	-695.2(19)	6355.6(12)	17.2(5)
C29	1179.9(13)	3542.9(19)	5354.5(12)	17.6(5)
C22	-65.4(12)	3111(2)	7294.7(13)	19.4(5)
C16	998.3(14)	-1433(2)	5987.9(12)	20.5(6)
C64	3041.3(13)	8333.5(19)	4709.8(11)	17.4(5)
C61	5358.5(14)	7810(2)	2956.4(12)	21.7(6)
C3	2596.2(13)	-138.7(19)	6893.7(11)	16.2(5)
C45	3996.5(14)	12489(2)	3574.9(14)	24.0(6)
C51	2582.5(13)	8822(2)	1690.7(12)	21.8(6)
C23	-144.8(13)	3113(2)	6668.8(13)	20.5(6)
C12	2949.0(14)	-2236(2)	6822.2(13)	24.5(6)
C69	2386.5(13)	8269(2)	4338.8(11)	18.0(5)
C20	311.8(13)	1319(2)	7346.3(13)	20.5(6)
C21	146.5(13)	2195(2)	7622.7(13)	20.4(6)
C46	3645.9(13)	11812(2)	3099.6(13)	20.0(6)
C48	2945.0(14)	11612(2)	2058.3(13)	24.5(6)
C15	1246.5(15)	-2390(2)	5848.2(12)	23.4(6)
C17	319.2(15)	-1247(2)	5782.7(14)	26.4(6)
C44	4199.5(14)	12167(2)	4167.5(14)	24.0(6)
C32	1467.4(15)	2734(2)	4352.4(12)	24.3(6)
C9	3632.1(13)	132(2)	7703.2(12)	21.1(6)
C68	2014.4(14)	7420(2)	4389.4(12)	21.6(6)
C41	3804.0(14)	10105(2)	5121.5(12)	21.6(6)
C31	936.3(15)	3380(2)	4252.9(13)	27.5(7)
C47	3338.5(14)	12213(2)	2496.3(13)	24.1(6)
C30	797.4(14)	3782(2)	4757.9(12)	22.8(6)
C72	2068.9(14)	9092(2)	3865.7(13)	23.1(6)
C34	1031.9(14)	4065(2)	5884.3(13)	22.5(6)
C43	4018.3(13)	11175(2)	4331.6(12)	19.3(5)
C63	4115.6(13)	6160(2)	4231.9(13)	24.2(6)
C36	2391.7(14)	1697(2)	5007.8(13)	24.3(6)
C14	1878.3(15)	-2629(2)	6099.0(12)	24.1(6)
C42	4082.6(14)	10953(2)	4962.4(12)	23.1(6)
C62	6546.7(14)	6047(2)	4941.1(13)	24.4(6)
C67	2265.2(14)	6606(2)	4788.7(12)	22.7(6)
C25	535.7(15)	346(2)	7727.0(15)	30.6(7)
C66	2903.0(15)	6670(2)	5154.3(12)	23.7(6)
C50	2548.4(13)	9876(2)	1650.6(12)	22.6(6)
C18	63.4(14)	-387(2)	5951.0(15)	28.3(7)
C26	-172.6(14)	4096(2)	7603.9(14)	25.4(6)
B2	2125.7(14)	2508(2)	6122.4(13)	16.0(6)
C70	3983.9(15)	7500(2)	5536.2(13)	29.3(7)
B3	4098.9(14)	7427(2)	3147.3(13)	14.5(6)
C27	-100.8(15)	2282(2)	5695.8(13)	29.3(7)
C71	1848.1(16)	5673(2)	4806.3(14)	31.5(7)
C35	517(2)	3638(3)	3610.1(14)	47.1(10)
B4	3451.8(15)	9302(2)	4640.6(13)	17.2(6)
B1	489.3(16)	397(2)	6404.0(15)	22.7(7)
Br1A	-829.9(19)	-263(3)	5715.9(19)	84.9(13)
Br1	-854.4(10)	-195.2(11)	5607.4(9)	29.8(2)
Br4	4001(6)	9996(10)	5940(6)	79(4)
Br4A	3797.4(4)	10018.2(10)	5954.8(5)	28.51(14)

Table S12. Anisotropic Displacement Parameters ($Å^2$×10^3) for **BN[5]-Br_2**. The Anisotropic displacement factor exponent takes the form: $-2\pi^2[h^2a^{*2}U_{11}+2hka^*b^*U_{12}+\ldots]$.

Atom	U_{11}	U_{22}	U_{33}	U_{23}	U_{13}	U_{12}
Br2	23.07(15)	14.05(12)	25.56(14)	-0.94(10)	3.87(11)	-3.84(10)
Br3	29.63(17)	16.30(13)	30.33(15)	-9.00(11)	2.86(12)	-2.56(11)
N2	16.0(11)	14.7(10)	12.7(10)	-0.9(8)	2.6(9)	-0.5(9)
N4	17.7(11)	12.1(10)	13.5(10)	-2.1(8)	2.2(9)	-2.7(9)
N3	11.3(11)	14.9(10)	11.9(10)	-1.7(8)	-0.9(8)	-2.6(8)
N1	19.1(12)	13.0(10)	22.2(11)	-4.3(9)	7.6(9)	-2.6(9)
C55	15.9(13)	8.3(11)	14.9(12)	-3.5(9)	3.0(10)	-1.6(9)
C60	18.4(13)	11.4(11)	18.9(12)	-0.7(9)	5.9(10)	-0.9(10)
C5	18.8(13)	11.0(11)	18.2(12)	-1.3(9)	8.2(10)	-2.0(10)
C54	19.9(14)	11.8(11)	20.5(13)	-3.2(10)	8.3(11)	-2.1(10)
C37	11.2(12)	19.5(12)	11.3(11)	3.7(9)	3.4(9)	-0.1(10)
C6	14.3(13)	21.6(13)	14.6(12)	-4.0(10)	5.1(10)	-3.5(10)
C38	11.9(12)	18.6(12)	16.2(12)	4.6(10)	5.2(10)	2.0(10)
C56	20.3(14)	10.4(11)	14.5(12)	-2.2(9)	5.1(10)	-1.1(10)

Atom	U_{11}	U_{22}	U_{33}	U_{23}	U_{13}	U_{12}
C28	20.8(14)	11.0(11)	14.5(12)	0.3(9)	4.7(10)	-5.2(10)
C7	16.5(13)	22.3(13)	11.7(11)	1.6(10)	6.8(10)	0.7(10)
C52	10.5(13)	25.1(13)	14.2(12)	1.4(10)	3.6(10)	-0.9(10)
C58	17.9(14)	11.2(11)	18.5(12)	-0.6(9)	1.6(10)	0.9(10)
C53	13.7(13)	26.3(14)	14.2(12)	-4.3(10)	2.6(10)	-4.9(11)
C10	21.2(14)	21.0(13)	17.1(12)	6.4(10)	10.5(11)	4.7(11)
C65	28.7(15)	17.2(12)	13.6(12)	-0.7(10)	6.0(11)	0.5(11)
C57	14.4(13)	17.1(12)	16.7(12)	-2.2(10)	5.0(10)	-1.9(10)
C4	16.1(13)	18.5(12)	13.4(12)	1.5(9)	7.3(10)	2.0(10)
C8	15.9(13)	30.0(14)	12.9(12)	2.6(10)	5.4(10)	-2.4(11)
C59	22.2(14)	10.4(11)	17.7(12)	3.7(9)	5.3(11)	-0.6(10)
C19	11.7(13)	21.0(13)	27.1(14)	-5.3(11)	6.6(11)	-4.9(10)
C40	14.4(13)	11.9(11)	19.5(12)	0.5(9)	6.1(10)	0.1(9)
C33	25.2(15)	13.7(12)	17.9(12)	-2.0(10)	6.4(11)	-5.9(11)
C2	24.9(14)	14.6(12)	13.7(12)	2.7(9)	9.1(10)	1.7(10)
C24	14.2(13)	23.2(13)	22.9(14)	-3.1(11)	5.6(11)	-4.3(11)
C13	29.2(16)	15.3(12)	20.8(13)	4.4(10)	15.0(12)	3.9(11)
C39	12.6(13)	16.5(12)	20.3(13)	1.6(10)	7.1(10)	2.3(10)
C49	16.0(13)	27.0(14)	19.8(13)	7.1(11)	8.8(11)	6.3(11)
C11	22.1(15)	24.4(14)	24.5(14)	9.3(11)	10.8(12)	6.8(11)
C1	23.8(14)	13.3(11)	17.1(12)	1.3(10)	10.1(11)	0.7(10)
C29	19.7(14)	13.7(12)	17.8(12)	1.5(10)	3.6(10)	-4.5(10)
C22	12.7(13)	18.7(13)	27.8(14)	-4.4(11)	7.7(11)	-3.2(10)
C16	27.5(15)	15.7(12)	19.2(13)	-0.5(10)	9.0(11)	-0.4(11)
C64	25.6(15)	15.0(12)	11.8(12)	-0.9(9)	6.2(10)	0.2(10)
C61	21.7(15)	26.7(14)	17.6(13)	4.0(11)	7.3(11)	-0.8(11)
C3	20.5(14)	17.7(12)	13.1(11)	2.6(9)	9.1(10)	2.2(10)
C45	26.2(16)	11.9(12)	37.7(16)	2.3(11)	15.6(13)	1.5(11)
C51	14.3(14)	36.2(16)	12.2(12)	0.1(11)	0.6(10)	-0.1(12)
C23	15.1(14)	17.6(13)	27.7(14)	0.0(11)	5.1(11)	0.9(10)
C12	30.4(17)	18.4(13)	29.1(15)	6.0(11)	15.7(13)	8.0(12)
C69	23.9(15)	17.8(12)	14.0(12)	-1.8(10)	8.5(11)	2.6(11)
C20	12.0(13)	20.0(13)	28.7(14)	1.1(11)	5.1(11)	-2.0(10)
C21	15.4(14)	24.8(14)	21.1(13)	-2.8(11)	6.1(11)	-2.5(11)
C46	19.0(14)	17.0(12)	28.8(15)	4.2(11)	14.5(12)	2.6(10)
C48	25.1(16)	27.7(15)	24.1(14)	13.6(12)	12.7(12)	11.2(12)
C15	34.9(17)	15.7(13)	19.9(13)	-2.2(10)	8.9(12)	-0.8(12)
C17	28.6(16)	19.0(13)	32.0(16)	-8.8(12)	9.9(13)	-7.8(12)
C44	25.7(16)	12.5(12)	34.9(16)	-3.7(11)	11.2(13)	-2.8(11)
C32	38.6(18)	20.4(13)	13.4(12)	-2.7(10)	7.4(12)	-7.1(12)
C9	16.0(13)	31.4(15)	17.1(12)	9.3(11)	6.7(10)	4.0(11)
C68	22.1(15)	24.8(14)	18.7(13)	-4.2(11)	7.7(11)	-3.0(11)
C41	29.3(16)	21.1(13)	11.9(12)	-2.3(10)	2.8(11)	0.0(11)
C31	37.1(18)	21.3(14)	18.2(14)	3.9(11)	0.2(12)	-6.7(12)
C47	28.3(16)	17.8(13)	31.9(16)	11.8(11)	17.7(13)	6.4(11)
C30	22.6(15)	17.1(13)	23.3(14)	3.0(11)	-0.4(11)	-2.8(11)
C72	21.7(15)	23.3(14)	23.1(14)	3.8(11)	5.3(11)	3.3(11)
C34	21.0(15)	21.7(14)	24.1(14)	-0.6(11)	6.3(11)	0.2(11)
C43	17.9(14)	14.1(12)	24.8(14)	-1.8(10)	5.3(11)	-1.1(10)
C63	20.4(15)	24.7(14)	29.0(15)	8.0(12)	9.9(12)	-0.5(11)
C36	27.6(16)	23.3(14)	24.3(14)	-6.1(11)	11.6(12)	-3.6(12)
C14	39.6(18)	14.7(12)	21.4(14)	0.9(11)	14.5(13)	5.8(12)
C42	24.8(15)	18.9(13)	20.3(13)	-5.8(11)	-0.3(11)	-1.2(11)
C62	21.0(15)	23.9(14)	23.0(14)	3.3(11)	-0.4(11)	0.6(11)
C67	32.8(17)	20.6(13)	18.7(13)	-2.9(11)	13.8(12)	-4.6(12)
C25	24.6(16)	28.1(15)	39.6(18)	8.1(13)	11.0(13)	4.1(13)
C66	40.1(18)	15.4(13)	17.1(13)	3.0(10)	11.2(12)	1.1(12)
C50	15.2(13)	37.3(16)	14.3(12)	7.5(11)	3.1(10)	6.3(12)
C18	13.9(14)	24.8(14)	43.9(18)	-9.9(13)	6.0(13)	-6.1(12)
C26	24.5(16)	19.7(14)	36.1(16)	-8.6(12)	15.1(13)	-2.0(11)
B2	17.4(15)	16.9(13)	14.8(13)	-1.2(11)	6.7(11)	-1.1(11)
C70	33.8(18)	21.6(14)	25.0(15)	5.8(12)	-1.5(13)	2.4(13)
B3	13.9(14)	16.5(13)	13.1(13)	0.5(11)	4.0(11)	-1.6(11)
C27	31.9(18)	29.2(16)	24.7(15)	-4.0(12)	6.0(13)	-6.5(13)
C71	42.4(19)	25.1(15)	30.4(16)	-2.2(12)	16.3(14)	-11.1(14)
C35	66(3)	42(2)	18.7(15)	6.1(14)	-7.1(16)	5.0(18)
B4	19.0(15)	15.3(13)	15.1(13)	1.6(11)	2.1(11)	2.9(11)
B1	22.7(17)	16.8(14)	31.9(17)	-2.7(13)	13.3(14)	-3.8(12)
Br1A	23.0(12)	76.4(18)	150(3)	-59.2(17)	19.5(16)	-11.4(11)
Br1	12.5(5)	17.3(4)	55.7(4)	-14.3(3)	5.1(3)	-6.6(3)
Br4	179(12)	32(4)	18(3)	-8(2)	19(6)	-35(7)
Br4A	47.5(3)	24.0(3)	12.2(2)	-1.54(18)	6.80(18)	0.2(2)

Table S13. Bond Lengths for **BN[5]-Br_2**.

Atom	Atom	Length/Å	Atom	Atom	Length/Å
Br2	C5	1.910(2)	C33	C32	1.392(4)
Br3	C54	1.901(2)	C33	C36	1.503(4)
N2	C4	1.393(3)	C2	C13	1.418(3)
N2	B2	1.425(4)	C2	C1	1.426(4)
N4	C40	1.382(3)	C2	C3	1.459(4)
N4	B4	1.431(4)	C24	C23	1.387(4)
N3	C37	1.391(3)	C24	C27	1.514(4)
N3	B3	1.418(4)	C13	C12	1.429(4)
N1	C1	1.394(3)	C13	C14	1.413(4)
N1	B1	1.421(4)	C39	C46	1.416(4)
C55	C60	1.403(3)	C49	C48	1.427(4)
C55	C56	1.401(4)	C49	C50	1.415(4)
C55	B3	1.570(4)	C11	C12	1.348(4)
C60	C59	1.389(4)	C1	C16	1.411(4)
C60	C63	1.509(4)	C29	C30	1.395(4)
C5	C6	1.351(4)	C29	C34	1.511(4)
C5	B2	1.527(4)	C22	C23	1.393(4)
C54	C53	1.348(4)	C22	C21	1.392(4)
C54	B3	1.532(4)	C22	C26	1.503(4)
C37	C38	1.425(3)	C16	C15	1.418(4)
C37	C52	1.407(3)	C16	C17	1.429(4)
C6	C7	1.427(4)	C64	C69	1.418(4)
C38	C39	1.470(4)	C64	B4	1.569(4)
C38	C49	1.417(3)	C45	C46	1.415(4)
C56	C57	1.397(4)	C45	C44	1.356(4)
C56	C61	1.508(3)	C51	C50	1.354(4)
C28	C33	1.415(4)	C69	C68	1.386(4)
C28	C29	1.408(4)	C69	C72	1.516(4)
C28	B2	1.577(4)	C20	C21	1.393(4)
C7	C4	1.405(4)	C20	C25	1.512(4)
C7	C8	1.422(4)	C46	C47	1.431(4)
C52	C53	1.438(4)	C48	C47	1.341(4)
C52	C51	1.421(4)	C15	C14	1.353(4)
C58	C57	1.389(4)	C17	C18	1.347(4)
C58	C59	1.393(4)	C44	C43	1.418(4)
C58	C62	1.509(4)	C32	C31	1.385(4)
C10	C11	1.426(4)	C68	C67	1.383(4)
C10	C3	1.418(4)	C41	C42	1.351(4)
C10	C9	1.414(4)	C41	B4	1.527(4)
C65	C64	1.410(4)	C41	Br4	1.797(12)
C65	C66	1.389(4)	C41	Br4A	1.923(3)
C65	C70	1.508(4)	C31	C30	1.388(4)
C4	C3	1.438(3)	C31	C35	1.508(4)
C8	C9	1.355(4)	C43	C42	1.440(4)
C19	C24	1.408(4)	C67	C66	1.384(4)
C19	C20	1.411(4)	C67	C71	1.512(4)
C19	B1	1.571(4)	C18	B1	1.531(4)
C40	C39	1.435(3)	C18	Br1A	1.861(5)
C40	C43	1.409(4)	C18	Br1	1.926(4)

Table S14. Bond Angles for **BN[5]-Br_2**.

Atom	Atom	Atom	Angle/°	Atom	Atom	Atom	Angle/°
C4	N2	B2	126.4(2)	N1	C1	C16	116.7(2)
C40	N4	B4	127.1(2)	C16	C1	C2	120.6(2)
C37	N3	B3	126.5(2)	C28	C29	C34	120.9(2)
C1	N1	B1	126.9(2)	C30	C29	C28	120.4(2)
C60	C55	B3	121.2(2)	C30	C29	C34	118.7(2)
C56	C55	C60	118.8(2)	C23	C22	C26	119.9(2)
C56	C55	B3	119.9(2)	C21	C22	C23	118.2(2)
C55	C60	C63	119.7(2)	C21	C22	C26	121.8(3)
C59	C60	C55	119.8(2)	C1	C16	C15	118.9(3)
C59	C60	C63	120.5(2)	C1	C16	C17	120.9(2)
C6	C5	Br2	117.00(19)	C15	C16	C17	120.1(3)
C6	C5	B2	121.0(2)	C65	C64	C69	117.8(2)
B2	C5	Br2	121.79(19)	C65	C64	B4	123.1(2)
C53	C54	Br3	118.90(19)	C69	C64	B4	119.1(2)
C53	C54	B3	120.9(2)	C10	C3	C4	116.3(2)
B3	C54	Br3	120.04(19)	C10	C3	C2	118.2(2)
N3	C37	C38	121.9(2)	C4	C3	C2	125.2(2)
N3	C37	C52	117.1(2)	C44	C45	C46	120.9(2)

Atom	Atom	Atom	Angle/°	Atom	Atom	Atom	Angle/°
C52	C37	C38	120.7(2)	C50	C51	C52	120.2(3)
C5	C6	C7	121.6(2)	C24	C23	C22	121.5(3)
C37	C38	C39	125.1(2)	C11	C12	C13	120.9(3)
C49	C38	C37	116.8(2)	C64	C69	C72	122.5(2)
C49	C38	C39	117.8(2)	C68	C69	C64	120.2(2)
C55	C56	C61	121.1(2)	C68	C69	C72	117.3(2)
C57	C56	C55	120.1(2)	C19	C20	C25	121.0(3)
C57	C56	C61	118.8(2)	C21	C20	C19	120.0(2)
C33	C28	B2	119.6(2)	C21	C20	C25	118.9(3)
C29	C28	C33	118.1(2)	C22	C21	C20	121.5(3)
C29	C28	B2	122.2(2)	C39	C46	C47	119.8(3)
C4	C7	C6	120.7(2)	C45	C46	C39	120.0(2)
C4	C7	C8	119.3(2)	C45	C46	C47	120.1(2)
C8	C7	C6	119.4(2)	C47	C48	C49	121.0(3)
C37	C52	C53	120.9(2)	C14	C15	C16	120.8(3)
C37	C52	C51	119.1(2)	C18	C17	C16	121.6(3)
C51	C52	C53	119.8(2)	C45	C44	C43	120.6(3)
C57	C58	C59	117.9(2)	C31	C32	C33	121.8(3)
C57	C58	C62	120.6(2)	C8	C9	C10	120.9(2)
C59	C58	C62	121.4(2)	C67	C68	C69	121.9(3)
C54	C53	C52	121.1(2)	C42	C41	B4	120.9(2)
C3	C10	C11	119.5(3)	C42	C41	Br4	111.5(4)
C9	C10	C11	119.9(2)	C42	C41	Br4A	117.5(2)
C9	C10	C3	120.5(2)	B4	C41	Br4	127.2(5)
C64	C65	C70	122.0(2)	B4	C41	Br4A	121.4(2)
C66	C65	C64	119.9(3)	Br4	C41	Br4A	13.6(4)
C66	C65	C70	118.1(2)	C32	C31	C30	118.5(3)
C58	C57	C56	121.4(2)	C32	C31	C35	120.7(3)
N2	C4	C7	117.3(2)	C30	C31	C35	120.8(3)
N2	C4	C3	121.8(2)	C48	C47	C46	120.9(3)
C7	C4	C3	120.4(2)	C31	C30	C29	121.2(3)
C9	C8	C7	120.2(3)	C40	C43	C44	118.9(2)
C60	C59	C58	121.9(2)	C40	C43	C42	120.7(2)
C24	C19	C20	118.3(2)	C44	C43	C42	119.9(2)
C24	C19	B1	120.4(2)	C15	C14	C13	120.8(2)
C20	C19	B1	121.3(2)	C41	C42	C43	121.5(2)
N4	C40	C39	122.0(2)	C68	C67	C66	118.0(3)
N4	C40	C43	116.9(2)	C68	C67	C71	119.9(3)
C43	C40	C39	120.6(2)	C66	C67	C71	122.1(3)
C28	C33	C36	121.7(2)	C67	C66	C65	122.2(3)
C32	C33	C28	119.9(3)	C51	C50	C49	121.0(2)
C32	C33	C36	118.5(2)	C17	C18	B1	120.9(3)
C13	C2	C1	117.1(2)	C17	C18	Br1A	118.6(2)
C13	C2	C3	117.5(2)	C17	C18	Br1	117.4(2)
C1	C2	C3	125.0(2)	B1	C18	Br1A	119.9(2)
C19	C24	C27	120.3(2)	B1	C18	Br1	121.7(2)
C23	C24	C19	120.4(3)	Br1A	C18	Br1	7.42(18)
C23	C24	C27	119.4(3)	N2	B2	C5	112.5(2)
C2	C13	C12	119.8(3)	N2	B2	C28	119.0(2)
C14	C13	C2	120.3(3)	C5	B2	C28	128.3(2)
C14	C13	C12	119.7(2)	N3	B3	C55	120.7(2)
C40	C39	C38	125.1(2)	N3	B3	C54	112.9(2)
C46	C39	C38	117.5(2)	C54	B3	C55	126.4(2)
C46	C39	C40	117.1(2)	N4	B4	C64	118.1(2)
C38	C49	C48	119.6(3)	N4	B4	C41	112.4(2)
C50	C49	C38	120.2(2)	C41	B4	C64	129.3(2)
C50	C49	C48	120.0(2)	N1	B1	C19	120.1(3)
C12	C11	C10	120.8(3)	N1	B1	C18	112.5(2)
N1	C1	C2	122.4(2)	C18	B1	C19	127.3(3)

Table S15. Torsion Angles for **BN[5]-Br$_2$**.

A	B	C	D	Angle/°	A	B	C	D	Angle/°
Br2	C5	C6	C7	-174.39(19)	C1	C2	C13	C12	-160.8(2)
Br2	C5	B2	N2	179.91(18)	C1	C2	C13	C14	13.6(4)
Br2	C5	B2	C28	5.0(4)	C1	C2	C3	C10	151.4(2)
Br3	C54	C53	C52	-177.07(19)	C1	C2	C3	C4	-35.1(4)
Br3	C54	B3	N3	-177.91(18)	C1	C16	C15	C14	4.9(4)
Br3	C54	B3	C55	5.4(4)	C1	C16	C17	C18	-2.7(4)
N2	C4	C3	C10	156.3(2)	C29	C28	C33	C32	-0.5(4)
N2	C4	C3	C2	-17.2(4)	C29	C28	C33	C36	180.0(2)
N4	C40	C39	C38	-12.2(4)	C29	C28	B2	N2	117.0(3)
N4	C40	C39	C46	160.8(2)	C29	C28	B2	C5	-68.4(4)
N4	C40	C43	C44	-172.8(2)	C16	C15	C14	C13	-4.0(4)
N4	C40	C43	C42	-0.9(4)	C16	C17	C18	B1	-3.9(5)
N3	C37	C38	C39	-15.2(4)	C16	C17	C18	Br1A	-174.9(3)
N3	C37	C38	C49	158.0(2)	C16	C17	C18	Br1	176.8(2)
N3	C37	C52	C53	5.9(4)	C64	C65	C66	C67	0.0(4)
N3	C37	C52	C51	-168.4(2)	C64	C69	C68	C67	-1.2(4)
N1	C1	C16	C15	-171.3(2)	C61	C56	C57	C58	-178.2(2)
N1	C1	C16	C17	5.7(4)	C3	C10	C11	C12	2.5(4)
C55	C60	C59	C58	-1.2(4)	C3	C10	C9	C8	-4.4(4)
C55	C56	C57	C58	-0.1(4)	C3	C2	C13	C12	12.1(4)
C60	C55	C56	C57	-2.5(3)	C3	C2	C13	C14	-173.6(2)
C60	C55	C56	C61	175.6(2)	C3	C2	C1	N1	-10.3(4)
C60	C55	B3	N3	104.2(3)	C3	C2	C1	C16	175.1(2)
C60	C55	B3	C54	-79.4(3)	C45	C46	C47	C48	-172.4(3)
C5	C6	C7	C4	-5.1(4)	C45	C44	C43	C40	8.8(4)
C5	C6	C7	C8	166.3(2)	C45	C44	C43	C42	-163.1(3)
C37	N3	B3	C55	171.0(2)	C51	C52	C53	C54	169.0(2)
C37	N3	B3	C54	-5.8(4)	C23	C22	C21	C20	3.6(4)
C37	C38	C39	C40	-34.9(4)	C12	C13	C14	C15	168.8(3)
C37	C38	C39	C46	152.1(2)	C69	C64	B4	N4	-52.6(3)
C37	C38	C49	C48	-159.8(2)	C69	C64	B4	C41	121.0(3)
C37	C38	C49	C50	15.1(4)	C69	C68	C67	C66	1.6(4)
C37	C52	C53	C54	-5.2(4)	C69	C68	C67	C71	-177.2(2)
C37	C52	C51	C50	5.6(4)	C20	C19	C24	C23	4.3(4)
C6	C5	B2	N2	5.7(4)	C20	C19	C24	C27	-175.3(2)
C6	C5	B2	C28	-169.3(3)	C20	C19	B1	N1	-70.2(4)
C6	C7	C4	N2	3.6(4)	C20	C19	B1	C18	106.9(4)
C6	C7	C4	C3	176.3(2)	C21	C22	C23	C24	-2.9(4)
C6	C7	C8	C9	-164.3(2)	C46	C45	C44	C43	-5.4(4)
C38	C37	C52	C53	179.6(2)	C48	C49	C50	C51	170.2(3)
C38	C37	C52	C51	5.4(4)	C15	C16	C17	C18	174.2(3)
C38	C39	C46	C45	-171.5(2)	C17	C16	C15	C14	-172.1(3)
C38	C39	C46	C47	12.7(4)	C17	C18	B1	N1	6.8(4)
C38	C49	C48	C47	2.3(4)	C17	C18	B1	C19	-170.6(3)
C38	C49	C50	C51	-4.7(4)	C44	C45	C46	C39	-6.9(4)
C56	C55	C60	C59	3.1(4)	C44	C45	C46	C47	169.0(3)
C56	C55	C60	C63	-176.2(2)	C44	C43	C42	C41	167.1(3)
C56	C55	B3	N3	-78.7(3)	C32	C31	C30	C29	-0.2(4)
C56	C55	B3	C54	97.7(3)	C9	C10	C11	C12	-173.6(3)
C28	C33	C32	C31	-2.6(4)	C9	C10	C3	C4	15.9(3)
C28	C29	C30	C31	-2.9(4)	C9	C10	C3	C2	-170.1(2)
C7	C4	C3	C10	-16.1(3)	C68	C67	C66	C65	-1.0(4)
C7	C4	C3	C2	170.4(2)	C72	C69	C68	C67	177.3(2)
C7	C8	C9	C10	-7.6(4)	C34	C29	C30	C31	175.7(2)
C52	C37	C38	C39	171.4(2)	C43	C40	C39	C38	175.5(2)
C52	C37	C38	C49	-15.5(4)	C43	C40	C39	C46	-11.5(4)
C52	C51	C50	C49	-6.0(4)	C63	C60	C59	C58	178.1(2)
C53	C54	B3	N3	6.4(4)	C36	C33	C32	C31	176.9(3)
C53	C54	B3	C55	-170.2(2)	C14	C13	C12	C11	-170.2(3)
C53	C52	C51	C50	-168.7(3)	C42	C41	B4	N4	0.6(4)
C10	C11	C12	C13	-11.7(4)	C42	C41	B4	C64	-173.3(3)
C65	C64	C69	C68	0.1(4)	C62	C58	C57	C56	-175.1(2)
C65	C64	C69	C72	-178.3(2)	C62	C58	C59	C60	175.8(2)
C65	C64	B4	N4	127.0(3)	C25	C20	C21	C22	-179.7(2)
C65	C64	B4	C41	-59.4(4)	C66	C65	C64	C69	0.5(4)
C57	C58	C59	C60	-1.4(4)	C66	C65	C64	B4	-179.1(2)
C4	N2	B2	C5	-7.4(4)	C50	C49	C48	C47	-172.7(3)
C4	N2	B2	C28	168.0(2)	C26	C22	C23	C24	173.7(2)
C4	C7	C8	C9	7.3(4)	C26	C22	C21	C20	-172.9(2)
C8	C7	C4	N2	-167.8(2)	B2	N2	C4	C7	3.1(4)
C8	C7	C4	C3	4.9(4)	B2	N2	C4	C3	-169.5(2)
C59	C58	C57	C56	2.0(4)	B2	C5	C6	C7	0.1(4)
C19	C24	C23	C22	-1.0(4)	B2	C28	C33	C32	179.5(2)
C19	C20	C21	C22	-0.4(4)	B2	C28	C33	C36	-0.1(4)
C40	N4	B4	C64	167.9(2)	B2	C28	C29	C30	-176.8(2)
C40	N4	B4	C41	-6.8(4)	B2	C28	C29	C34	4.6(4)
C40	C39	C46	C45	15.0(4)	C70	C65	C64	C69	179.7(2)
C40	C39	C46	C47	-160.8(2)	C70	C65	C64	B4	0.0(4)
C40	C43	C42	C41	-4.7(4)	C70	C65	C66	C67	-179.2(3)
C33	C28	C29	C30	3.2(4)	B3	N3	C37	C38	-173.7(2)
C33	C28	C29	C34	-175.4(2)	B3	N3	C37	C52	0.0(4)
C33	C28	B2	N2	-63.0(3)	B3	C55	C60	C59	-179.8(2)
C33	C28	B2	C5	111.6(3)	B3	C55	C60	C63	0.9(4)

A	B	C	D	Angle/°	A	B	C	D	Angle/°
C33	C32	C31	C30	3.0(4)	B3	C55	C56	C57	-179.6(2)
C33	C32	C31	C35	-176.8(3)	B3	C55	C56	C61	-1.6(3)
C2	C13	C12	C11	4.1(4)	B3	C54	C53	C52	-1.4(4)
C2	C13	C14	C15	-5.5(4)	C27	C24	C23	C22	178.5(3)
C2	C1	C16	C15	3.7(4)	C71	C67	C66	C65	177.8(3)
C2	C1	C16	C17	-179.3(2)	C35	C31	C30	C29	179.6(3)
C24	C19	C20	C21	-3.6(4)	B4	N4	C40	C39	-165.6(3)
C24	C19	C20	C25	175.7(2)	B4	N4	C40	C43	7.0(4)
C24	C19	B1	N1	109.1(3)	B4	C64	C69	C68	179.7(2)
C24	C19	B1	C18	-73.7(4)	B4	C64	C69	C72	1.3(4)
C13	C2	C1	N1	162.0(2)	B4	C41	C42	C43	4.7(4)
C13	C2	C1	C16	-12.6(4)	B1	N1	C1	C2	-177.1(3)
C13	C2	C3	C10	-20.8(3)	B1	N1	C1	C16	-2.2(4)
C13	C2	C3	C4	152.6(2)	B1	C19	C24	C23	-175.1(2)
C39	C38	C49	C48	13.9(4)	B1	C19	C24	C27	5.3(4)
C39	C38	C49	C50	-171.2(2)	B1	C19	C20	C21	175.8(2)
C39	C40	C43	C44	-0.1(4)	B1	C19	C20	C25	-4.9(4)
C39	C40	C43	C42	171.8(2)	Br1A	C18	B1	N1	177.7(3)
C39	C46	C47	C48	3.4(4)	Br1A	C18	B1	C19	0.4(5)
C49	C38	C39	C40	152.0(2)	Br1	C18	B1	N1	-173.9(2)
C49	C38	C39	C46	-21.0(3)	Br1	C18	B1	C19	8.7(4)
C49	C48	C47	C46	-11.2(4)	Br4	C41	C42	C43	177.0(5)
C11	C10	C3	C4	-160.1(2)	Br4	C41	B4	N4	-170.4(5)
C11	C10	C3	C2	13.9(3)	Br4	C41	B4	C64	15.6(7)
C11	C10	C9	C8	171.6(2)	Br4A	C41	C42	C43	-169.5(2)
C1	N1	B1	C19	173.8(2)	Br4A	C41	B4	N4	174.61(19)
C1	N1	B1	C18	-3.7(4)	Br4A	C41	B4	C64	0.7(4)

Table S16. Hydrogen Atom Coordinates (Å×10^4) and Isotropic Displacement Parameters (Å^2×10^3) for **BN[5]-Br$_2$**.

Atom	*x*	*y*	*z*	U(eq)
H6	3281.82	3162.65	7431.97	20
H53	2872.94	6816.5	1878.3	22
H57	6306.42	7037.45	3871.8	19
H8	3805.33	1605.74	8005.57	23
H59	5322.23	5728.16	4901.27	20
H11	3727.44	-1885.11	7528.46	27
H61A	5271.64	7316.86	2613.93	33
H61B	5786.98	8118.06	3031.99	33
H61C	5032.55	8364.07	2854.42	33
H45	4091.04	13178.79	3477.42	29
H51	2307.2	8406.35	1372.31	26
H23	-308.39	3720.93	6434.33	25
H12	3096.3	-2905.78	6749.54	29
H21	179.09	2167.15	8044.64	24
H48	2686.57	11921.72	1686.15	29
H15	965.93	-2868.67	5575.2	28
H17	41.28	-1742.13	5521.01	32
H44	4465.71	12611.1	4475.63	29
H32	1578.25	2482.44	4009.96	29
H9	4010.21	-152.79	7987.77	25
H68	1574.42	7395.98	4142.86	26
H47	3414.18	12915.31	2404.7	29
H30	435.18	4227.67	4696.23	27
H72A	2177.31	9787.49	4046.76	35
H72B	1600.17	8997.24	3733.27	35
H72C	2223.85	9023.62	3511.26	35
H34A	1107.73	3570.42	6225.38	34
H34B	579.97	4287.66	5753.14	34
H34C	1311.95	4674.36	6017.97	34
H63A	3832.52	6772.06	4154.66	36
H63B	4196.06	5921.99	4654.96	36
H63C	3908.29	5599.17	3947.67	36
H36A	2759.39	1901.9	5360.77	36
H36B	2518.19	1713.02	4635.01	36
H36C	2255.07	989.23	5071.42	36
H14	2030.57	-3292.35	6020.98	29
H42	4326.29	11413.18	5273.88	28
H62A	6887.56	6020.84	4748.67	37
H62B	6503.42	5360.12	5111.74	37
H62C	6658.06	6567.31	5270.65	37
H25A	283.65	-254.67	7516.98	46
H25B	475.31	435.3	8128.92	46
H25C	993.3	226.8	7781.92	46
H66	3079.73	6121.78	5435.45	28
H50	2278.39	10193.27	1286	27
H26A	155.32	4612.43	7595.65	38
H26B	-141.2	3943.81	8030.33	38
H26C	-601.82	4374.77	7387.23	38
H70A	4247.4	7926.74	5353.21	44
H70B	4145.41	6781.39	5584.92	44
H70C	4007.79	7785.91	5938.48	44
H27A	290.79	2053.2	5611.92	44
H27B	-206.09	2996.94	5546.32	44
H27C	-458.69	1816.9	5486.18	44
H71A	1424.47	5912.54	4812.15	47
H71B	2053.77	5261.02	5176	47
H71C	1795.61	5239.72	4442.05	47
H35A	788.02	3886.56	3370.76	71
H35B	208.4	4183	3625.25	71
H35C	283.27	3010.85	3416.57	71
H1	1434(15)	570(20)	6817(14)	19(8)
H4	3271(14)	9170(20)	3752(14)	18(8)
H3	4132(15)	8860(20)	3385(14)	22(8)
H2	1881(15)	980(20)	6023(14)	22(8)

3.3. 3,12-Dicyano-1,14-dihydro-2,13-dimesityl-1,14-diaza-2,13-diborapentahelicene (BN[5]-(CN)$_2$)

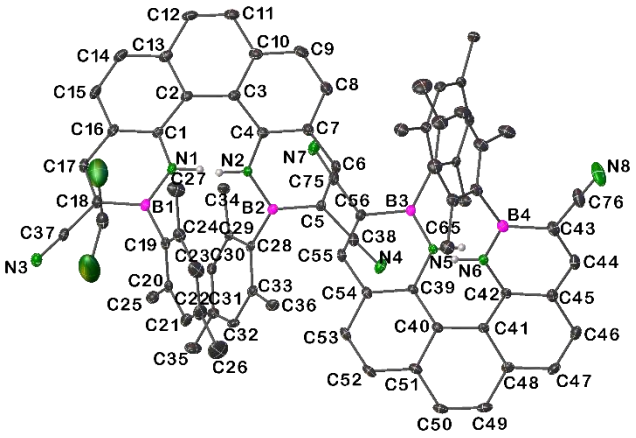

Pale-yellow single crystals of $C_{38}H_{32}B_2N_4$ (**BN[5]-(CN)$_2$**, two molecules of the helicene co-crystallized with one molecule of dichloromethane, net molecular formula $C_{77}H_{66}B_4Cl_2N_8$) were grown by dissolving a small amount (ca. 2 mg) of the compound in DCM (ca. 1 mL) in a sample vial. Ethanol (ca. 5 mL) was added to a second, larger vial. The small vial was placed in the larger vial, which was capped. DCM was allowed to evaporate slowly at 25 °C, while letting the ethanol diffuse into the small vial over the course of 3 d. CCDC Deposition Number: 2212000.

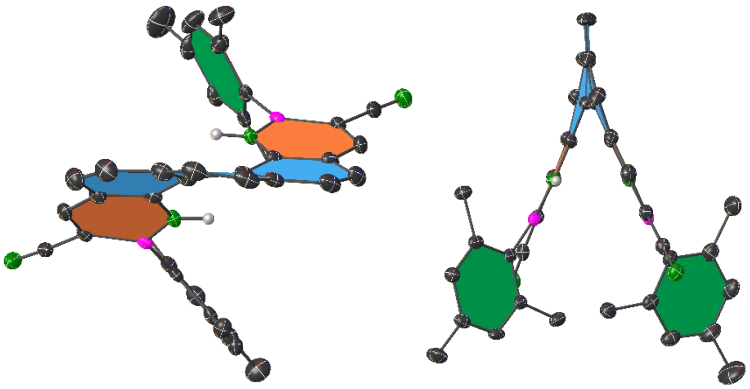

Fig. S7. Top view and view along the central phenyl-unit of **BN[5]-(CN)$_2$**.

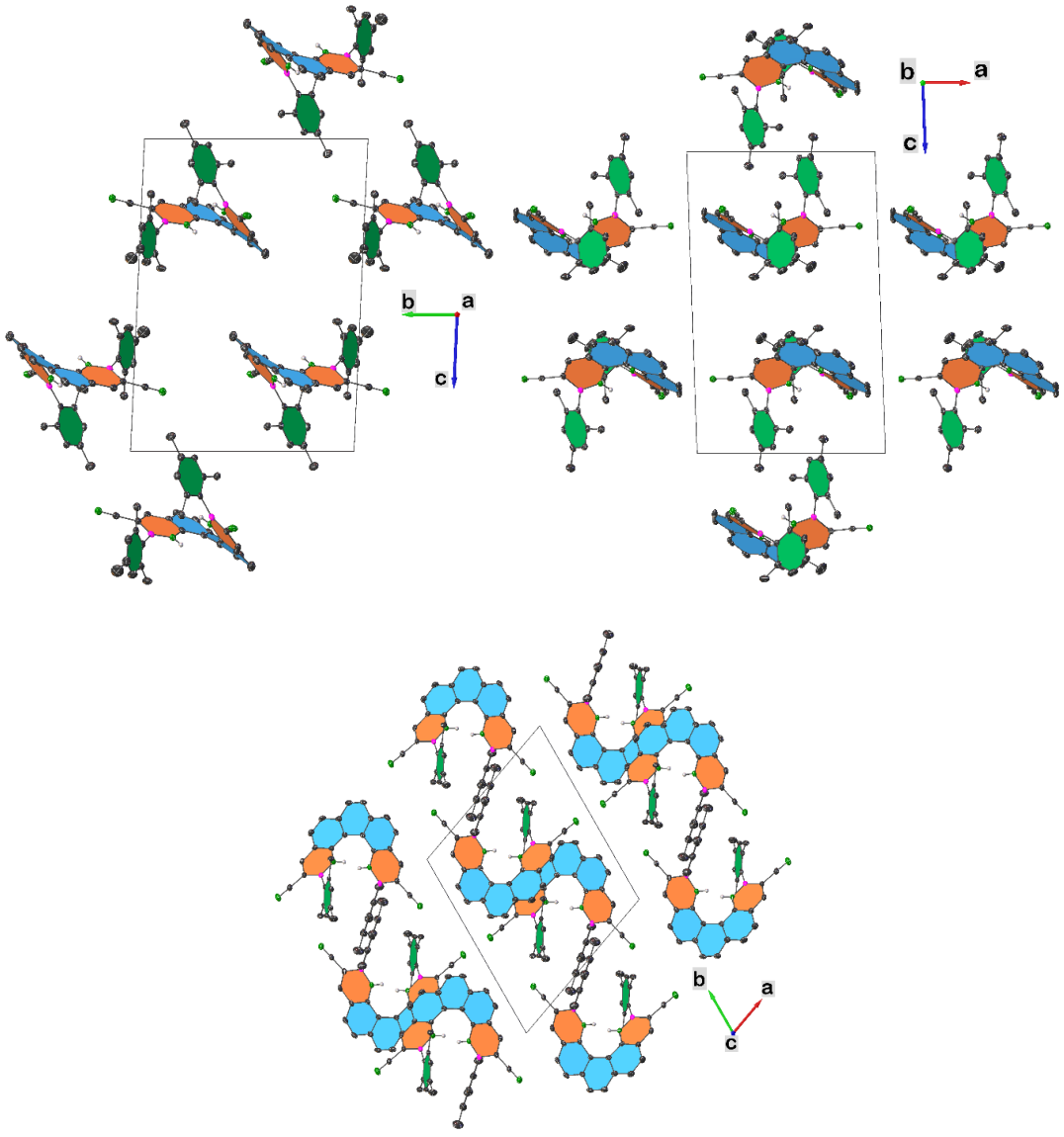

Fig. S8. Unit cell packing view of a **BN[5]-(CN)$_2$** crystal along the *a*, *b* and *c*-axes

Table S17. Crystal data and structure refinement for **BN[5]-(CN)$_2$**.

Empirical formula	$C_{38.5}H_{33}B_2ClN_4$
Formula weight	608.76
Temperature/K	100.00
Crystal system	triclinic
Space group	P-1
a/Å	13.0913(14)
b/Å	14.9897(16)
c/Å	19.698(2)
α/°	86.550(4)
β/°	86.961(4)
γ/°	69.776(4)
Volume/Å^3	3618.3(7)
Z	4
ρ_{calc}g/cm^3	1.117
μ/mm^{-1}	0.136
F(000)	1276.0
Crystal size/mm^3	0.403 × 0.129 × 0.038
Radiation	MoKα (λ = 0.71073)
2Θ range for data collection/°	4.01 to 57.18
Index ranges	-17 ≤ h ≤ 17, -20 ≤ k ≤ 19, -26 ≤ l ≤ 26
Reflections collected	112802
Independent reflections	18466 [R_{int} = 0.0673, R_{sigma} = 0.0497]
Data/restraints/parameters	18466/0/848
Goodness-of-fit on F^2	1.026
Final R indexes [I>=2σ (I)]	R_1 = 0.0610, wR_2 = 0.1369
Final R indexes [all data]	R_1 = 0.0950, wR_2 = 0.1527
Largest diff. peak/hole / e Å^{-3}	0.46/-0.81

Table S18. Fractional Atomic Coordinates (×10^4) and Equivalent Isotropic Displacement Parameters (Å^2×10^3) for **BN[5]-(CN)$_2$**. U_{eq} is defined as 1/3 of the trace of the orthogonalized U_{IJ} tensor.

Atom	*x*	*y*	*z*	$U_{(eq)}$
Cl2	7763.3(6)	1946.4(6)	9487.0(3)	55.6(2)
Cl1	6589.6(8)	709.2(5)	10024.0(6)	75.2(3)
N1	6718.3(13)	2063.2(11)	7245.1(8)	17.7(3)
N5	-137.1(13)	6630.7(11)	8608.1(8)	15.6(3)
N2	4994.1(13)	3710.1(11)	7672.9(8)	17.9(3)
N6	-1070.6(13)	6643.1(11)	7296.9(8)	17.0(3)
N3	8222.4(14)	-1318.5(12)	8090.6(9)	25.7(4)
N4	975.5(14)	4748.0(13)	7536.7(8)	26.3(4)
N7	3566.8(15)	6248.3(14)	9249.8(10)	32.1(4)
C62	417.1(14)	8603.6(13)	9038.0(9)	16.9(4)
C39	-268.0(15)	5756.0(12)	8765.0(9)	15.5(4)
C40	-1260.4(15)	5591.6(13)	8643.7(9)	16.7(4)
C28	3768.1(14)	3205.6(13)	8570.7(10)	17.3(4)
C29	4235.5(15)	3321.7(13)	9179.4(10)	18.5(4)
C38	1894.0(16)	4614.4(14)	7511.0(9)	20.2(4)
C54	592.1(16)	5033.0(13)	9088.7(9)	17.8(4)
C57	929.8(15)	7857.2(13)	8599.9(9)	16.3(4)
C33	3144.9(15)	2604.4(14)	8599.8(10)	19.9(4)
C5	3041.2(15)	4454.9(13)	7439.2(9)	18.2(4)
C55	1590.2(16)	5170.6(13)	9202.9(9)	19.4(4)
C42	-2061.3(15)	6789.3(13)	7648.6(9)	17.4(4)
C61	690.1(15)	9431.1(13)	8983.1(9)	18.0(4)
C2	7334.3(15)	3446.8(14)	7316.4(9)	19.3(4)
C6	3337.6(16)	5001.2(14)	6938.3(10)	21.6(4)
C1	7440.8(15)	2467.3(14)	7470.0(9)	18.4(4)
C58	1698.2(15)	7976.4(14)	8104.1(10)	19.7(4)
C53	461.5(17)	4163.4(13)	9324.1(9)	22.0(4)
C60	1458.1(16)	9542.8(14)	8501.9(10)	20.5(4)
C56	1749.1(15)	6010.9(14)	9027.4(9)	18.6(4)
C52	-519.2(18)	4053.2(14)	9294.0(10)	23.3(4)
C41	-2160.5(15)	6219.8(13)	8246.4(9)	17.7(4)
C59	1939.4(16)	8812.2(14)	8058.6(10)	21.9(4)
C20	5217.8(15)	403.6(13)	7458.3(10)	21.2(4)
C37	8005.4(15)	-526.1(14)	7939.2(10)	21.0(4)
C19	5928.5(15)	725.6(13)	7034.9(10)	19.3(4)
C75	2764.8(16)	6126.0(14)	9161.1(10)	23.5(4)
C4	5282.7(16)	4254.7(13)	7157.2(10)	19.5(4)
C51	-1404.5(17)	4777.2(13)	8988.3(9)	20.6(4)
C16	8347.1(15)	1859.1(14)	7821.9(10)	21.7(4)
C65	-396.9(16)	8523.4(14)	9589.8(10)	22.7(4)
C18	7760.4(16)	475.7(14)	7764.4(10)	20.5(4)
C66	203.9(17)	6912.0(15)	6259.9(10)	23.8(4)
C7	4435.6(16)	4942.6(14)	6803.5(10)	22.9(4)
C45	-3004.5(16)	7456.1(14)	7362.4(10)	22.3(4)
C30	4041.5(15)	2870.4(14)	9785.6(10)	20.2(4)
C3	6393.7(16)	4185.2(14)	7025.5(10)	20.5(4)
C36	2663.9(17)	2400.6(15)	7972.0(11)	25.5(4)
C13	8274.6(16)	3691.9(15)	7406.7(10)	23.4(4)
C34	4954.2(17)	3924.4(14)	9203.0(10)	23.8(4)
C50	-2468.9(18)	4713.8(15)	9069.6(10)	25.3(4)
C31	3428.7(16)	2268.1(14)	9814.6(10)	23.5(4)
C17	8475.4(16)	883.4(14)	7965.6(10)	23.3(4)
C15	9176.5(16)	2199.5(16)	8000.7(11)	27.4(5)
C32	2993.6(16)	2143.7(14)	9217.1(10)	22.3(4)
C14	9163.3(17)	3070.9(16)	7775.7(11)	28.0(5)
C49	-3345.9(18)	5432.9(15)	8846.3(11)	27.1(5)
C10	6558.4(17)	4969.8(15)	6652.0(11)	25.4(4)
C47	-4154.7(17)	6875.3(15)	8127.3(11)	26.6(4)
C63	2285.3(18)	7192.1(15)	7625.2(11)	28.2(5)
C48	-3218.1(16)	6196.6(14)	8416.9(10)	22.1(4)
C44	-2926.3(17)	8018.2(15)	6766.1(10)	26.5(4)
C12	8359.2(18)	4547.0(15)	7085.1(11)	28.2(5)
C71	651.0(17)	6088.2(15)	5878.6(10)	24.9(4)
C24	5890.0(18)	682.4(15)	6325.5(11)	27.2(4)
C46	-4048.4(17)	7517.9(16)	7636.6(11)	27.3(4)
C25	5249.8(17)	406.3(16)	8222.9(11)	26.5(4)
C74	144.3(19)	5319.4(16)	5918.2(11)	29.1(5)
C64	1787.9(17)	10413.7(15)	8461.8(12)	28.3(5)
C43	-1963.4(18)	7895.8(15)	6421.2(10)	27.1(4)
C21	4468.2(17)	76.4(15)	7171.4(12)	27.9(5)
C67	702.6(19)	7610.6(16)	6186.3(10)	29.2(5)
C11	7573.8(18)	5113.8(16)	6681.2(11)	28.7(5)
N8	-1977(2)	8870.8(18)	5295.0(11)	59.2(7)
C8	4678.5(18)	5618.4(16)	6347.2(11)	30.0(5)
C9	5699.1(19)	5651.9(16)	6296.5(12)	31.4(5)
C70	1557.2(19)	5978.9(17)	5444.9(10)	30.2(5)
C22	4416(2)	36.3(17)	6475.0(13)	35.2(5)
C23	5140(2)	334.9(18)	6060.1(12)	37.7(6)
C27	6653(2)	1006.8(19)	5853.6(11)	37.2(6)
C68	1610(2)	7477.6(18)	5745.2(11)	35.0(5)
C69	2040(2)	6675.2(18)	5367.8(11)	35.3(5)
B3	809.2(17)	6847.9(15)	8724.3(10)	16.0(4)
C72	249(2)	8524.0(17)	6564.8(12)	37.5(6)
C76	-1972(2)	8447.9(17)	5797.7(12)	38.3(6)
B2	3920.7(17)	3765.6(15)	7896.6(11)	17.7(4)
B1	6785.6(17)	1093.3(15)	7349.3(11)	18.1(4)
C35	3263(2)	1772.9(18)	10478.5(12)	35.5(5)
C77	6909(2)	1733.9(17)	10148.4(12)	35.7(5)
B4	-910.9(19)	7131.5(16)	6678.7(11)	22.1(5)
C73	2985(2)	6567(2)	4861.1(13)	48.0(7)
C26	3615(3)	-351(2)	6180.5(16)	58.4(8)

Table S19. Anisotropic Displacement Parameters (Å^2×10^3) for **BN[5]-(CN)$_2$**. The Anisotropic displacement factor exponent takes the form: $-2\pi^2[h^2a^{*2}U_{11}+2hka^*b^*U_{12}+\ldots]$.

Atom	U_{11}	U_{22}	U_{33}	U_{23}	U_{13}	U_{12}
Cl2	52.5(4)	58.7(4)	37.1(3)	-1.0(3)	6.0(3)	3.0(3)
Cl1	75.3(6)	35.5(4)	117.5(8)	-1.9(4)	-42.4(5)	-17.3(4)
N1	13.0(8)	18.0(8)	20.1(8)	-2.8(6)	-1.7(6)	-2.3(6)
N5	15.6(8)	12.4(7)	17.2(7)	-0.2(6)	-0.3(6)	-3.1(6)
N2	14.5(8)	14.9(8)	22.8(8)	0.0(6)	-0.7(6)	-3.4(6)
N6	17.2(8)	15.4(8)	17.5(8)	-0.9(6)	-0.4(6)	-4.5(7)
N3	23.2(9)	22.4(9)	29.0(9)	-2.6(7)	-3.0(7)	-4.0(7)
N4	18.4(9)	36.1(10)	21.1(8)	-4.9(7)	-0.4(7)	-4.5(8)
N7	21.6(10)	30.1(10)	41.7(11)	-2.5(8)	-6.5(8)	-4.4(8)

Atom	U_{11}	U_{22}	U_{33}	U_{23}	U_{13}	U_{12}
C62	12.2(9)	17.5(9)	19.7(9)	-0.2(7)	-2.6(7)	-3.4(7)
C39	19.9(9)	12.8(8)	13.5(8)	-1.2(6)	3.3(7)	-5.7(7)
C40	20.7(9)	13.6(9)	15.6(8)	-3.2(7)	4.2(7)	-5.7(7)
C28	11.1(8)	13.7(9)	24.2(9)	-3.9(7)	2.5(7)	-0.8(7)
C29	12.2(9)	13.5(9)	27.4(10)	-0.9(7)	-0.3(7)	-1.4(7)
C38	20.9(10)	19.5(9)	16.6(9)	-3.1(7)	-1.4(7)	-2.0(8)
C54	21.7(10)	14.0(9)	14.2(8)	-2.9(7)	3.4(7)	-2.0(7)
C57	13.8(9)	15.7(9)	18.3(9)	-0.8(7)	-2.7(7)	-3.5(7)
C33	14.0(9)	18.5(9)	25.4(10)	-4.1(7)	2.3(7)	-3.4(7)
C5	14.6(9)	16.1(9)	22.1(9)	-3.9(7)	1.0(7)	-2.6(7)
C55	20.2(10)	16.8(9)	15.6(9)	-1.8(7)	-1.2(7)	0.9(7)
C42	18.9(9)	15.1(9)	19.5(9)	-3.6(7)	-2.0(7)	-7.1(7)
C61	16.8(9)	15.2(9)	21.5(9)	-2.9(7)	-4.2(7)	-3.9(7)
C2	16.8(9)	20.9(9)	20.5(9)	-7.2(7)	6.7(7)	-6.8(8)
C6	20.4(10)	16.4(9)	24.0(10)	-1.6(7)	-2.8(8)	-0.7(8)
C1	13.7(9)	20.3(9)	21.0(9)	-6.5(7)	3.3(7)	-5.2(7)
C58	17.7(9)	19.4(9)	21.1(9)	-0.9(7)	0.4(7)	-5.6(8)
C53	30.6(11)	12.3(9)	17.4(9)	-0.7(7)	2.0(8)	-0.5(8)
C60	19.0(10)	16.7(9)	26.6(10)	2.6(7)	-6.2(8)	-7.1(8)
C56	15.8(9)	20.1(9)	18.3(9)	-3.4(7)	0.1(7)	-3.8(7)
C52	37.9(12)	12.9(9)	18.0(9)	0.5(7)	4.6(8)	-8.4(8)
C41	19.6(9)	13.9(9)	21.0(9)	-4.6(7)	1.4(7)	-7.3(7)
C59	17.7(10)	23.6(10)	24.3(10)	0.8(8)	2.3(8)	-7.7(8)
C20	15.4(9)	15.0(9)	29.8(10)	-1.9(8)	-4.5(8)	-0.4(7)
C37	14.7(9)	23.9(10)	21.6(9)	-3.5(8)	-2.6(7)	-2.5(8)
C19	16.9(9)	14.2(9)	24.3(10)	-2.7(7)	-4.3(7)	-1.2(7)
C75	18.9(10)	20.4(10)	26.5(10)	-3.3(8)	-1.6(8)	-0.3(8)
C4	20.4(10)	16.3(9)	21.4(9)	-3.5(7)	3.8(7)	-5.9(8)
C51	29.4(11)	17.4(9)	17.1(9)	-2.7(7)	4.6(8)	-11.0(8)
C16	14.2(9)	25.9(10)	24.1(10)	-6.0(8)	1.2(7)	-5.2(8)
C65	21.9(10)	18.3(9)	27.9(10)	-6.3(8)	5.7(8)	-6.8(8)
C18	17.4(9)	19.7(9)	21.1(9)	-2.5(7)	-0.6(7)	-2.0(8)
C66	29.7(11)	24.7(10)	15.4(9)	4.8(8)	0.4(8)	-8.4(9)
C7	22.4(10)	18.7(10)	25.6(10)	0.1(8)	1.5(8)	-4.9(8)
C45	23.4(10)	20.7(10)	22.7(10)	-2.3(8)	-4.0(8)	-6.7(8)
C30	16.8(9)	20.1(9)	21.9(9)	0.6(7)	-2.8(7)	-4.1(8)
C3	19.5(10)	20.7(10)	22.6(9)	-4.5(8)	4.6(7)	-8.7(8)
C36	23.9(11)	22.8(10)	32.8(11)	-5.4(8)	0.0(8)	-11.4(9)
C13	19.4(10)	26.0(10)	26.4(10)	-11.5(8)	6.4(8)	-9.5(8)
C34	25.4(11)	21.7(10)	27.1(10)	1.1(8)	-4.2(8)	-11.7(9)
C50	34.2(12)	21.5(10)	25.7(10)	-3.5(8)	6.9(9)	-17.4(9)
C31	19.4(10)	22.7(10)	27.7(10)	1.0(8)	3.8(8)	-7.3(8)
C17	16.1(9)	24.3(10)	24.2(10)	-1.3(8)	-3.9(8)	0.1(8)
C15	15.1(10)	30.6(11)	36.0(12)	-8.7(9)	-4.0(8)	-5.5(9)
C32	17.1(10)	20.3(10)	32.1(11)	-1.3(8)	3.8(8)	-10.4(8)
C14	16.5(10)	34.5(12)	36.3(12)	-14.5(9)	2.6(8)	-11.3(9)
C49	27.1(11)	29.7(11)	31.4(11)	-7.1(9)	8.6(9)	-18.9(9)
C10	26.1(11)	22.8(10)	28.3(11)	-3.9(8)	8.5(8)	-10.4(9)
C47	16.2(10)	28.8(11)	36.7(12)	-6.2(9)	0.3(8)	-9.7(9)
C63	31.1(12)	25.7(11)	26.5(11)	-6.1(8)	8.6(9)	-8.8(9)
C48	22.0(10)	20.5(10)	26.2(10)	-6.0(8)	2.4(8)	-10.3(8)
C44	26.0(11)	23.3(10)	25.0(10)	-0.4(8)	-7.7(8)	-0.8(9)
C12	25.3(11)	28.6(11)	37.6(12)	-12.4(9)	11.2(9)	-18.1(9)
C71	27.8(11)	27.6(11)	17.3(9)	2.4(8)	-0.9(8)	-7.5(9)
C24	31.1(12)	24.5(11)	25.7(10)	-1.1(8)	-6.6(9)	-8.5(9)
C46	19.1(10)	27.3(11)	33.5(11)	-3.8(9)	-4.4(8)	-4.6(9)
C25	22.6(11)	27.7(11)	29.1(11)	-3.1(9)	3.1(8)	-8.5(9)
C74	33.0(12)	31.2(12)	22.9(10)	-4.2(9)	2.1(9)	-10.8(10)
C64	22.9(11)	19.7(10)	44.2(13)	1.3(9)	-1.5(9)	-10.1(9)
C43	33.6(12)	24.6(11)	18.8(9)	1.5(8)	-2.2(8)	-4.7(9)
C21	19.3(10)	23.9(11)	40.6(12)	-1.4(9)	-5.5(9)	-6.9(8)
C67	38.5(13)	29.5(11)	20.4(10)	3.9(8)	2.4(9)	-14.1(10)
C11	30.4(12)	26.5(11)	33.6(11)	-5.8(9)	10.2(9)	-16.2(9)
N8	68.8(17)	49.2(14)	28.5(11)	14.9(10)	10.7(11)	14.9(12)
C8	29.9(12)	24.3(11)	32.9(11)	5.8(9)	0.1(9)	-6.7(9)
C9	36.3(13)	24.0(11)	34.7(12)	5.3(9)	5.8(10)	-13.4(10)
C70	34.0(12)	35.2(12)	19.2(10)	-3.3(9)	5.7(9)	-9.5(10)
C22	32.6(13)	33.5(12)	42.9(13)	-1.0(10)	-16.9(10)	-13.6(10)
C23	50.9(15)	40.3(14)	27.1(11)	0.6(10)	-15.6(11)	-20.6(12)
C27	52.0(15)	43.2(14)	21.9(11)	-3.3(10)	-1.3(10)	-23.0(12)
C68	44.6(14)	38.9(13)	27.3(11)	3.7(10)	4.9(10)	-23.6(11)
C69	40.2(14)	46.4(14)	20.5(10)	2.3(10)	7.2(9)	-18.3(12)
B3	15.7(10)	15.7(10)	14.6(9)	-3.0(7)	1.8(8)	-2.9(8)
C72	48.6(15)	31.1(12)	36.3(13)	-0.7(10)	6.8(11)	-19.5(11)
C76	41.5(14)	32.1(12)	25.3(11)	4.2(9)	1.9(10)	6.3(11)
B2	15.7(10)	15.7(10)	21.1(10)	-5.4(8)	1.9(8)	-4.0(8)
B1	14.8(10)	18.4(10)	17.9(10)	-4.6(8)	2.1(8)	-1.4(8)
C35	41.2(14)	40.9(14)	30.8(12)	6.3(10)	2.9(10)	-24.1(12)
C77	34.1(13)	28.3(12)	39.7(13)	-1.5(10)	-8.9(10)	-3.3(10)
B4	25.8(12)	20.4(11)	19.7(10)	-1.0(8)	-2.0(9)	-7.0(9)
C73	49.4(16)	66.3(19)	31.5(13)	-2.1(12)	16.8(12)	-26.4(15)
C26	58.6(19)	71(2)	60.6(18)	-4.1(16)	-27.6(15)	-37.8(17)

Table S20. Bond Lengths for **BN[5]-(CN)$_2$**.

Atom	Atom	Length/Å	Atom	Atom	Length/Å
Cl2	C77	1.758(3)	C41	C48	1.419(3)
Cl1	C77	1.759(3)	C20	C19	1.405(3)
N1	C1	1.389(2)	C20	C25	1.509(3)
N1	B1	1.429(3)	C20	C21	1.396(3)
N5	C39	1.395(2)	C37	C18	1.447(3)
N5	B3	1.418(3)	C19	C24	1.407(3)
N2	C4	1.383(2)	C19	B1	1.577(3)
N2	B2	1.426(3)	C4	C7	1.408(3)
N6	C42	1.392(2)	C4	C3	1.433(3)
N6	B4	1.426(3)	C51	C50	1.429(3)
N3	C37	1.146(3)	C16	C17	1.426(3)
N4	C38	1.147(3)	C16	C15	1.417(3)
N7	C75	1.150(3)	C18	C17	1.368(3)
C62	C57	1.408(3)	C18	B1	1.535(3)
C62	C61	1.402(3)	C66	C71	1.413(3)
C62	C65	1.510(3)	C66	C67	1.410(3)
C39	C40	1.438(3)	C66	B4	1.579(3)
C39	C54	1.414(3)	C7	C8	1.421(3)
C40	C41	1.459(3)	C45	C44	1.424(3)
C40	C51	1.426(3)	C45	C46	1.417(3)
C28	C29	1.421(3)	C30	C31	1.397(3)
C28	C33	1.406(3)	C3	C10	1.423(3)
C28	B2	1.569(3)	C13	C14	1.417(3)
C29	C30	1.392(3)	C13	C12	1.432(3)
C29	C34	1.517(3)	C50	C49	1.347(3)
C38	C5	1.437(3)	C31	C32	1.384(3)
C54	C55	1.422(3)	C31	C35	1.507(3)
C54	C53	1.420(3)	C15	C14	1.348(3)
C57	C58	1.413(3)	C49	C48	1.434(3)
C57	B3	1.578(3)	C10	C11	1.423(3)
C33	C36	1.510(3)	C10	C9	1.415(3)
C33	C32	1.401(3)	C47	C48	1.416(3)
C5	C6	1.370(3)	C47	C46	1.359(3)
C5	B2	1.543(3)	C44	C43	1.360(3)
C55	C56	1.368(3)	C12	C11	1.347(3)
C42	C41	1.439(3)	C71	C74	1.512(3)
C42	C45	1.412(3)	C71	C70	1.392(3)
C61	C60	1.390(3)	C24	C23	1.396(3)
C2	C1	1.441(3)	C24	C27	1.510(3)
C2	C3	1.458(3)	C43	C76	1.437(3)
C2	C13	1.423(3)	C43	B4	1.543(3)
C6	C7	1.421(3)	C21	C22	1.383(3)
C1	C16	1.408(3)	C67	C68	1.398(3)
C58	C59	1.391(3)	C67	C72	1.516(3)
C58	C63	1.515(3)	N8	C76	1.142(3)
C53	C52	1.355(3)	C8	C9	1.352(3)
C60	C59	1.392(3)	C70	C69	1.392(3)
C60	C64	1.507(3)	C22	C23	1.391(4)
C56	C75	1.438(3)	C22	C26	1.517(3)
C56	B3	1.538(3)	C68	C69	1.382(3)
C52	C51	1.417(3)	C69	C73	1.518(3)
C56	B3	1.538(3)	C68	C69	1.382(3)

Table S21. Bond Angles for **BN[5]-(CN)$_2$**.

Atom	Atom	Atom	Angle/°	Atom	Atom	Atom	Angle/°
C1	N1	B1	126.56(17)	C17	C18	C37	117.01(17)
C39	N5	B3	125.31(16)	C17	C18	B1	118.39(18)
C4	N2	B2	127.29(17)	C71	C66	B4	122.03(19)
C42	N6	B4	125.79(17)	C67	C66	C71	118.02(19)

Atom	Atom	Atom	Angle/°	Atom	Atom	Atom	Angle/°
C57	C62	C65	121.58(16)	C67	C66	B4	119.41(19)
C61	C62	C57	119.85(17)	C4	C7	C6	120.11(18)
C61	C62	C65	118.52(16)	C4	C7	C8	119.52(19)
N5	C39	C40	122.27(16)	C8	C7	C6	120.22(19)
N5	C39	C54	117.85(17)	C42	C45	C44	120.75(19)
C54	C39	C40	119.78(16)	C42	C45	C46	119.93(18)
C39	C40	C41	125.90(16)	C46	C45	C44	119.12(19)
C51	C40	C39	116.40(17)	C29	C30	C31	122.01(18)
C51	C40	C41	117.52(17)	C4	C3	C2	124.99(17)
C29	C28	B2	120.10(16)	C10	C3	C2	118.55(17)
C33	C28	C29	118.11(17)	C10	C3	C4	115.95(18)
C33	C28	B2	121.76(17)	C2	C13	C12	119.82(19)
C28	C29	C34	122.67(17)	C14	C13	C2	120.89(19)
C30	C29	C28	119.91(17)	C14	C13	C12	119.16(19)
C30	C29	C34	117.41(17)	C49	C50	C51	120.64(18)
N4	C38	C5	176.9(2)	C30	C31	C35	120.27(19)
C39	C54	C55	120.91(17)	C32	C31	C30	117.72(18)
C39	C54	C53	120.34(18)	C32	C31	C35	122.01(19)
C53	C54	C55	118.73(17)	C18	C17	C16	123.25(18)
C62	C57	C58	118.39(17)	C14	C15	C16	120.4(2)
C62	C57	B3	121.57(16)	C31	C32	C33	122.09(18)
C58	C57	B3	119.31(16)	C15	C14	C13	120.63(19)
C28	C33	C36	121.76(18)	C50	C49	C48	120.65(19)
C32	C33	C28	120.11(18)	C11	C10	C3	119.5(2)
C32	C33	C36	118.07(17)	C9	C10	C3	120.92(19)
C38	C5	B2	125.12(17)	C9	C10	C11	119.36(19)
C6	C5	C38	115.43(17)	C46	C47	C48	120.17(19)
C6	C5	B2	119.38(17)	C41	C48	C49	119.95(19)
C56	C55	C54	121.93(17)	C47	C48	C41	121.18(18)
N6	C42	C41	122.09(17)	C47	C48	C49	118.68(18)
N6	C42	C45	117.78(17)	C43	C44	C45	122.12(19)
C45	C42	C41	119.82(17)	C11	C12	C13	120.98(19)
C60	C61	C62	121.76(17)	C66	C71	C74	121.02(18)
C1	C2	C3	126.34(17)	C70	C71	C66	120.4(2)
C13	C2	C1	116.31(18)	C70	C71	C74	118.56(19)
C13	C2	C3	117.13(18)	C19	C24	C27	120.46(19)
C5	C6	C7	122.80(18)	C23	C24	C19	119.4(2)
N1	C1	C2	122.79(17)	C23	C24	C27	120.1(2)
N1	C1	C16	117.09(17)	C47	C46	C45	120.4(2)
C16	C1	C2	119.98(17)	C44	C43	C76	118.4(2)
C57	C58	C63	120.67(17)	C44	C43	B4	119.75(19)
C59	C58	C57	120.19(17)	C76	C43	B4	121.8(2)
C59	C58	C63	119.13(17)	C22	C21	C20	121.9(2)
C52	C53	C54	120.10(18)	C66	C67	C72	120.9(2)
C61	C60	C59	118.01(17)	C68	C67	C66	120.0(2)
C61	C60	C64	121.83(18)	C68	C67	C72	119.1(2)
C59	C60	C64	120.15(18)	C12	C11	C10	120.8(2)
C55	C56	C75	120.19(18)	C9	C8	C7	120.1(2)
C55	C56	B3	119.31(17)	C8	C9	C10	120.8(2)
C75	C56	B3	120.41(17)	C69	C70	C71	121.4(2)
C53	C52	C51	120.54(18)	C21	C22	C23	117.9(2)
C42	C41	C40	125.79(17)	C21	C22	C26	120.5(2)
C48	C41	C40	117.51(17)	C23	C22	C26	121.6(2)
C48	C41	C42	116.35(17)	C22	C23	C24	122.1(2)
C58	C59	C60	121.75(18)	C69	C68	C67	121.9(2)
C19	C20	C25	120.96(17)	C70	C69	C73	120.4(2)
C21	C20	C19	119.86(19)	C68	C69	C70	118.3(2)
C21	C20	C25	119.17(19)	C68	C69	C73	121.2(2)
N3	C37	C18	178.0(2)	N5	B3	C57	125.51(17)
C20	C19	C24	118.85(18)	N5	B3	C56	114.44(17)
C20	C19	B1	120.64(17)	C56	B3	C57	119.99(16)
C24	C19	B1	120.48(18)	N8	C76	C43	178.6(3)
N7	C75	C56	177.3(2)	N2	B2	C28	118.83(17)
N2	C4	C7	117.54(17)	N2	B2	C5	112.30(17)
N2	C4	C3	121.48(18)	C5	B2	C28	128.73(17)
C7	C4	C3	120.75(18)	N1	B1	C19	120.83(17)
C40	C51	C50	119.86(18)	N1	B1	C18	113.98(17)
C52	C51	C40	121.10(18)	C18	B1	C19	125.18(18)
C52	C51	C50	118.90(18)	Cl2	C77	Cl1	111.77(14)
C1	C16	C17	120.65(18)	N6	B4	C66	125.23(19)
C1	C16	C15	120.02(19)	N6	B4	C43	113.56(19)
C15	C16	C17	119.22(18)	C43	B4	C66	121.16(18)
C37	C18	B1	124.56(17)				

Table S22. Torsion Angles for **BN[5]-(CN)$_2$**.

A	B	C	D	Angle/°	A	B	C	D	Angle/°
N1	C1	C16	C17	-3.0(3)	C75	C56	B3	N5	179.00(17)
N1	C1	C16	C15	173.18(17)	C75	C56	B3	C57	-3.7(3)
N5	C39	C40	C41	11.5(3)	C4	N2	B2	C28	-169.56(17)
N5	C39	C40	C51	-163.39(16)	C4	N2	B2	C5	6.5(3)
N5	C39	C54	C55	-4.7(2)	C4	C7	C8	C9	-5.6(3)
N5	C39	C54	C53	173.45(16)	C4	C3	C10	C11	160.08(18)
N2	C4	C7	C6	-5.6(3)	C4	C3	C10	C9	-14.8(3)
N2	C4	C7	C8	170.00(18)	C51	C40	C41	C42	-150.44(18)
N2	C4	C3	C2	11.6(3)	C51	C40	C41	C48	22.5(2)
N2	C4	C3	C10	-160.05(18)	C51	C50	C49	C48	11.3(3)
N6	C42	C41	C40	14.5(3)	C16	C15	C14	C13	5.4(3)
N6	C42	C41	C48	-158.50(17)	C65	C62	C57	C58	-178.80(17)
N6	C42	C45	C44	-5.4(3)	C65	C62	C57	B3	-8.6(3)
N6	C42	C45	C46	169.54(17)	C65	C62	C61	C60	177.94(17)
C62	C57	C58	C59	0.4(3)	C66	C71	C70	C69	-0.7(3)
C62	C57	C58	C63	179.21(18)	C66	C67	C68	C69	0.5(4)
C62	C57	B3	N5	73.5(2)	C7	C4	C3	C2	-174.09(18)
C62	C57	B3	C56	-103.4(2)	C7	C4	C3	C10	14.3(3)
C62	C61	C60	C59	1.4(3)	C7	C8	C9	C10	5.2(3)
C62	C61	C60	C64	-177.33(18)	C45	C42	C41	C40	-172.05(17)
C39	N5	B3	C57	-175.06(16)	C45	C42	C41	C48	15.0(3)
C39	N5	B3	C56	2.0(3)	C45	C44	C43	C76	175.6(2)
C39	C40	C41	C42	34.8(3)	C45	C44	C43	B4	-0.4(3)
C39	C40	C41	C48	-152.33(18)	C30	C31	C32	C33	-0.5(3)
C39	C40	C51	C52	-14.9(3)	C3	C2	C1	N1	11.8(3)
C39	C40	C51	C50	160.84(17)	C3	C2	C1	C16	-172.74(18)
C39	C54	C55	C56	2.2(3)	C3	C2	C13	C14	170.59(18)
C39	C54	C53	C52	-5.8(3)	C3	C2	C13	C12	-13.5(3)
C40	C39	C54	C55	178.78(16)	C3	C4	C7	C6	179.82(18)
C40	C39	C54	C53	-3.1(3)	C3	C4	C7	C8	-4.5(3)
C40	C41	C48	C49	-14.4(3)	C3	C10	C11	C12	-3.5(3)
C40	C41	C48	C47	170.71(17)	C3	C10	C9	C8	5.3(3)
C40	C51	C50	C49	-2.5(3)	C36	C33	C32	C31	178.31(19)
C28	C29	C30	C31	2.5(3)	C13	C2	C1	N1	-162.72(17)
C28	C33	C32	C31	0.9(3)	C13	C2	C1	C16	12.8(3)
C29	C28	C33	C36	-176.93(17)	C13	C2	C3	C4	-151.24(18)
C29	C28	C33	C32	0.4(3)	C13	C2	C3	C10	20.2(3)
C29	C28	B2	N2	52.3(2)	C13	C12	C11	C10	10.7(3)
C29	C28	B2	C5	-123.0(2)	C34	C29	C30	C31	-177.32(18)
C29	C30	C31	C32	-1.3(3)	C50	C49	C48	C41	-2.6(3)
C29	C30	C31	C35	178.36(19)	C50	C49	C48	C47	172.43(19)
C38	C5	C6	C7	179.26(18)	C17	C16	C15	C14	169.32(19)
C38	C5	B2	N2	175.96(17)	C17	C18	B1	N1	-2.6(3)
C38	C5	B2	C28	-8.5(3)	C17	C18	B1	C19	175.71(18)
C54	C39	C40	C41	-172.21(17)	C15	C16	C17	C18	-174.73(19)
C54	C39	C40	C51	12.9(2)	C14	C13	C12	C11	174.2(2)
C54	C55	C56	C75	179.04(17)	C63	C58	C59	C60	-177.46(19)
C54	C55	C56	B3	2.5(3)	C48	C47	C46	C45	6.3(3)
C54	C53	C52	C51	4.1(3)	C44	C45	C46	C47	168.3(2)
C57	C62	C61	C60	0.3(3)	C44	C43	B4	N6	-2.6(3)
C57	C58	C59	C60	1.4(3)	C44	C43	B4	C66	175.0(2)
C33	C28	C29	C30	-2.0(3)	C12	C13	C14	C15	-170.37(19)
C33	C28	C29	C34	177.82(17)	C71	C66	C67	C68	0.1(3)
C33	C28	B2	N2	-129.74(19)	C71	C66	C67	C72	178.3(2)
C33	C28	B2	C5	55.0(3)	C71	C66	B4	N6	72.8(3)
C5	C6	C7	C4	4.7(3)	C71	C66	B4	C43	-104.5(2)
C5	C6	C7	C8	-170.9(2)	C71	C70	C69	C68	1.3(3)
C55	C54	C53	C52	172.39(17)	C71	C70	C69	C73	-176.4(2)
C55	C56	B3	N5	-4.5(3)	C24	C19	B1	N1	67.0(3)
C55	C56	B3	C57	172.76(17)	C24	C19	B1	C18	-111.2(2)
C42	N6	B4	C66	-175.77(18)	C46	C45	C44	C43	-170.4(2)
C42	N6	B4	C43	1.7(3)	C46	C47	C48	C41	5.3(3)
C42	C41	C48	C49	159.22(18)	C46	C47	C48	C49	-169.66(19)
C42	C41	C48	C47	-15.7(3)	C25	C20	C19	C24	178.11(18)
C42	C45	C44	C43	4.6(3)	C25	C20	C19	B1	0.4(3)
C42	C45	C46	C47	-6.8(3)	C25	C20	C21	C22	-178.5(2)
C61	C62	C57	C58	-1.2(3)	C74	C71	C70	C69	177.8(2)
C61	C62	C57	B3	168.96(17)	C64	C60	C59	C58	176.53(19)
C61	C60	C59	C58	-2.3(3)	C21	C20	C19	C24	-2.0(3)
C2	C1	C16	C17	-178.73(17)	C21	C20	C19	B1	-179.69(18)
C2	C1	C16	C15	-2.6(3)	C21	C22	C23	C24	-1.1(4)

A	B	C	D	Angle/°	A	B	C	D	Angle/°
C2	C3	C10	C11	-12.1(3)	C67	C66	C71	C74	-178.53(19)
C2	C3	C10	C9	173.05(19)	C67	C66	C71	C70	0.0(3)
C2	C13	C14	C15	5.6(3)	C67	C66	B4	N6	-115.9(2)
C2	C13	C12	C11	-1.8(3)	C67	C66	B4	C43	66.9(3)
C6	C5	B2	N2	-7.1(3)	C67	C68	C69	C70	-1.2(4)
C6	C5	B2	C28	168.47(18)	C67	C68	C69	C73	176.5(2)
C6	C7	C8	C9	170.0(2)	C11	C10	C9	C8	-169.5(2)
C1	N1	B1	C19	-177.32(17)	C9	C10	C11	C12	171.4(2)
C1	N1	B1	C18	1.1(3)	C27	C24	C23	C22	-179.4(2)
C1	C2	C3	C4	34.3(3)	B3	N5	C39	C40	178.86(17)
C1	C2	C3	C10	-154.24(19)	B3	N5	C39	C54	2.5(3)
C1	C2	C13	C14	-14.4(3)	B3	C57	C58	C59	-169.98(17)
C1	C2	C13	C12	161.51(18)	B3	C57	C58	C63	8.8(3)
C1	C16	C17	C18	1.4(3)	C72	C67	C68	C69	-177.7(2)
C1	C16	C15	C14	-6.9(3)	C76	C43	B4	N6	-178.5(2)
C58	C57	B3	N5	-116.4(2)	C76	C43	B4	C66	-0.9(3)
C58	C57	B3	C56	66.7(2)	B2	N2	C4	C7	-0.4(3)
C53	C54	C55	C56	-175.98(17)	B2	N2	C4	C3	174.15(18)
C53	C52	C51	C40	6.6(3)	B2	C28	C29	C30	175.98(17)
C53	C52	C51	C50	-169.18(18)	B2	C28	C29	C34	-4.2(3)
C52	C51	C50	C49	173.27(19)	B2	C28	C33	C36	5.1(3)
C41	C40	C51	C52	169.86(17)	B2	C28	C33	C32	-177.62(17)
C41	C40	C51	C50	-14.5(3)	B2	C5	C6	C7	2.0(3)
C41	C42	C45	C44	-179.19(18)	B1	N1	C1	C2	177.30(18)
C41	C42	C45	C46	-4.2(3)	B1	N1	C1	C16	1.7(3)
C20	C19	C24	C23	0.9(3)	B1	C19	C24	C23	178.6(2)
C20	C19	C24	C27	-179.0(2)	B1	C19	C24	C27	-1.3(3)
C20	C19	B1	N1	-115.3(2)	B1	C18	C17	C16	1.4(3)
C20	C19	B1	C18	66.5(3)	C35	C31	C32	C33	179.9(2)
C20	C21	C22	C23	0.0(3)	B4	N6	C42	C41	175.82(18)
C20	C21	C22	C26	178.1(2)	B4	N6	C42	C45	2.2(3)
C37	C18	C17	C16	179.17(18)	B4	C66	C71	C74	-7.0(3)
C37	C18	B1	N1	179.88(17)	B4	C66	C71	C70	171.49(19)
C37	C18	B1	C19	-1.8(3)	B4	C66	C67	C68	-171.6(2)
C19	C20	C21	C22	1.6(3)	B4	C66	C67	C72	6.6(3)
C19	C24	C23	C22	0.7(4)	C26	C22	C23	C24	-179.2(3)

Table S23. Hydrogen Atom Coordinates (Å×10^4) and Isotropic Displacement Parameters (Å^2×10^3) for **BN[5]-(CN)$_2$**.

Atom	*x*	*y*	*z*	U(eq)
H55	2163.19	4663.99	9406.98	23
H61	341.26	9928.99	9282.65	22
H6	2785.7	5437.87	6669.62	26
H53	1062.79	3658.12	9502.95	26
H52	-614.49	3486.09	9479.32	28
H59	2446.16	8886.6	7716.03	26
H65A	-710.61	8049.08	9471.39	34
H65B	-978.14	9141.77	9633.01	34
H65C	-30.23	8327.24	10022.87	34
H30	4334.73	2975.08	10192.1	24
H36A	1868.17	2684.55	8006.1	38
H36B	2874.35	1710.95	7934.1	38
H36C	2937.16	2674.1	7568.23	38
H34A	5706.37	3543.5	9076.26	36
H34B	4926.02	4143.67	9664.72	36
H34C	4694.46	4475.57	8883.39	36
H50	-2558.78	4159.06	9283.14	30
H17	9087.81	497.34	8213.35	28
H15	9745.29	1811.44	8280.74	33
H32	2579.27	1732.87	9225.86	27
H14	9755.34	3270.29	7865.44	34
H49	-4056.13	5433.99	8974.71	33
H47	-4859.15	6881.56	8276.47	32
H63A	2540.84	7465.74	7214.64	42
H63B	1785.23	6875.91	7499.45	42
H63C	2909.79	6727.07	7851.67	42
H44	-3567.66	8494.01	6604.08	32
H12	8978.56	4717.09	7157.71	34
H46	-4677.33	8011.14	7476.67	33
H25A	5892.22	-114.59	8382.61	40
H25B	4590.24	320.74	8429.25	40
H25C	5287.79	1014.49	8353.24	40
H74A	487.31	4858.84	5569.43	44
H74B	-637.86	5606.72	5841.72	44
H74C	255.1	4994.45	6369.29	44
H64A	2569.97	10224.7	8536.36	42
H64B	1379.78	10849.15	8811.65	42
H64C	1628.54	10733.77	8011.24	42
H21	3979.71	-124.45	7462.82	33
H11	7699.24	5616.1	6412.39	34
H8	4122.98	6047.64	6076.98	36
H9	5840.94	6139.4	6018.86	38
H70	1852.44	5417.26	5196.35	36
H23	5124.36	301.3	5580.9	45
H27A	6673.91	757.42	5402.47	56
H27B	7386.04	769.55	6035.33	56
H27C	6394.57	1703.77	5816.79	56
H68	1941.47	7951.96	5703.59	42
H72A	825.57	8792.18	6609.66	56
H72B	-23.83	8388.73	7018.13	56
H72C	-348.26	8981.71	6311.4	56
H35A	3943.75	1551.69	10724.67	53
H35B	3050.09	1227.15	10387.56	53
H35C	2689.24	2218.02	10754.99	53
H77A	6227.27	2290.41	10174.32	43
H77B	7273.92	1656.93	10586.48	43
H73A	3465.96	5899.49	4866.32	72
H73B	3394.42	6966.35	4985.87	72
H73C	2705.4	6763.57	4403.93	72
H26A	3980.49	-1025.37	6090.26	88
H26B	3343.76	4.66	5754.83	88
H26C	3003.22	-282.83	6506.22	88
H5	-699(18)	7078(16)	8437(11)	17(5)
H1	6167(19)	2461(16)	6986(11)	22(6)
H6A	-490(20)	6178(18)	7465(12)	27(6)
H2	5540(20)	3347(17)	7924(12)	26(6)

3.4. 1,16-Dihydro-2,15-dimesityl-1,16-diaza-2,15-diborahexahelicene (BN[6])

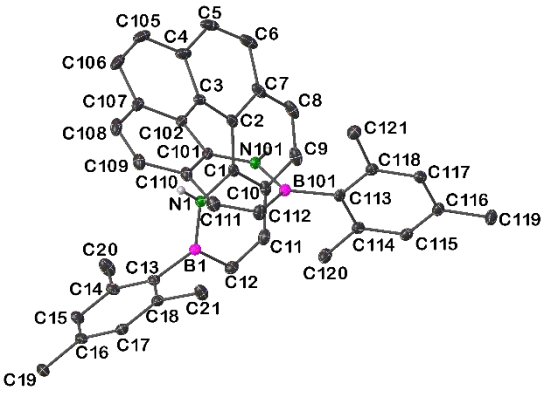

Colorless single crystals of $C_{40}H_{36}B_2N_2$ (**BN[6]**) were grown by dissolving a small amount (ca. 10 mg) of the compound in DCM (ca. 0.5 mL) in a snap cap sample vial. The vial was placed in a larger, capped vial, filled with cyclohexane (ca. 5 mL). Over 7 d, DCM slowly evaporated while cyclohexane was allowed to diffuse into the DCM solution. CCDC Deposition Number: 2192803.

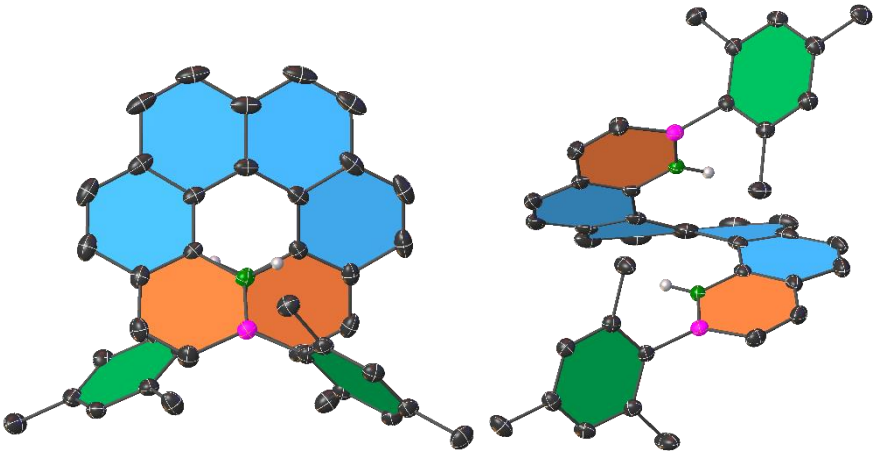

Fig. S9. Frontal view and representation of the helical structure of **BN[6]**.

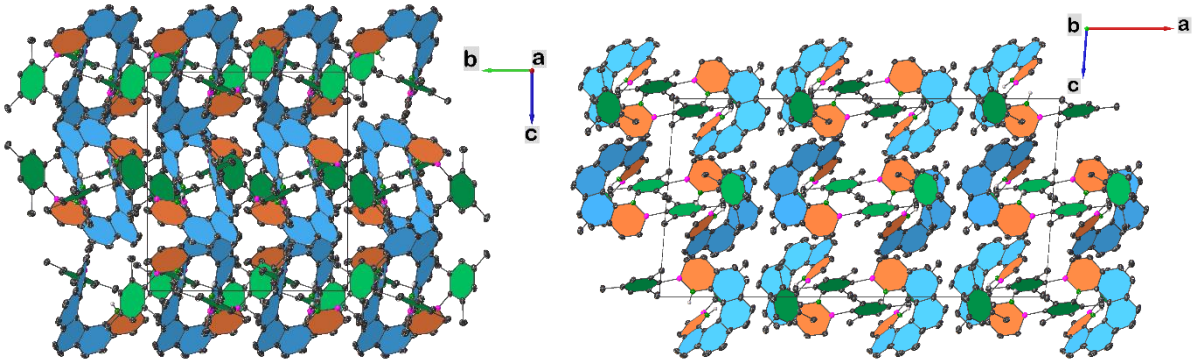

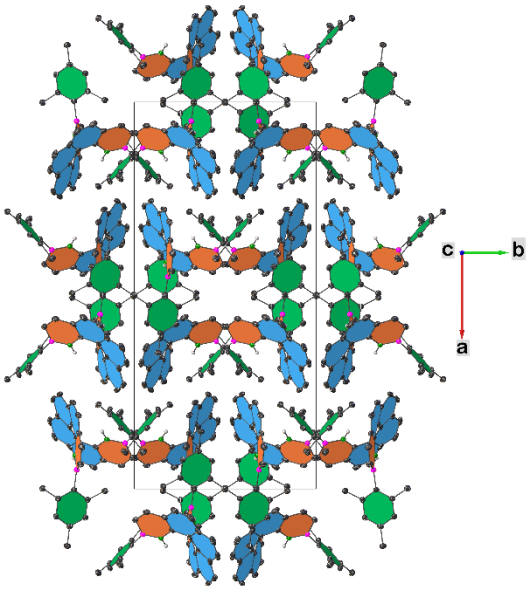

Fig. S10. Unit cell packing view of a **BN[6]** crystal along the a, b and c-axes.

Table S24. Crystal data and structure refinement for **BN[6].**

Empirical formula	$C_{40}H_{36}B_2N_2$
Formula weight	566.33
Temperature/K	100.00
Crystal system	monoclinic
Space group	C2/c
a/Å	29.2871(11)
b/Å	13.7319(5)
c/Å	15.0245(5)
α/°	90
β/°	94.365(2)
γ/°	90
Volume/Å^3	6024.8(4)
Z	8
ρ_{calc}g/cm^3	1.249
μ/mm^{-1}	0.071
F(000)	2400.0
Crystal size/mm^3	0.24 × 0.23 × 0.18
Radiation	MoKα (λ = 0.71073)
2Θ range for data collection/°	4.19 to 56.564
Index ranges	-38 ≤ h ≤ 38, -18 ≤ k ≤ 16, -20 ≤ l ≤ 20
Reflections collected	76344
Independent reflections	7480 [R_{int} = 0.0575, R_{sigma} = 0.0327]
Data/restraints/parameters	7480/0/403
Goodness-of-fit on F^2	1.031
Final R indexes [I>=2σ (I)]	R_1 = 0.0528, wR_2 = 0.1348
Final R indexes [all data]	R_1 = 0.0721, wR_2 = 0.1471
Largest diff. peak/hole / e Å^{-3}	0.64/-0.32

Table S25. Fractional Atomic Coordinates (×10^4) and Equivalent Isotropic Displacement Parameters (Å^2×10^3) for **BN[6]**. U_{eq} is defined as 1/3 of the trace of the orthogonalized U_{IJ} tensor.

Atom	*x*	*y*	*z*	U(eq)
N1	3723.8(4)	6489.5(9)	4068.6(8)	16.9(2)
C1	3924.2(5)	7093.9(11)	3468.7(9)	18.8(3)
B1	3820.0(6)	5481.5(12)	4199.8(11)	18.5(3)
C2	3761.5(5)	8067.4(11)	3295.4(10)	21.3(3)
C3	3410.7(5)	8533.3(10)	3774.4(10)	21.9(3)
C4	3113.6(6)	9186.5(11)	3279.3(12)	29.7(4)
C5	3253.1(7)	9594.7(13)	2471.1(13)	37.1(4)
C6	3651.6(7)	9339.8(13)	2139.6(12)	37.0(4)
C7	3902.2(6)	8521.6(12)	2504.2(11)	29.0(4)
C8	4248.6(6)	8115.6(14)	2032.8(11)	33.6(4)
C9	4429.0(6)	7236.3(14)	2259.7(11)	31.6(4)
C10	4259.0(5)	6683.5(12)	2961.9(10)	23.0(3)
C11	4393.9(5)	5688.6(13)	3093.8(11)	26.1(3)
C12	4196.0(5)	5081.0(12)	3658.4(10)	24.3(3)
C13	3543.0(5)	4860.4(10)	4857.9(10)	18.9(3)
C14	3184.8(5)	4246.9(11)	4526.9(10)	23.5(3)
C15	2955.0(6)	3672.0(11)	5116.2(11)	25.9(3)
C16	3073.4(5)	3672.3(11)	6026.8(11)	23.4(3)
C17	3428.1(5)	4282.0(11)	6344.0(10)	20.9(3)
C18	3660.3(5)	4870.2(11)	5781.2(10)	20.6(3)
C19	2827.4(6)	3038.4(12)	6666.1(13)	30.9(4)
C20	3046.1(7)	4215.5(14)	3536.9(11)	36.0(4)
C21	4046.8(6)	5506.6(13)	6162.1(11)	28.9(4)
N101	4142.6(4)	8224.1(9)	5256.3(8)	18.0(2)
C101	3680.3(5)	8179.1(10)	5404.4(10)	18.5(3)
B101	4512.6(6)	8145.0(12)	5929.1(11)	20.2(3)
C102	3327.8(5)	8385.2(10)	4704.6(10)	20.6(3)
C105	2685.9(6)	9431.1(12)	3596.5(13)	35.5(4)
C106	2557.3(6)	9077.4(13)	4377.7(13)	33.6(4)
C107	2881.8(5)	8583.7(11)	4976.8(12)	26.3(3)
C108	2769.7(6)	8358.6(13)	5848.9(12)	30.6(4)
C109	3097.4(6)	8048.7(12)	6473.0(12)	27.9(4)
C110	3565.6(5)	8011.0(11)	6283.9(10)	23.0(3)
C111	3915.9(6)	7875.9(12)	6990.5(10)	26.1(3)
C112	4366.2(5)	7936.0(13)	6863.9(10)	26.1(3)
C113	5028.1(5)	8292.8(11)	5713.1(9)	19.1(3)
C114	5285.6(5)	7546.1(11)	5348.6(10)	21.1(3)
C115	5748.9(5)	7675.8(12)	5252.7(10)	22.9(3)
C116	5973.9(5)	8535.9(12)	5499.6(10)	23.4(3)
C117	5720.0(5)	9278.4(11)	5854.0(10)	22.8(3)
C118	5254.1(5)	9171.6(11)	5959.8(9)	20.8(3)
C119	6482.5(5)	8662.5(13)	5402.0(12)	30.8(4)
C120	5056.7(6)	6596.3(12)	5067.3(12)	29.2(4)
C121	4990.0(6)	10014.3(12)	6309.4(11)	26.6(3)

Table S26. Anisotropic Displacement Parameters (Å^2×10^3) for **BN[6]**. The Anisotropic displacement factor exponent takes the form: $-2\pi^2[h^2a^{*2}U_{11}+2hka^*b^*U_{12}+\ldots]$.

Atom	U_{11}	U_{22}	U_{33}	U_{23}	U_{13}	U_{12}
N1	16.5(6)	17.4(6)	16.9(6)	-1.0(4)	2.5(4)	-0.6(4)
C1	17.8(7)	21.5(7)	16.7(6)	-0.7(5)	-2.3(5)	-4.9(5)
B1	19.2(7)	18.2(8)	17.6(7)	-1.0(6)	-1.5(6)	0.0(6)
C2	21.8(7)	21.2(7)	19.7(7)	1.5(6)	-5.5(5)	-8.2(6)
C3	20.6(7)	14.2(7)	29.3(8)	0.5(6)	-8.6(6)	-4.3(5)
C4	32.6(9)	16.2(7)	37.6(9)	-0.5(6)	-16.2(7)	-1.4(6)
C5	47.7(11)	18.9(8)	40.8(10)	8.4(7)	-21.9(8)	-5.3(7)
C6	53.8(12)	26.1(9)	28.5(9)	10.0(7)	-12.9(8)	-15.8(8)

Atom	U_{11}	U_{22}	U_{33}	U_{23}	U_{13}	U_{12}
C7	37.0(9)	26.1(8)	22.5(8)	4.6(6)	-6.9(6)	-15.7(7)
C8	42.0(10)	39.1(10)	19.6(8)	3.4(7)	2.1(7)	-21.6(8)
C9	30.8(9)	42.7(10)	22.1(8)	-3.7(7)	7.0(6)	-13.9(8)
C10	19.6(7)	30.6(8)	18.9(7)	-2.6(6)	1.5(5)	-7.5(6)
C11	19.5(7)	33.2(9)	25.9(8)	-9.4(6)	4.8(6)	-0.4(6)
C12	23.7(7)	22.1(7)	26.8(8)	-5.4(6)	-0.2(6)	4.1(6)
C13	21.1(7)	14.0(6)	21.4(7)	-0.3(5)	1.0(5)	2.4(5)
C14	28.9(8)	17.8(7)	23.3(7)	0.1(6)	-0.8(6)	-1.5(6)
C15	28.2(8)	18.2(7)	31.0(8)	0.1(6)	0.5(6)	-5.6(6)
C16	23.3(7)	18.2(7)	29.0(8)	4.6(6)	3.4(6)	1.3(6)
C17	20.8(7)	21.9(7)	19.7(7)	0.9(6)	-0.8(5)	3.1(6)
C18	20.2(7)	18.1(7)	23.2(7)	0.3(5)	-0.3(6)	2.2(5)
C19	25.9(8)	24.1(8)	42.7(10)	10.5(7)	2.7(7)	-4.2(6)
C20	44.0(10)	37.9(10)	24.9(8)	0.0(7)	-6.3(7)	-18.1(8)
C21	30.8(8)	33.6(9)	21.6(7)	1.9(6)	-3.2(6)	-9.5(7)
N101	16.2(6)	19.7(6)	18.0(6)	-2.0(5)	0.9(4)	-1.4(5)
C101	15.9(6)	14.8(6)	24.7(7)	-4.9(5)	0.6(5)	-1.1(5)
B101	18.8(8)	20.6(8)	20.7(8)	-2.4(6)	-0.8(6)	-0.8(6)
C102	17.5(7)	13.4(6)	30.1(8)	-4.1(6)	-2.7(6)	-1.4(5)
C105	30.7(9)	20.1(8)	52.4(11)	-5.5(7)	-19.4(8)	6.9(7)
C106	19.0(8)	24.9(8)	55.2(11)	-12.4(8)	-8.3(7)	5.2(6)
C107	17.9(7)	18.1(7)	42.1(9)	-9.3(6)	-3.4(6)	-0.7(6)
C108	20.0(7)	28.5(8)	44.1(10)	-16.8(7)	7.7(7)	-4.5(6)
C109	25.5(8)	25.8(8)	33.6(9)	-11.3(7)	9.6(6)	-5.7(6)
C110	23.0(7)	19.7(7)	26.7(8)	-7.6(6)	5.2(6)	-3.9(6)
C111	30.7(8)	29.6(8)	18.5(7)	-4.4(6)	5.4(6)	-3.7(7)
C112	24.2(8)	34.1(9)	19.2(7)	-3.0(6)	-2.9(6)	-2.8(6)
C113	16.6(6)	23.8(7)	16.3(6)	-0.2(5)	-3.5(5)	-0.2(5)
C114	21.1(7)	22.3(7)	19.1(7)	-0.4(5)	-3.1(5)	-0.4(6)
C115	21.3(7)	23.4(7)	23.2(7)	0.2(6)	-2.5(6)	2.2(6)
C116	18.4(7)	27.7(8)	23.6(7)	2.1(6)	-2.6(6)	-0.3(6)
C117	22.3(7)	21.5(7)	23.4(7)	0.1(6)	-4.9(6)	-3.0(6)
C118	20.8(7)	23.3(7)	17.6(7)	-0.7(5)	-3.3(5)	0.8(6)
C119	19.4(8)	32.3(9)	40.3(10)	-2.6(7)	0.7(7)	-2.4(6)
C120	23.1(8)	25.0(8)	38.9(9)	-8.2(7)	-1.7(7)	-0.7(6)
C121	27.2(8)	25.3(8)	27.0(8)	-5.5(6)	0.1(6)	1.8(6)

Table S27. Bond Lengths for **BN[6].**

Atom	Atom	Length/Å	Atom	Atom	Length/Å
N1	C1	1.3877(18)	C17	C18	1.385(2)
N1	B1	1.423(2)	C18	C21	1.508(2)
C1	C2	1.436(2)	N101	C101	1.3901(18)
C1	C10	1.404(2)	N101	B101	1.429(2)
B1	C12	1.521(2)	C101	C102	1.444(2)
B1	C13	1.576(2)	C101	C110	1.407(2)
C2	C3	1.448(2)	B101	C112	1.527(2)
C2	C7	1.431(2)	B101	C113	1.581(2)
C3	C4	1.420(2)	C102	C107	1.425(2)
C3	C102	1.451(2)	C105	C106	1.350(3)
C4	C5	1.425(3)	C106	C107	1.429(2)
C4	C105	1.414(3)	C107	C108	1.409(3)
C5	C6	1.349(3)	C108	C109	1.358(3)
C6	C7	1.428(3)	C109	C110	1.422(2)
C7	C8	1.397(3)	C110	C111	1.431(2)
C8	C9	1.351(3)	C111	C112	1.349(2)
C9	C10	1.420(2)	C113	C114	1.408(2)
C10	C11	1.432(2)	C113	C118	1.412(2)
C11	C12	1.351(2)	C114	C115	1.387(2)
C13	C14	1.406(2)	C114	C120	1.512(2)
C13	C18	1.404(2)	C115	C116	1.389(2)
C14	C15	1.397(2)	C116	C117	1.391(2)
C14	C20	1.512(2)	C116	C119	1.518(2)
C15	C16	1.386(2)	C117	C118	1.393(2)
C16	C17	1.390(2)	C118	C121	1.508(2)
C16	C19	1.518(2)			

Table S28. Bond Angles for **BN[6]**.

Atom	Atom	Atom	Angle/°	Atom	Atom	Atom	Angle/°
C1	N1	B1	125.64(13)	C13	C18	C21	120.06(13)
N1	C1	C2	121.57(13)	C17	C18	C13	120.21(14)
N1	C1	C10	117.34(13)	C17	C18	C21	119.71(13)
C10	C1	C2	120.72(14)	C101	N101	B101	125.38(13)
N1	B1	C12	114.91(14)	N101	C101	C102	121.71(13)
N1	B1	C13	120.48(13)	N101	C101	C110	117.55(13)
C12	B1	C13	124.60(14)	C110	C101	C102	120.50(13)
C1	C2	C3	124.02(13)	N101	B101	C112	114.47(13)
C7	C2	C1	116.35(15)	N101	B101	C113	121.99(13)
C7	C2	C3	118.72(14)	C112	B101	C113	123.52(13)
C2	C3	C102	126.44(13)	C101	C102	C3	124.48(13)
C4	C3	C2	116.65(15)	C107	C102	C3	118.29(14)
C4	C3	C102	116.90(15)	C107	C102	C101	116.66(14)
C3	C4	C5	119.39(17)	C106	C105	C4	121.35(15)
C105	C4	C3	119.77(16)	C105	C106	C107	120.15(16)
C105	C4	C5	120.83(16)	C102	C107	C106	119.35(16)
C6	C5	C4	121.63(16)	C108	C107	C102	120.57(15)
C5	C6	C7	119.74(16)	C108	C107	C106	119.93(15)
C6	C7	C2	119.32(17)	C109	C108	C107	120.55(15)
C8	C7	C2	120.90(16)	C108	C109	C110	120.99(16)
C8	C7	C6	119.43(16)	C101	C110	C109	118.96(15)
C9	C8	C7	120.92(15)	C101	C110	C111	120.61(14)
C8	C9	C10	120.84(16)	C109	C110	C111	120.27(15)
C1	C10	C9	119.14(15)	C112	C111	C110	122.72(15)
C1	C10	C11	120.30(14)	C111	C112	B101	119.16(14)
C9	C10	C11	120.28(15)	C114	C113	B101	122.30(13)
C12	C11	C10	123.30(14)	C114	C113	C118	118.04(13)
C11	C12	B1	118.36(14)	C118	C113	B101	119.44(13)
C14	C13	B1	120.52(13)	C113	C114	C120	119.84(13)
C18	C13	B1	121.05(13)	C115	C114	C113	120.27(14)
C18	C13	C14	118.37(14)	C115	C114	C120	119.88(14)
C13	C14	C20	120.14(14)	C114	C115	C116	121.97(14)
C15	C14	C13	119.79(14)	C115	C116	C117	117.95(14)
C15	C14	C20	120.07(14)	C115	C116	C119	121.38(14)
C16	C15	C14	121.97(15)	C117	C116	C119	120.66(14)
C15	C16	C17	117.58(14)	C116	C117	C118	121.53(14)
C15	C16	C19	121.97(15)	C113	C118	C121	120.29(13)
C17	C16	C19	120.45(14)	C117	C118	C113	120.23(14)
C18	C17	C16	122.07(14)	C117	C118	C121	119.44(14)

Table S29. Torsion Angles for **BN[6]**.

A	B	C	D	Angle/°	A	B	C	D	Angle/°
N1	C1	C2	C3	5.8(2)	C14	C15	C16	C19	-179.26(15)
N1	C1	C2	C7	-163.17(13)	C15	C16	C17	C18	-0.3(2)
N1	C1	C10	C9	171.76(13)	C16	C17	C18	C13	-0.4(2)
N1	C1	C10	C11	-2.1(2)	C16	C17	C18	C21	-179.14(15)
N1	B1	C12	C11	-1.8(2)	C18	C13	C14	C15	0.3(2)
N1	B1	C13	C14	100.99(17)	C18	C13	C14	C20	179.82(15)
N1	B1	C13	C18	-81.97(18)	C19	C16	C17	C18	179.99(14)
C1	N1	B1	C12	3.6(2)	C20	C14	C15	C16	179.44(16)
C1	N1	B1	C13	-175.80(13)	N101	C101	C102	C3	8.1(2)
C1	C2	C3	C4	-145.91(14)	N101	C101	C102	C107	-163.03(13)
C1	C2	C3	C102	32.9(2)	N101	C101	C110	C109	174.35(13)
C1	C2	C7	C6	160.85(14)	N101	C101	C110	C111	-1.1(2)
C1	C2	C7	C8	-12.3(2)	N101	B101	C112	C111	-2.1(2)
C1	C10	C11	C12	3.9(2)	N101	B101	C113	C114	-81.74(19)
B1	N1	C1	C2	171.39(13)	N101	B101	C113	C118	103.74(17)
B1	N1	C1	C10	-1.7(2)	C101	N101	B101	C112	3.7(2)
B1	C13	C14	C15	177.43(14)	C101	N101	B101	C113	-174.75(13)
B1	C13	C14	C20	-3.1(2)	C101	C102	C107	C106	160.80(14)
B1	C13	C18	C17	-176.71(13)	C101	C102	C107	C108	-14.8(2)
B1	C13	C18	C21	2.0(2)	C101	C110	C111	C112	2.5(2)
C2	C1	C10	C9	-1.3(2)	B101	N101	C101	C102	172.22(14)
C2	C1	C10	C11	-175.25(13)	B101	N101	C101	C110	-2.1(2)
C2	C3	C4	C5	-20.3(2)	B101	C113	C114	C115	-173.57(14)
C2	C3	C4	C105	160.26(14)	B101	C113	C114	C120	6.0(2)
C2	C3	C102	C101	33.1(2)	B101	C113	C118	C117	173.76(13)
C2	C3	C102	C107	-155.94(14)	B101	C113	C118	C121	-8.4(2)
C2	C7	C8	C9	6.5(2)	C102	C3	C4	C5	160.76(14)
C3	C2	C7	C6	-8.7(2)	C102	C3	C4	C105	-18.7(2)
C3	C2	C7	C8	178.14(14)	C102	C101	C110	C109	-0.1(2)
C3	C4	C5	C6	3.3(2)	C102	C101	C110	C111	-175.49(14)
C3	C4	C105	C106	1.9(2)	C102	C107	C108	C109	7.2(2)
C3	C102	C107	C106	-10.9(2)	C105	C4	C5	C6	-177.28(16)
C3	C102	C107	C108	173.49(14)	C105	C106	C107	C102	-6.1(2)

A	B	C	D	Angle/°	A	B	C	D	Angle/°
C4	C3	C102	C101	-148.16(14)	C105	C106	C107	C108	169.52(16)
C4	C3	C102	C107	22.8(2)	C106	C107	C108	C109	-168.34(15)
C4	C5	C6	C7	11.6(3)	C107	C108	C109	C110	4.6(2)
C4	C105	C106	C107	10.9(3)	C108	C109	C110	C101	-8.1(2)
C5	C4	C105	C106	-177.51(16)	C108	C109	C110	C111	167.29(15)
C5	C6	C7	C2	-8.7(2)	C109	C110	C111	C112	-172.89(16)
C5	C6	C7	C8	164.52(16)	C110	C101	C102	C3	-177.69(14)
C6	C7	C8	C9	-166.61(16)	C110	C101	C102	C107	11.2(2)
C7	C2	C3	C4	22.8(2)	C110	C111	C112	B101	-0.7(3)
C7	C2	C3	C102	-158.40(14)	C112	B101	C113	C114	99.97(18)
C7	C8	C9	C10	2.5(3)	C112	B101	C113	C118	-74.5(2)
C8	C9	C10	C1	-5.0(2)	C113	B101	C112	C111	176.25(15)
C8	C9	C10	C11	168.89(15)	C113	C114	C115	C116	-0.6(2)
C9	C10	C11	C12	-169.95(15)	C114	C113	C118	C117	-1.0(2)
C10	C1	C2	C3	178.60(14)	C114	C113	C118	C121	176.86(13)
C10	C1	C2	C7	9.6(2)	C114	C115	C116	C117	0.1(2)
C10	C11	C12	B1	-1.7(2)	C114	C115	C116	C119	179.18(15)
C12	B1	C13	C14	-78.4(2)	C115	C116	C117	C118	-0.1(2)
C12	B1	C13	C18	98.68(18)	C116	C117	C118	C113	0.5(2)
C13	B1	C12	C11	177.57(14)	C116	C117	C118	C121	-177.32(14)
C7	C8	C9	C10	2.5(3)	C112	B101	C113	C118	-74.5(2)
C13	C14	C15	C16	-1.1(2)	C118	C113	C114	C115	1.0(2)
C14	C13	C18	C17	0.4(2)	C118	C113	C114	C120	-179.44(14)
C14	C13	C18	C21	179.12(14)	C119	C116	C117	C118	-179.15(15)
C14	C15	C16	C17	1.0(2)	C120	C114	C115	C116	179.85(15)

Table S30. Hydrogen Atom Coordinates (Å×10^4) and Isotropic Displacement Parameters (Å^2×10^3) for **BN[6]**.

Atom	*x*	*y*	*z*	U(eq)
H1	3519.71	6752.15	4396.06	20
H5	3060.83	10057.69	2157.88	45
H6	3765.07	9703.22	1665.66	44
H8	4358.94	8462.58	1545.93	40
H9	4672.54	6984.58	1945.47	38
H11	4634.6	5443.24	2768.05	31
H12	4289.46	4420.02	3715.62	29
H15	2710.25	3268.85	4885.81	31
H17	3513.82	4295.75	6966.57	25
H19A	2924.8	2360.11	6608.25	46
H19B	2496	3085.43	6523.06	46
H19C	2902.43	3260.6	7279.68	46
H20A	2984.49	4878.21	3317.42	54
H20B	2769.47	3818.02	3430.39	54
H20C	3294.61	3930	3221.45	54
H21A	3995.18	5678.17	6779.59	43
H21B	4059.25	6101.53	5804.56	43
H21C	4337.04	5153.59	6149.74	43
H101	4213.15	8308.3	4702.61	22
H105	2484.87	9852.87	3252.73	43
H106	2250.55	9156.94	4529.55	40
H108	2462.3	8424.16	6001.56	37
H109	3012.62	7854.11	7044.39	33
H111	3827.68	7738.24	7572.9	31
H112	4589.32	7849.44	7350.25	31
H115	5917.37	7161.09	5010.83	27
H117	5867.73	9871.89	6027.85	27
H11A	6655.46	8461.41	5955.57	46
H11B	6547.36	9347.98	5280.89	46
H11C	6573.19	8259.89	4906.51	46
H12D	4955.73	6261.7	5593.97	44
H12E	5274.71	6183.19	4778.15	44
H12F	4791.32	6728.42	4647.37	44
H12A	4807.25	10323.89	5814.1	40
H12B	5204.49	10490.43	6590.85	40
H12C	4786.76	9776.06	6750.35	40

3.5. 2,13-Dimesitylpentahelicene (CC[5])

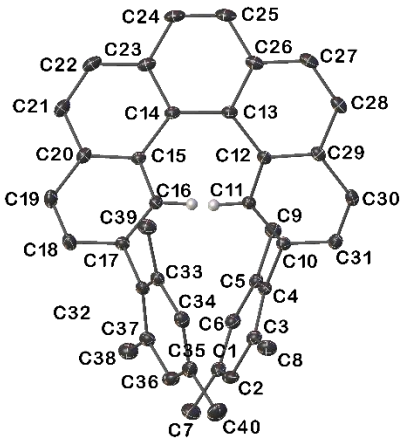

Colorless single crystals of $C_{40}H_{34}$ (**CC[5]**) were grown by dissolving a small amount (ca. 5 mg) of the compound in DCM (ca. 1 mL) in a sample vial. *n*-Hexane (ca. 5 mL) was added to a second, larger vial. The small vial was placed in the larger vial, which was capped. DCM was allowed to evaporate slowly at 25 °C, while letting the *n*-hexane diffuse into the small vial over the course of 1 d. CCDC Deposition Number: 2192799.

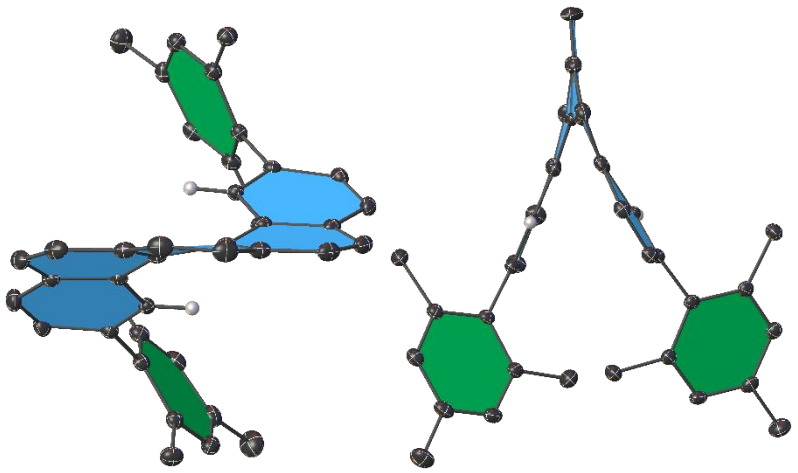

Fig. S11. Top view and view along the central phenyl-unit of **CC[5]**.

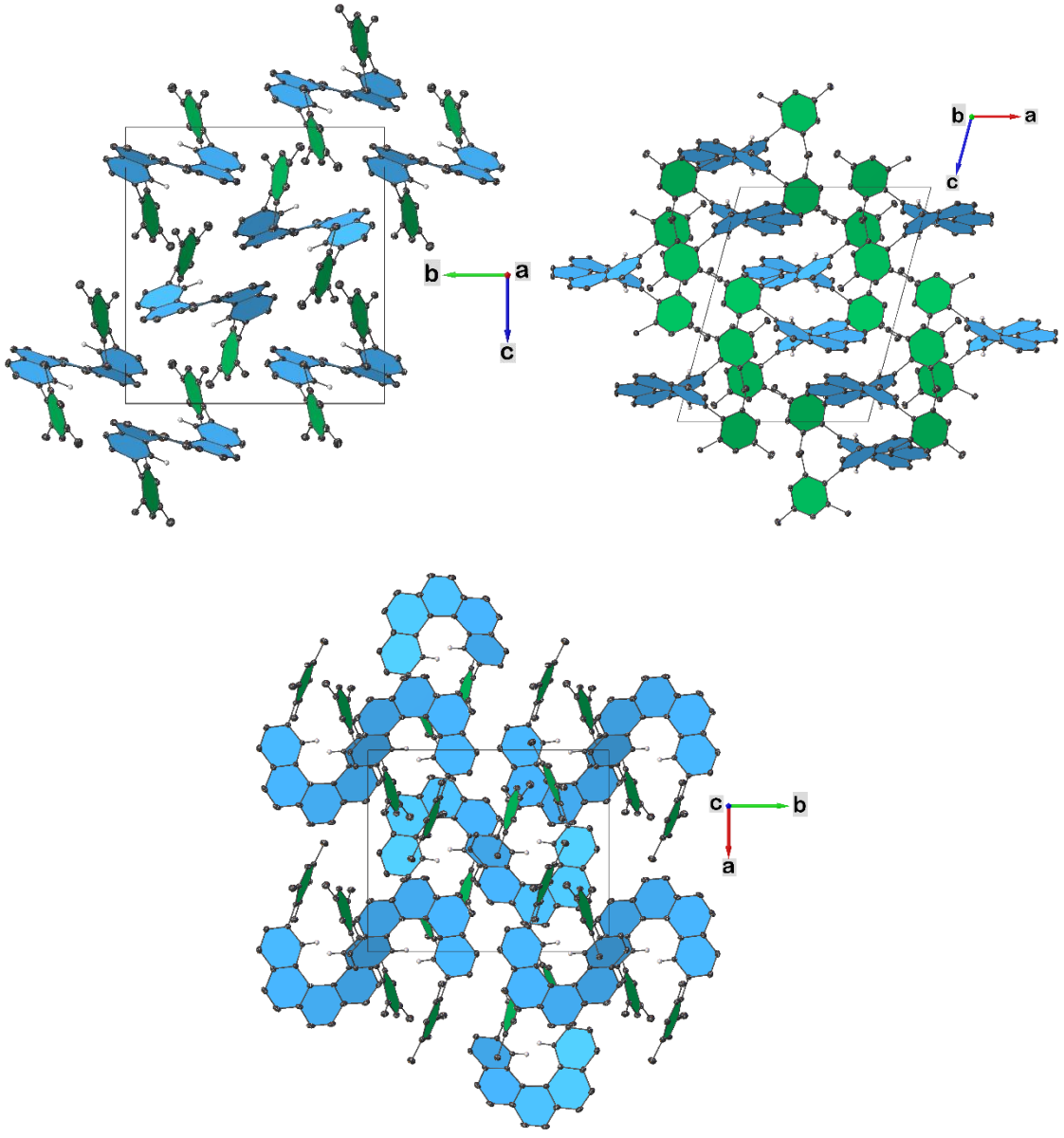

Fig. S12. Unit cell packing view of a **CC[5]** crystal along the a, b and c-axes.

Table S31. Crystal data and structure refinement for **CC[5]**.

Empirical formula	$C_{40}H_{34}$
Formula weight	514.67
Temperature/K	100.00
Crystal system	monoclinic
Space group	$P2_1/n$
a/Å	12.554(5)
b/Å	14.479(4)
c/Å	15.943(6)
α/°	90
β/°	105.032(14)
γ/°	90
Volume/Å^3	2798.8(16)
Z	4
ρ_{calc}g/cm^3	1.221
μ/mm^{-1}	0.069
F(000)	1096.0
Crystal size/mm^3	0.453 × 0.375 × 0.174
Radiation	MoKα (λ = 0.71073)
2Θ range for data collection/°	4.784 to 61.21
Index ranges	-17 ≤ h ≤ 17, -20 ≤ k ≤ 20, -21 ≤ l ≤ 22
Reflections collected	55723
Independent reflections	8551 [R_{int} = 0.0505, R_{sigma} = 0.0356]
Data/restraints/parameters	8551/0/368
Goodness-of-fit on F^2	1.032
Final R indexes [I>=2σ (I)]	R_1 = 0.0498, wR_2 = 0.1253
Final R indexes [all data]	R_1 = 0.0694, wR_2 = 0.1399
Largest diff. peak/hole / e Å^{-3}	0.44/-0.40

Table S32. Fractional Atomic Coordinates (×10^4) and Equivalent Isotropic Displacement Parameters (Å^2×10^3) for **CC[5]**. U_{eq} is defined as 1/3 of the trace of the orthogonalized U_{IJ} tensor.

Atom	*x*	*y*	*z*	$U_{(eq)}$
C6	6563.3(10)	3946.3(9)	938.6(8)	16.9(2)
C5	5929.6(10)	4294.8(8)	1466.4(8)	15.0(2)
C26	2429.0(10)	3990.3(9)	3939.0(8)	16.9(2)
C12	4218.6(9)	4216.3(8)	3624.5(7)	12.8(2)
C13	3357.0(9)	3584.2(8)	3730.3(7)	13.5(2)
C10	5710.3(9)	4634.2(8)	2959.1(7)	13.6(2)
C11	4950.9(9)	4003.9(8)	3109.4(7)	12.6(2)
C1	7656.1(10)	3674.0(9)	1275.6(8)	17.5(2)
C16	5365.5(9)	2271.5(8)	4181.6(7)	12.8(2)
C30	5085.8(10)	5743.8(8)	3854.5(8)	16.5(2)
C35	9346.0(10)	2750.5(9)	5895.8(9)	19.8(3)
C33	7485.6(10)	2175.5(8)	5774.8(8)	15.5(2)
C29	4250.0(10)	5130.9(8)	3955.6(7)	14.5(2)
C17	6261.3(10)	1678.6(8)	4339.0(8)	14.1(2)
C15	4299.5(9)	2000.7(8)	3696.1(7)	12.7(2)
C23	2288.0(10)	2151.0(9)	3357.6(8)	16.7(2)
C4	6407.9(10)	4372.3(8)	2365.1(8)	13.8(2)
C37	8249.9(10)	2123.9(9)	4522.9(8)	16.7(2)
C25	1423.0(10)	3486.8(10)	3800.2(9)	21.5(3)
C20	4161.2(10)	1067.2(9)	3406.6(8)	16.1(2)
C36	9227.1(10)	2501.1(9)	5034.2(9)	19.5(3)
C32	7355.6(10)	1990.5(8)	4888.9(8)	14.2(2)
C14	3330.1(9)	2594.8(8)	3575.0(7)	13.1(2)
C24	1336.5(10)	2622.9(10)	3459.6(9)	21.3(3)
C18	6120.9(11)	780.2(9)	3986.5(9)	19.1(2)
C22	2182.4(10)	1216.7(10)	3054.7(8)	19.7(3)
C2	8132.1(10)	3809.6(9)	2155.6(8)	17.5(2)
C31	5799.4(10)	5509.0(8)	3366.0(8)	16.5(2)
C3	7527.7(10)	4162.3(9)	2706.9(8)	16.0(2)
C21	3080.3(11)	706.9(9)	3037.6(8)	19.3(2)
C19	5092.4(11)	484.7(9)	3536.3(9)	20.0(3)
C28	3383.3(11)	5448.4(9)	4313.6(8)	18.0(2)
C9	4761.7(10)	4617.7(9)	1072.2(8)	18.3(2)
C34	8471.1(10)	2569.7(9)	6257.0(8)	18.0(2)
C27	2480.6(10)	4918.4(10)	4253.5(8)	19.1(3)
C39	6602.2(11)	1937.7(10)	6222.3(9)	20.4(3)
C8	8073.3(11)	4306.9(10)	3657.0(8)	20.7(3)
C7	8304.9(12)	3257.1(10)	694.1(10)	24.8(3)
C38	8160.4(11)	1877.6(10)	3589.2(9)	22.6(3)
C40	10393.6(12)	3191.9(11)	6427.4(10)	28.2(3)

Table S33. Anisotropic Displacement Parameters (Å^2×10^3) for **CC[5]**. The Anisotropic displacement factor exponent takes the form: $-2\pi^2[h^2a^{*2}U_{11}+2hka^*b^*U_{12}+\ldots]$.

Atom	U_{11}	U_{22}	U_{33}	U_{23}	U_{13}	U_{12}
C6	17.4(6)	17.2(5)	16.6(5)	-0.5(4)	5.4(4)	-2.0(4)
C5	15.1(5)	13.4(5)	16.9(5)	1.3(4)	4.6(4)	-1.6(4)
C26	13.9(5)	23.0(6)	14.2(5)	2.9(4)	4.4(4)	4.1(5)
C12	11.9(5)	14.1(5)	11.4(5)	1.8(4)	1.3(4)	2.3(4)
C13	10.7(5)	18.4(5)	10.9(5)	1.8(4)	2.0(4)	1.0(4)
C10	12.3(5)	15.1(5)	12.8(5)	1.9(4)	2.3(4)	1.0(4)
C11	11.8(5)	13.2(5)	12.7(5)	0.7(4)	3.2(4)	1.0(4)
C1	18.3(6)	15.5(5)	21.2(6)	-0.2(5)	9.5(5)	-2.2(4)
C16	13.0(5)	12.7(5)	12.7(5)	0.4(4)	3.3(4)	-0.6(4)
C30	17.9(6)	12.9(5)	17.1(5)	-1.1(4)	1.9(4)	2.3(4)
C35	14.9(6)	16.5(6)	25.1(6)	1.5(5)	-0.1(5)	1.4(4)
C33	14.5(5)	14.1(5)	17.3(5)	1.2(4)	3.1(4)	3.0(4)
C29	14.8(5)	15.6(5)	12.2(5)	0.7(4)	1.8(4)	3.8(4)
C17	12.9(5)	14.9(5)	14.5(5)	1.4(4)	3.4(4)	0.5(4)
C15	12.2(5)	14.5(5)	11.5(5)	1.5(4)	3.4(4)	-1.1(4)
C23	12.6(5)	23.6(6)	13.4(5)	2.9(4)	2.4(4)	-2.7(4)
C4	13.2(5)	12.5(5)	16.4(5)	1.4(4)	5.0(4)	-1.0(4)
C37	14.5(5)	17.3(5)	18.2(5)	3.3(4)	4.0(4)	2.5(4)
C25	12.6(5)	31.2(7)	22.6(6)	3.2(5)	7.9(5)	3.1(5)
C20	17.1(5)	16.0(5)	15.0(5)	0.1(4)	3.5(4)	-3.6(4)
C36	13.7(5)	20.8(6)	23.9(6)	5.0(5)	4.4(5)	0.6(5)
C32	11.8(5)	13.1(5)	16.8(5)	1.7(4)	2.4(4)	2.5(4)
C14	10.6(5)	18.0(5)	10.8(5)	1.7(4)	2.8(4)	-0.7(4)
C24	10.8(5)	31.4(7)	22.3(6)	3.4(5)	5.2(5)	-2.3(5)
C18	17.9(6)	15.0(6)	23.6(6)	-0.7(5)	3.7(5)	3.1(4)
C22	15.8(6)	24.9(6)	16.9(5)	1.7(5)	1.8(4)	-8.4(5)
C2	12.5(5)	19.3(6)	21.6(6)	3.8(5)	5.9(4)	0.6(4)
C31	15.3(5)	14.5(5)	18.7(5)	0.9(4)	2.4(4)	-0.8(4)
C3	14.8(5)	16.6(5)	16.6(5)	3.0(4)	4.2(4)	-1.3(4)
C21	20.2(6)	18.0(6)	18.0(6)	-0.7(5)	2.0(5)	-6.7(5)
C19	22.3(6)	13.3(5)	23.6(6)	-3.8(5)	4.3(5)	-1.0(5)
C28	19.7(6)	18.9(6)	15.2(5)	-0.6(4)	4.2(4)	6.9(5)
C9	16.2(5)	20.3(6)	17.2(5)	0.3(5)	2.5(4)	1.5(5)
C34	17.5(6)	17.4(6)	17.2(5)	-0.3(4)	1.2(4)	2.8(5)
C27	16.4(6)	25.2(6)	16.9(5)	1.3(5)	6.6(4)	7.5(5)
C39	18.2(6)	25.5(6)	18.4(6)	2.2(5)	6.4(5)	2.1(5)
C8	15.8(6)	27.6(7)	17.4(6)	2.1(5)	2.0(4)	2.1(5)
C7	23.6(7)	26.9(7)	27.4(7)	-4.1(6)	13.1(5)	2.0(5)
C38	21.2(6)	28.0(7)	20.3(6)	1.5(5)	8.3(5)	0.6(5)
C40	19.4(6)	28.0(7)	33.0(8)	-2.6(6)	-0.9(6)	-5.2(5)

Table S34. Bond Lengths for **CC[5]**.

Atom	Atom	Length/Å	Atom	Atom	Length/Å
C6	C5	1.3938(17)	C33	C32	1.4049(18)
C6	C1	1.3943(18)	C33	C34	1.3979(18)
C5	C4	1.4071(17)	C33	C39	1.5059(18)
C5	C9	1.5118(18)	C29	C28	1.4293(17)
C26	C13	1.4194(17)	C17	C32	1.4952(17)
C26	C25	1.4250(19)	C17	C18	1.4098(17)
C26	C27	1.4300(19)	C15	C20	1.4243(17)
C12	C13	1.4598(17)	C15	C14	1.4617(16)
C12	C11	1.4163(16)	C23	C14	1.4176(17)
C12	C29	1.4223(17)	C23	C24	1.4217(18)
C13	C14	1.4526(17)	C23	C22	1.4309(19)
C10	C11	1.3847(16)	C4	C3	1.4031(17)
C10	C4	1.4959(17)	C37	C36	1.3961(18)
C10	C31	1.4142(17)	C37	C32	1.4065(17)
C1	C2	1.3890(19)	C37	C38	1.5063(19)
C1	C7	1.5095(18)	C25	C24	1.357(2)
C16	C17	1.3850(16)	C20	C21	1.4302(18)
C16	C15	1.4166(16)	C20	C19	1.4126(18)

C30	C29	1.4150(18)	C18	C19	1.3728(18)
C30	C31	1.3736(18)	C22	C21	1.354(2)
C35	C36	1.390(2)	C2	C3	1.3981(18)
C35	C34	1.3910(19)	C3	C8	1.5064(18)
C35	C40	1.5094(19)	C28	C27	1.3513(19)

Table S35. Bond Angles for **CC[5]**.

Atom	Atom	Atom	Angle/°	Atom	Atom	Atom	Angle/°
C5	C6	C1	121.90(12)	C16	C15	C14	123.06(11)
C6	C5	C4	118.95(11)	C20	C15	C14	119.24(10)
C6	C5	C9	120.33(11)	C14	C23	C24	120.25(12)
C4	C5	C9	120.69(11)	C14	C23	C22	120.66(11)
C13	C26	C25	119.99(12)	C24	C23	C22	119.07(11)
C13	C26	C27	120.41(11)	C5	C4	C10	119.97(11)
C25	C26	C27	119.54(11)	C3	C4	C5	119.88(11)
C11	C12	C13	122.87(11)	C3	C4	C10	120.09(11)
C11	C12	C29	117.24(11)	C36	C37	C32	119.12(12)
C29	C12	C13	119.40(11)	C36	C37	C38	119.91(12)
C26	C13	C12	116.43(11)	C32	C37	C38	120.97(11)
C26	C13	C14	117.67(11)	C24	C25	C26	120.64(12)
C14	C13	C12	125.72(10)	C15	C20	C21	120.15(11)
C11	C10	C4	119.00(11)	C19	C20	C15	119.50(11)
C11	C10	C31	119.14(11)	C19	C20	C21	120.23(12)
C31	C10	C4	121.86(11)	C35	C36	C37	122.09(12)
C10	C11	C12	122.46(11)	C33	C32	C17	119.77(11)
C6	C1	C7	120.67(12)	C33	C32	C37	119.60(11)
C2	C1	C6	118.14(12)	C37	C32	C17	120.61(11)
C2	C1	C7	121.17(12)	C13	C14	C15	125.18(10)
C17	C16	C15	122.35(11)	C23	C14	C13	117.90(11)
C31	C30	C29	121.42(11)	C23	C14	C15	116.71(11)
C36	C35	C34	117.79(12)	C25	C24	C23	120.43(12)
C36	C35	C40	121.29(13)	C19	C18	C17	119.96(12)
C34	C35	C40	120.92(13)	C21	C22	C23	121.17(11)
C32	C33	C39	121.66(11)	C1	C2	C3	121.68(12)
C34	C33	C32	119.09(12)	C30	C31	C10	119.75(11)
C34	C33	C39	119.23(12)	C4	C3	C8	120.59(11)
C12	C29	C28	119.80(11)	C2	C3	C4	119.18(11)
C30	C29	C12	119.45(11)	C2	C3	C8	120.24(11)
C30	C29	C28	120.50(11)	C22	C21	C20	119.94(12)
C16	C17	C32	119.90(11)	C18	C19	C20	121.40(12)
C16	C17	C18	119.21(11)	C27	C28	C29	120.02(12)
C18	C17	C32	120.89(11)	C35	C34	C33	122.03(12)
C16	C15	C20	117.27(11)	C28	C27	C26	121.29(11)

Table S36. Torsion Angles for **CC[5]**.

A	B	C	D	Angle/°	A	B	C	D	Angle/°
C6	C5	C4	C10	-172.57(11)	C23	C22	C21	C20	6.34(19)
C6	C5	C4	C3	4.51(17)	C4	C10	C11	C12	-176.48(10)
C6	C1	C2	C3	3.39(19)	C4	C10	C31	C30	175.18(11)
C5	C6	C1	C2	-3.82(19)	C25	C26	C13	C12	161.12(11)
C5	C6	C1	C7	177.09(12)	C25	C26	C13	C14	-14.22(17)
C5	C4	C3	C2	-4.92(18)	C25	C26	C27	C28	-173.51(12)
C5	C4	C3	C8	175.55(11)	C20	C15	C14	C13	-171.39(11)
C26	C13	C14	C15	-154.11(11)	C20	C15	C14	C23	14.05(16)
C26	C13	C14	C23	20.40(16)	C36	C35	C34	C33	-1.83(19)
C26	C25	C24	C23	9.6(2)	C36	C37	C32	C33	-4.54(18)
C12	C13	C14	C15	31.04(18)	C36	C37	C32	C17	173.79(11)
C12	C13	C14	C23	-154.45(11)	C32	C33	C34	C35	-2.66(19)
C12	C29	C28	C27	-7.08(18)	C32	C17	C18	C19	175.28(12)
C13	C26	C25	C24	-0.79(19)	C32	C37	C36	C35	-0.04(19)
C13	C26	C27	C28	3.81(18)	C14	C15	C20	C21	-2.78(17)
C13	C12	C11	C10	174.96(11)	C14	C15	C20	C19	-178.83(11)
C13	C12	C29	C30	179.91(11)	C14	C23	C24	C25	-2.83(19)
C13	C12	C29	C28	-5.86(16)	C14	C23	C22	C21	5.70(19)
C10	C4	C3	C2	172.15(11)	C24	C23	C14	C13	-12.24(17)
C10	C4	C3	C8	-7.38(18)	C24	C23	C14	C15	162.73(11)
C11	C12	C13	C26	-154.70(11)	C24	C23	C22	C21	-172.69(12)
C11	C12	C13	C14	20.21(18)	C18	C17	C32	C33	-113.05(14)
C11	C12	C29	C30	-7.88(16)	C18	C17	C32	C37	68.62(16)
C11	C12	C29	C28	166.35(11)	C22	C23	C14	C13	169.38(11)
C11	C10	C4	C5	70.77(15)	C22	C23	C14	C15	-15.65(16)
C11	C10	C4	C3	-106.30(13)	C22	C23	C24	C25	175.57(12)
C11	C10	C31	C30	-4.37(17)	C31	C10	C11	C12	3.09(17)
C1	C6	C5	C4	-0.08(18)	C31	C10	C4	C5	-108.79(13)
C1	C6	C5	C9	177.59(11)	C31	C10	C4	C3	74.14(15)
C1	C2	C3	C4	0.93(19)	C31	C30	C29	C12	6.85(18)
C1	C2	C3	C8	-179.54(12)	C31	C30	C29	C28	-167.34(12)
C16	C17	C32	C33	65.97(16)	C21	C20	C19	C18	-171.72(13)
C16	C17	C32	C37	-112.36(13)	C19	C20	C21	C22	168.35(12)
C16	C17	C18	C19	-3.75(19)	C9	C5	C4	C10	9.77(17)
C16	C15	C20	C21	169.91(11)	C9	C5	C4	C3	-173.16(11)
C16	C15	C20	C19	-6.14(17)	C34	C35	C36	C37	3.20(19)
C16	C15	C14	C13	16.37(18)	C34	C33	C32	C17	-172.50(11)
C16	C15	C14	C23	-158.20(11)	C34	C33	C32	C37	5.84(18)
C30	C29	C28	C27	167.09(12)	C27	C26	C13	C12	-16.18(16)
C29	C12	C13	C26	17.05(16)	C27	C26	C13	C14	168.48(11)
C29	C12	C13	C14	-168.04(11)	C27	C26	C25	C24	176.54(12)
C29	C12	C11	C10	3.04(17)	C39	C33	C32	C17	9.08(17)
C29	C30	C31	C10	-0.58(18)	C39	C33	C32	C37	-172.57(11)
C29	C28	C27	C26	8.25(19)	C39	C33	C34	C35	175.79(12)
C17	C16	C15	C20	3.20(17)	C7	C1	C2	C3	-177.52(12)
C17	C16	C15	C14	175.59(11)	C38	C37	C36	C35	179.18(12)
C17	C18	C19	C20	0.7(2)	C38	C37	C32	C33	176.25(12)
C15	C16	C17	C32	-177.31(11)	C38	C37	C32	C17	-5.42(18)
C15	C16	C17	C18	1.73(18)	C40	C35	C36	C37	-177.56(13)
C15	C20	C21	C22	-7.67(19)	C40	C35	C34	C33	178.93(12)
C15	C20	C19	C18	4.34(19)					

Table S37. Hydrogen Atom Coordinates (Å×10^4) and Isotropic Displacement Parameters (Å^2×10^3) for **CC[5]**.

Atom	*x*	*y*	*z*	U(eq)
H6	6241.29	3892.73	331.78	20
H11	4920.05	3406.68	2857.52	15
H16	5469.78	2881.58	4407.27	15
H30	5154.8	6330.38	4130.43	20
H25	807.04	3758.58	3947.68	26
H36	9830.08	2590.22	4785.45	23
H24	635.46	2331.53	3288.02	26
H18	6737.59	379.54	4060.51	23
H22	1469.46	949.52	2862.15	24
H2	8887.52	3658.84	2388.95	21
H31	6350.75	5932.56	3301.8	20
H21	2992.59	110.4	2780.77	23
H19	5005.18	-124.34	3307.08	24
H28	3441.94	6032.17	4593.79	22
H9A	4713.23	5283.88	1164.4	27
H9B	4258.32	4292.31	1348.85	27
H9C	4556.41	4486.21	447.85	27
H34	8545.58	2718.68	6849.81	22
H27	1868.32	5167.32	4423.64	23
H39A	6162.75	2489.4	6255.56	31
H39B	6945.84	1713	6810.12	31
H39C	6123.27	1456.07	5892.57	31
H8A	8107.78	4969.31	3787.72	31
H8B	8821.97	4052.37	3795.35	31
H8C	7645.03	3993.25	4006.17	31
H7A	7924.47	2704.46	410.92	37
H7B	9043.1	3088.08	1042.49	37
H7C	8368.15	3708.27	251.28	37
H38A	8783.76	2145.89	3410.27	34
H38B	7468.31	2122.37	3221.19	34
H38C	8171.06	1204.39	3528.73	34
H40A	10890.71	3309.8	6056.22	42
H40B	10753.88	2776	6901.06	42
H40C	10216.23	3776.53	6670.01	42

3.6. 2,15-Dimesitylhexahelicene (CC[6])

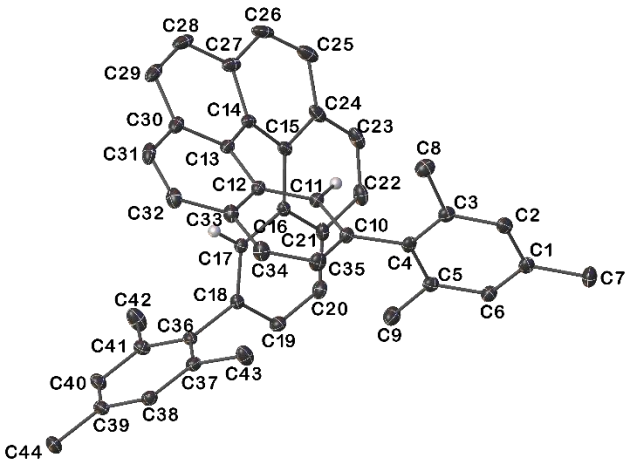

Colorless single crystals of $C_{44}H_{36}$ (**CC[6]**) were grown by dissolving a small amount (ca. 1 mg) of the compound in DCM (ca. 1 mL) in a sample vial. Cyclohexane (ca. 5 mL) was added to a second, larger vial. The small vial was placed in the larger vial, which was capped. DCM was allowed to evaporate slowly at 25 °C, while letting the cyclohexane diffuse into the small vial over the course of 14 d. CCDC Deposition Number: 2192801.

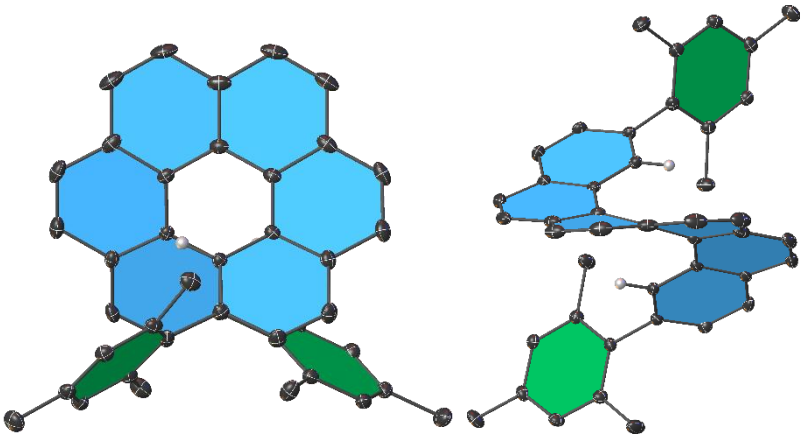

Fig. S13. Frontal view and representation of the helical structure of **CC[6]**.

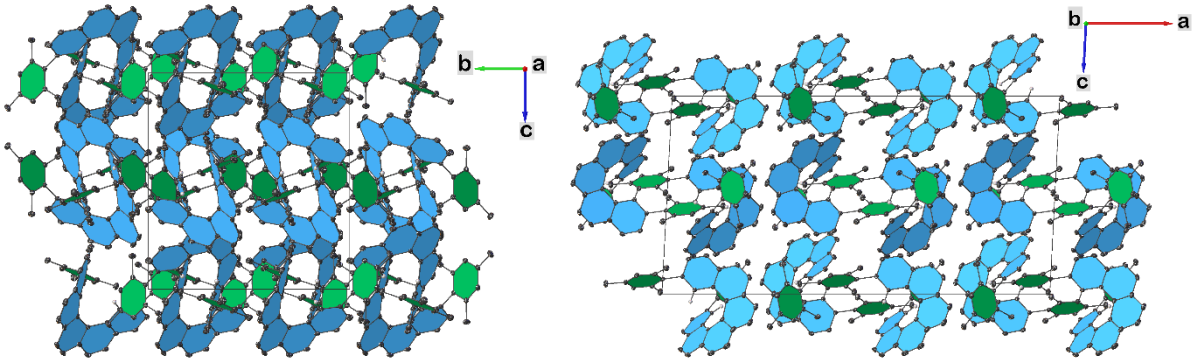

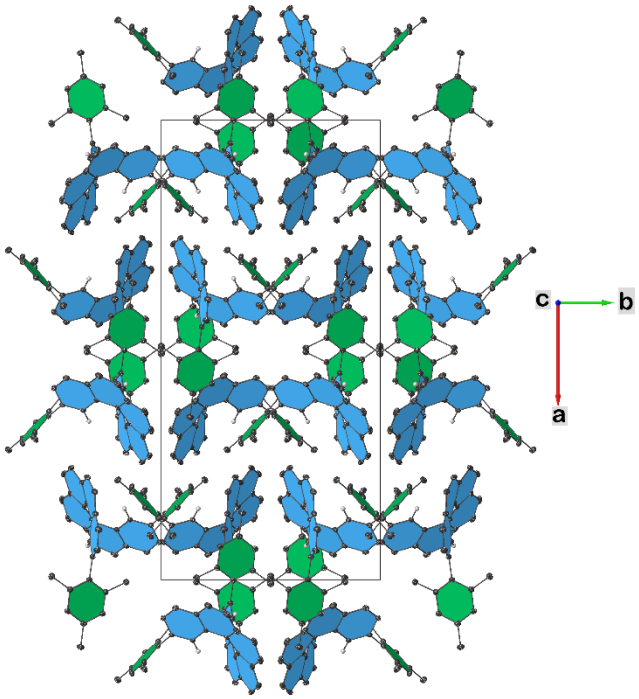

Fig. S14. Unit cell packing view of a **CC[6]** crystal along the a, b and c-axes.

Table S38. Crystal data and structure refinement for **CC[6].**

Empirical formula	$C_{44}H_{36}$
Formula weight	564.73
Temperature/K	100.00
Crystal system	monoclinic
Space group	C2/c
a/Å	29.1349(9)
b/Å	13.8389(5)
c/Å	14.8881(6)
α/°	90
β/°	92.9530(10)
γ/°	90
Volume/Å^3	5994.8(4)
Z	8
ρcalcg/cm^3	1.251
μ/mm^{-1}	0.071
F(000)	2400.0
Crystal size/mm^3	0.333 × 0.295 × 0.166
Radiation	MoKα (λ = 0.71073)
2Θ range for data collection/°	5.128 to 61.118
Index ranges	-37 ≤ h ≤ 41, -19 ≤ k ≤ 19, -19 ≤ l ≤ 21
Reflections collected	55111
Independent reflections	9154 [R_{int} = 0.0535, R_{sigma} = 0.0400]
Data/restraints/parameters	9154/0/403
Goodness-of-fit on F^2	1.017
Final R indexes [I>=2σ (I)]	R1 = 0.0534, wR2 = 0.1227
Final R indexes [all data]	R1 = 0.0745, wR2 = 0.1345
Largest diff. peak/hole / e Å^{-3}	0.40/-0.27

Table S39. Fractional Atomic Coordinates (×10^4) and Equivalent Isotropic Displacement Parameters (Å^2×10^3) for **CC[6]**. U_{eq} is defined as 1/3 of the trace of the orthogonalized U_{IJ} tensor.

Atom	*x*	*y*	*z*	U(eq)
C17	6311.4(4)	3570.3(9)	5932.7(8)	11.9(2)
C12	6313.4(4)	1808.5(9)	4625.0(8)	12.7(2)
C16	6091.7(4)	2960.6(9)	6545.0(8)	12.1(2)
C38	6570.4(4)	5736.5(9)	3690.1(8)	15.0(2)
C18	6189.8(4)	4528.6(9)	5808.5(8)	12.5(2)
C21	5743.4(4)	3379.5(9)	7053.3(8)	14.6(2)
C10	5503.8(4)	1849.8(9)	4086.2(8)	13.7(2)
C6	4266.1(4)	2306.7(9)	4649.6(8)	16.2(2)
C14	6591.6(4)	1478.5(9)	6264.1(8)	13.8(2)
C36	6442.6(4)	5159.9(9)	5186.4(8)	12.7(2)
C4	5003.1(4)	1706.1(9)	4228.6(8)	13.9(2)
C11	5837.7(4)	1741.6(9)	4776.4(8)	12.8(2)
C37	6332.9(4)	5140.4(9)	4258.0(8)	14.3(2)
C5	4737.0(4)	2448.2(9)	4577.5(8)	15.0(2)
C2	4321.7(4)	708.6(9)	4052.7(8)	16.6(2)
C19	5825.5(4)	4911.8(9)	6284.8(9)	15.9(2)
C13	6672.0(4)	1591.9(9)	5317.2(8)	13.5(2)
C35	5640.6(4)	2063.8(10)	3209.8(8)	18.0(3)
C30	7115.6(4)	1374.9(9)	5028.3(9)	17.0(2)
C1	4051.4(4)	1444.7(10)	4387.3(8)	16.7(2)
C40	7024.3(4)	6360.3(9)	4938.0(9)	17.3(2)
C33	6441.2(4)	1987.4(9)	3730.3(8)	15.6(2)
C41	6792.1(4)	5778.3(9)	5532.7(8)	15.8(2)
C3	4793.9(4)	820.7(9)	3976.8(8)	15.2(2)
C20	5608.1(4)	4344.3(10)	6885.8(9)	16.7(2)
C39	6917.4(4)	6355.5(9)	4015.5(9)	15.9(2)
C24	6105.7(5)	1564.0(10)	7564.1(8)	18.0(3)
C15	6248.9(4)	1982.6(9)	6756.2(8)	13.2(2)
C22	5560.8(5)	2851.5(11)	7781.2(9)	19.6(3)
C34	6097.2(5)	2131.9(10)	3040.3(9)	18.6(3)
C32	6915.0(4)	1952.8(10)	3519.4(9)	18.8(3)
C31	7235.7(4)	1618.3(10)	4138.9(10)	19.7(3)
C8	5078.0(5)	-17.0(10)	3671.9(9)	20.6(3)
C28	7308.5(5)	544.9(10)	6421.3(10)	23.1(3)
C27	6883.6(5)	828.0(9)	6764.2(9)	18.9(3)
C23	5746.7(5)	1994.8(11)	8039.7(9)	21.1(3)
C25	6347.4(5)	751.2(10)	7951.6(9)	23.1(3)
C29	7437.5(5)	877.1(10)	5616.2(10)	21.7(3)
C7	3539.9(5)	1308.0(11)	4463.2(10)	23.6(3)
C44	7172.1(5)	6990.0(10)	3378.7(10)	22.2(3)
C43	5957.3(5)	4492.4(11)	3870.1(9)	20.9(3)
C9	4953.2(5)	3394.3(10)	4874.0(10)	20.8(3)
C26	6744.4(5)	457.0(10)	7602.7(10)	23.6(3)
C42	6921.8(5)	5801.6(11)	6527.7(9)	25.3(3)

Table S40. Anisotropic Displacement Parameters ($Å^2×10^3$) for **CC[6]**. The Anisotropic displacement factor exponent takes the form: $-2π^2[h^2a^{*2}U_{11}+2hka^*b^*U_{12}+…]$.

Atom	U_{11}	U_{22}	U_{33}	U_{23}	U_{13}	U_{12}
C17	11.2(5)	13.7(5)	10.9(5)	-0.8(4)	1.1(4)	0.0(4)
C12	12.0(5)	11.9(5)	14.1(5)	-2.8(4)	-0.1(4)	0.0(4)
C16	11.9(5)	13.9(5)	10.2(5)	-0.2(4)	-1.1(4)	-1.9(4)
C38	14.9(5)	16.5(6)	13.7(5)	1.6(4)	0.8(4)	2.1(4)
C18	12.7(5)	13.5(5)	11.5(5)	-0.1(4)	0.6(4)	-1.2(4)
C21	12.7(5)	18.7(6)	12.5(5)	-0.6(4)	1.3(4)	-3.6(4)
C10	12.1(5)	15.3(6)	13.7(5)	-2.3(4)	0.0(4)	-0.1(4)
C6	14.2(6)	17.3(6)	16.9(6)	0.0(5)	-0.5(4)	1.0(4)
C14	13.5(5)	10.0(5)	17.5(6)	0.3(4)	-4.0(4)	-1.9(4)
C36	12.8(5)	10.7(5)	14.6(5)	0.6(4)	2.3(4)	1.0(4)
C4	11.9(5)	18.3(6)	11.3(5)	0.7(4)	-2.3(4)	-0.1(4)
C11	12.6(5)	13.7(5)	12.0(5)	-1.2(4)	0.5(4)	0.4(4)
C37	13.3(5)	13.7(6)	15.9(5)	0.4(4)	0.1(4)	1.2(4)
C5	15.1(6)	15.7(6)	13.8(5)	-0.1(4)	-1.9(4)	-0.2(4)
C2	16.1(6)	16.5(6)	16.7(6)	0.7(5)	-3.0(4)	-2.2(5)
C19	15.4(6)	14.9(6)	17.4(6)	-1.1(5)	1.0(4)	2.5(4)
C13	12.9(5)	9.7(5)	17.7(6)	-1.8(4)	-1.5(4)	0.0(4)
C35	16.9(6)	23.9(7)	12.7(5)	-1.2(5)	-2.4(4)	-0.7(5)
C30	12.9(6)	12.8(6)	25.1(6)	-5.6(5)	-1.5(5)	0.4(4)
C1	14.3(6)	19.9(6)	15.6(6)	3.0(5)	-1.9(4)	-0.2(5)
C40	18.8(6)	12.8(6)	20.2(6)	0.3(5)	1.0(5)	-3.7(5)
C33	15.5(6)	15.9(6)	15.6(6)	-4.4(5)	3.0(4)	-1.7(4)
C41	18.7(6)	12.9(6)	15.8(6)	0.1(4)	0.6(4)	-0.7(4)
C3	16.2(6)	16.5(6)	12.6(5)	-1.1(4)	-2.7(4)	0.9(4)
C20	13.1(5)	21.0(6)	16.4(6)	-3.9(5)	4.2(4)	0.8(5)
C39	16.2(6)	12.9(6)	18.9(6)	3.0(5)	4.2(4)	0.6(4)
C24	22.5(6)	17.2(6)	14.0(5)	2.9(5)	-3.2(5)	-7.9(5)
C15	14.2(5)	12.7(5)	12.4(5)	1.2(4)	-3.0(4)	-3.1(4)
C22	18.0(6)	26.3(7)	14.9(6)	-1.6(5)	5.0(5)	-6.3(5)
C34	19.9(6)	23.7(7)	12.5(5)	-2.3(5)	2.6(4)	-2.5(5)
C32	17.5(6)	19.7(6)	19.8(6)	-6.1(5)	6.7(5)	-2.5(5)
C31	12.1(6)	20.0(6)	27.5(7)	-10.6(5)	5.1(5)	-2.5(5)
C8	21.9(6)	18.9(6)	20.7(6)	-4.7(5)	-1.0(5)	2.7(5)
C28	20.5(6)	14.4(6)	33.0(7)	-2.9(5)	-11.2(5)	4.8(5)
C27	20.8(6)	11.2(6)	23.6(6)	-0.6(5)	-9.4(5)	-0.1(5)
C23	24.0(7)	25.3(7)	14.2(6)	2.9(5)	2.8(5)	-10.7(5)
C25	32.2(7)	18.0(6)	18.2(6)	6.7(5)	-6.3(5)	-7.6(5)
C29	13.7(6)	17.0(6)	33.8(7)	-7.3(5)	-4.8(5)	3.5(5)
C7	14.1(6)	25.2(7)	31.4(7)	0.4(6)	0.7(5)	-3.0(5)
C44	19.2(6)	20.1(7)	27.6(7)	8.7(5)	3.3(5)	-4.2(5)
C43	22.1(6)	23.9(7)	16.5(6)	2.0(5)	-2.3(5)	-7.4(5)
C9	17.0(6)	17.5(6)	27.6(7)	-5.7(5)	-1.2(5)	-0.5(5)
C26	30.7(7)	12.9(6)	25.8(7)	6.3(5)	-11.9(6)	-1.1(5)
C42	31.5(8)	27.9(7)	16.2(6)	-0.4(5)	-2.3(5)	-13.3(6)

Table S41. Bond Lengths for **CC[6].**

Atom	Atom	Length/Å	Atom	Atom	Length/Å
C17	C16	1.4188(16)	C5	C9	1.5090(18)
C17	C18	1.3826(17)	C2	C1	1.3951(19)
C12	C11	1.4184(16)	C2	C3	1.3950(18)
C12	C13	1.4604(16)	C19	C20	1.3702(18)
C12	C33	1.4232(17)	C13	C30	1.4152(17)
C16	C21	1.4205(17)	C35	C34	1.3701(18)
C16	C15	1.4580(17)	C30	C31	1.427(2)
C38	C37	1.3909(18)	C30	C29	1.4268(18)
C38	C39	1.3929(18)	C1	C7	1.5121(18)
C18	C36	1.4947(17)	C40	C41	1.3971(18)
C18	C19	1.4099(17)	C40	C39	1.3926(18)
C21	C20	1.4107(18)	C33	C34	1.4120(18)
C21	C22	1.4320(18)	C33	C32	1.4320(18)
C10	C4	1.4982(17)	C41	C42	1.5101(18)
C10	C11	1.3863(16)	C3	C8	1.5078(18)
C10	C35	1.4151(17)	C39	C44	1.5144(18)
C6	C5	1.3955(17)	C24	C15	1.4172(17)
C6	C1	1.3934(18)	C24	C23	1.424(2)
C14	C13	1.4495(18)	C24	C25	1.4326(19)
C14	C15	1.4477(18)	C22	C23	1.351(2)
C14	C27	1.4224(17)	C32	C31	1.360(2)
C36	C37	1.4028(17)	C28	C27	1.418(2)
C36	C41	1.4074(17)	C28	C29	1.355(2)
C4	C5	1.4024(18)	C27	C26	1.428(2)
C4	C3	1.4107(17)	C25	C26	1.355(2)
C37	C43	1.5065(17)			

Table S42. Bond Angles for **BN[6]**.

Atom	Atom	Atom	Angle/°	Atom	Atom	Atom	Angle/°
C18	C17	C16	122.36(11)	C34	C35	C10	120.43(11)
C11	C12	C13	122.94(11)	C13	C30	C31	120.21(12)
C11	C12	C33	117.71(11)	C13	C30	C29	119.85(13)
C33	C12	C13	118.94(11)	C29	C30	C31	119.89(12)
C17	C16	C21	117.26(11)	C6	C1	C2	118.15(11)
C17	C16	C15	122.92(11)	C6	C1	C7	121.07(12)
C21	C16	C15	119.28(11)	C2	C1	C7	120.79(12)
C37	C38	C39	121.88(11)	C39	C40	C41	122.08(12)
C17	C18	C36	120.82(11)	C12	C33	C32	120.07(11)
C17	C18	C19	119.20(11)	C34	C33	C12	119.69(11)
C19	C18	C36	119.97(11)	C34	C33	C32	120.09(12)
C16	C21	C22	119.89(12)	C36	C41	C42	120.80(11)
C20	C21	C16	119.53(11)	C40	C41	C36	118.89(11)
C20	C21	C22	120.36(12)	C40	C41	C42	120.30(12)
C11	C10	C4	122.14(11)	C4	C3	C8	120.77(11)
C11	C10	C35	119.07(11)	C2	C3	C4	119.30(12)
C35	C10	C4	118.74(10)	C2	C3	C8	119.86(12)
C1	C6	C5	121.83(12)	C19	C20	C21	121.57(11)
C15	C14	C13	126.18(11)	C38	C39	C44	120.60(12)
C27	C14	C13	117.08(11)	C40	C39	C38	117.87(12)
C27	C14	C15	116.72(11)	C40	C39	C44	121.52(12)
C37	C36	C18	120.31(11)	C15	C24	C23	120.46(12)
C37	C36	C41	119.77(11)	C15	C24	C25	120.17(13)
C41	C36	C18	119.92(11)	C23	C24	C25	119.14(12)
C5	C4	C10	121.07(11)	C14	C15	C16	123.74(11)
C5	C4	C3	119.67(11)	C24	C15	C16	117.36(11)
C3	C4	C10	119.22(11)	C24	C15	C14	118.26(11)
C10	C11	C12	121.95(11)	C23	C22	C21	120.28(12)
C38	C37	C36	119.49(11)	C35	C34	C33	121.06(12)
C38	C37	C43	119.62(11)	C31	C32	C33	119.94(13)
C36	C37	C43	120.89(11)	C32	C31	C30	121.13(12)
C6	C5	C4	119.35(11)	C29	C28	C27	120.79(12)
C6	C5	C9	119.76(12)	C14	C27	C26	119.73(13)
C4	C5	C9	120.89(11)	C28	C27	C14	119.74(13)
C3	C2	C1	121.66(12)	C28	C27	C26	120.54(12)
C20	C19	C18	119.89(12)	C22	C23	C24	121.32(12)
C14	C13	C12	124.26(11)	C26	C25	C24	119.55(13)
C30	C13	C12	117.42(11)	C28	C29	C30	120.19(12)
C30	C13	C14	117.94(11)	C25	C26	C27	120.93(12)

Table S43. Torsion Angles for **CC[6]**.

A	B	C	D	Angle/°	A	B	C	D	Angle/°
C17	C16	C21	C20	4.63(17)	C13	C14	C15	C24	158.10(12)
C17	C16	C21	C22	-169.98(11)	C13	C14	C27	C28	18.35(17)
C17	C16	C15	C14	-10.53(17)	C13	C14	C27	C26	-160.97(12)
C17	C16	C15	C24	160.11(11)	C13	C30	C31	C32	-7.99(19)
C17	C18	C36	C37	82.13(15)	C13	C30	C29	C28	5.19(19)
C17	C18	C36	C41	-97.96(14)	C35	C10	C4	C5	-99.77(14)
C17	C18	C19	C20	2.32(18)	C35	C10	C4	C3	77.95(16)
C12	C13	C30	C31	16.83(18)	C35	C10	C11	C12	-2.04(19)
C12	C13	C30	C29	-160.70(11)	C1	C6	C5	C4	0.25(19)
C12	C33	C34	C35	-2.7(2)	C1	C6	C5	C9	-179.79(12)
C12	C33	C32	C31	9.21(19)	C1	C2	C3	C4	-1.18(19)
C16	C17	C18	C36	177.36(11)	C1	C2	C3	C8	175.79(12)
C16	C17	C18	C19	-1.95(17)	C33	C12	C11	C10	-0.34(18)
C16	C21	C20	C19	-4.42(18)	C33	C12	C13	C14	174.48(11)
C16	C21	C22	C23	6.06(19)	C33	C12	C13	C30	-12.78(17)
C18	C17	C16	C21	-1.53(17)	C33	C32	C31	C30	-5.4(2)
C18	C17	C16	C15	-173.04(11)	C41	C36	C37	C38	-0.22(18)
C18	C36	C37	C38	179.69(11)	C41	C36	C37	C43	-179.42(12)
C18	C36	C37	C43	0.49(18)	C41	C40	C39	C38	-0.78(19)
C18	C36	C41	C40	179.88(11)	C41	C40	C39	C44	-179.97(12)
C18	C36	C41	C42	1.04(19)	C3	C4	C5	C6	-1.56(18)
C18	C19	C20	C21	0.86(19)	C3	C4	C5	C9	178.49(11)

A	B	C	D	Angle/°	A	B	C	D	Angle/°
C21	C16	C15	C14	178.12(11)	C3	C2	C1	C6	-0.11(19)
C21	C16	C15	C24	-11.23(16)	C3	C2	C1	C7	179.95(12)
C21	C22	C23	C24	-4.2(2)	C20	C21	C22	C23	-168.51(12)
C10	C4	C5	C6	176.15(11)	C39	C38	C37	C36	0.17(19)
C10	C4	C5	C9	-3.80(18)	C39	C38	C37	C43	179.38(12)
C10	C4	C3	C2	-175.74(11)	C39	C40	C41	C36	0.73(19)
C10	C4	C3	C8	7.31(17)	C39	C40	C41	C42	179.58(13)
C10	C35	C34	C33	0.3(2)	C24	C25	C26	C27	-11.2(2)
C14	C13	C30	C31	-169.96(11)	C15	C16	C21	C20	176.46(11)
C14	C13	C30	C29	12.51(17)	C15	C16	C21	C22	1.84(17)
C14	C27	C26	C25	-3.2(2)	C15	C14	C13	C12	-32.73(19)
C36	C18	C19	C20	-177.00(11)	C15	C14	C13	C30	154.56(12)
C4	C10	C11	C12	175.29(11)	C15	C14	C27	C28	-160.21(12)
C4	C10	C35	C34	-175.33(12)	C15	C14	C27	C26	20.47(17)
C11	C12	C13	C14	-12.96(19)	C15	C24	C23	C22	-5.75(19)
C11	C12	C13	C30	159.78(12)	C15	C24	C25	C26	7.77(19)
C11	C12	C33	C34	2.69(18)	C22	C21	C20	C19	170.17(12)
C11	C12	C33	C32	-172.89(12)	C34	C33	C32	C31	-166.35(13)
C11	C10	C4	C5	82.90(16)	C32	C33	C34	C35	172.88(13)
C11	C10	C4	C3	-99.39(14)	C31	C30	C29	C28	-172.34(13)
C11	C10	C35	C34	2.1(2)	C28	C27	C26	C25	177.50(13)
C37	C38	C39	C40	0.32(19)	C27	C14	C13	C12	148.87(12)
C37	C38	C39	C44	179.52(12)	C27	C14	C13	C30	-23.84(16)
C37	C36	C41	C40	-0.22(18)	C27	C14	C15	C16	147.08(11)
C37	C36	C41	C42	-179.06(12)	C27	C14	C15	C24	-23.49(16)
C5	C6	C1	C2	0.58(19)	C27	C28	C29	C30	-11.2(2)
C5	C6	C1	C7	-179.48(12)	C23	C24	C15	C16	13.26(17)
C5	C4	C3	C2	2.01(18)	C23	C24	C15	C14	-175.56(11)
C5	C4	C3	C8	-174.94(12)	C23	C24	C25	C26	-166.87(13)
C19	C18	C36	C37	-98.56(14)	C25	C24	C15	C16	-161.30(11)
C19	C18	C36	C41	81.35(15)	C25	C24	C15	C14	9.88(17)
C13	C12	C11	C10	-172.99(12)	C25	C24	C23	C22	168.87(13)
C13	C12	C33	C34	175.64(12)	C29	C30	C31	C32	169.53(13)
C13	C12	C33	C32	0.06(18)	C29	C28	C27	C14	-0.9(2)
C13	C14	C15	C16	-31.33(18)	C29	C28	C27	C26	178.46(13)
C17	C16	C21	C20	4.63(17)	C13	C14	C15	C24	158.10(12)

Atom	*x*	*y*	*z*	U(eq)
H26	6932.73	-2.47	7920.4	28
H42A	6667.19	6073.01	6851.48	38
H42B	7196.03	6203.49	6635.46	38
H42C	6986.19	5143.4	6741.86	38

Table S44. Hydrogen Atom Coordinates (Å×10^4) and Isotropic Displacement Parameters (Å^2×10^3) for **CC[6]**.

Atom	*x*	*y*	*z*	U(eq)
H17	6550.72	3310.84	5595.86	14
H38	6493.75	5721.02	3062.24	18
H6	4086.89	2812.18	4883.96	19
H11	5745.26	1618.91	5368.35	15
H2	4180.55	116.02	3871.96	20
H19	5731.06	5562.36	6189.17	19
H35	5414.29	2160.74	2735.89	22
H40	7262.74	6772.35	5170.35	21
H20	5360.25	4606.81	7197.12	20
H22	5307.87	3104.56	8083.55	23
H34	6183.74	2278.79	2449.11	22
H32	7005.14	2163.34	2947.29	23
H31	7544.92	1545.45	3976.91	24
H8A	5270.59	196.15	3189.02	31
H8B	4873.93	-536.86	3449.47	31
H8C	5274.04	-254.73	4179.18	31
H28	7504.9	117.35	6760.11	28
H23	5635.76	1673.53	8549.04	25
H25	6230.08	420.63	8449.91	28
H29	7743.21	778.22	5442.66	26
H7A	3427.31	1768.57	4900.77	35
H7B	3479.21	647.49	4662.65	35
H7C	3381.82	1419.31	3875.34	35
H44A	7098.32	6786.29	2757.5	33
H44B	7503.73	6929.85	3512.43	33
H44C	7079.04	7664.49	3453.87	33
H43A	5658.1	4797.97	3943.02	31
H43B	5968.47	3870.75	4185.67	31
H43C	6001.15	4387.02	3229.25	31
H9A	5050.62	3748.44	4346.53	31
H9B	5220.78	3267.65	5282.98	31
H9C	4728.57	3781.08	5184.91	31

4. Chiral Resolution & Racemization Behavior

4.1. Separation of Enantiomers

A saturated solution (ca. 1 mL) of the respective helicene (~1 mg) in a mixture of *n*-hexane and DCM (9:1 for BN-helicenes, 1:1 for **CC[5]**, pure DCM for **CC[6]**) was prepared and subsequently passed through a PTFE syringe filter (pore size: 0.20 µm). Depending on the obtained resolution during method development, 15 - 200 µL of the solutions were injected into the HPLC (Table S45) and the enantiomers were separated and collected. If required, impure fractions were subjected to further HPLC runs using the same conditions. This procedure was repeated until sufficient amounts of pure enantiomers were obtained. Enantiopure **BN[6]** was stored at ambient temperature (no notable racemization), while all five-membered helicenes were stored at –20 °C due to a significant racemization rate under these conditions.

Table S45. Conditions and retention times t_R for the chiral resolution of the described helicenes on a semi-preparative Daicel Chiralpak IA HPLC column with chiral amylose stationary phase. Note that slight variations (usually less than ±0.1 min) of the retention times were found.

Compound	Eluent mixture	Injection volume [µL]	t_R (*P*) [min]	t_R (*M*) [min]
BN[5]	8% DCM / *n*-Hexane	200	6.47	7.57
CC[5]	2% DCM / *n*-Hexane	25	10.14	11.46
BN[6]	8% DCM / *n*-Hexane	200	7.29	7.70
CC[6]	2% DCM / *n*-Hexane	15	13.60 *(no resolution achieved)*	
BN[5]-$(CN)_2$	40% DCM / *n*-Hexane	200	6.57	7.67

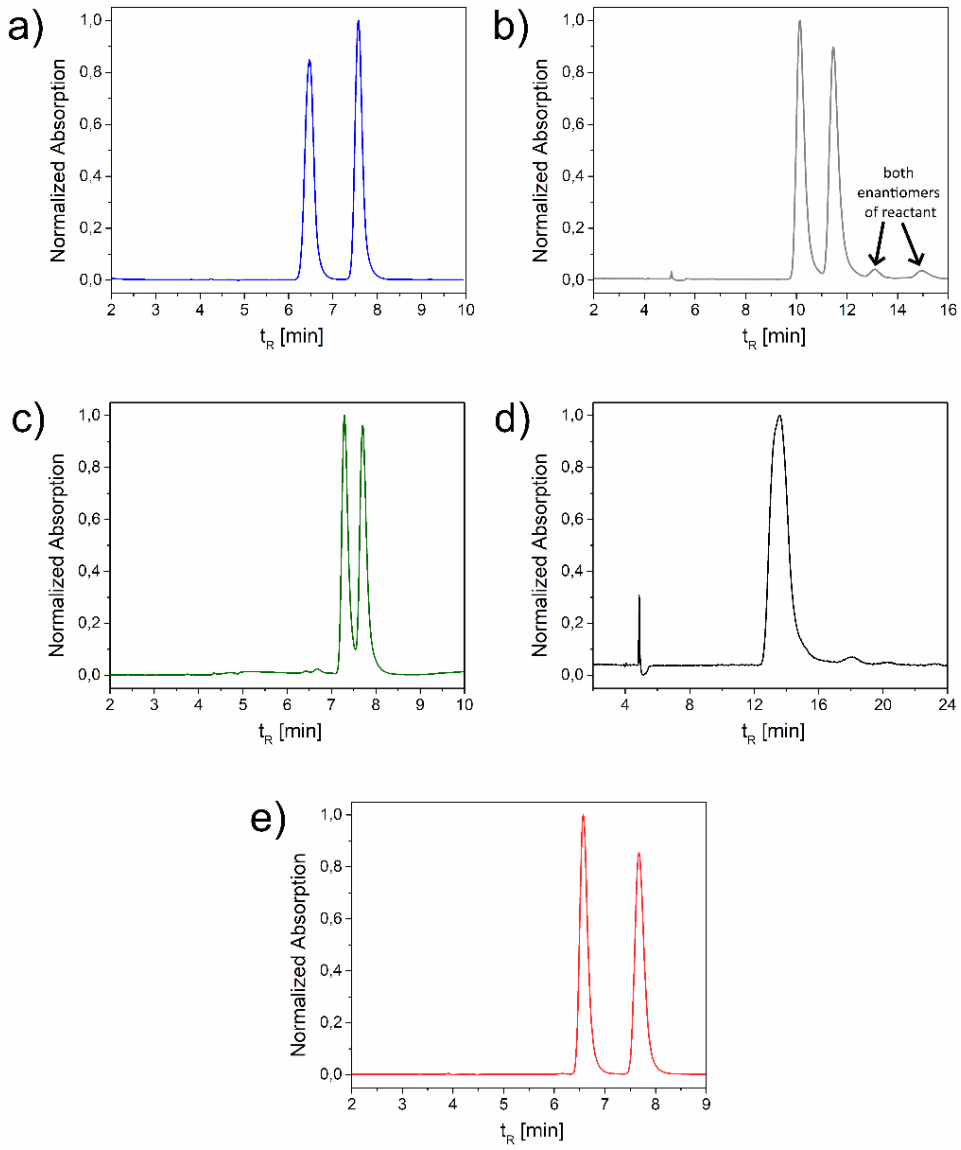

Fig. S15. (CSP)-HPLC chromatograms of **BN[5]** (a), **CC[5]** (b), **BN[6]** (c), **CC[6]** (d) and **BN[5]-(CN)$_2$** (e). The signals at t_R = 4-5 min represent the sample injection front. UV Vis absorption was recorded between λ = 280 – 350 nm, where all compounds showed intense absorptions. Therefore, the chosen wavelength did not have an impact on the peak shapes.

4.2. Kinetics of Racemization

The racemization of the pentahelicenes (initial enantiomeric excess ee_0 (**BN[5]**) = 99%, ee_0 (**CC[5]**) = 70%, ee_0 (**BN[5]-CN$_2$**) = 94%) was investigated by time-course ECD measurements at 50 °C, 60 °C and 70 °C in *n*-heptane (Fig. **S16** and Table S46). The respective ellipticities at the intensity maxima were collected at equal time intervals and the enantiomeric excess (ee_t) was monitored. ln(ee_t/ee_0) was plotted against time and a linear fitting was applied to calculate the rate constant of racemization (k_{rac} = slope). The half-life of racemization $t_{1/2rac}$ was calculated by applying the equation

$$t_{1/2rac} = \frac{\ln(2)}{k_{rac}}.$$

Using the Eyring-Polanyi equation

$$\Delta G^{\ddagger}(T) = -RT \ln\left(\frac{k_e \times h}{k_B \times T \times \kappa}\right),$$

the corresponding Gibbs' free activation energy of enantiomerization $\Delta G^{\ddagger}(T)$ could be calculated for the investigated temperatures, using the constants R = 8.31441 J × K^{-1}, h = 6.626176 × 10^{-34} J × s, k_B = 1.380662 × 10^{-23} J × K^{-1} and k_e = 0.5 k_{rac}. The transmission coefficient κ = 0.5 needs to be used because the enantiomerization process is a reversible reaction of first order.

Using the relation

$$\ln\left(\frac{k_e}{T}\right) = -\left(\frac{\Delta H^{\ddagger}}{R}\right) \times \left(\frac{1}{T}\right) + \ln\left(\frac{\kappa \times k_B}{h}\right) + \frac{\Delta S^{\ddagger}}{R},$$

the respective activation enthalpies ($\Delta H^{\ddagger}$) and entropies ($\Delta S^{\ddagger}$) of racemization were calculated. For that purpose, $\ln\left(\frac{k_e}{T}\right)$ was plotted against $\left(\frac{1}{T}\right)$ for each temperature. The respective linear fittings (y = a – b × x) with slope $-\left(\frac{\Delta H^{\ddagger}}{R}\right)$ and intercept $\ln\left(\frac{\kappa \times k_B}{h}\right) + \frac{\Delta S^{\ddagger}}{R}$ then allowed to derive these temperature-independent values (Table S47), which can be used to calculate $\Delta G^{\ddagger}(T)$ at any temperature via the relation

$$\Delta G^{\ddagger} = \Delta H^{\ddagger} - T \times \Delta S^{\ddagger}.$$

Table S46. Kinetic parameters that describe the racemization process of enantioenriched samples, determined by time-course ECD measurements.

Compound	k_{rac} [s^{-1}]	$t_{1/2rac}$ [min]	$\Delta G^{\ddagger}(T)$ [kcal mol^{-1}]
BN[5]			
50 °C	5.34×10^{-5}	216.4	25.3
60 °C	1.49×10^{-4}	77.6	25.4
70 °C	8.82×10^{-4}	13.1	25.0
CC[5]			
50 °C	1.55×10^{-4}	74.8	24.6
60 °C	5.47×10^{-4}	21.1	24.5
70 °C	1.20×10^{-3}	9.6	24.8
BN[5]-$(CN)_2$			
50 °C	7.77×10^{-5}	148.6	25.0
60 °C	2.30×10^{-4}	50.3	25.1
70 °C	9.38×10^{-4}	12.3	24.9

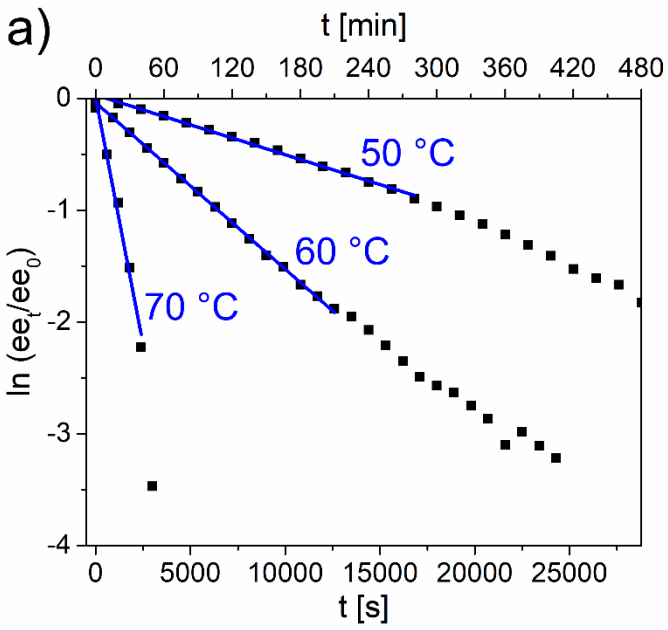

Equation	y = a + b*x		
Weight	No Weighting		
Residual Sum of Squares	0.00322		
Pearson's r	-0.9986		
Adj. R-Square	0.99699		
		Value	Standard Error
50 °C	Intercept	0.02971	0.00773
	Slope	-5.33871E-5	7.83402E-7

Equation	y = a + b*x		
Weight	No Weighting		
Residual Sum of Squares	0.00316		
Pearson's r	-0.99969		
Adj. R-Square	0.99932		
		Value	Standard Error
60 °C	Intercept	-0.03804	0.00766
	Slope	-1.48923E-4	1.03495E-6

Equation	y = a + b*x		
Weight	No Weighting		
Residual Sum of Squares	0.04135		
Pearson's r	-0.99269		
Adj. R-Square	0.98059		
		Value	Standard Error
70 °C	Intercept	0.00522	0.09094
	Slope	-8.81771E-4	6.1875E-5

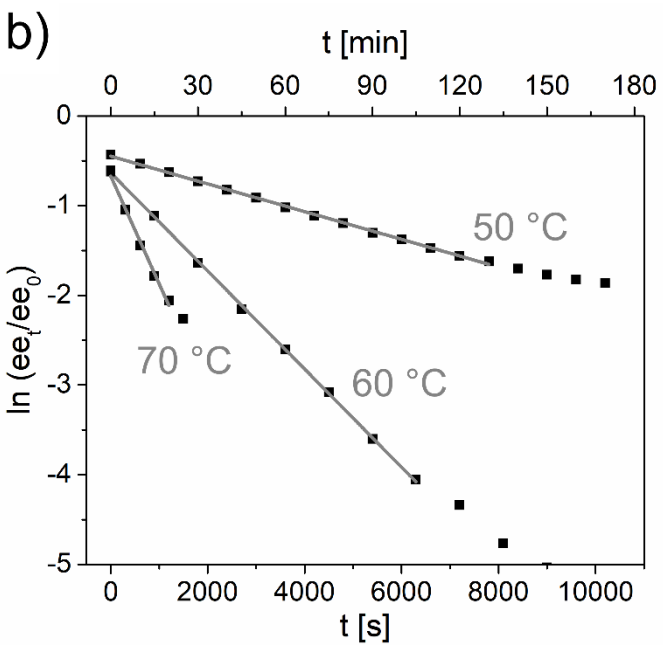

Equation	y = a + b*x		
Weight	No Weighting		
Residual Sum of Squares	0.00224		
Pearson's r	-0.99943		
Adj. R-Square	0.99876		
		Value	Standard Error
50 °C	Intercept	-0.44773	0.00693
	Slope	-1.54506E-4	1.5099E-6

Equation	y = a + b*x		
Weight	No Weighting		
Residual Sum of Squares	0.00431		
Pearson's r	-0.99979		
Adj. R-Square	0.99951		
		Value	Standard Error
60 °C	Intercept	-0.63253	0.01729
	Slope	-5.47287E-4	4.59326E-6

Equation	y = a + b*x		
Weight	No Weighting		
Residual Sum of Squares	0.00981		
Pearson's r	-0.99625		
Adj. R-Square	0.99001		
		Value	Standard Error
70 °C	Intercept	-0.67009	0.04431
	Slope	-0.0012	6.02917E-5

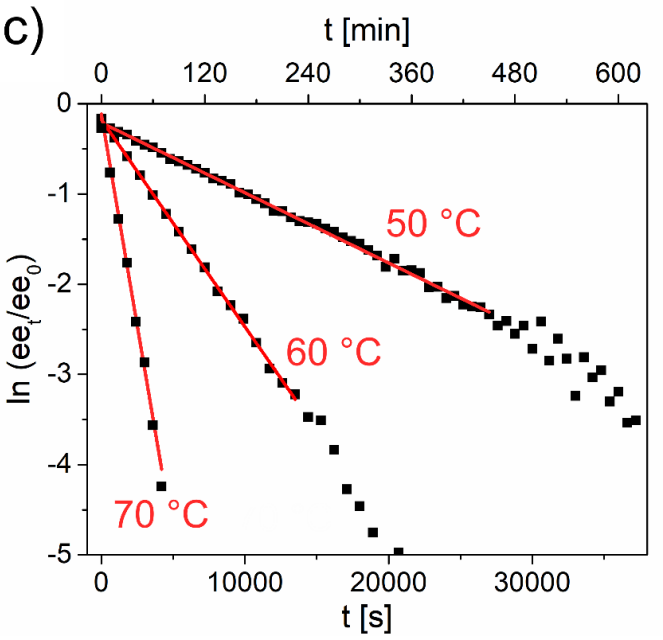

Equation	y = a + b*x		
Weight	No Weighting		
Residual Sum of Squares	0.05163		
Pearson's r	-0.99854		
Adj. R-Square	0.99702		
		Value	Standard Error
50 °C	Intercept	-0.2088	0.00994
	Slope	-7.77486E-5	6.34062E-7

Equation	y = a + b*x		
Weight	No Weighting		
Residual Sum of Squares	0.01575		
Pearson's r	-0.99946		
Adj. R-Square	0.99884		
		Value	Standard Error
60 °C	Intercept	-0.17391	0.01601
	Slope	-2.29709E-4	2.02128E-6

Equation	y = a + b*x		
Weight	No Weighting		
Residual Sum of Squares	0.05101		
Pearson's r	-0.99809		
Adj. R-Square	0.99554		
		Value	Standard Error
70 °C	Intercept	-0.11444	0.05952
	Slope	-9.37511E-4	2.37121E-5

Fig. S16. Plots of ln(ee$_t$/ee$_0$) against time and linear fittings for **BN[5]** (a), **CC[5]** (b) and **BN[5]-(CN)$_2$** (c) at different temperatures.

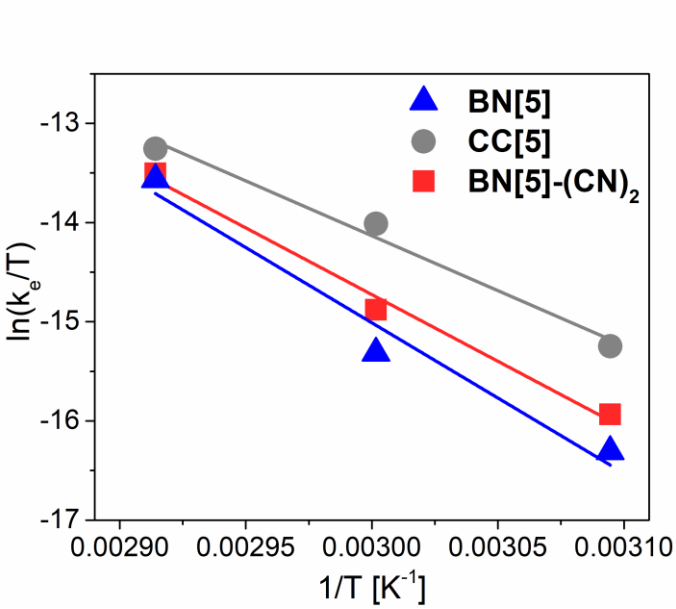

Equation	y = a + b*x		
Weight	No Weighting		
Residual Sum of Squares	0.11643		
Pearson's r	-0.9848		
Adj. R-Square	0.93968		
		Value	Standard Error
BN[5]	Intercept	30.49778	8.0368
	Slope	-15169.3324	2675.04582

Equation	y = a + b*x		
Weight	No Weighting		
Residual Sum of Squares	0.02901		
Pearson's r	-0.9928		
Adj. R-Square	0.97129		
		Value	Standard Error
CC[5]	Intercept	19.06096	4.012
	Slope	-11064.6747	1335.39234

Equation	y = a + b*x		
Weight	No Weighting		
Residual Sum of Squares	0.02625		
Pearson's r	-0.99557		
Adj. R-Square	0.98232		
		Value	Standard Error
BN[5]-(CN)2	Intercept	25.62197	3.81607
	Slope	-13449.31127	1270.17774

Fig. S17. Eyring-Polanyi plot of the investigated pentahelicenes at 50 °C, 60 °C and 70 °C.

Table S47. Fitting parameters of Eyring-Polanyi plot as well as calculated $\Delta H^{\ddagger}$, $\Delta S^{\ddagger}$ and $\Delta G^{\ddagger}$ at 25 °C.

Compound	Intercept (a)	Slope (b)	$\Delta H^{\ddagger}$ [kcal mol^{-1}]	$\Delta S^{\ddagger}$ [cal mol^{-1} K^{-1}]	$\Delta G^{\ddagger}$ (25 °C) [kcal mol^{-1}]
BN[5]	30.50	– 15 169	30.12	14.76	25.7
CC[5]	19.06	– 11 065	21.97	–7.96	24.3
BN[5]-(CN)$_2$	25.62	– 13 449	26.71	5.07	25.2

As carbohelicene **CC[6]** was not resolvable by (CSP)-HPLC, **BN[6]** was the only hexahelicene that was to be subjected to a racemization study. However, heating an enantiopure sample (ee_0 = 99%) of (*P*)-**BN[6]** in *n*-dodecane to 200 °C for 14 h did not lead to a detectable amount of the other enantiomer. Increasing the temperature to 220 °C for 30 min resulted in decomposition. Therefore, kinetic parameters of the hexahelicenes could not be collected.

5. Optical Spectroscopy

5.1. Molar Extinction Coefficients

1,14-Dihydro-2,13-dimesityl-1,14-diaza-2,13-diborapentahelicene (**BN[5]**)

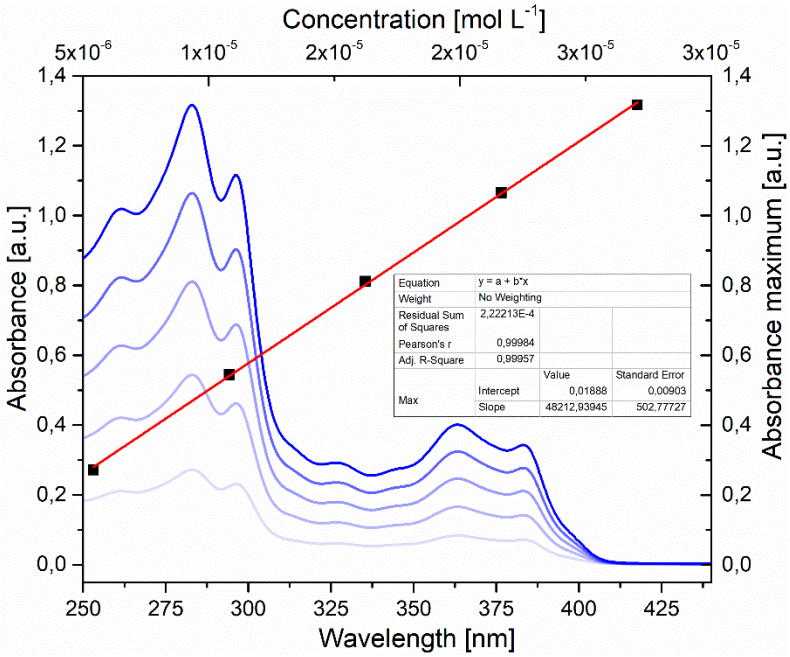

Fig. S18. Absorption spectra of **BN[5]** at different concentrations (5.4 × 10^{-6} to 2.7 × 10^{-5} mol L^{-1}) in DCM and linear fitting according to the Lambert-Beer law.

2,13-Dimesitylpentahelicene (**CC[5]**)

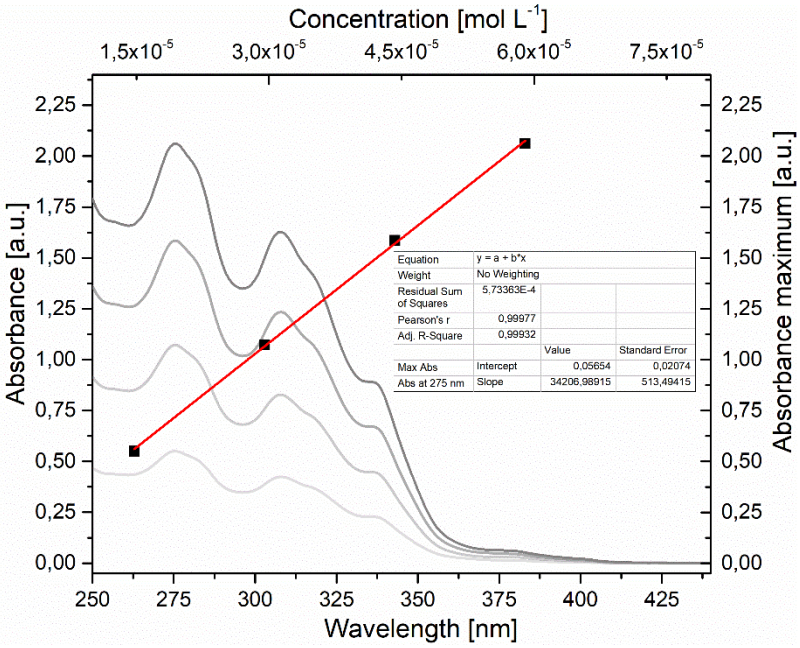

Fig. S19. Absorption spectra of **CC[5]** in different concentrations (1.5 × 10^{-5} to 5.9 × 10^{-5} mol L^{-1}) in DCM and linear fitting according to the Lambert-Beer law.

1,16-Dihydro-2,15-dimesityl-1,16-diaza-2,15-diborahexahelicene (**BN[6]**)

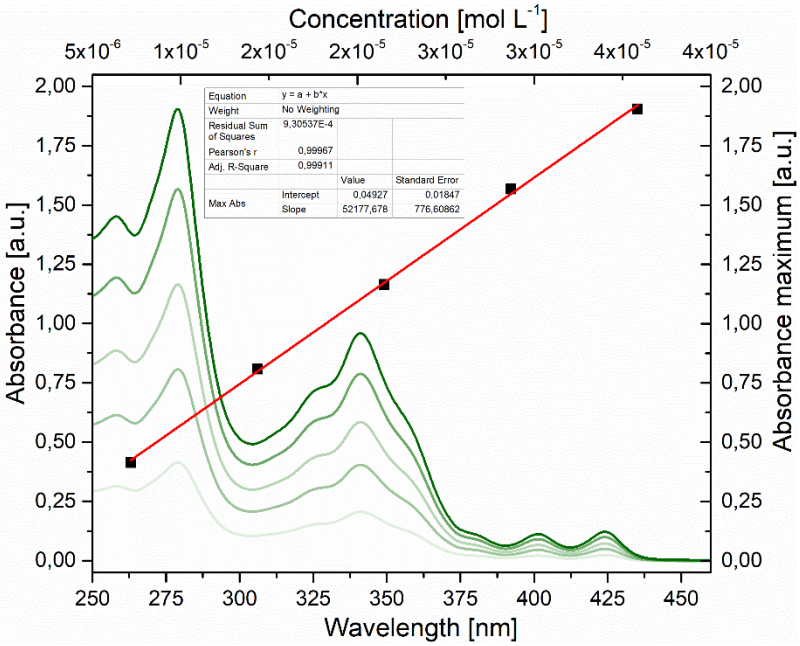

Fig. S20. Absorption spectra of **BN[6]** in different concentrations (7.2 × 10^{-6} to 3.6 × 10^{-5} mol L^{-1}) in DCM and linear fitting according to the Lambert-Beer law.

2,15-Dimesitylhexahelicene (**CC[6]**)

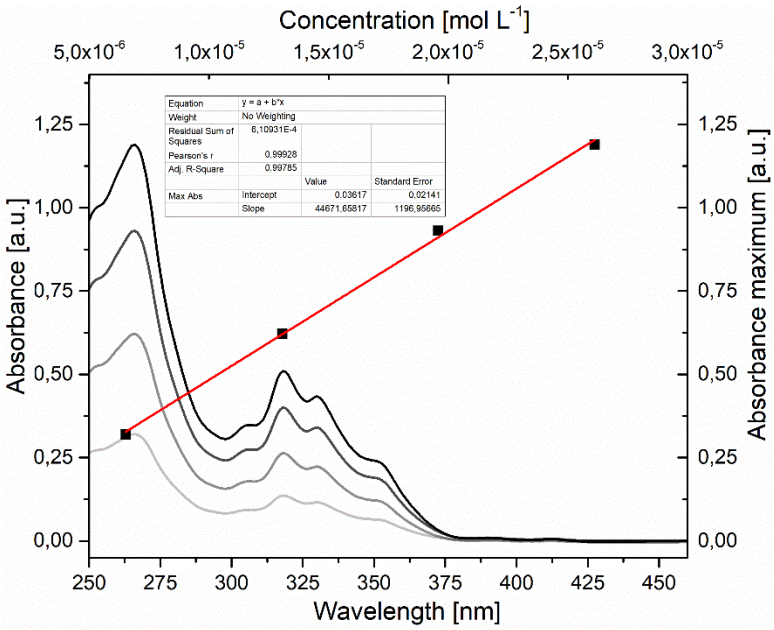

Fig. S21. Absorption spectra of **CC[6]** in different concentrations (6.5 × 10^{-6} to 2.6 × 10^{-5} mol L^{-1}) in DCM and linear fitting according to the Lambert-Beer law.

3,12-Dicyano-1,14-dihydro-2,13-dimesityl-1,14-diaza-2,13-diborapentahelicene (**BN[5]-(CN)$_2$**)

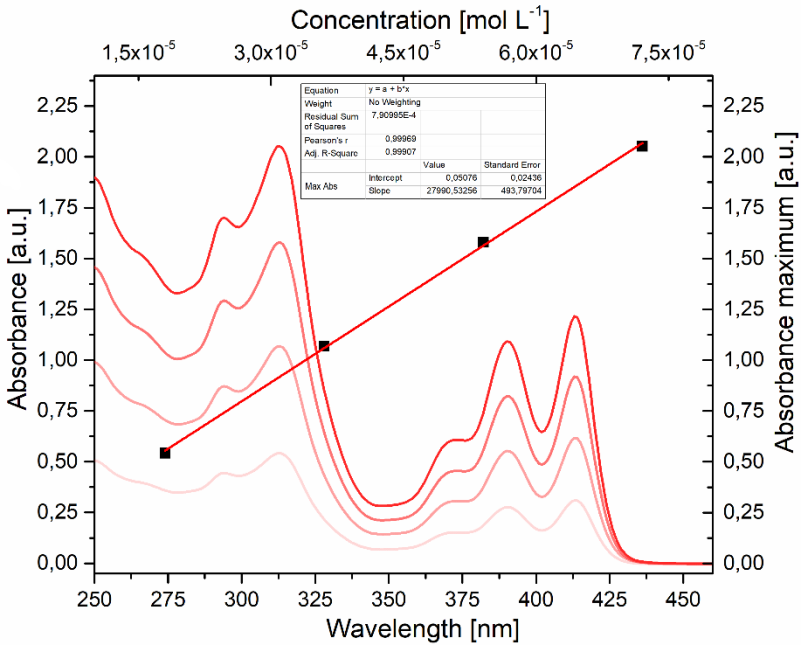

Fig. S22. Absorption spectra of **BN[5]-(CN)$_2$** in different concentrations (1.8×10^{-5} to 9.0×10^{-5} mol L^{-1}) in DCM and linear fitting according to the Lambert-Beer law.

5.2. Excitation Spectra

In order to choose the most suitable excitation wavelength (λ_{ex}) to carry out the emission measurements, we initially measured different excitation spectra in DCM as solvent. Fluorescence emission wavelengths (λ_{fl}) were fixed at different wavelengths around local maxima. Fig. S23 highlights that the highest intensities of the excitation curves of the BN-helicenes were between λ_{ex} = 360 nm and λ_{ex} = 380 nm, so we measured emission spectra with λ_{ex} = 375 nm. For the carbohelicenes, the highest intensities of the excitation curves (besides maxima in the high-energy region of 280 nm) were between λ_{ex} = 300 nm and λ_{ex} = 340 nm, so we chose to measure the emission spectra with λ_{ex} = 320 nm.

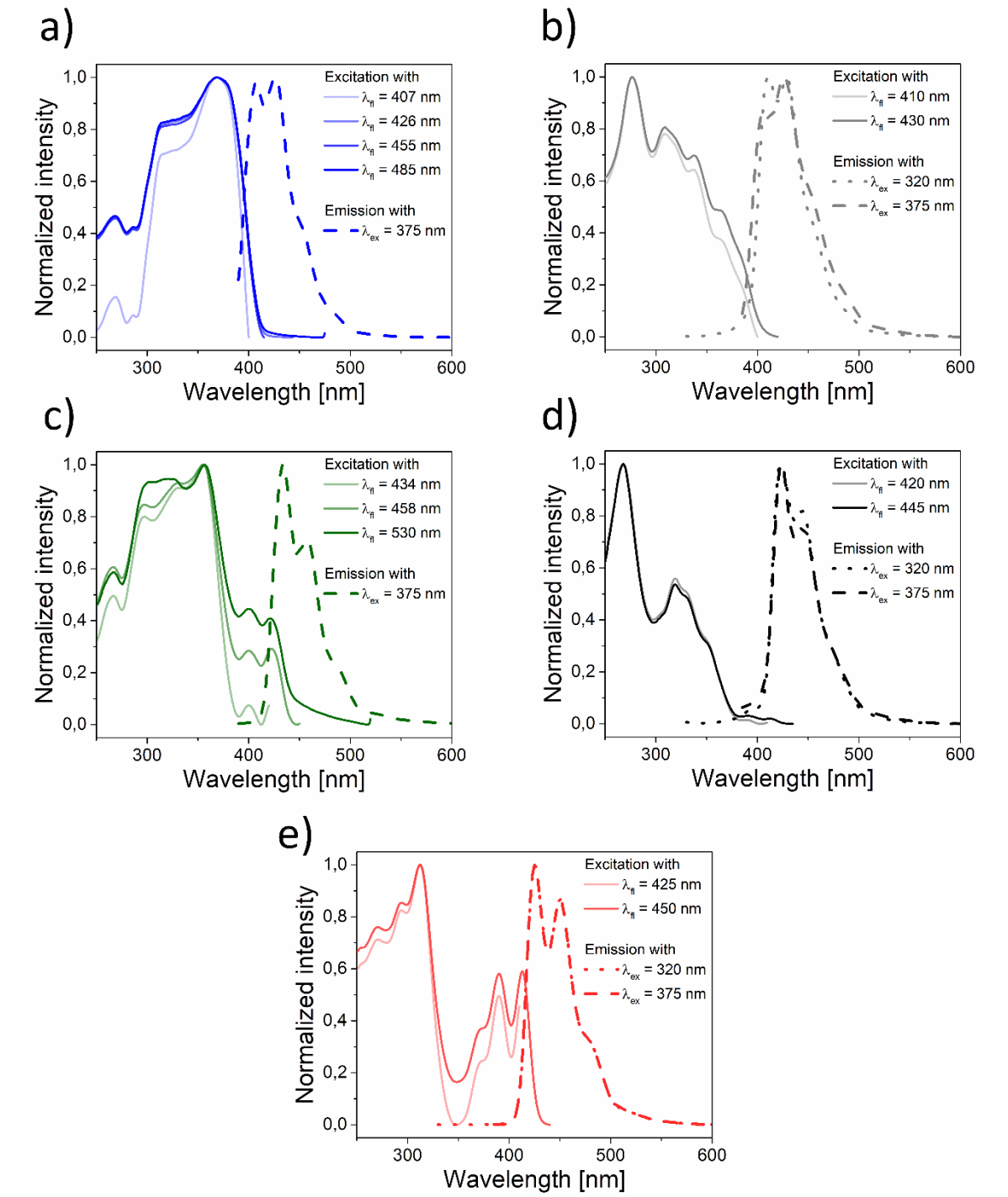

Fig. S23. Normalized excitation spectra at different, fixed emission wavelengths (solid lines) and normalized emission spectra, obtained at different excitation wavelengths (dashed and dotted lines) of **BN[5]** (a), **CC[5]** (b), **BN[6]** (c), **CC[6]** (d), **BN[5]-(CN)$_2$** (e) in DCM solution.

5.3. Fluorescence Lifetimes

Fluorescence lifetimes were measured in DCM around the main emissive peaks ($\Delta\lambda_{fl} \pm 10$ nm) observed in the fluorescence spectra, using a 375 nm laser as excitation source for the BN-helicenes and a 320 nm LED as excitation source for the carbohelicenes. Table S48 shows the lifetime distributions. While **BN[5]** and its substitute **BN[5]-(CN)$_2$** have just one lifetime component ($\tau = 4.7$ ns / $\tau = 3.5$ ns), the decay curves of **BN[6]**, **CC[5]** and **CC[6]** have biexponential character with higher average lifetimes of $\tau = 7$–10 ns. The influence of one additional, conjugated ring on the lifetime was small ($\Delta\tau < 1$ ns between **CC[5]** and **CC[6]**).

Table S48. Fluorescence lifetimes τ of the helicenes around the main emissive peaks.

Compound	Emission wavelength range [nm]	τ_1 [ns]	τ_2 [ns]	$\tau_{average}$ [ns]
BN[5]	405 – 425	4.73±0.02		4.73
CC[5]	410 – 430	11.09±0.04	1.03±0.002	9.66
BN[6]	430 – 460	7.21±0.02	1.58±0.37	7.13
CC[6]	425 – 445	8.95±0.03	3.27±0.26	8.71
BN[5]-(CN)$_2$	425 – 445	3.545±0.01		3.55

In order to extract more information about the multi-exponential characters, we also performed TRES of the compounds that showed more than one lifetime component. This enabled the deconvolution of the emission (Fig. S24). A 325 nm LED was used as excitation source.

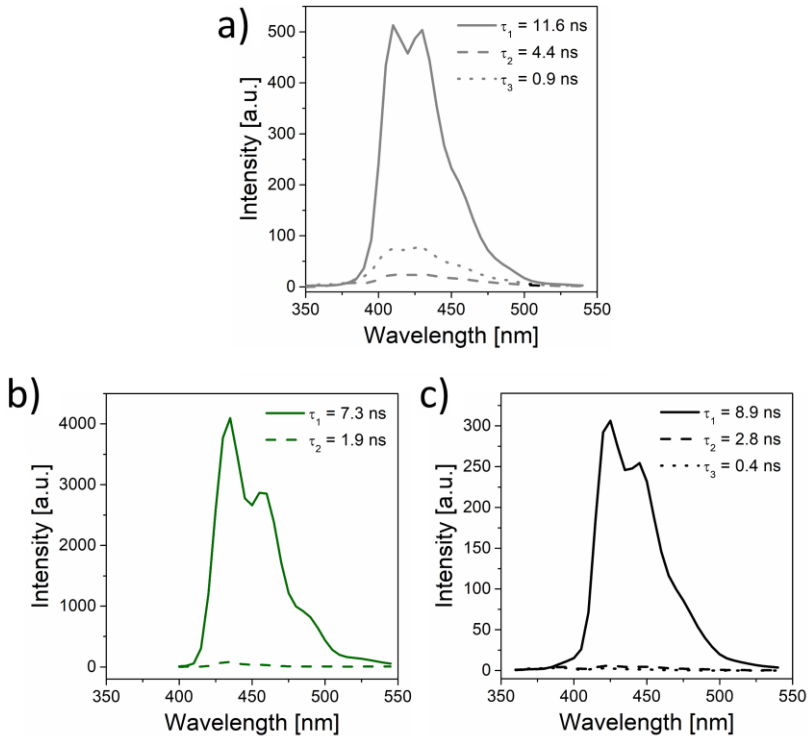

Fig. S24. SAEMS spectra of **CC[5]** (a), **BN[6]** (b) and **CC[6]** (c) in DCM solution.

The deconvolution of the spectra over the emission range showed that for all compounds, the species with the longest lifetimes contributed most to the shape and intensity of the fluorescence spectra. In case of both hexahelicenes, the contributions of the shorter lifetimes were negligibly small. Therefore, average lifetimes are similar to the comparably longest components. Both carbohelicenes showed three species in the excited state, although the shortest lifetime observed in **CC[6]** may be due to dispersion. These results also reveal the independence of fluorescence lifetimes and excitation wavelengths (note that values shown in Table S48 were recorded at λ_{ex} = 375 nm, whereas TRES was carried out at λ_{ex} = 325 nm).

5.4. ECD Spectra

Fig. S25 shows plots of the absorption dissymmetry factors (g_{abs}). The values as obtained from the ECD spectrometer can be interconverted between ellipticity in millidegrees (mdeg) and milliabsorbance (mAbs) using the relation

$$\text{mAbs} = \frac{\text{mdeg}}{32.982}.$$

The molar extinction Δε at a specific wavelength is calculated using the relation

$$\Delta\varepsilon = \frac{\text{mdeg} \times \text{M}}{32982 \times \text{c}}.$$

M is the molar weight in g mol^{-1}, L is the path length (1 cm) and c is the sample concentration in g L^{-1}. g_{abs} is obtained using the relation

$$g_{abs} = \frac{\Delta\varepsilon}{\varepsilon},$$

where ε is the molar extinction coefficient at a specific wavelength as calculated above.

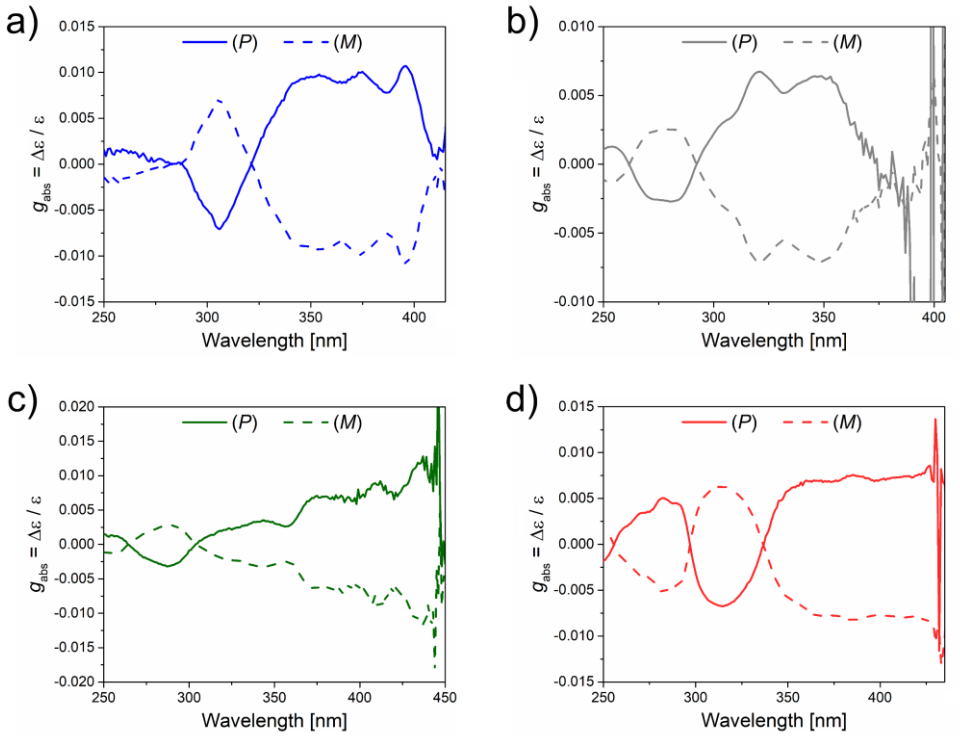

Fig. S25. Plots of the absorption dissymmetry factors (g_{abs}) for **BN[5]** (a), **CC[5]** (b), **BN[6]** (c) and **BN[5]-(CN)$_2$** (d) in DCM solution.

5.5. CPL Spectra

The obtained intensities of left- and right-handed polarized light (I_L and I_R, averaged over at least 50 scans, respectively) were used to calculate the luminescence dissymmetry factors g_{lum} (Fig. S27), using the equation

$$g_{lum} = 2 \times \frac{I_L - I_R}{I_L + I_R}$$

The g_{lum} value can range between –2 and +2, where 0 indicates entirely unpolarized light and |2| represents completely polarized light.

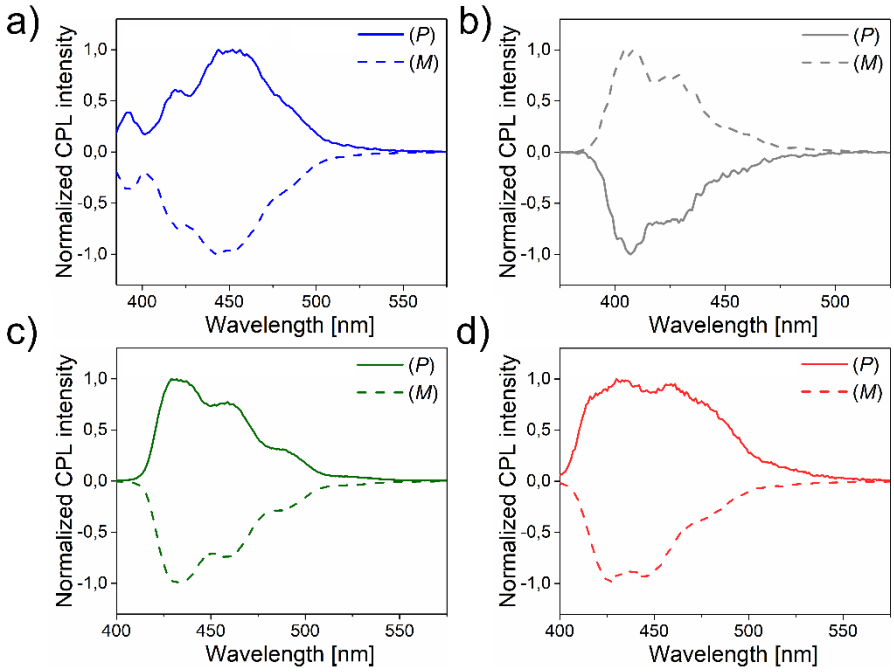

Fig. S26. Normalized CPL spectra of both enantiomers of **BN[5]** (a), **CC[5]** (b), **BN[6]** (c) and **BN[5]-(CN)$_2$** (d) in DCM solution.

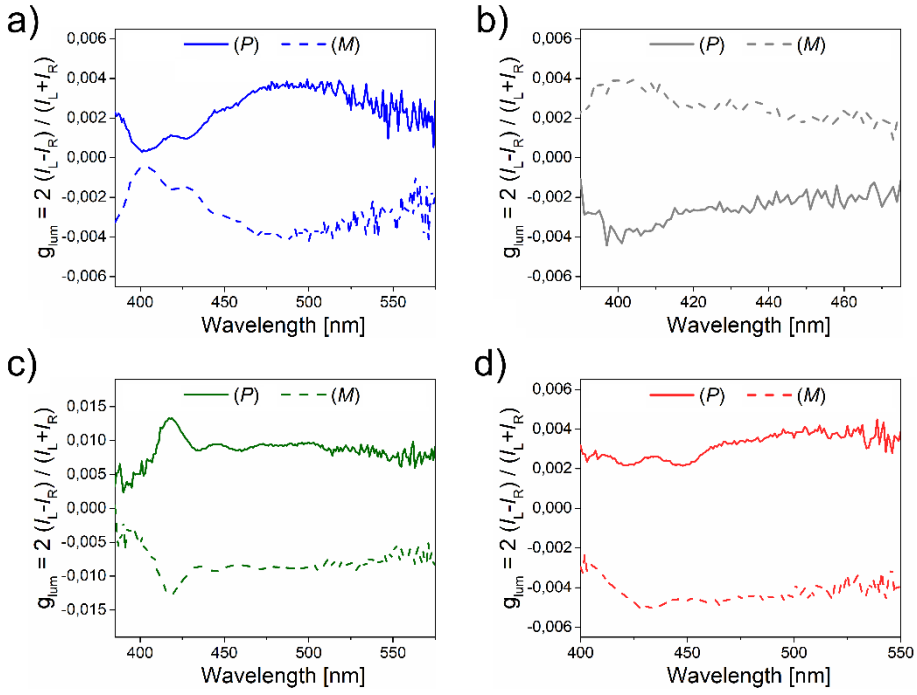

Fig. S27. Plots of the luminescence dissymmetry factors (g_{lum}) for **BN[5]** (a), **CC[5]** (b), **BN[6]** (c) and **BN[5]-(CN)$_2$** (d) in DCM solution.

6. NMR Spectra

6.1. 1-Hydro-2-mesityl-1,2-azaborinine (14)

^{1}H NMR (500 MHz, $CDCl_3$)

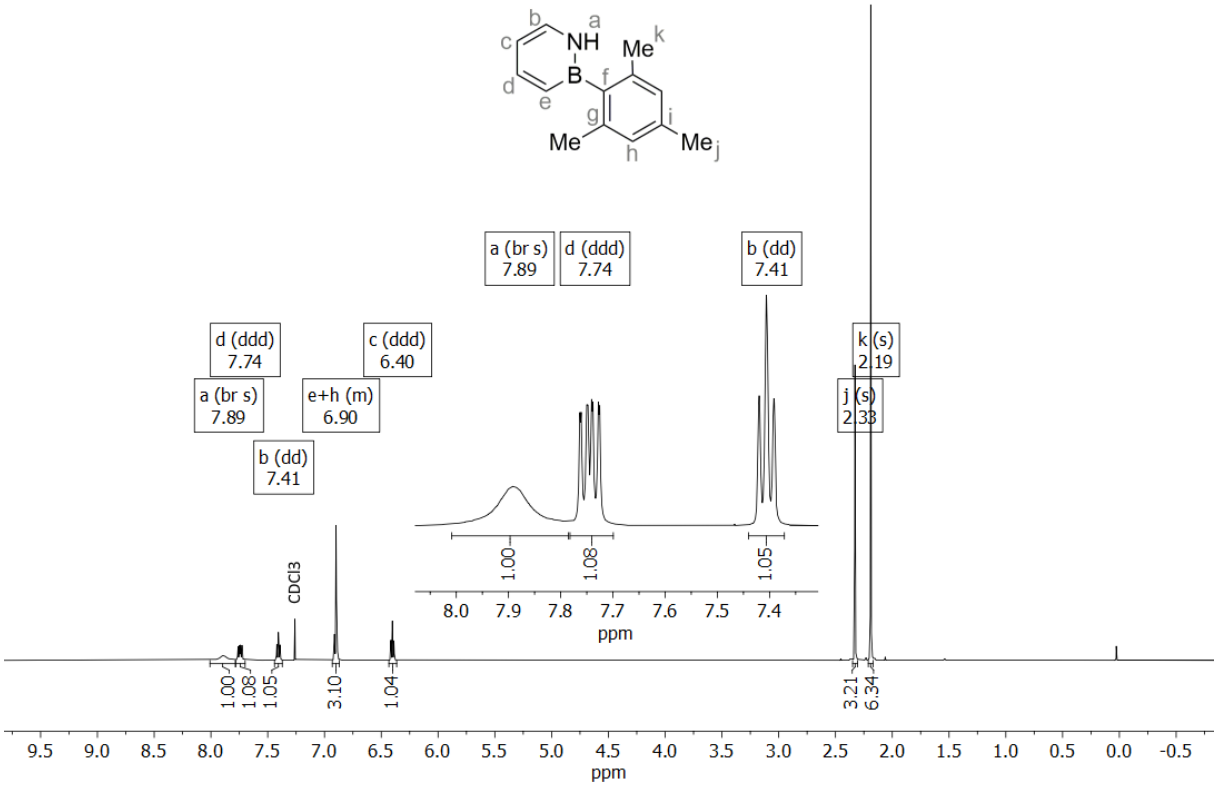

^{13}C{^{1}H} NMR (126 MHz, $CDCl_3$)

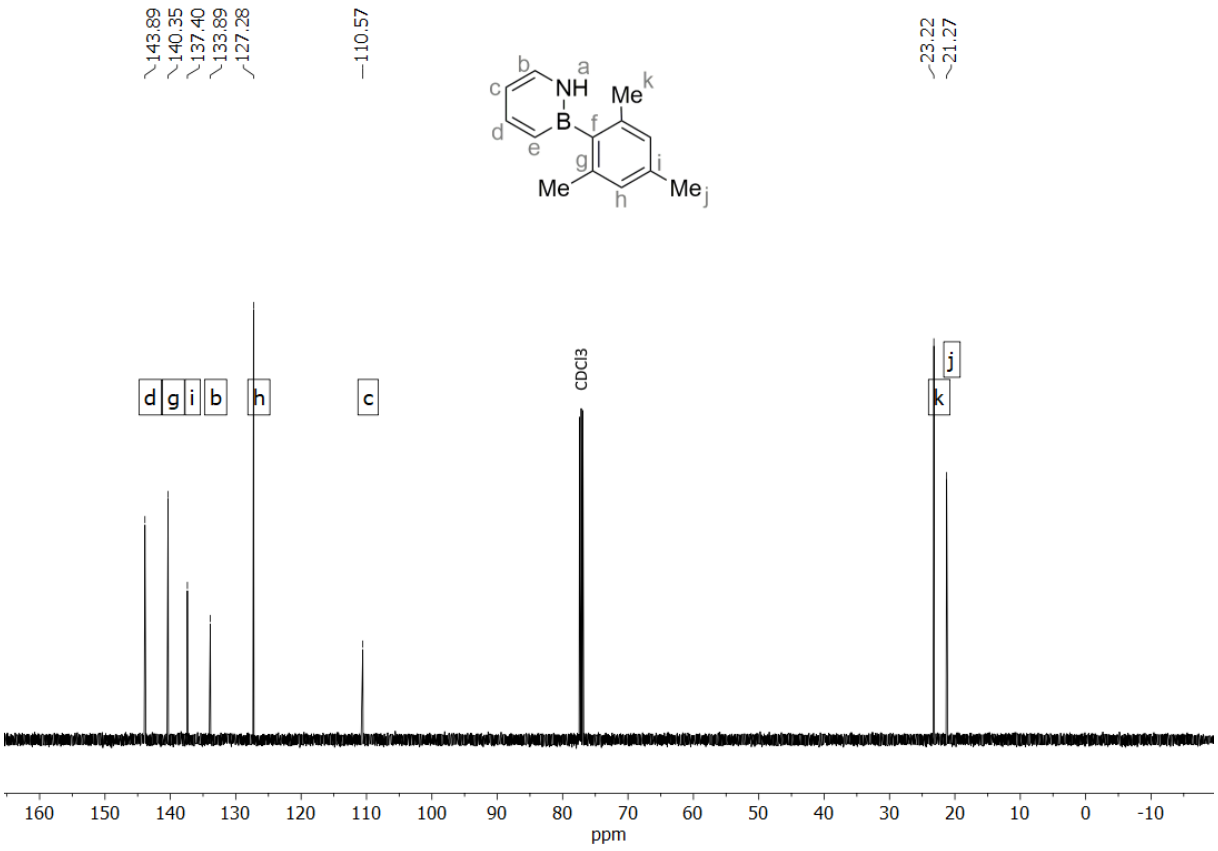

$^{11}B\{^{1}H\}$ NMR (160 MHz, $CDCl_3$)

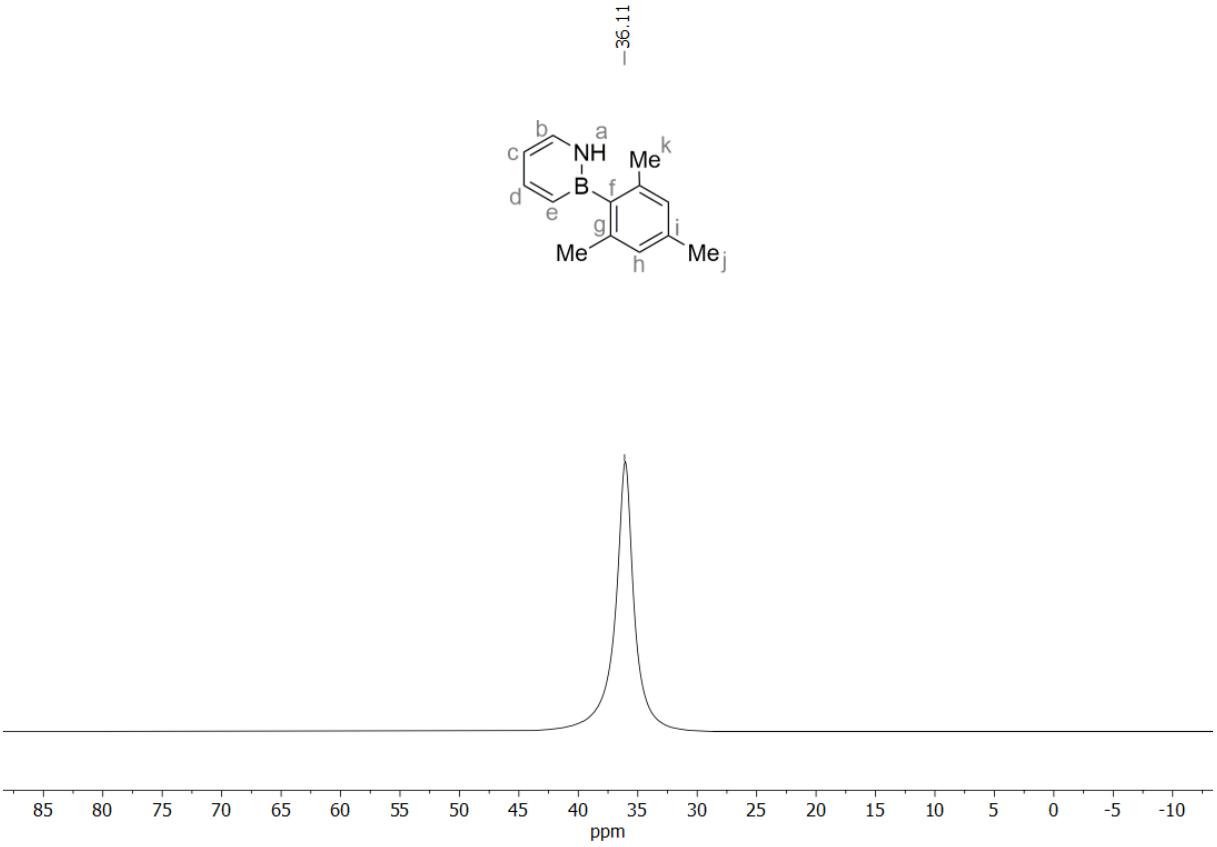

6.2. 1-Hydro-2-mesityl-6-(4,4,5,5-tetramethyl-1,3,2-dioxaborolan-2-yl)-1,2-azaborinine (3)

^{1}H NMR (500 MHz, $CDCl_3$)

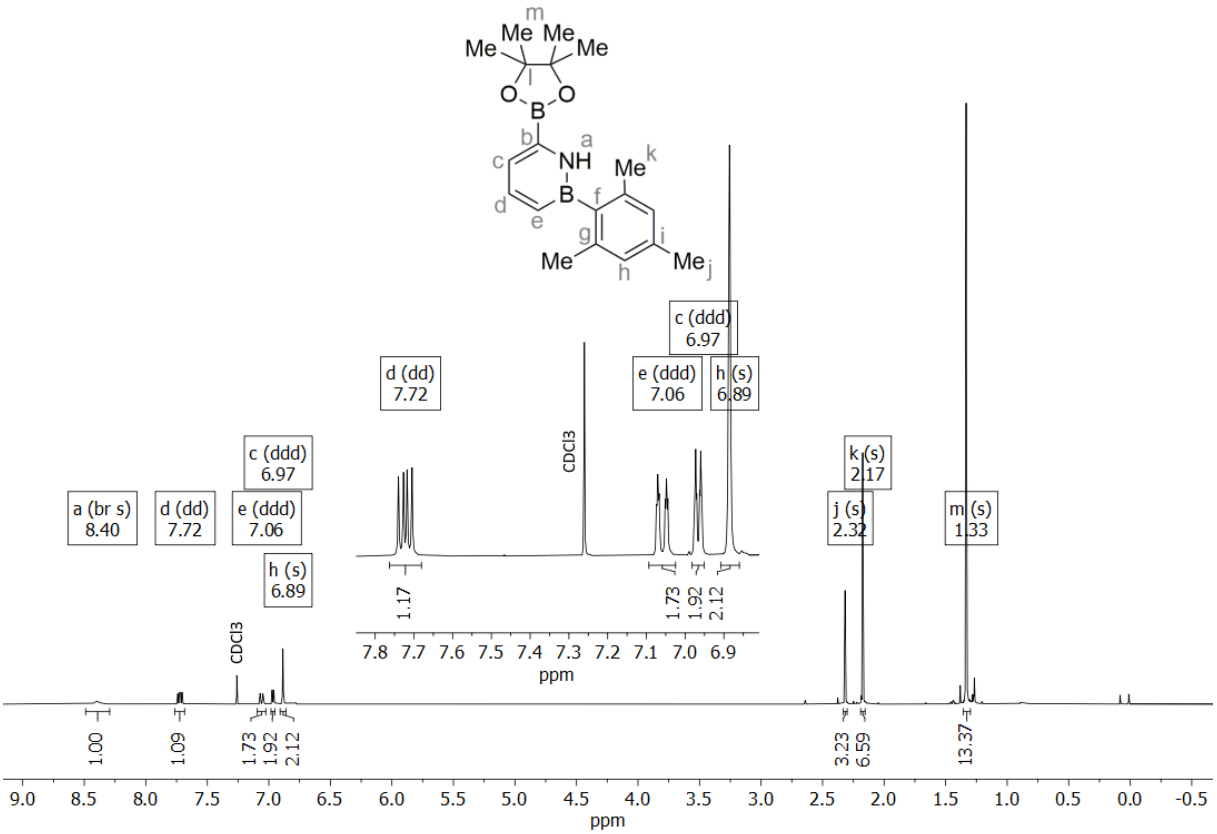

$^{13}C\{^{1}H\}$ NMR (126 MHz, $CDCl_3$)

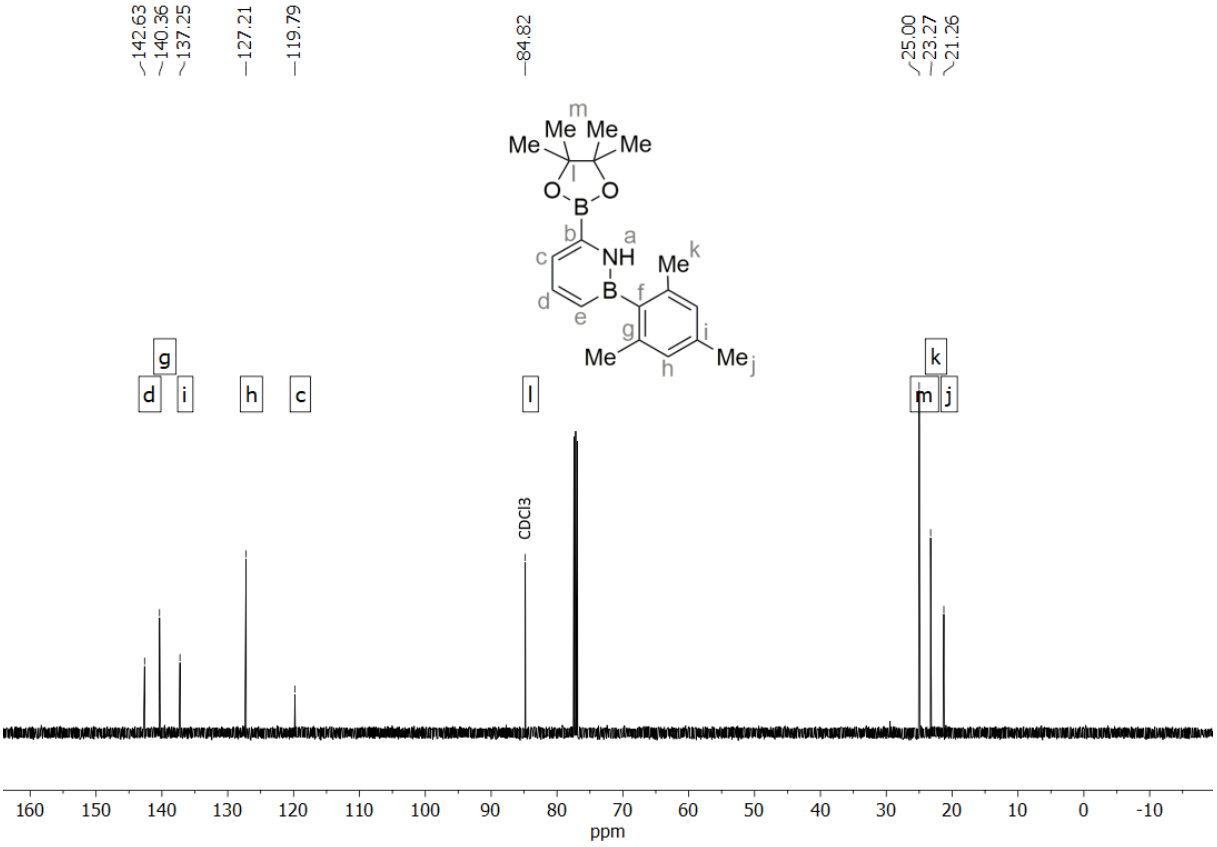

$^{11}B\{^{1}H\}$ NMR (160 MHz, $CDCl_3$)

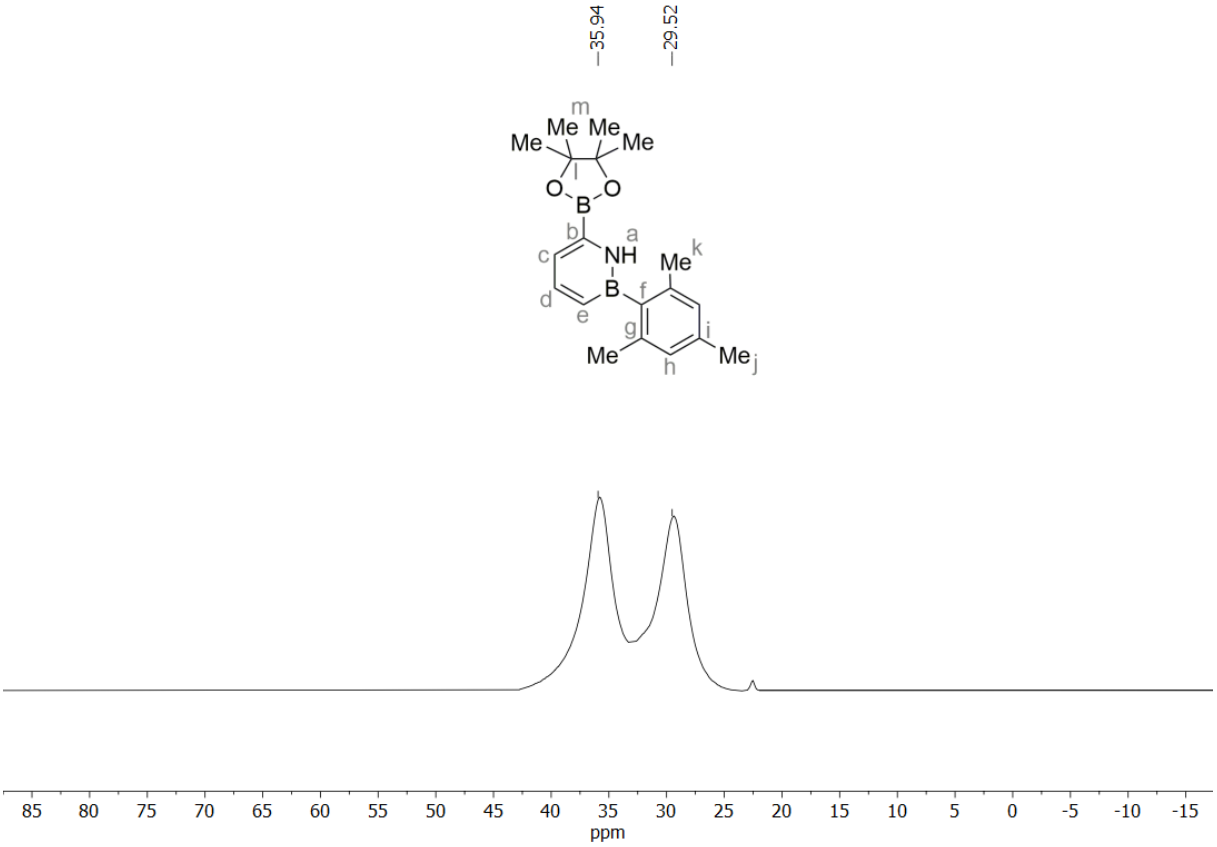

6.3. 1,4-bis(Trimethylsilyl)-2,3-dibromobenzene (15)

^{1}H NMR (500 MHz, $CDCl_3$)

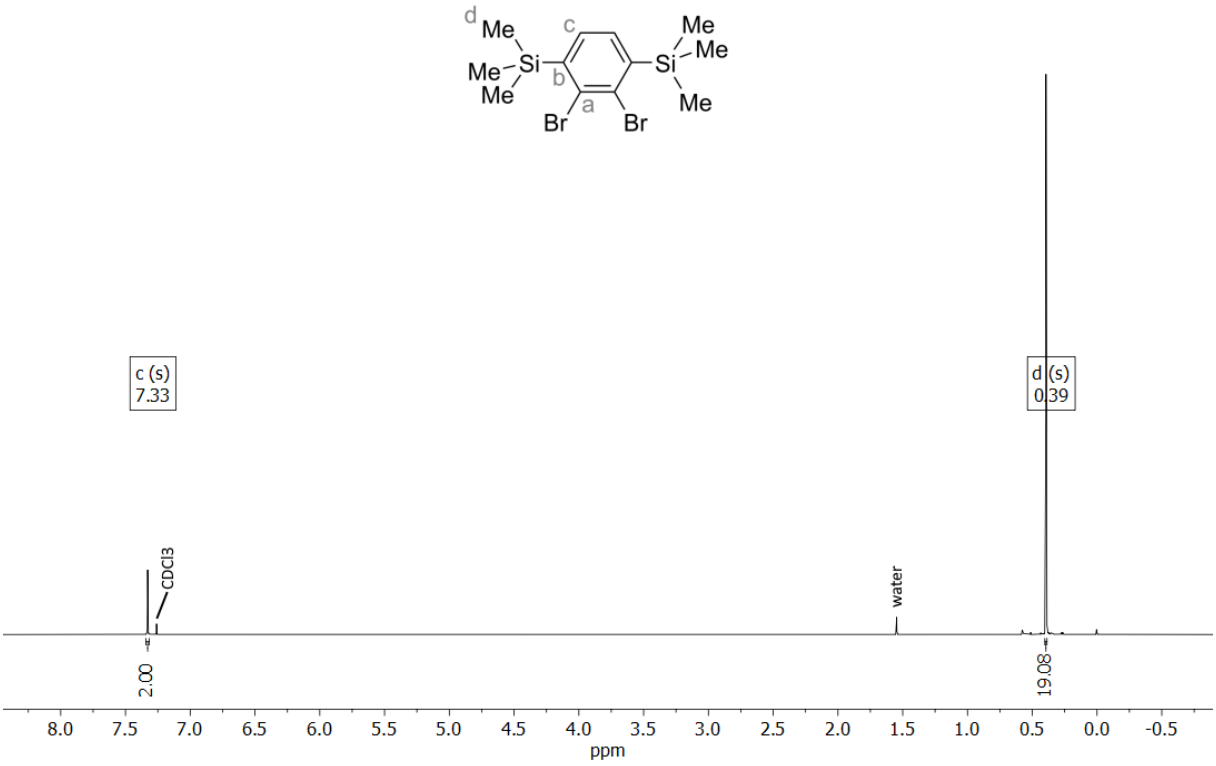

^{13}C{^{1}H} NMR (126 MHz, $CDCl_3$)

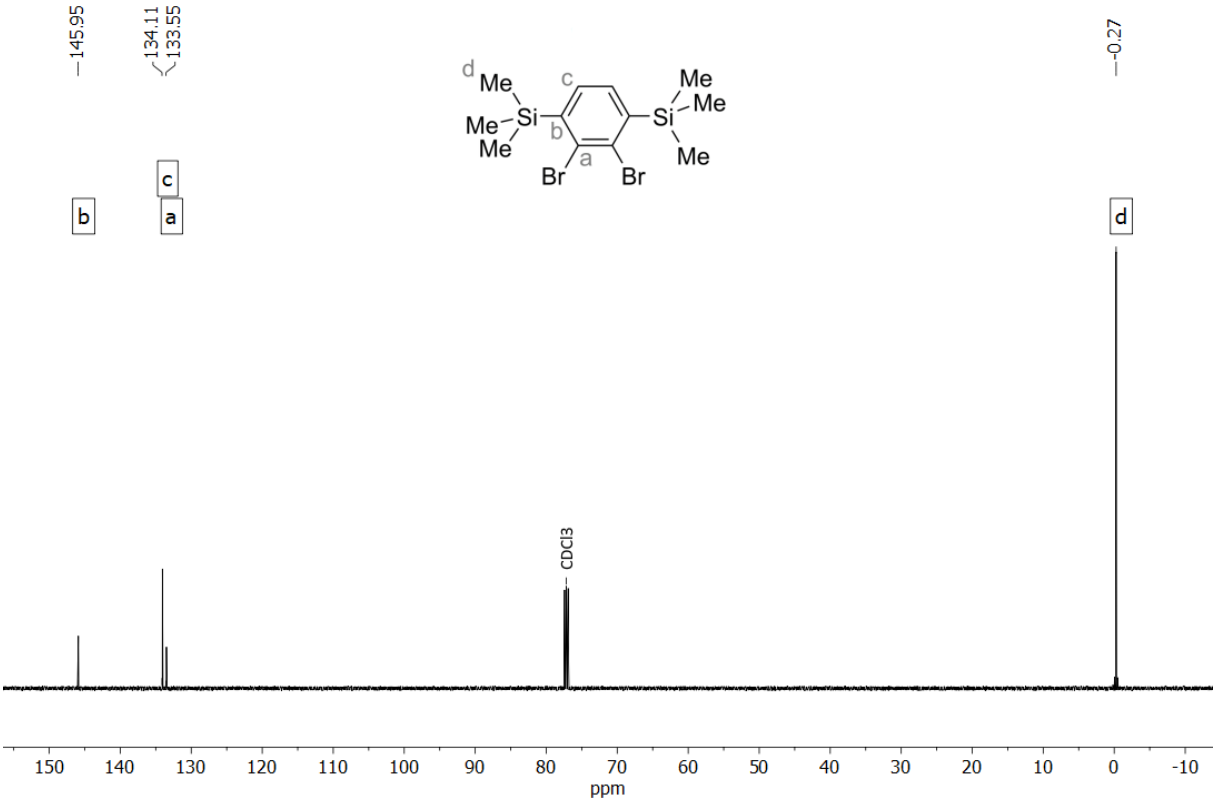

$^{29}Si\{^{1}H\}$ NMR (99 MHz, $CDCl_3$)

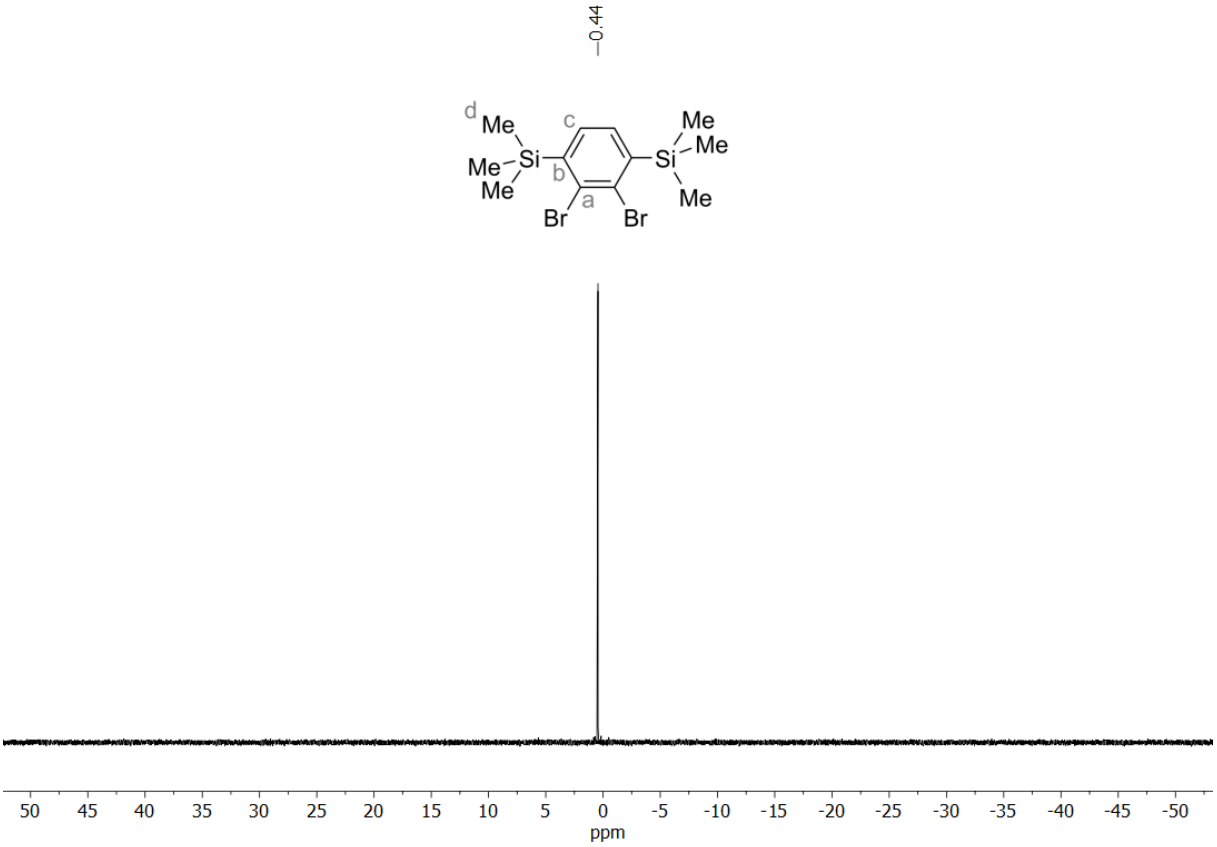

6.4. 2,3-Dibromo-1,4-diiodobenzene (16)

^{1}H NMR (500 MHz, $CDCl_3$)

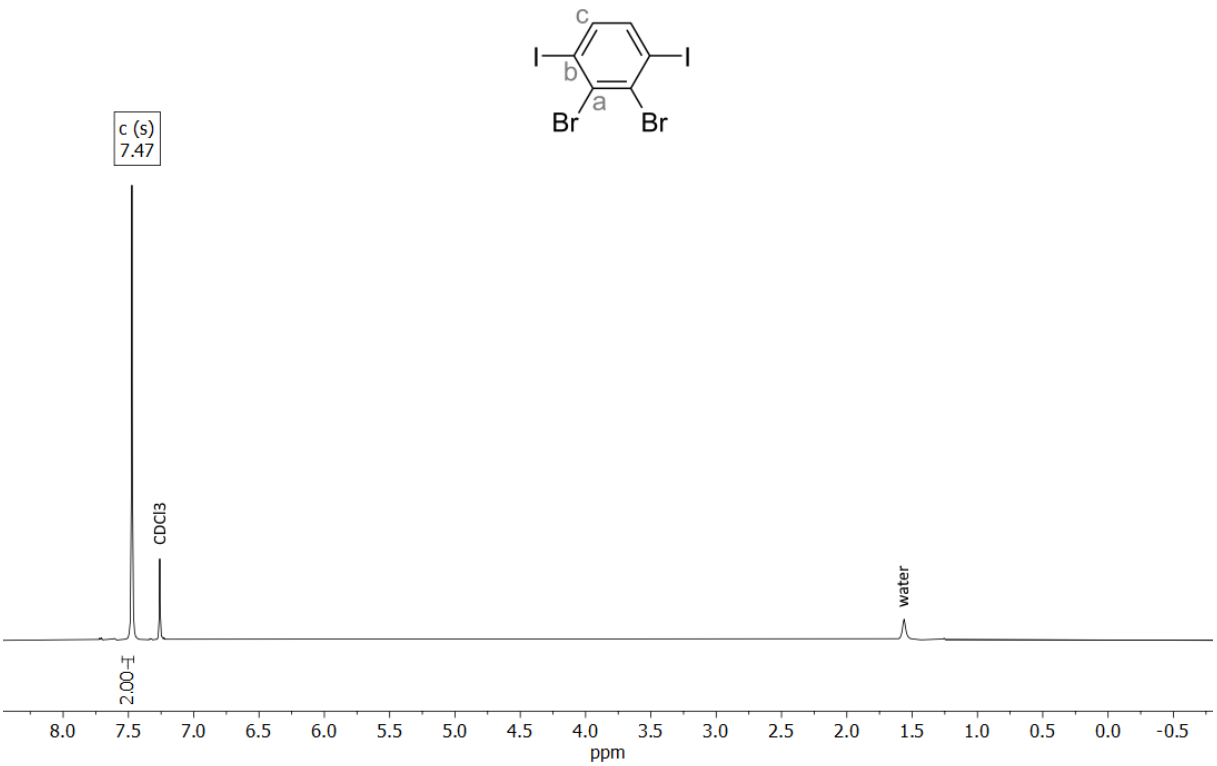

$^{13}C\{^{1}H\}$ NMR (126 MHz, $CDCl_3$)

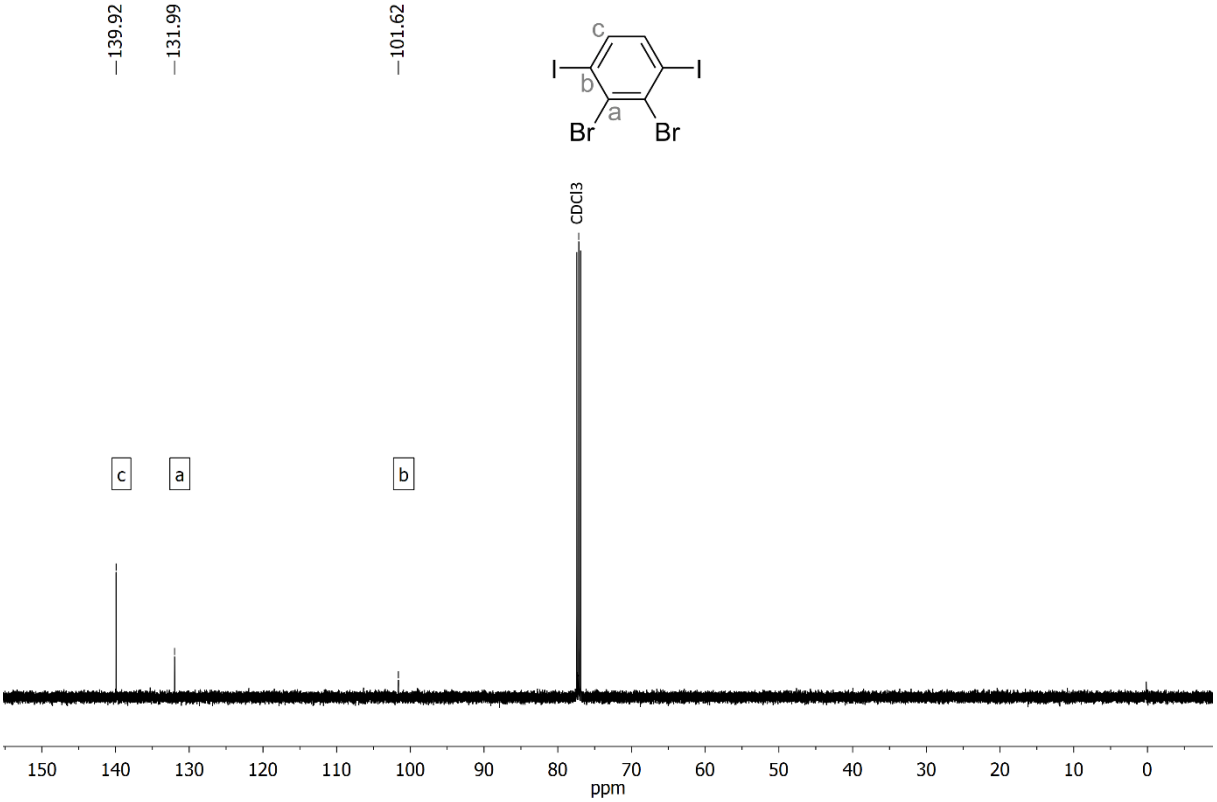

6.5. 2,3-Dibromo-1,4-bis(trimethylsilylethynyl)benzene (1)

^{1}H NMR (601 MHz, $CDCl_3$)

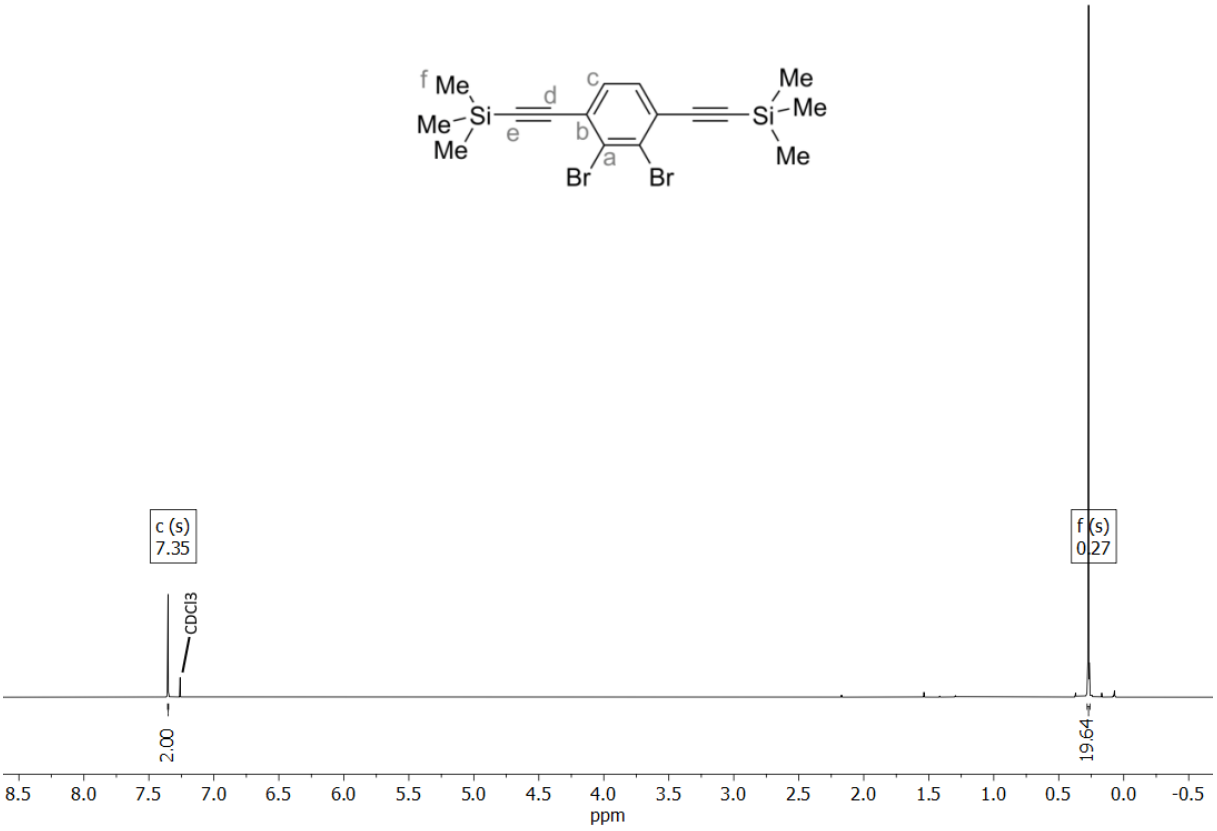

$^{13}C\{^{1}H\}$ NMR (151 MHz, $CDCl_3$)

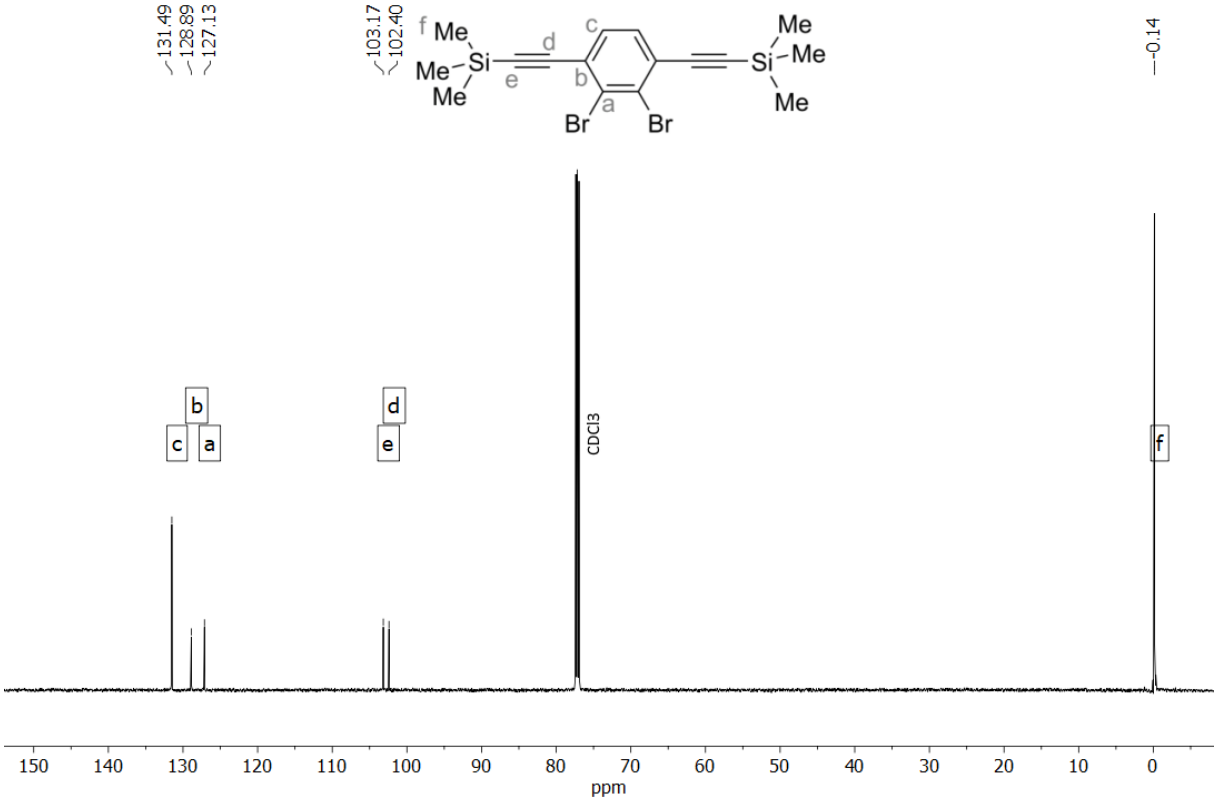

$^{29}Si\{^{1}H\}$ NMR (119 MHz, $CDCl_3$)

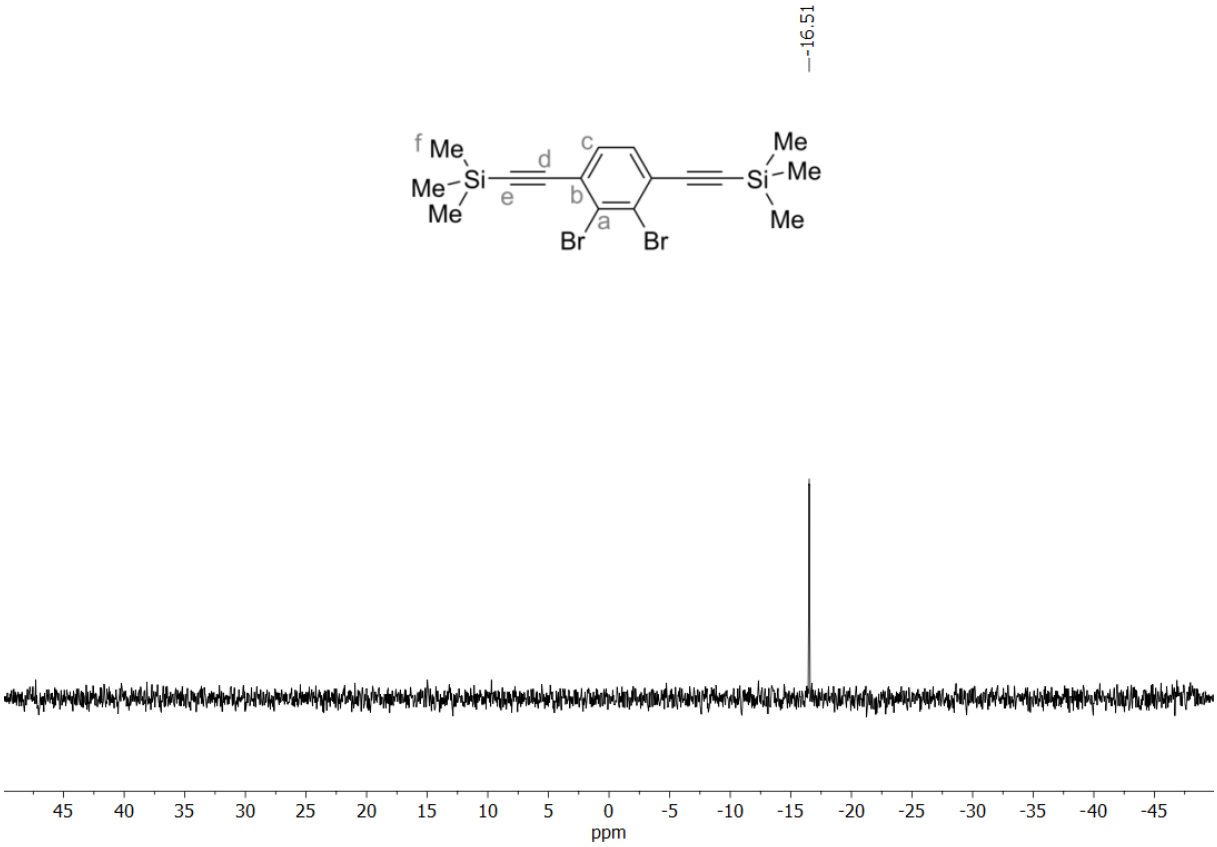

6.6. 1,2-bis(6-(1-Hydro-2-mesityl)-1,2-azaborinyl)-3,6-bis((trimethylsilyl)ethynyl)benzene (4)

^{1}H NMR (601 MHz, $CDCl_3$)

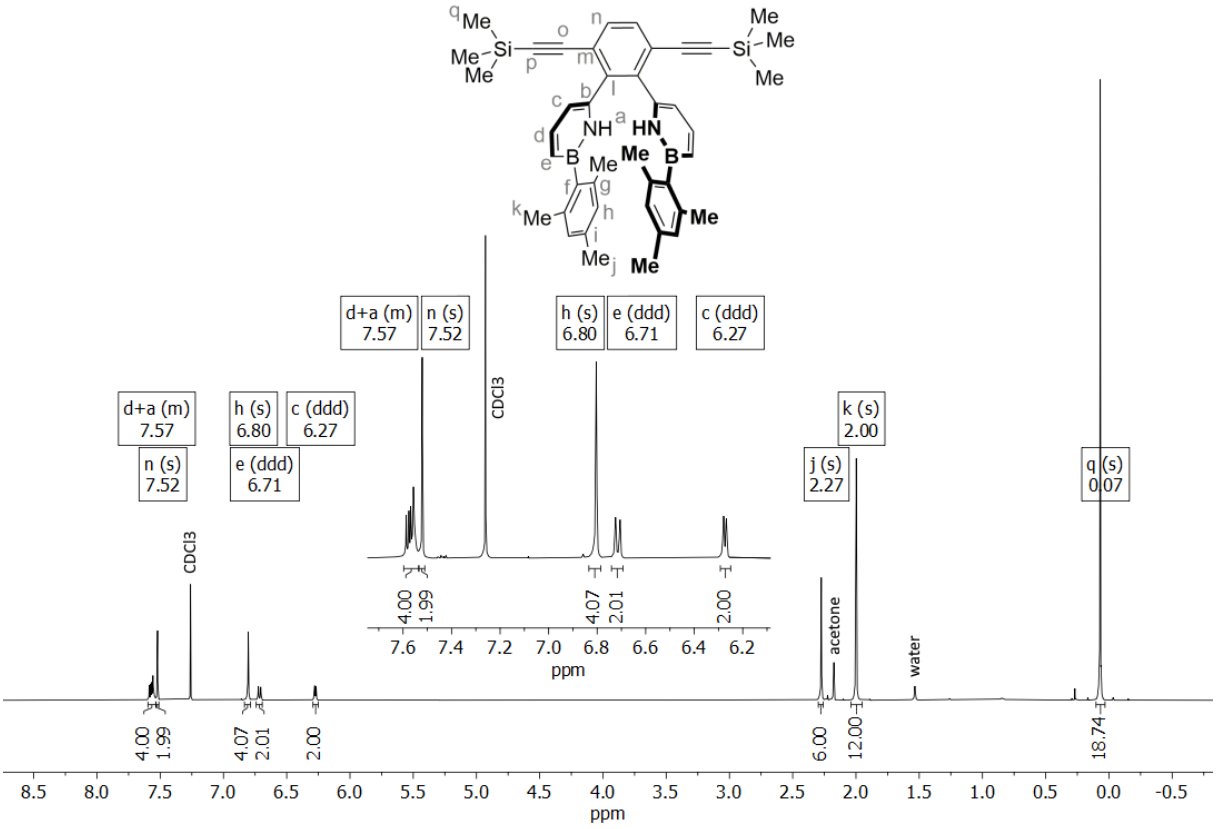

^{13}C{^{1}H} NMR (151 MHz, $CDCl_3$)

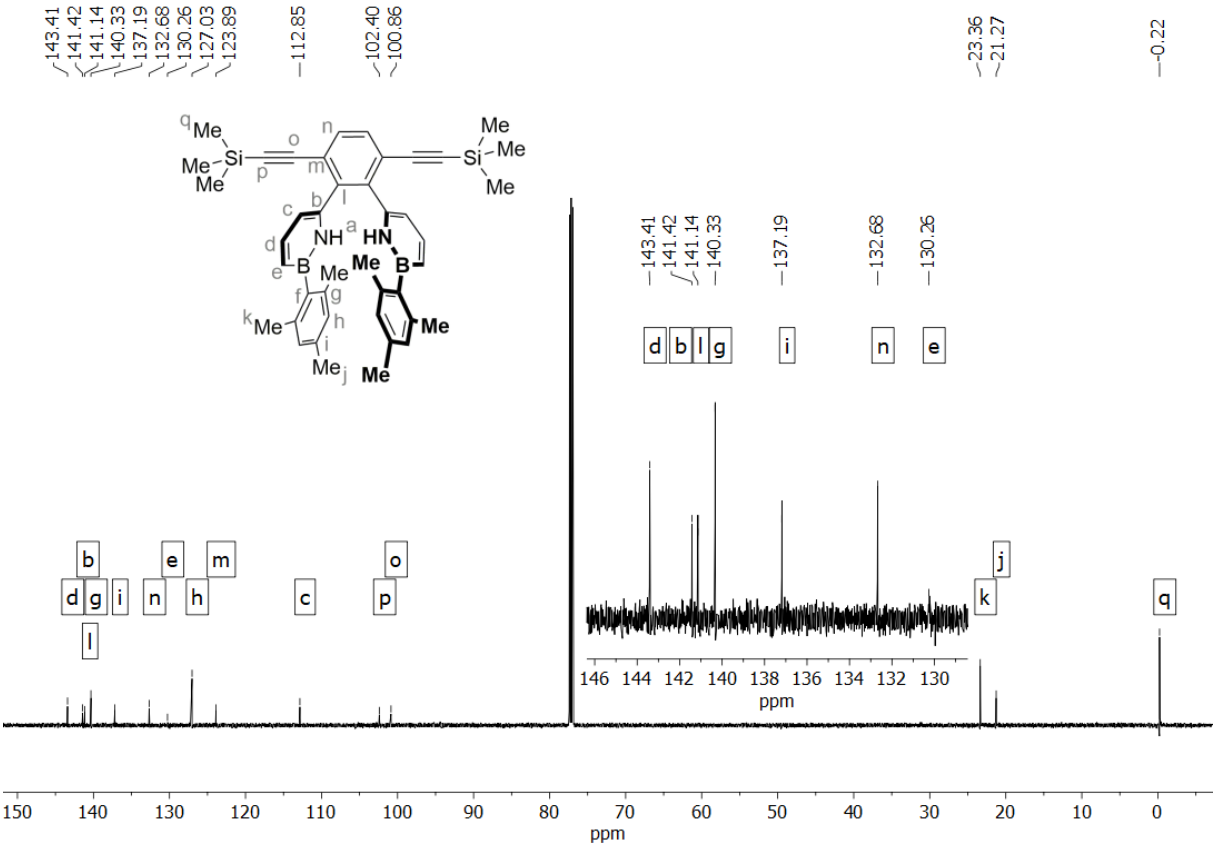

$^{11}B\{^{1}H\}$ NMR (193 MHz, $CDCl_3$)

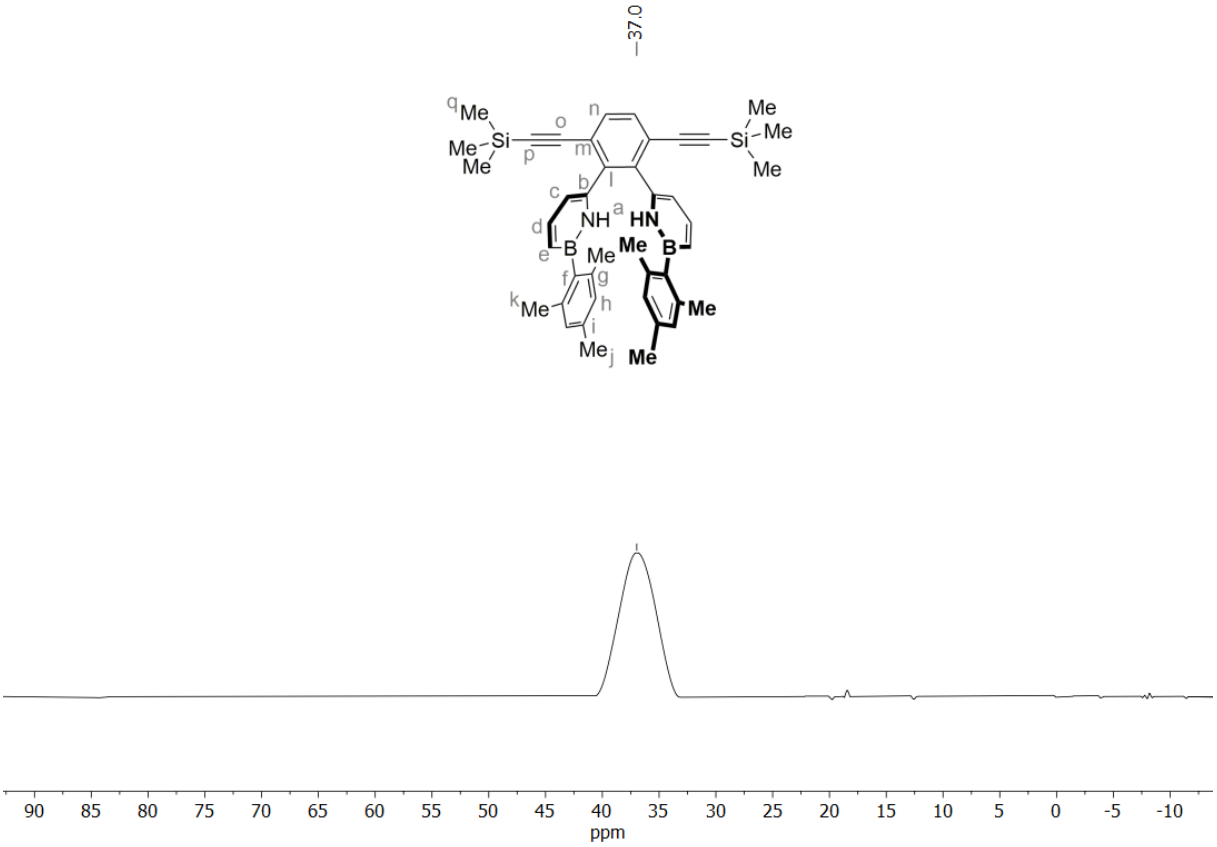

$^{29}Si\{^{1}H\}$ NMR (119 MHz, $CDCl_3$)

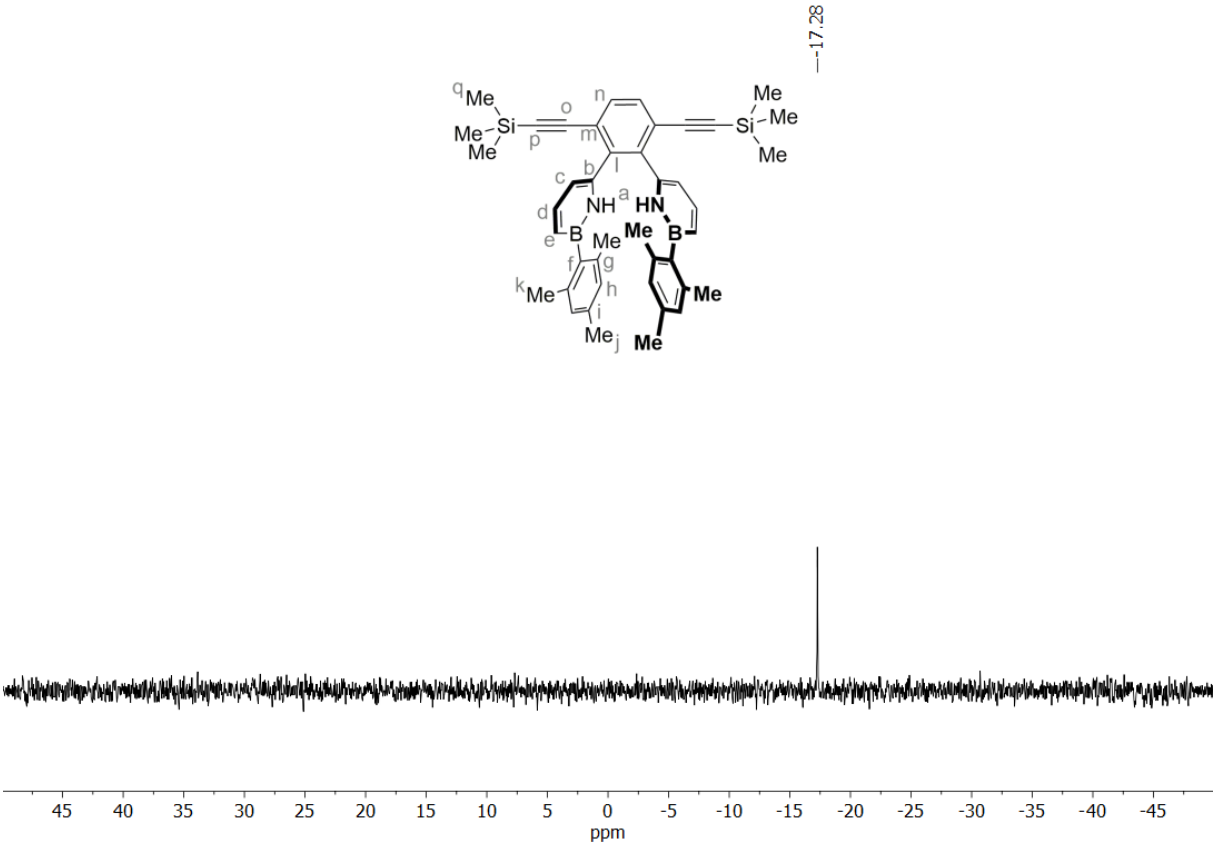

6.7. 1,14-Dihydro-2,13-dimesityl-1,14-diaza-2,13-diborapentahelicene (BN[5])

^{1}H NMR (601 MHz, $CDCl_3$)

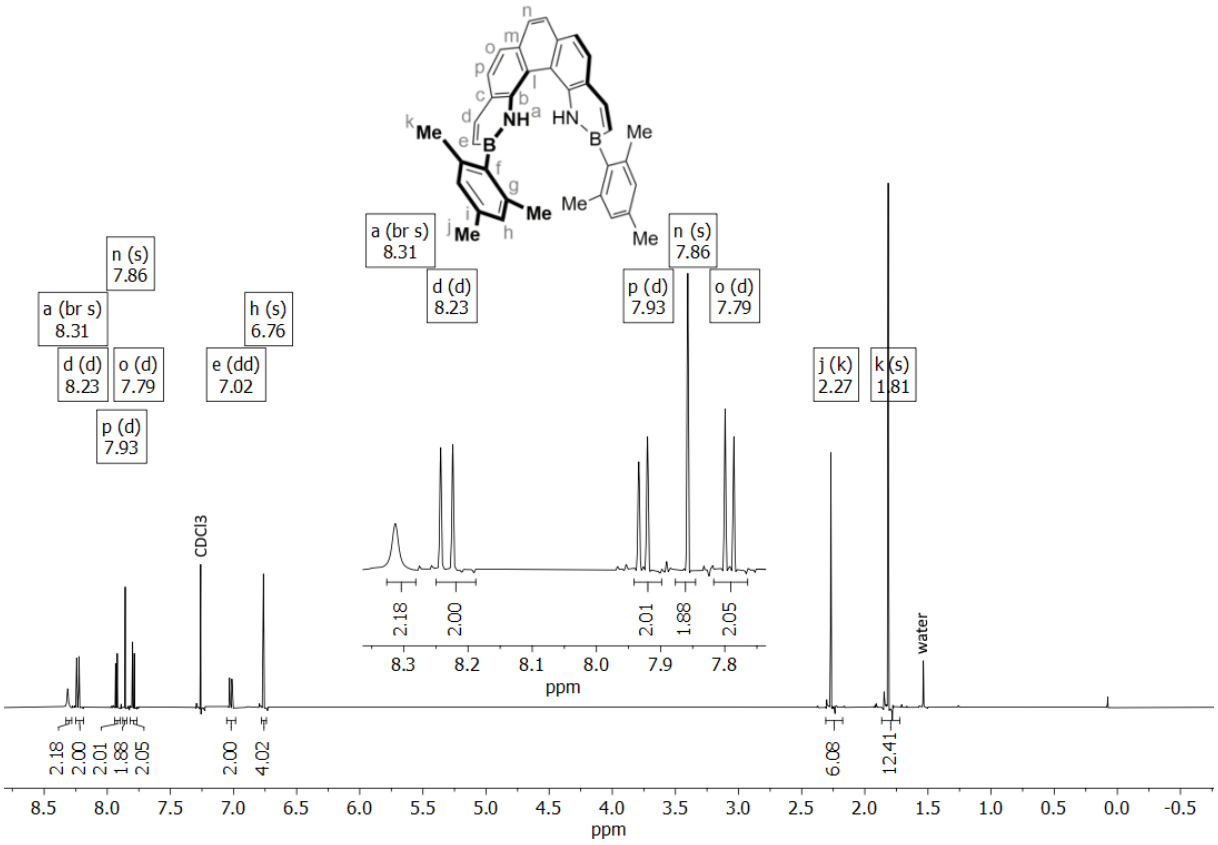

^{13}C{^{1}H} NMR (151 MHz, $CDCl_3$)

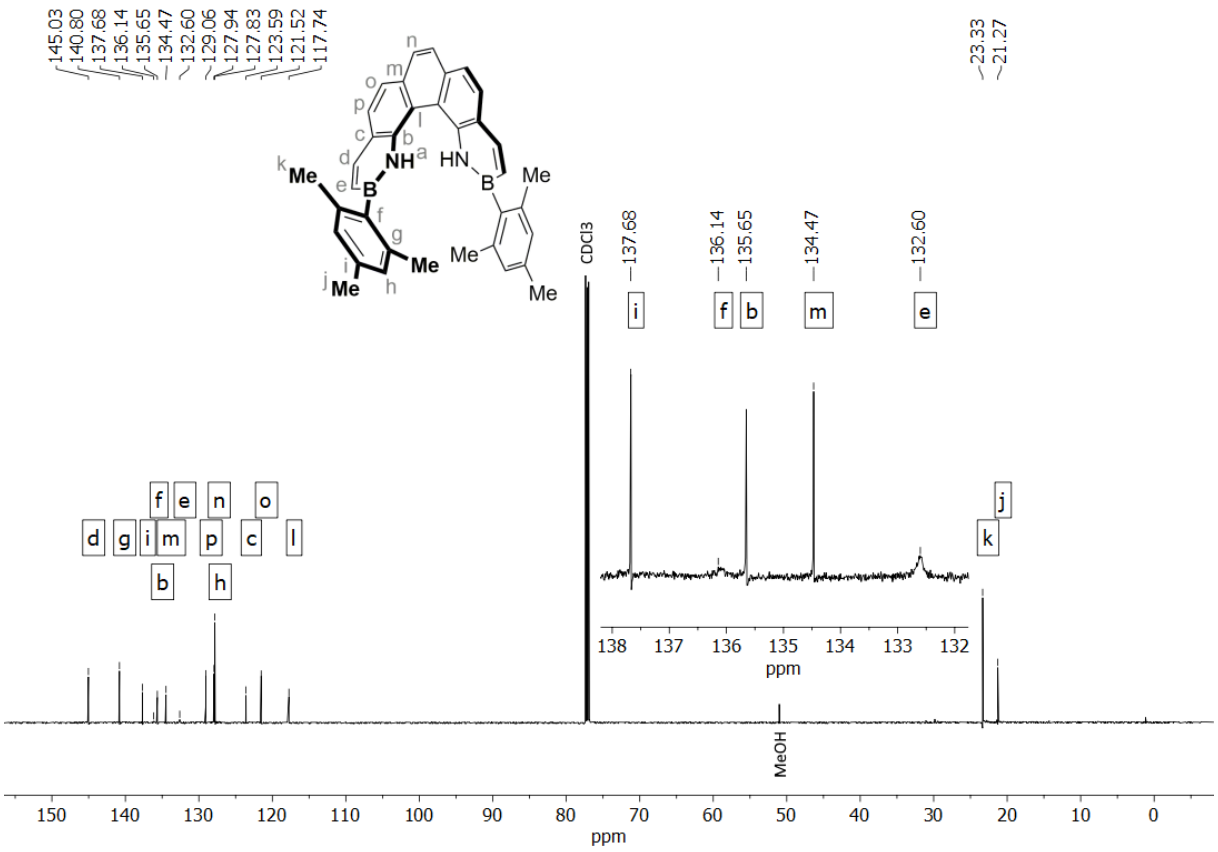

$^{11}B\{^{1}H\}$ NMR (193 MHz, $CDCl_3$)

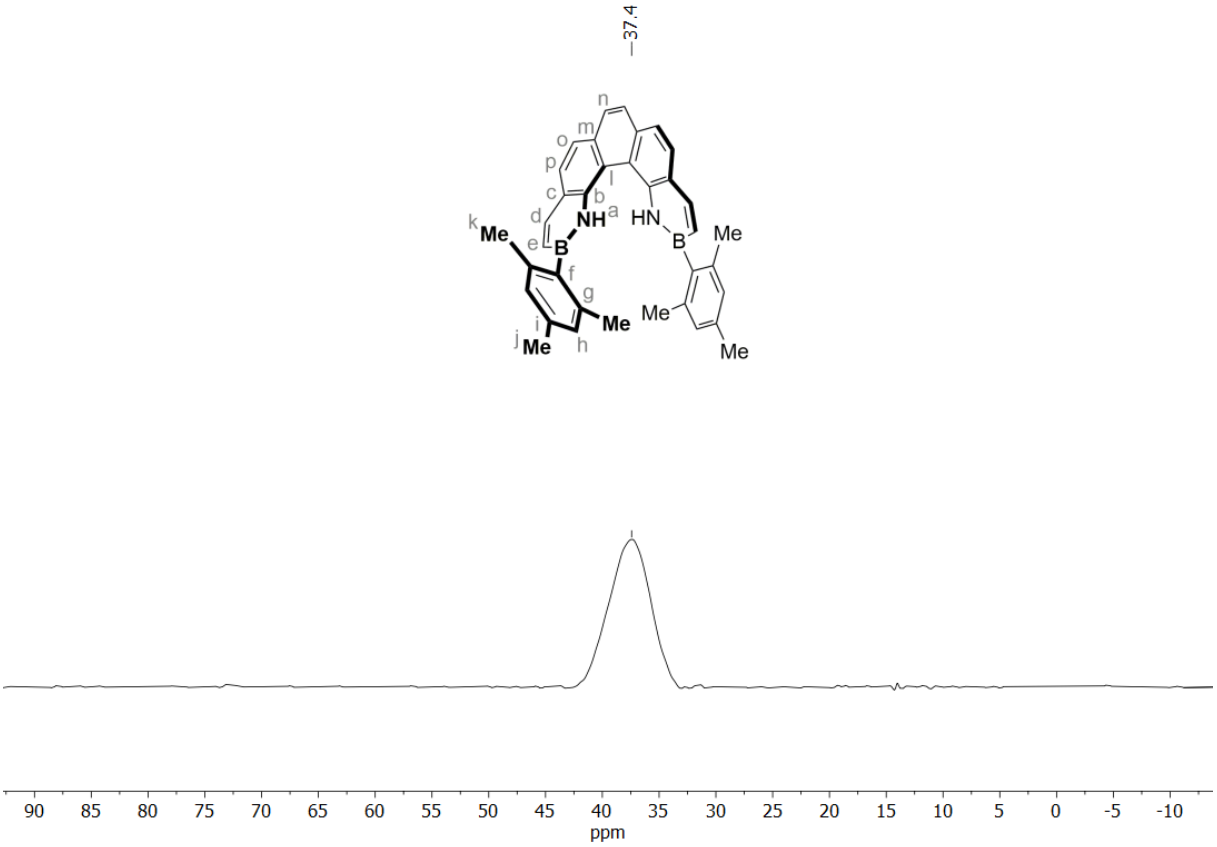

6.8. 3,12-Dibromo-1,14-dihydro-2,13-dimesityl-1,14-diaza-2,13-diborapentahelicene (BN[5]-Br_2)

^{1}H NMR (601 MHz, $CDCl_3$)

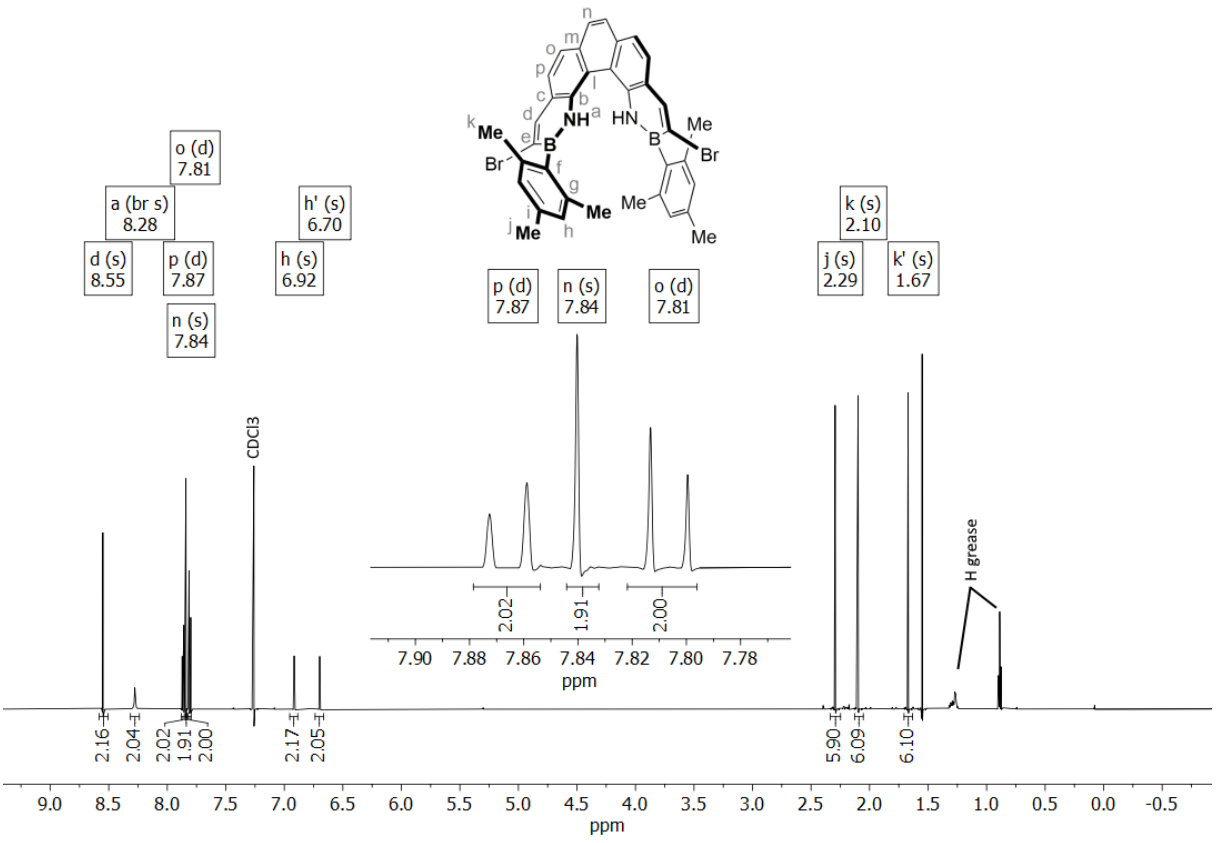

$^{13}C\{^{1}H\}$ NMR (151 MHz, $CDCl_3$)

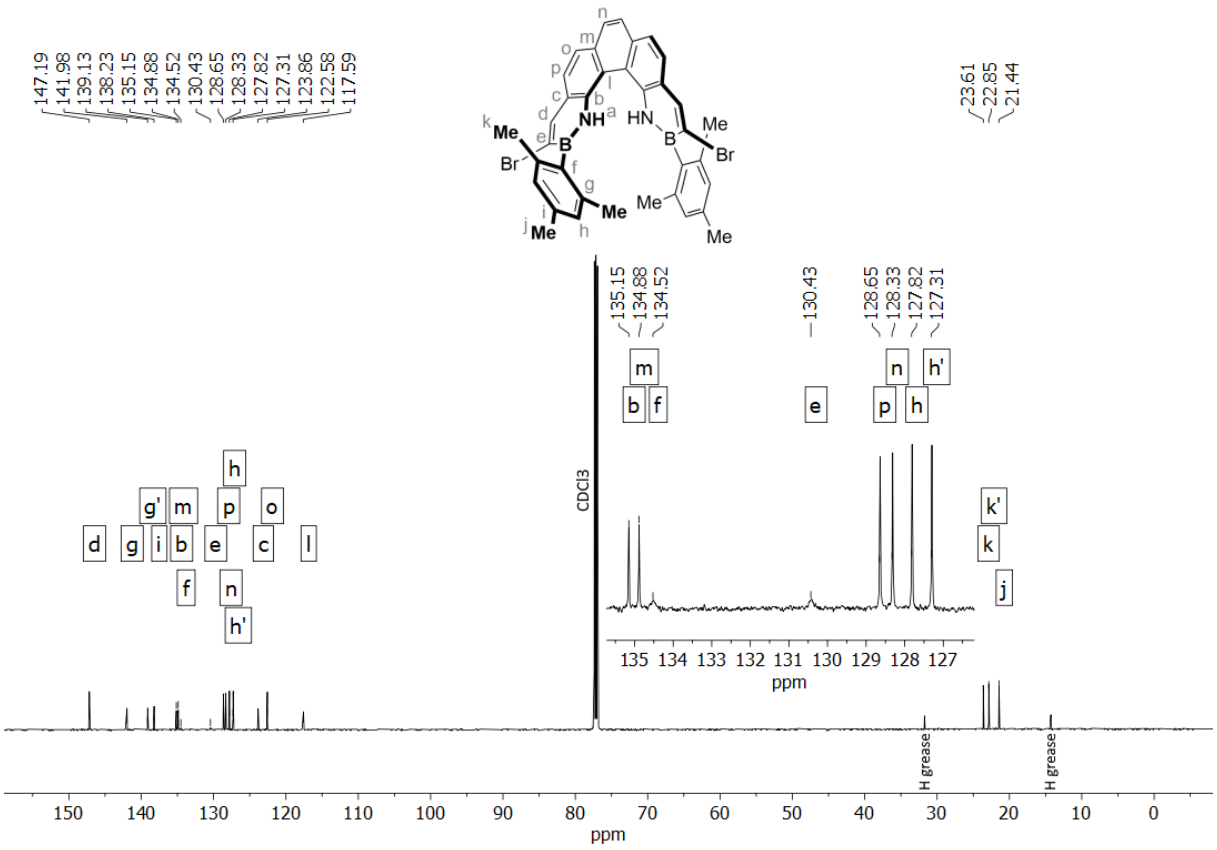

$^{11}B\{^{1}H\}$ NMR (193 MHz, $CDCl_3$)

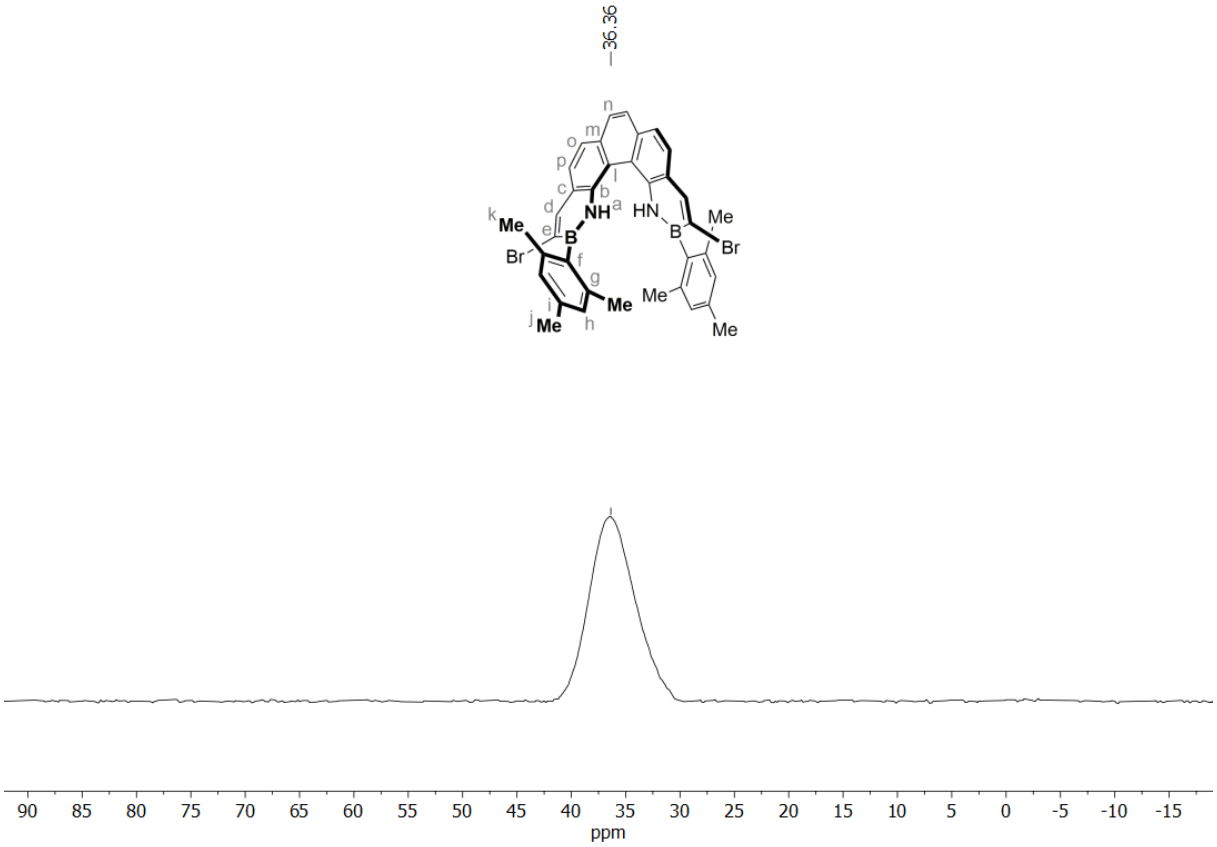

6.9. 3,12-Dicyano-1,14-dihydro-2,13-dimesityl-1,14-diaza-2,13-diborapentahelicene (BN[5]-(CN)$_2$)

^{1}H NMR (601 MHz, $CDCl_3$)

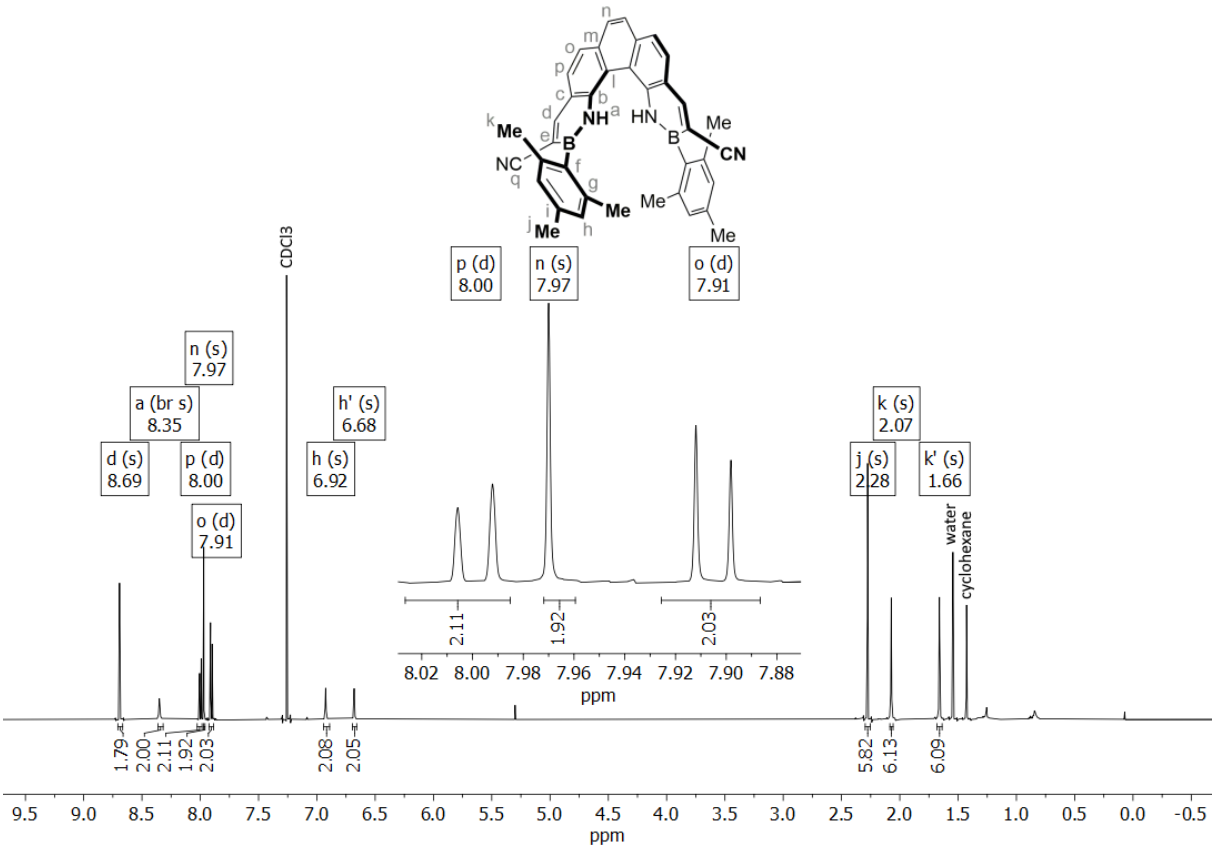

^{13}C{^{1}H} NMR (151 MHz, $CDCl_3$)

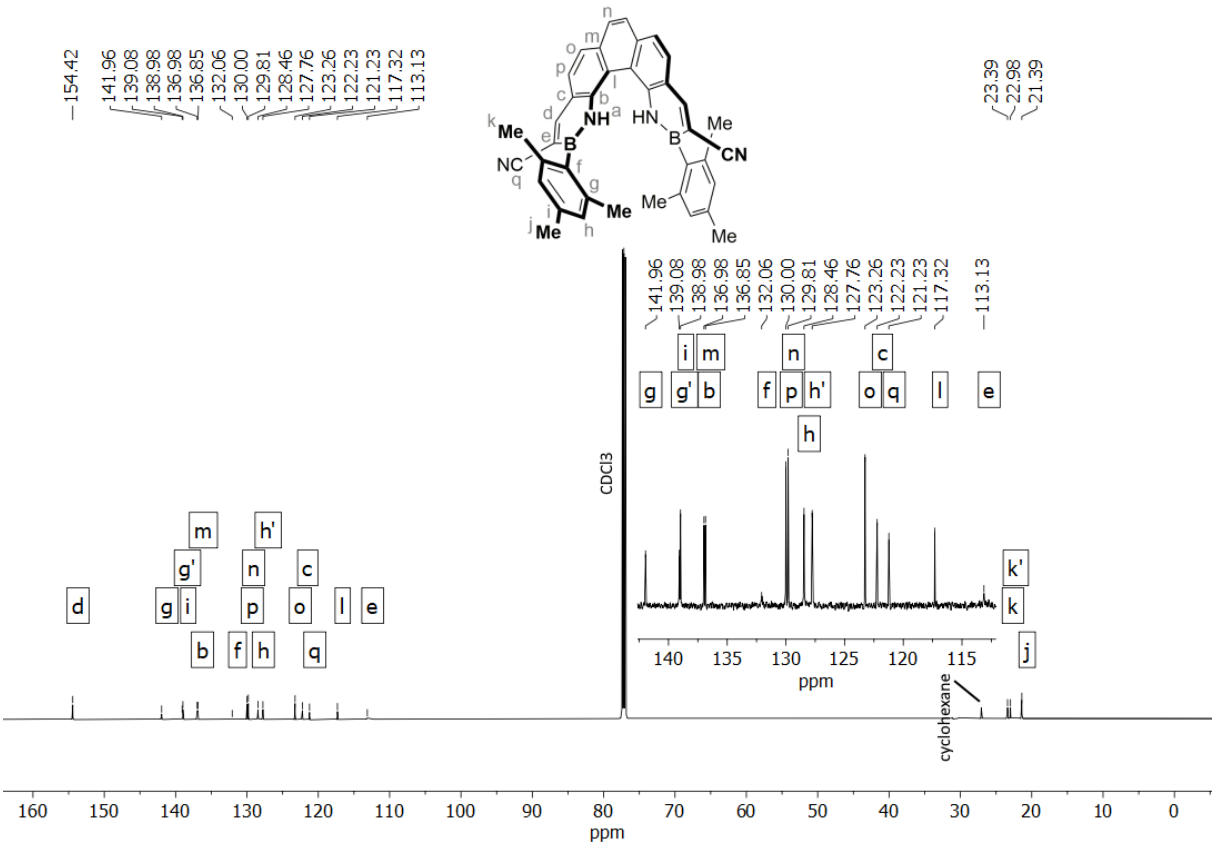

$^{11}B\{^{1}H\}$ NMR (193 MHz, $CDCl_3$)

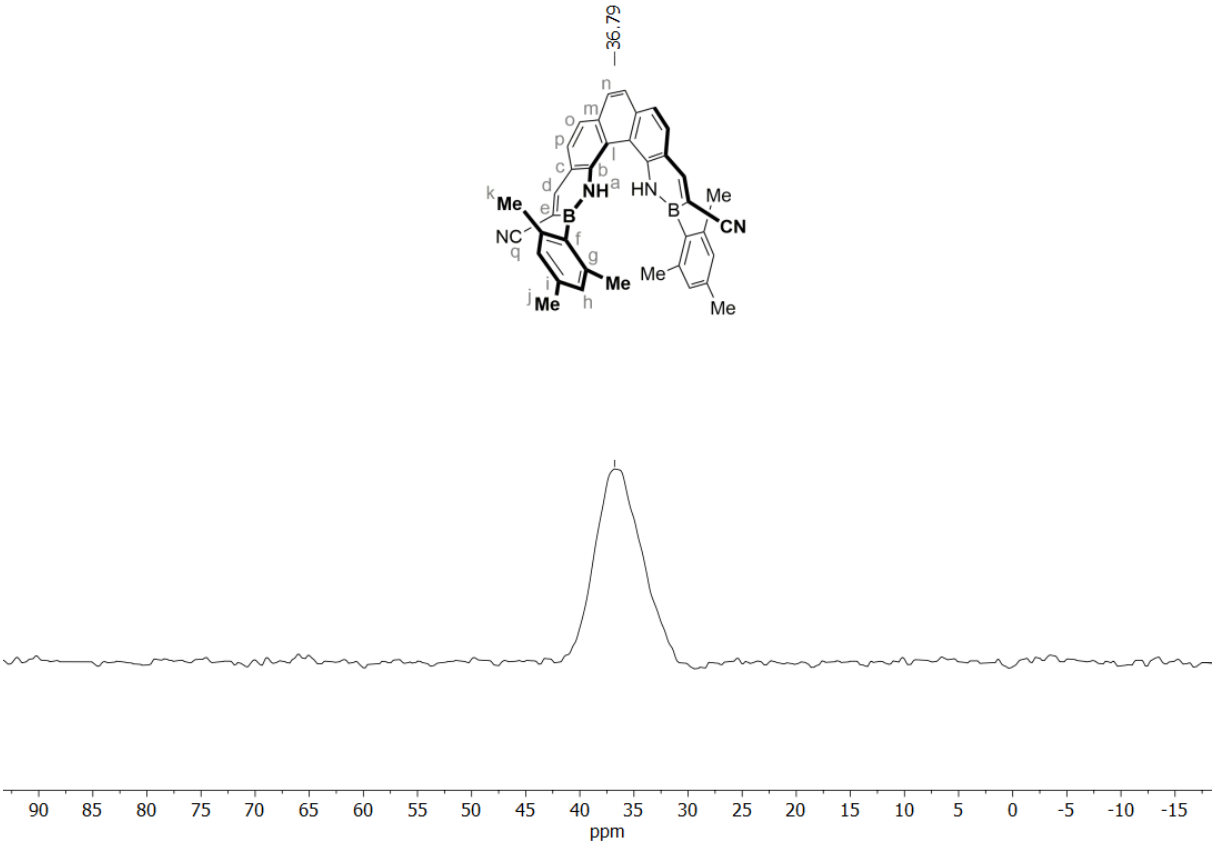

6.10. 1,8-Dibromo-2,7-bis(trifluoromethylsulfonyl)naphthalene (17)

^{1}H NMR (601 MHz, $CDCl_3$)

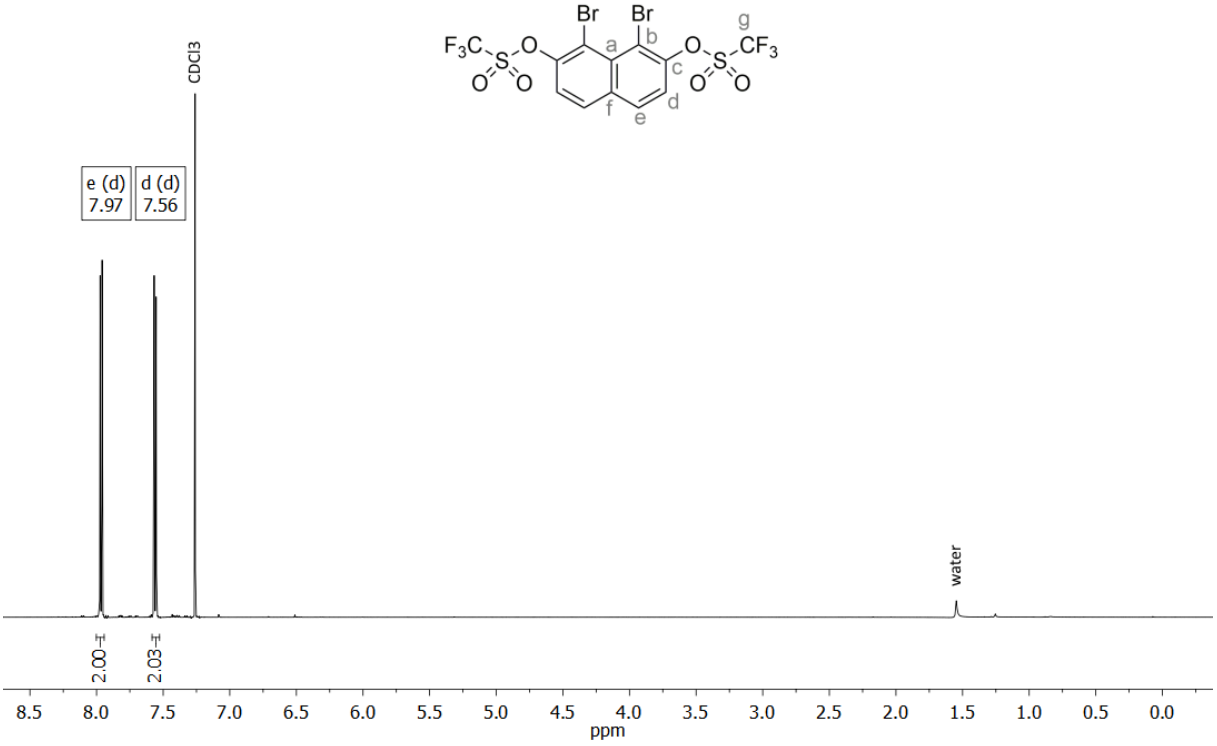

$^{13}C\{^{1}H\}$ NMR (151 MHz, $CDCl_3$)

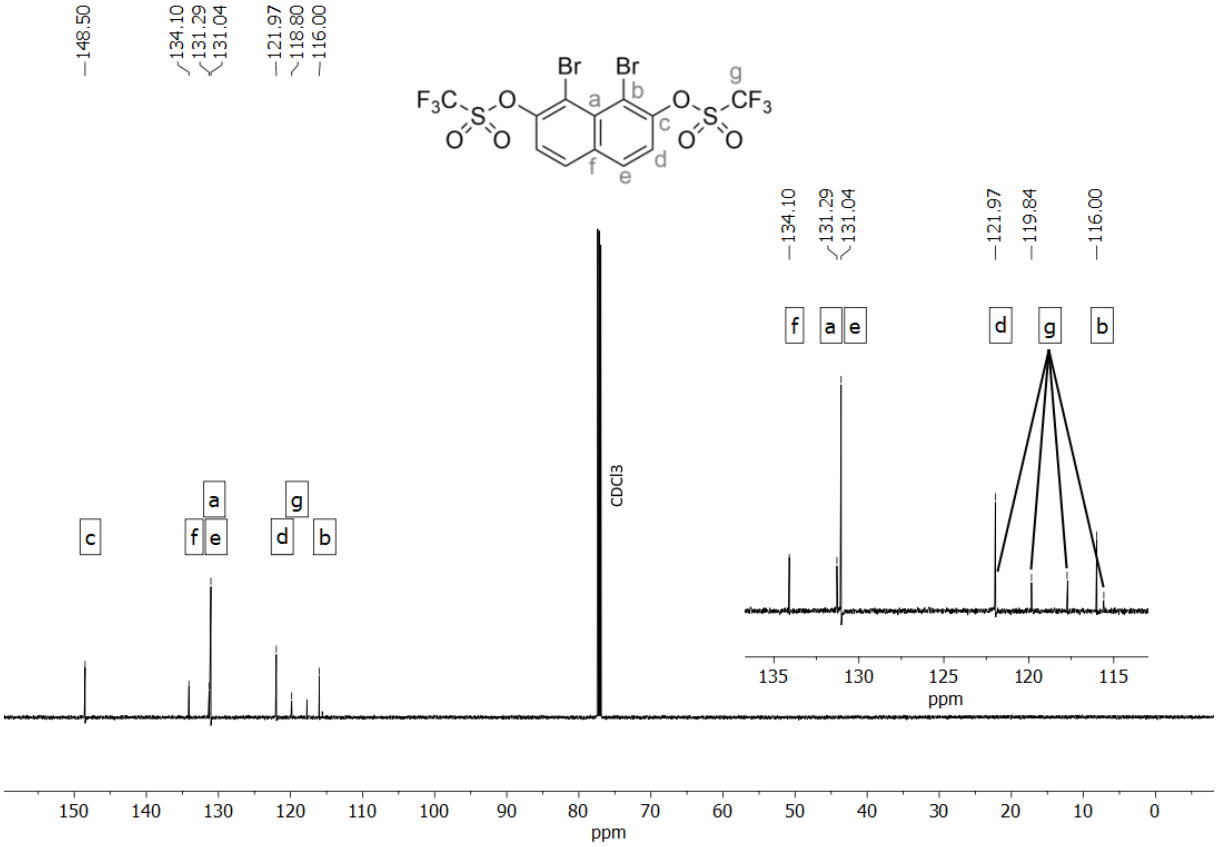

^{19}F NMR (565 MHz, $CDCl_3$)

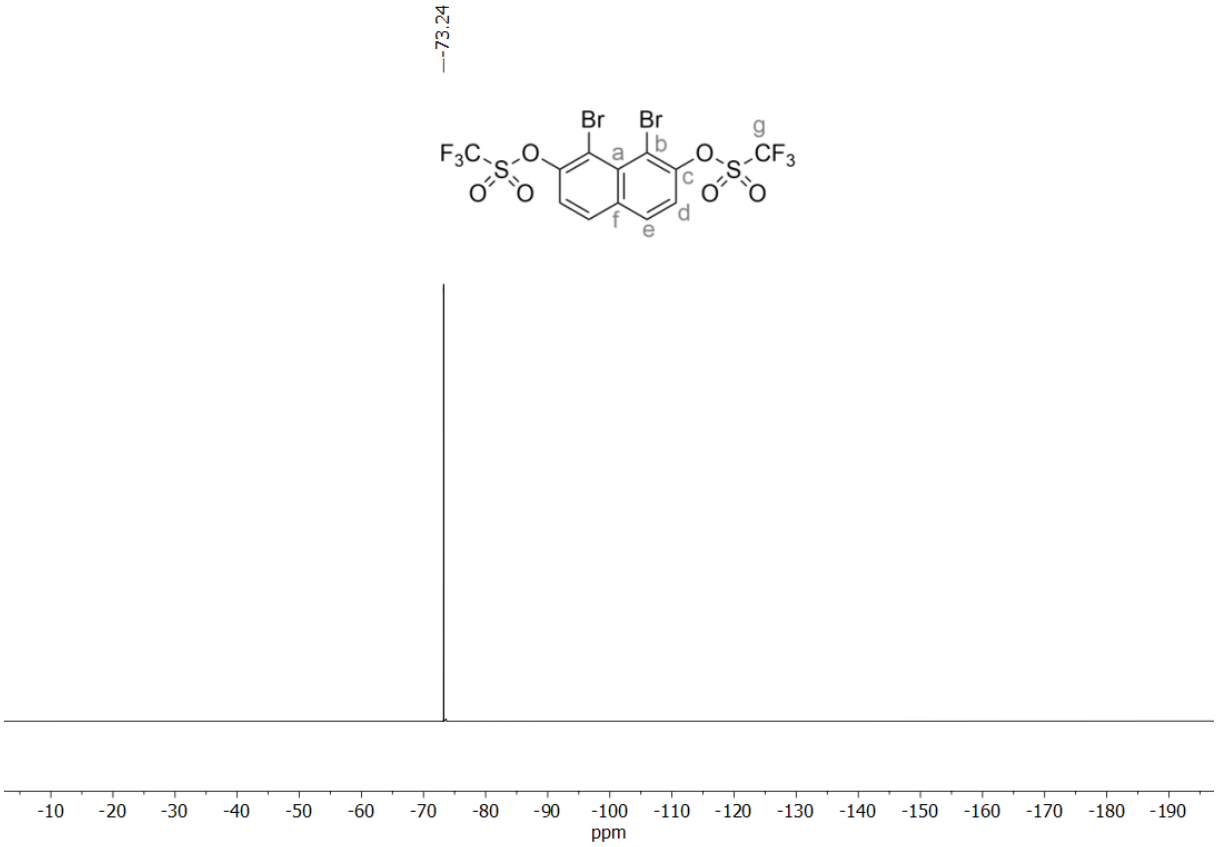

6.11. 1,8-Dibromo-2,7-bis(trimethylsilylethynyl)naphthalene (2)

^{1}H NMR (601 MHz, $CDCl_3$)

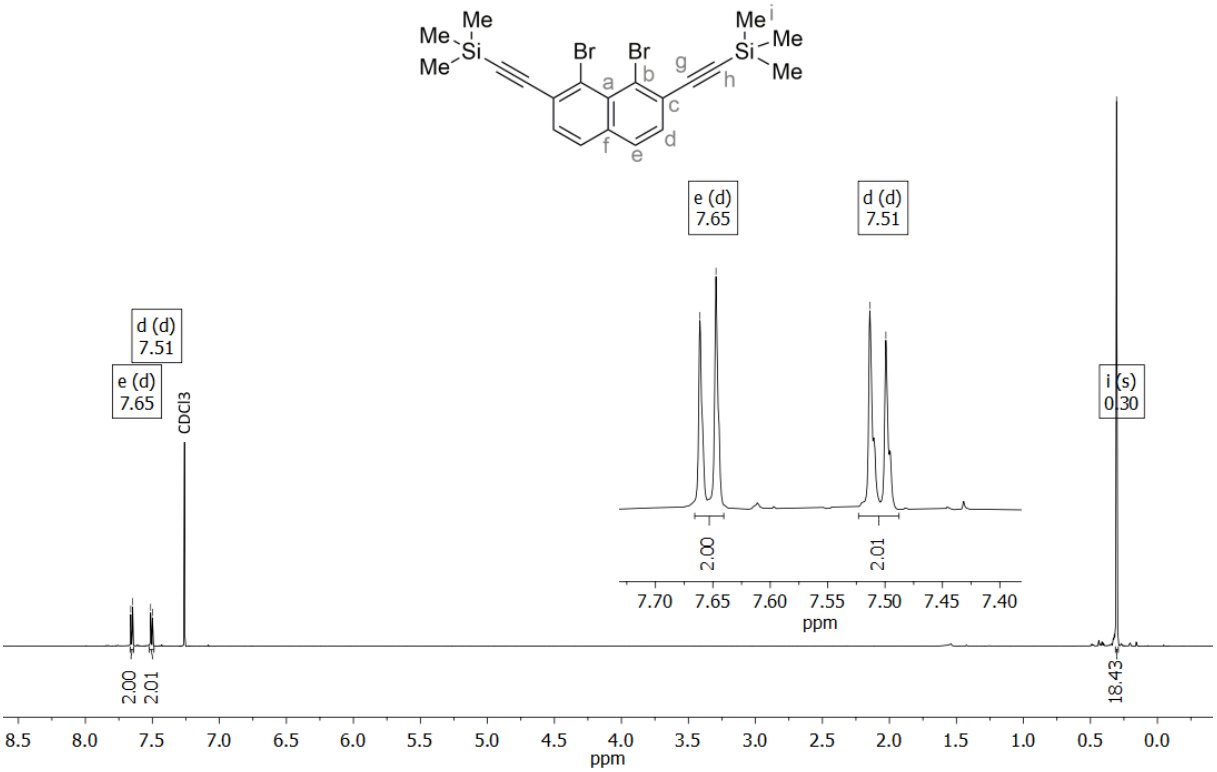

^{13}C{^{1}H} NMR (151 MHz, $CDCl_3$)

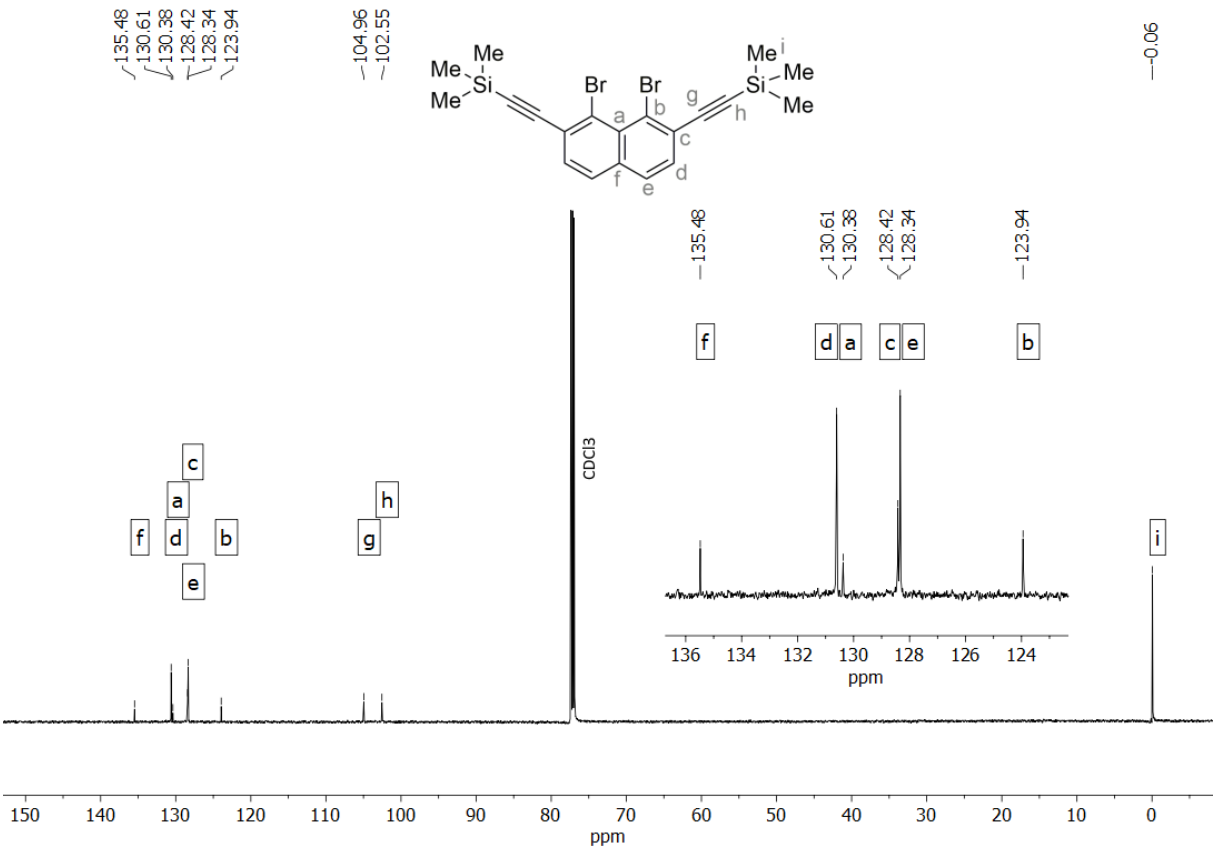

$^{29}Si\{^{1}H\}$ NMR (119 MHz, $CDCl_3$)

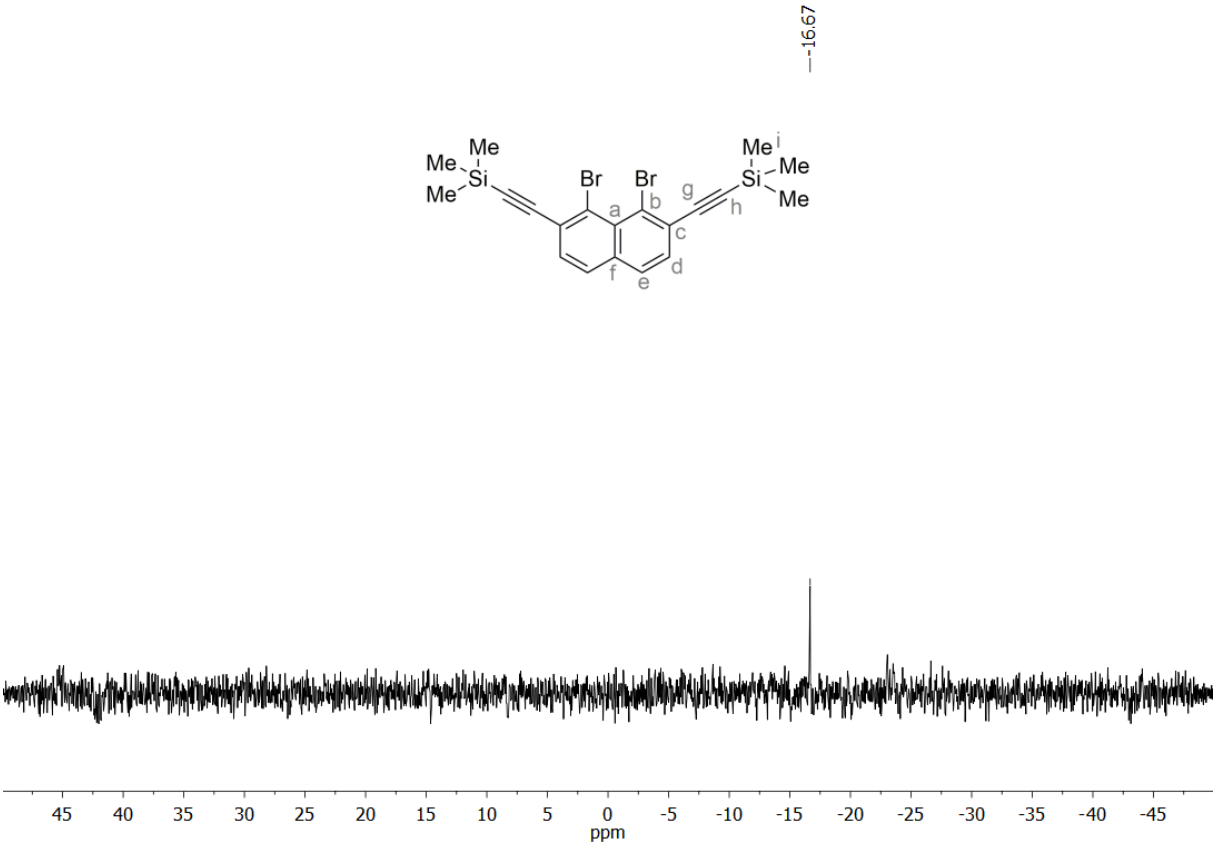

6.12. 1,8-bis(6-(1-Hydro-2-mesityl)-1,2-azaborinyl)-2,7-bis((trimethylsilyl)ethynyl)naphthalene (5)

^{1}H NMR (601 MHz, $CDCl_3$)

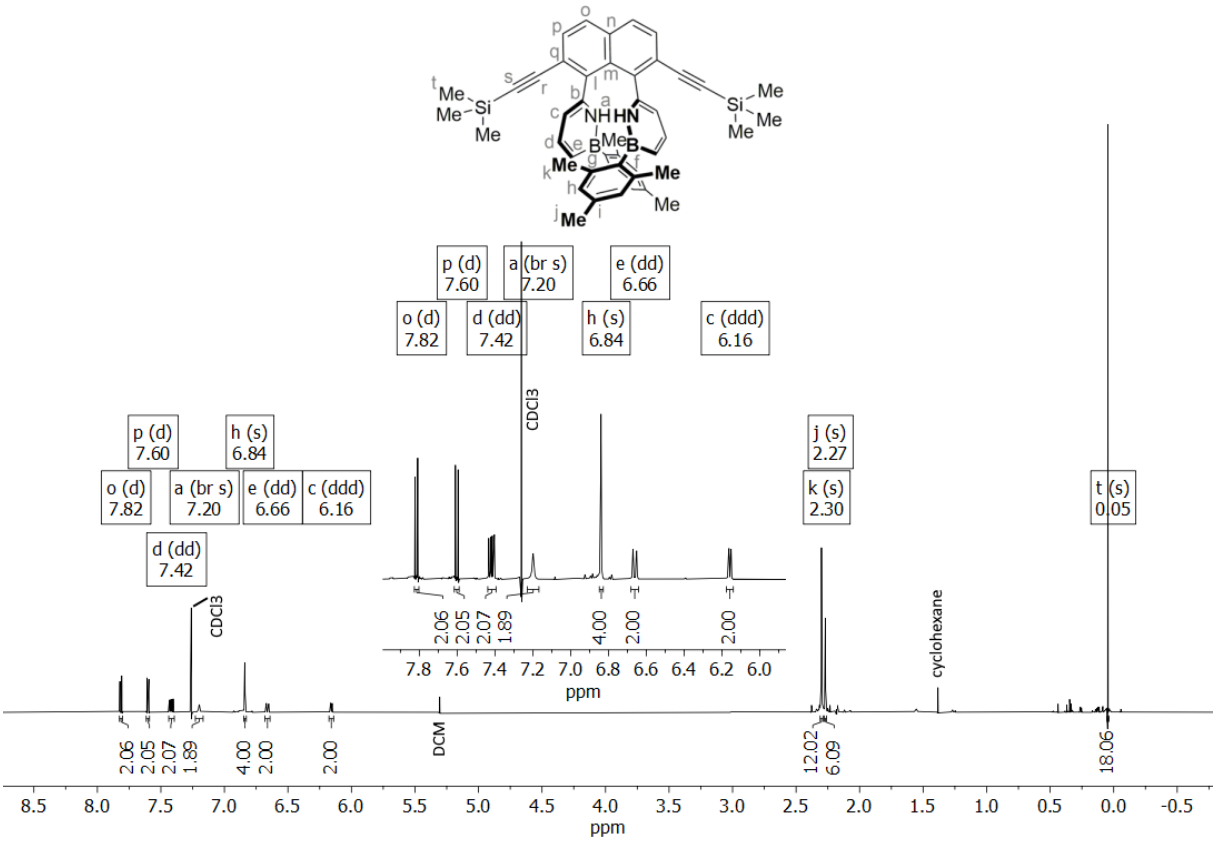

$^{13}C\{^{1}H\}$ NMR (151 MHz, $CDCl_3$)

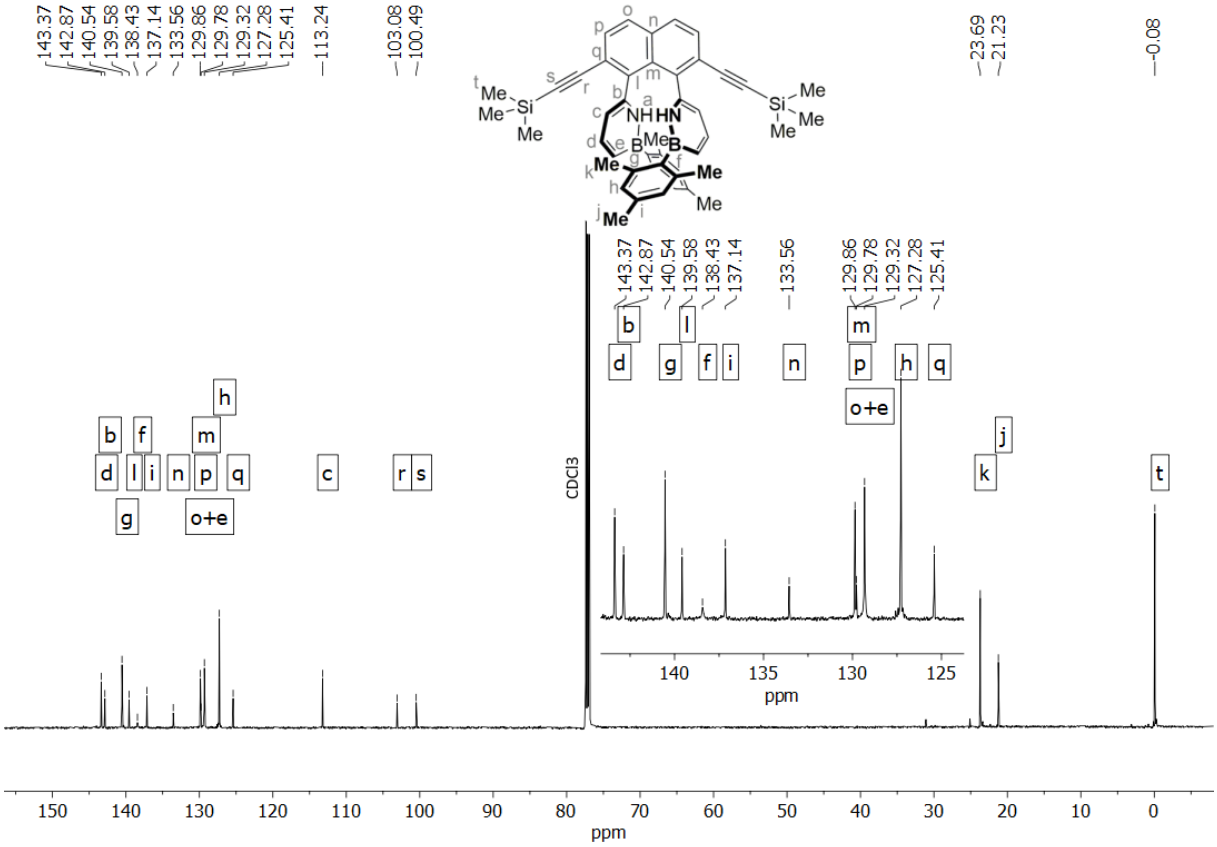

$^{11}B\{^{1}H\}$ NMR (193 MHz, $CDCl_3$)

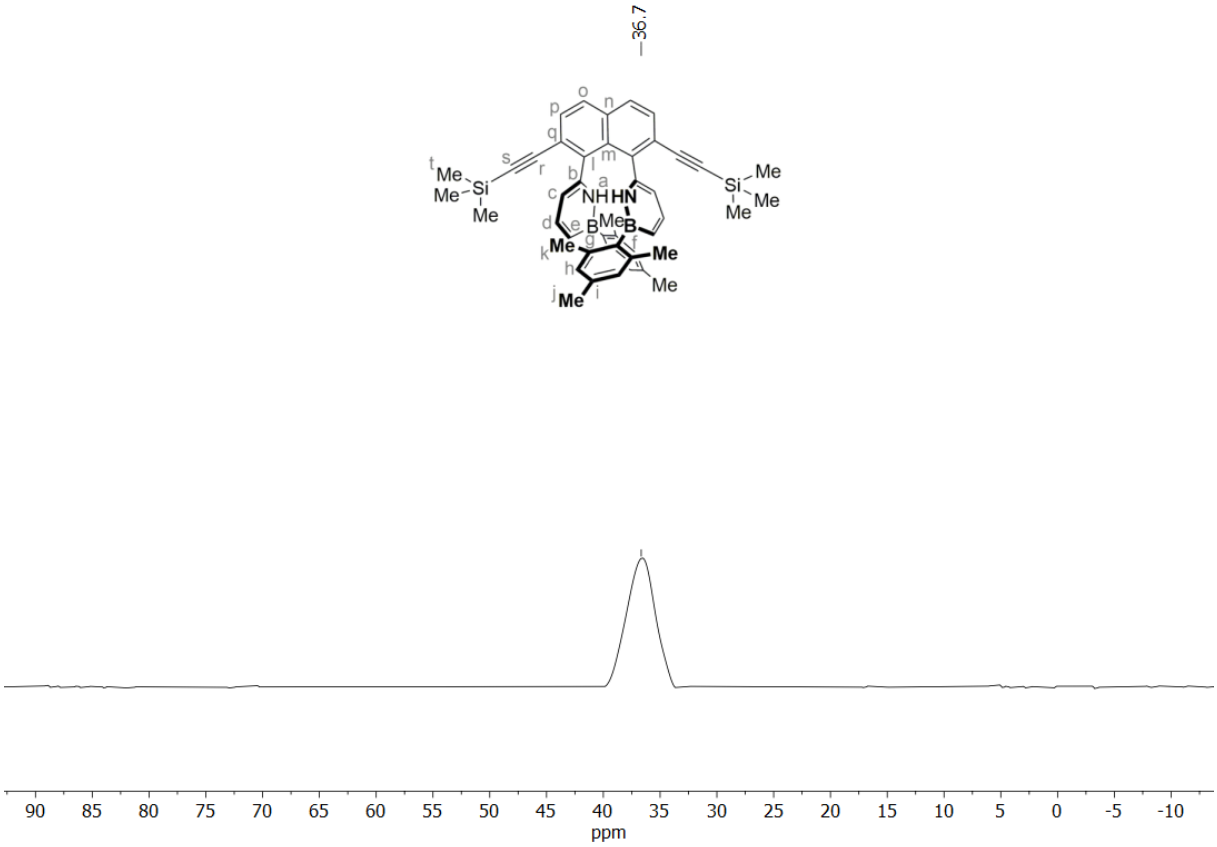

$^{29}Si\{^{1}H\}$ NMR (119 MHz, $CDCl_3$)

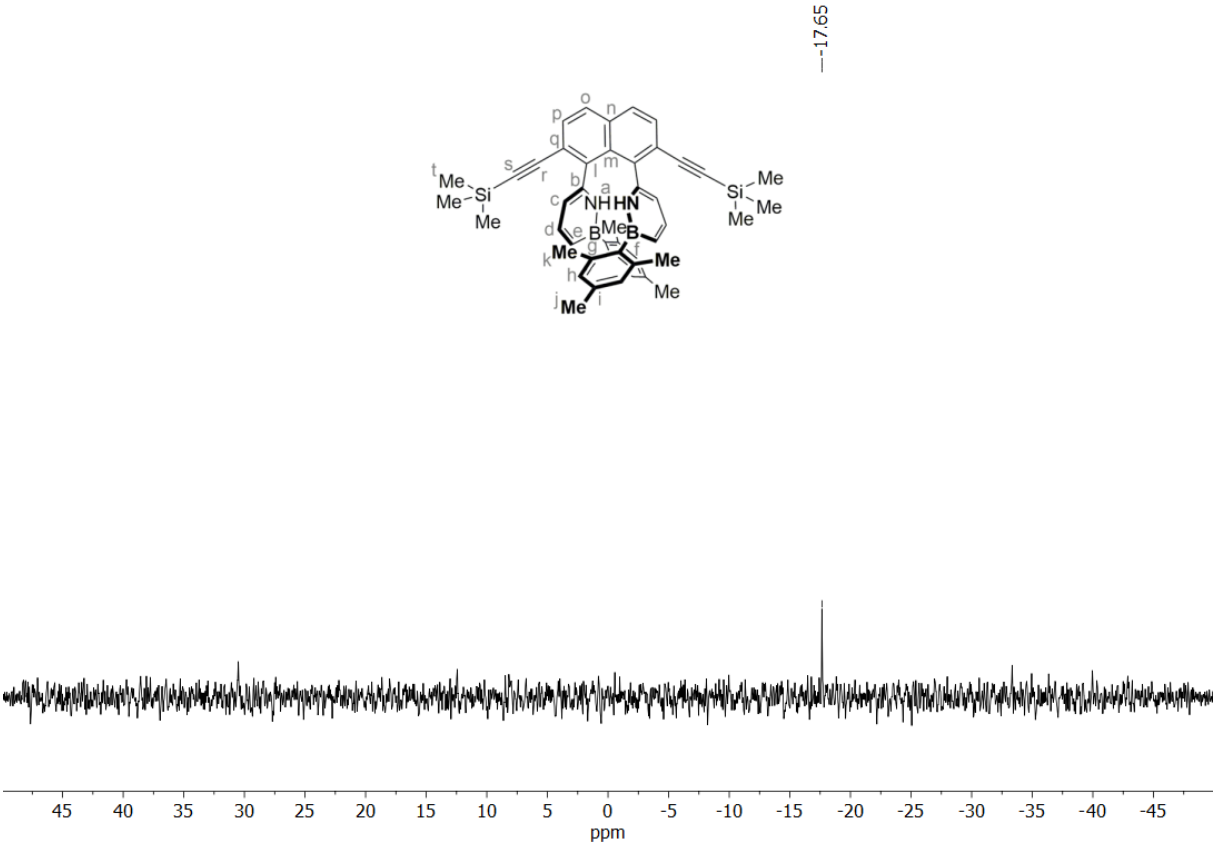

6.13. 1,16-Dihydro-2,15-dimesityl-1,16-diaza-2,15-diborahexahelicene (BN[6])

^{1}H NMR (601 MHz, $CDCl_3$)

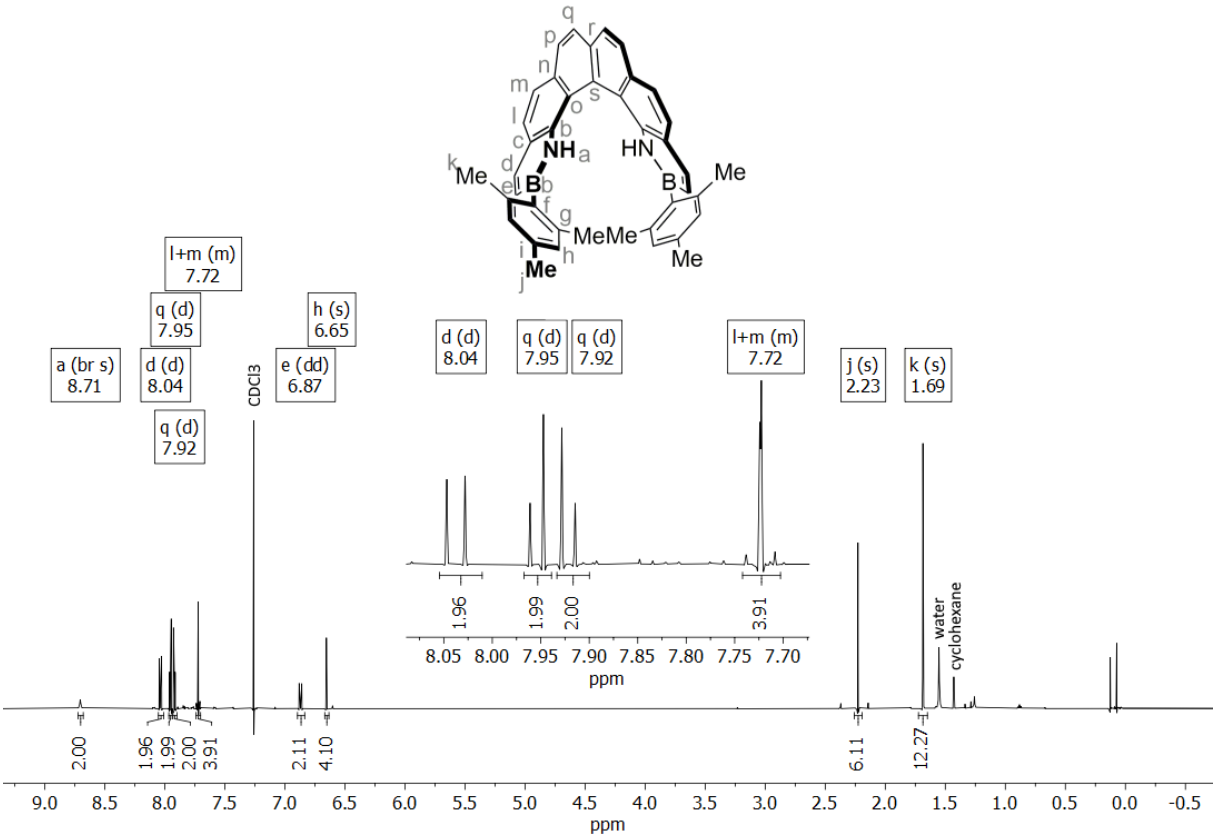

$^{13}C\{^{1}H\}$ NMR (151 MHz, $CDCl_3$)

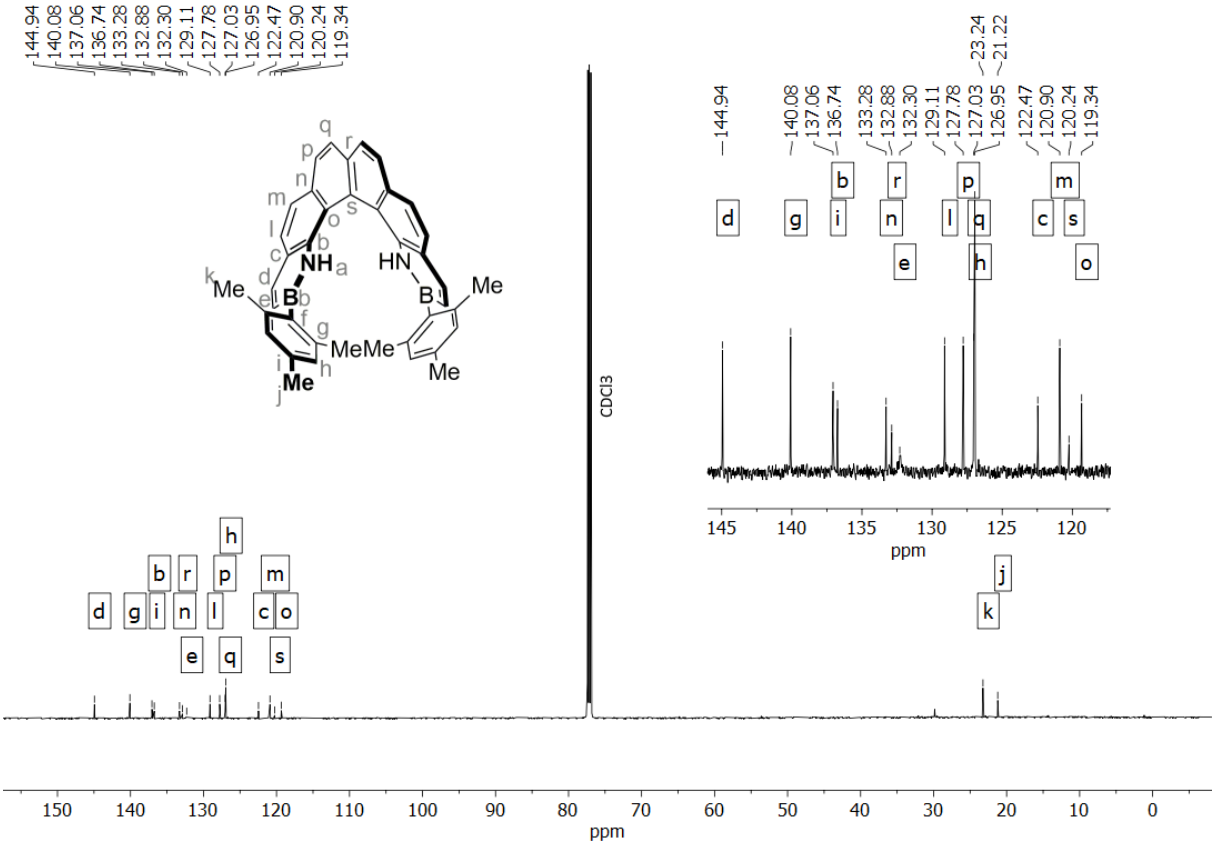

$^{11}B\{^{1}H\}$ NMR (193 MHz, $CDCl_3$)

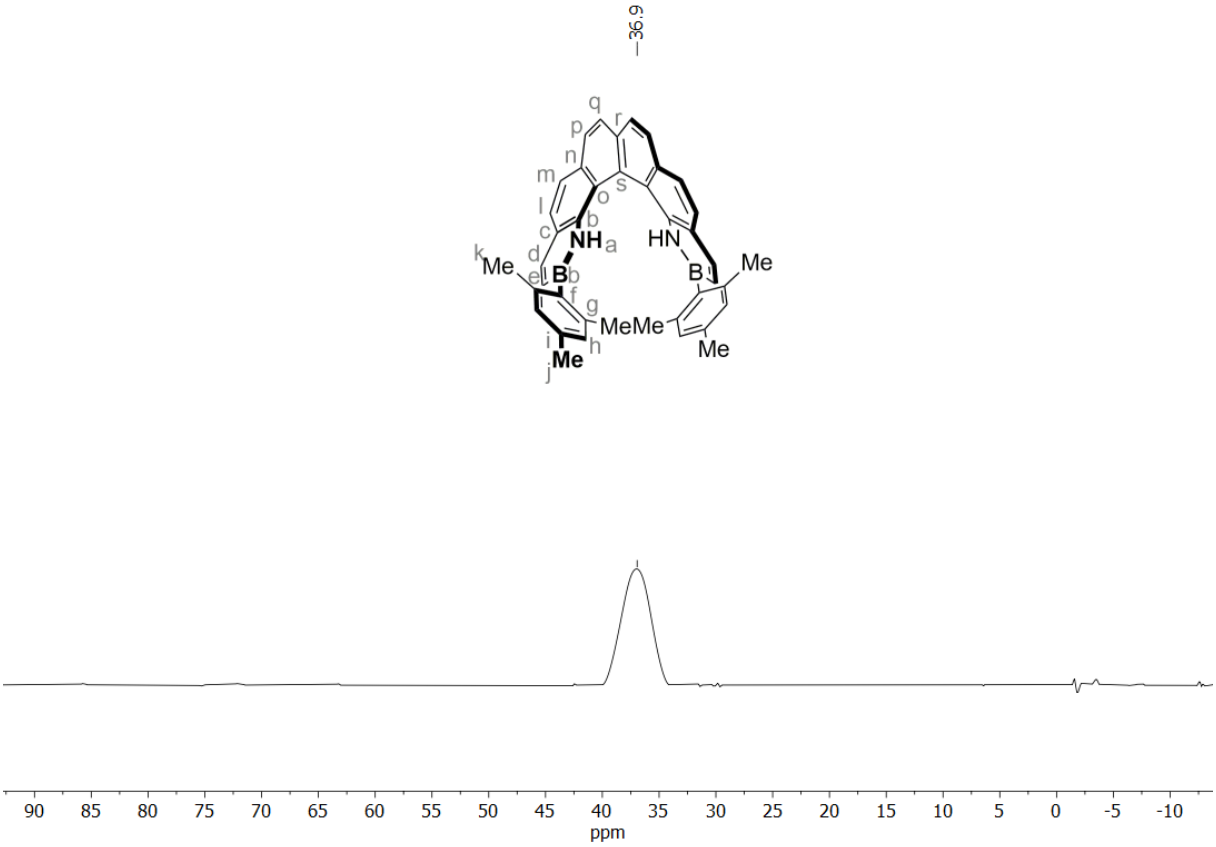

6.14. (*Z*)-4-Bromo-4'-formylstilbene (18)

^{1}H NMR (601 MHz, $CDCl_3$)

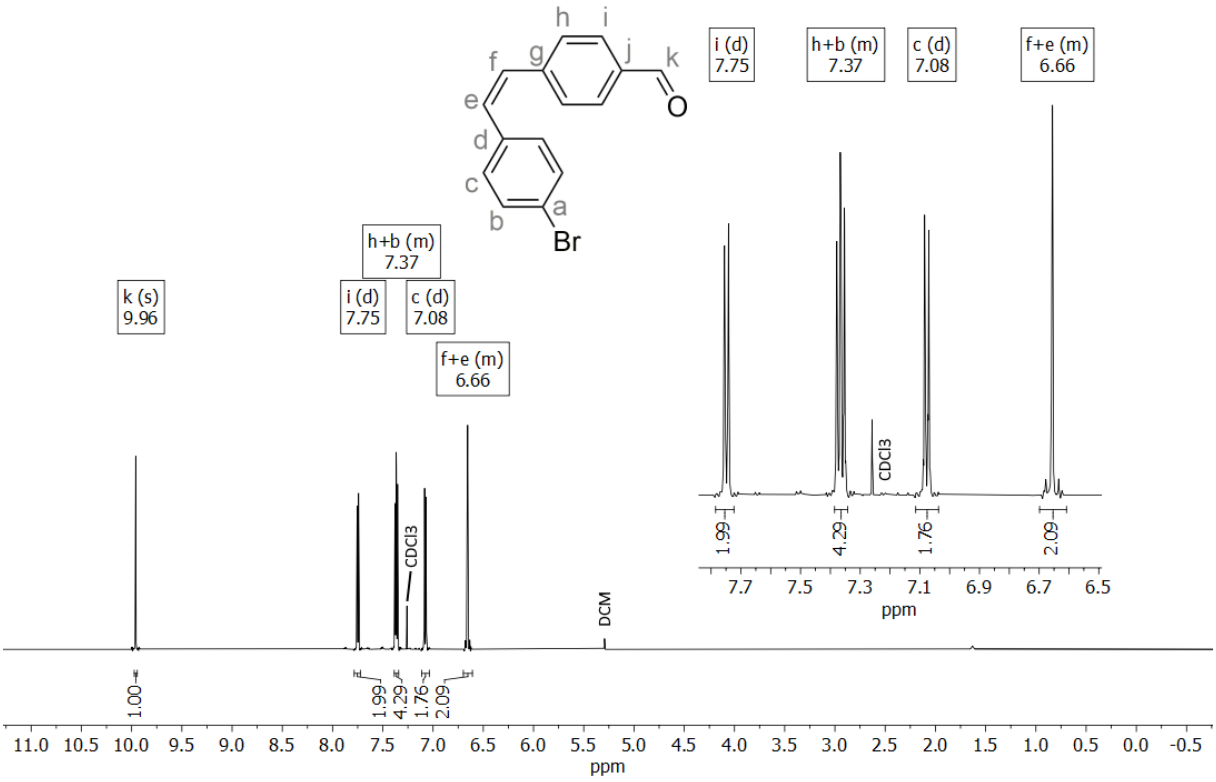

^{13}C{^{1}H} NMR (151 MHz, $CDCl_3$)

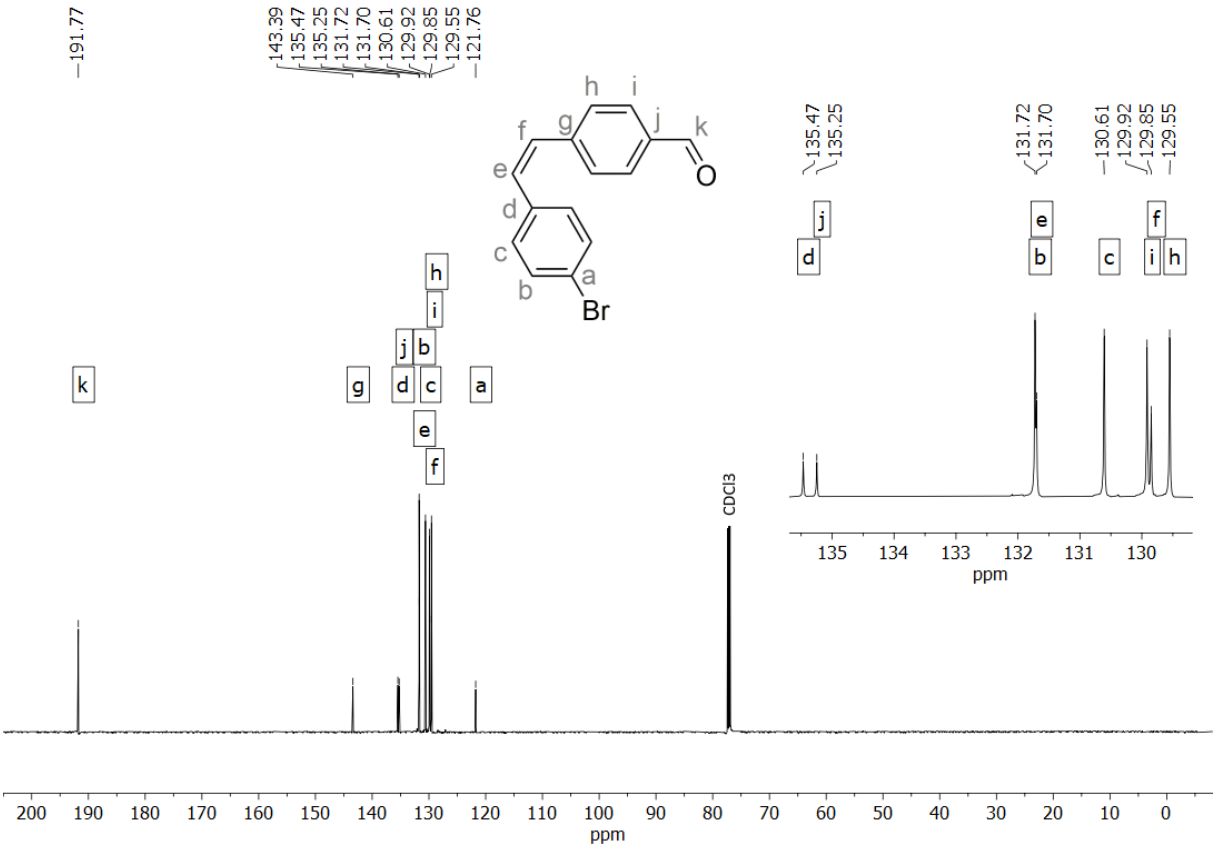

6.15. 6-Bromo-3-formylphenanthrene (19)

^{1}H NMR (601 MHz, $CDCl_3$)

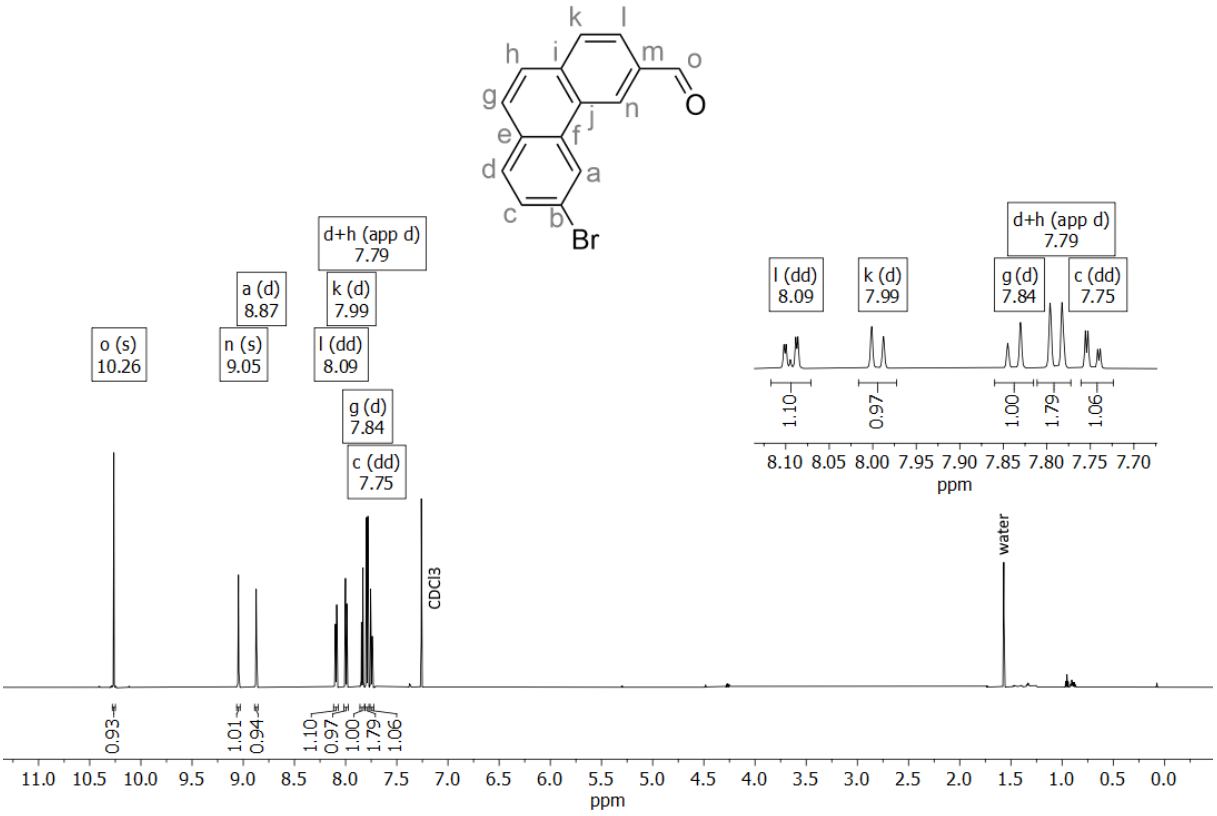

^{13}C{^{1}H} NMR (151 MHz, $CDCl_3$)

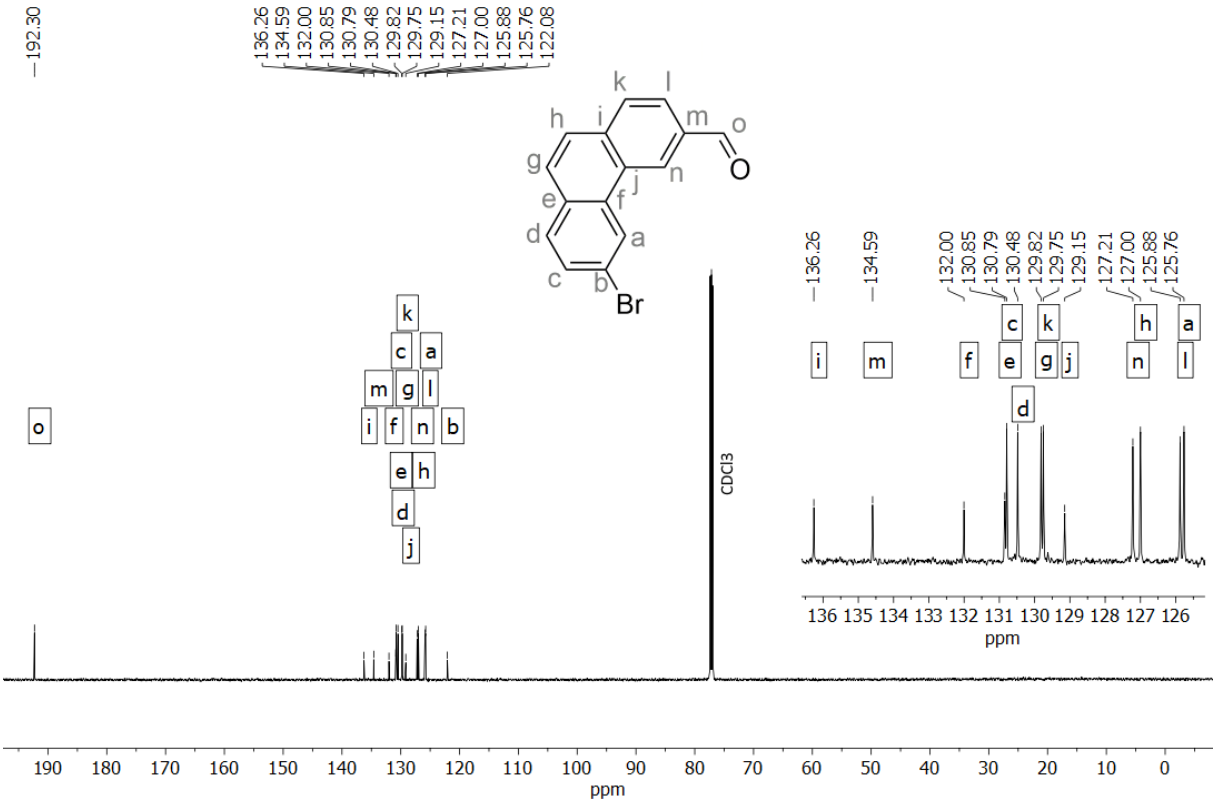

6.16. (*Z*)-6-Bromo-3-(2-(4-bromophenyl)ethenyl)phenanthrene (10)

^{1}H NMR (601 MHz, $CDCl_3$)

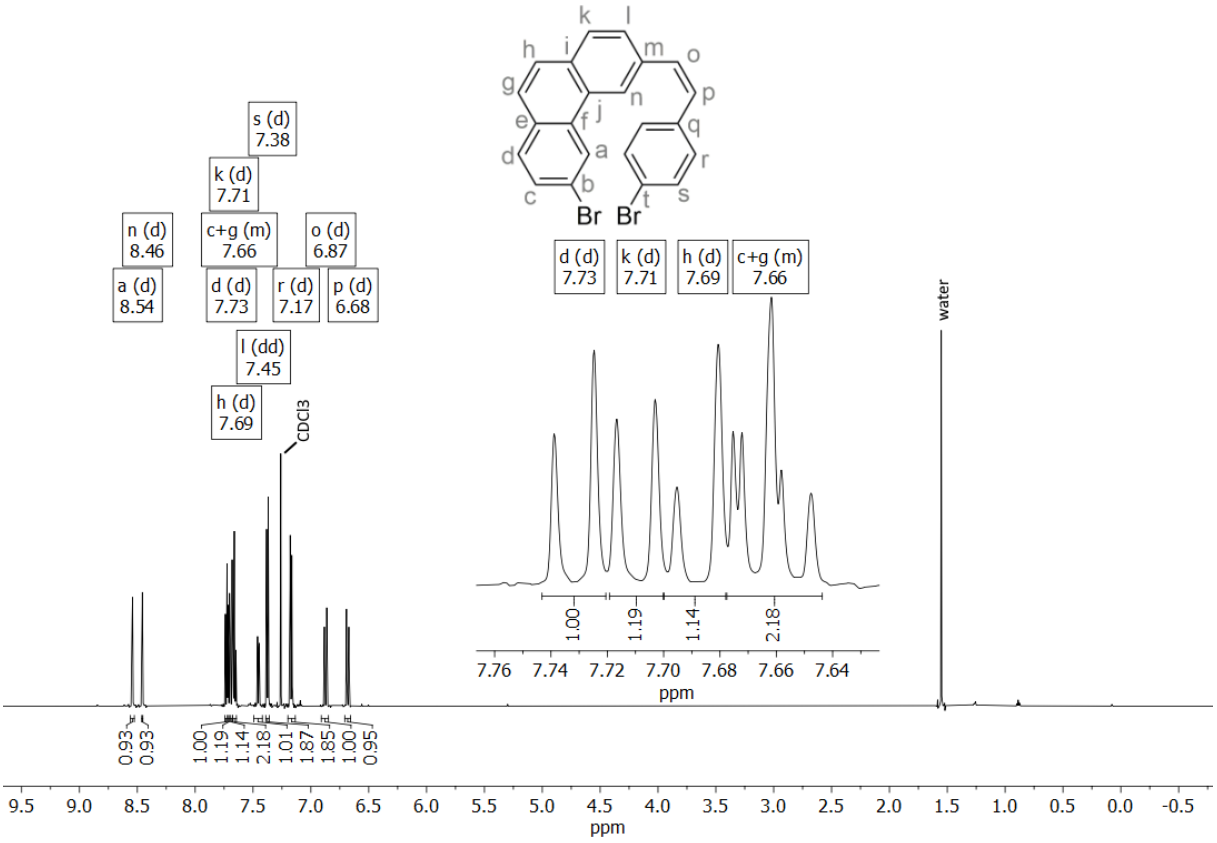

^{13}C{^{1}H} NMR (151 MHz, $CDCl_3$)

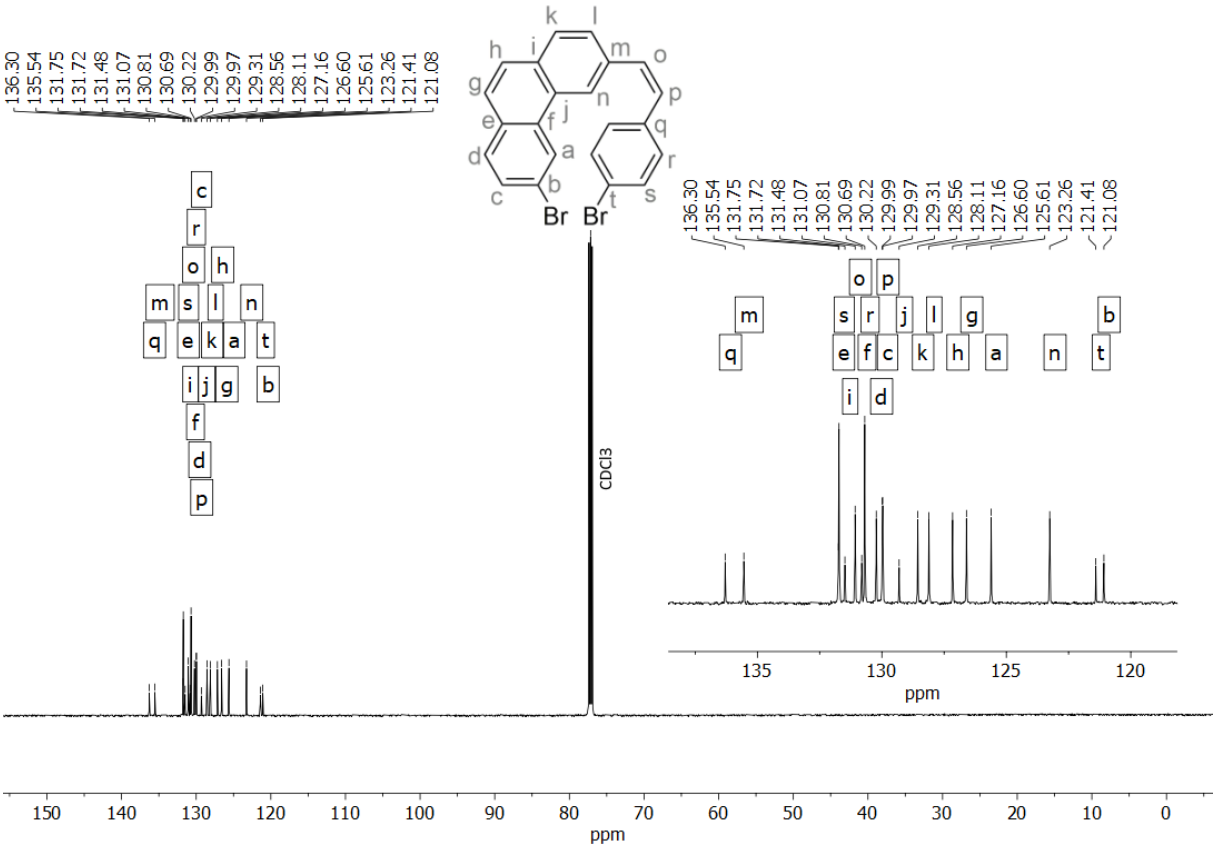

6.17. 2,13-Dibromopentahelicene (12)

^{1}H NMR (601 MHz, C_6D_6)

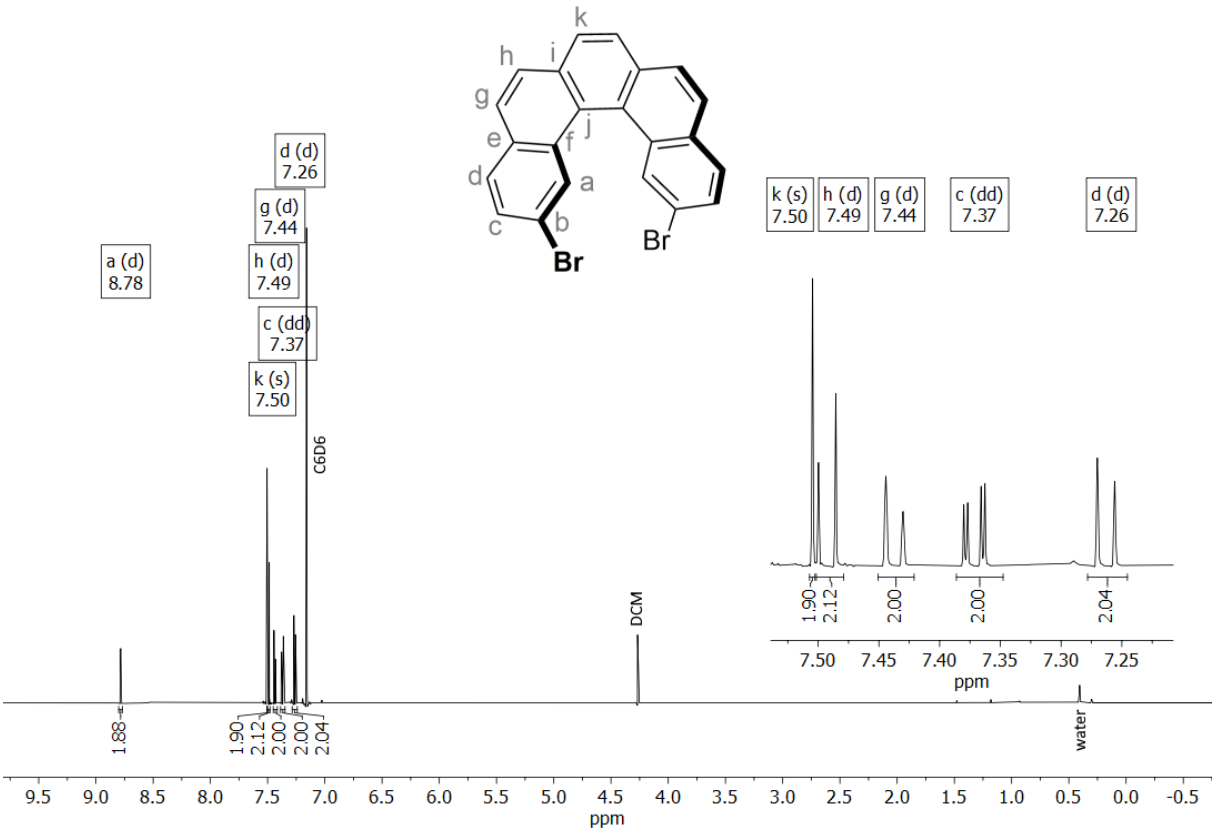

^{13}C{^{1}H} NMR (151 MHz, C_6D_6)

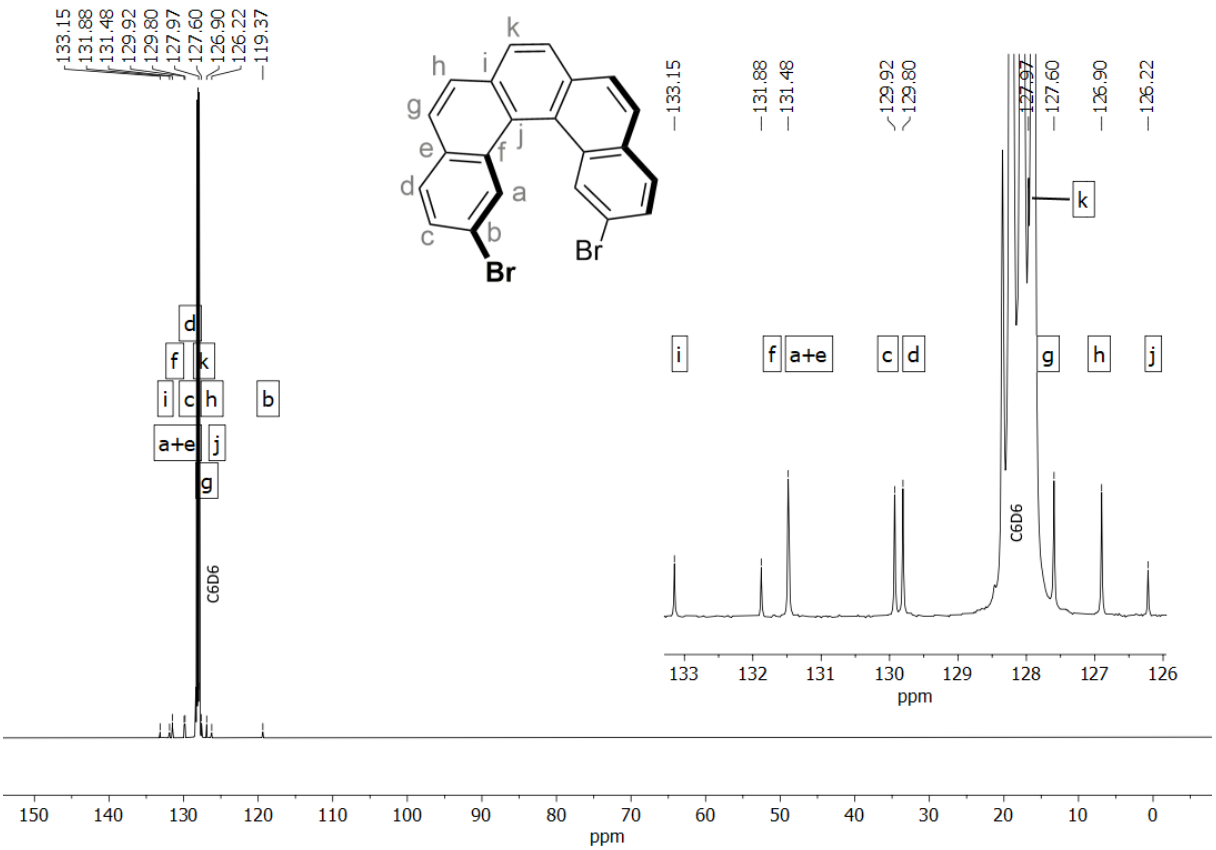

6.18. 2,13-Dimesitylpentahelicene (CC[5])

^{1}H NMR (601 MHz, CD_2Cl_2)

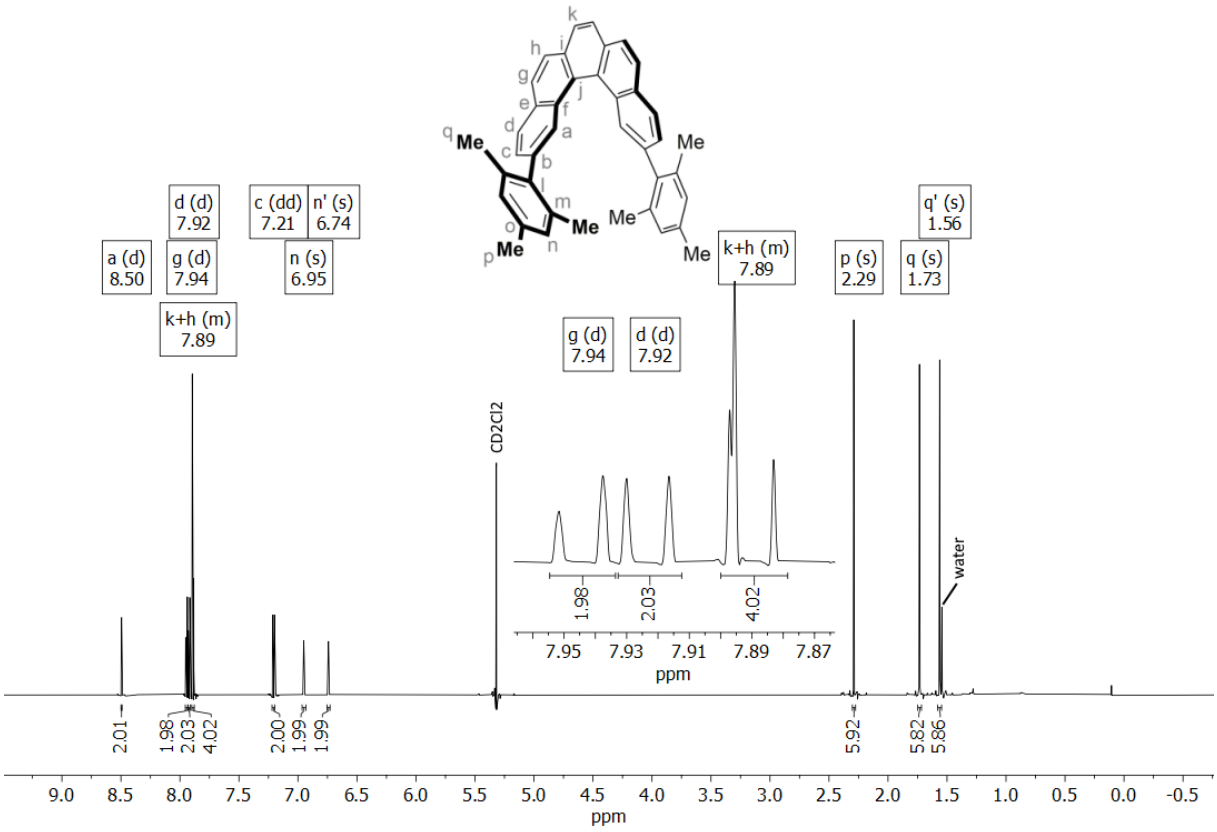

^{13}C{^{1}H} NMR (151 MHz, CD_2Cl_2)

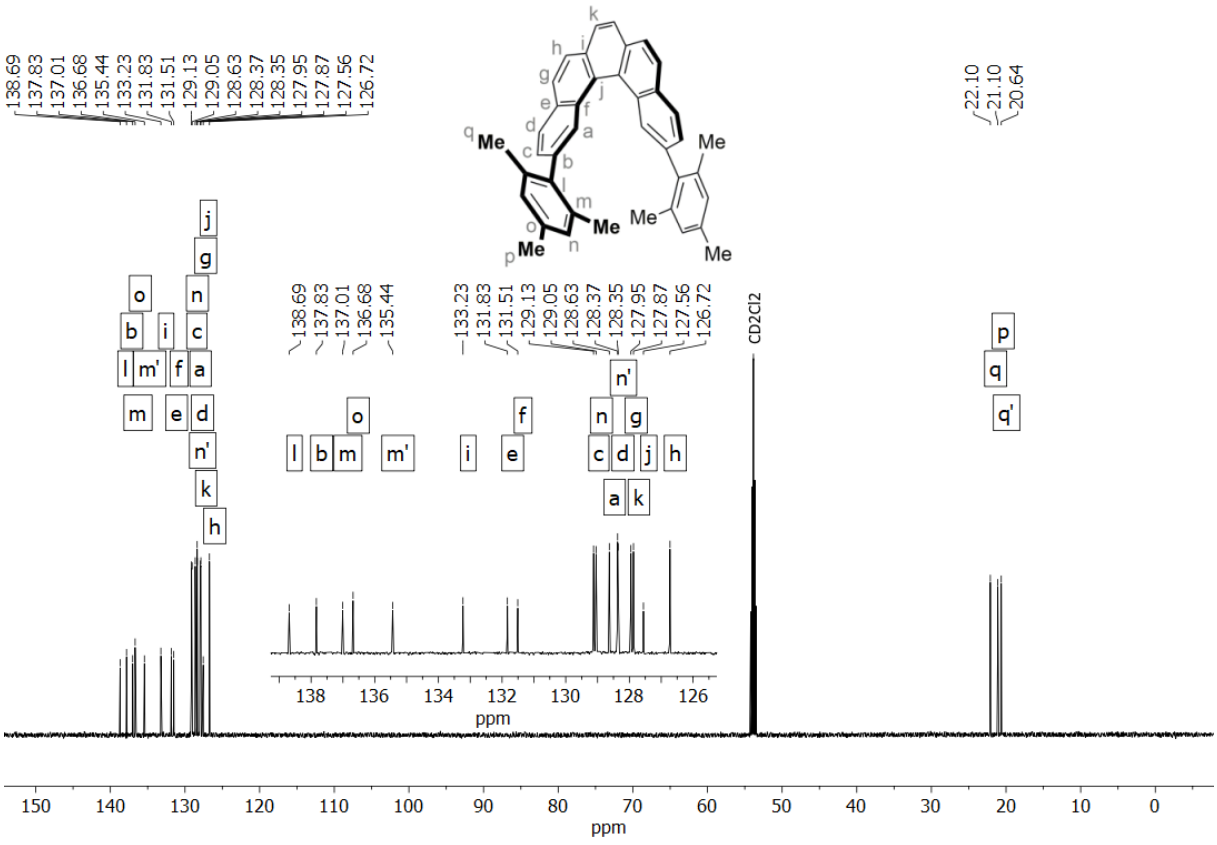

6.19. 2,7-bis(Trifluoromethylsulfonyl)naphthalene (20)

^{1}H NMR (601 MHz, $CDCl_3$)

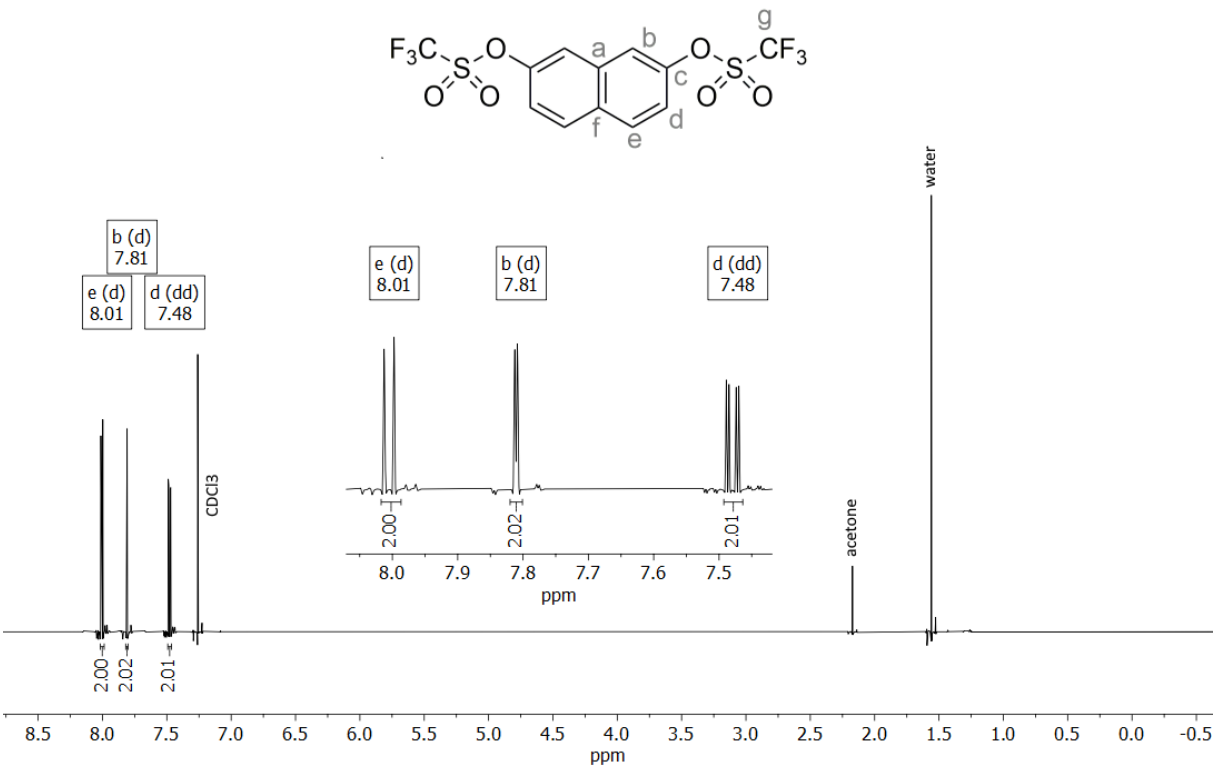

^{13}C{^{1}H} NMR (151 MHz, $CDCl_3$)

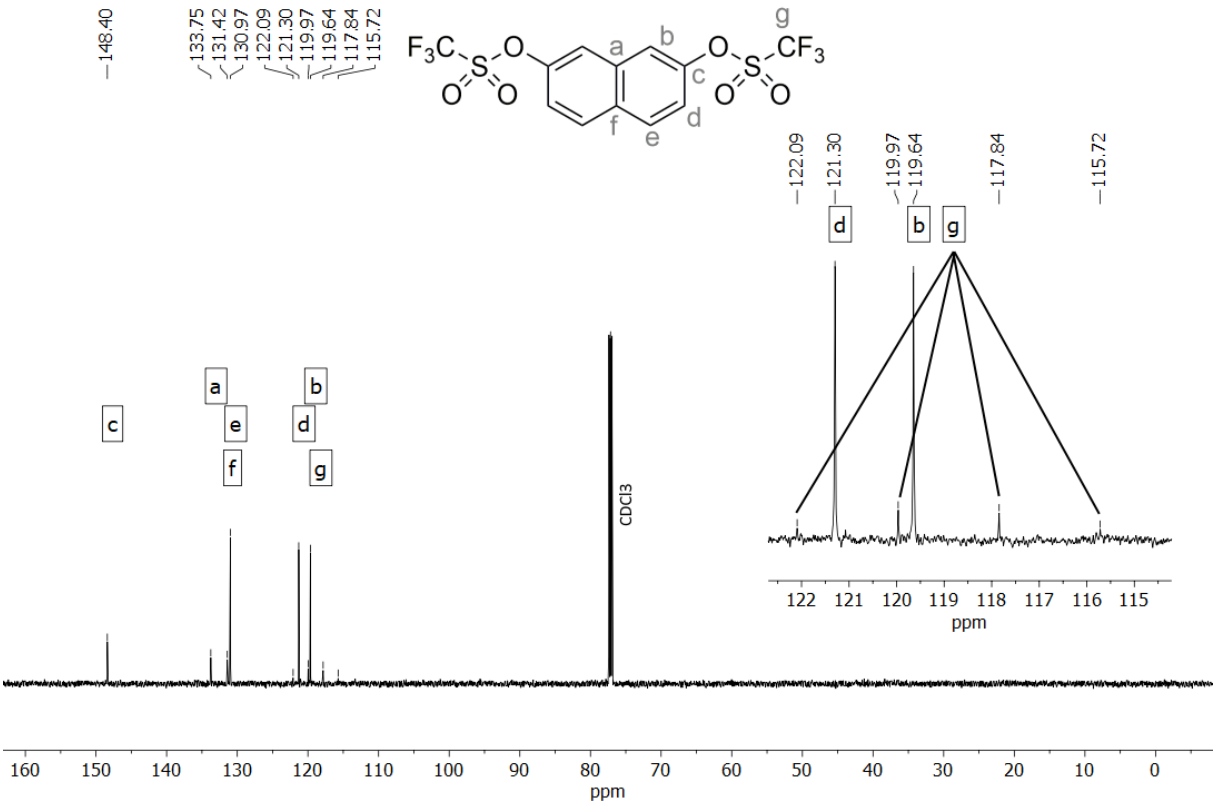

^{19}F NMR (565 MHz, $CDCl_3$)

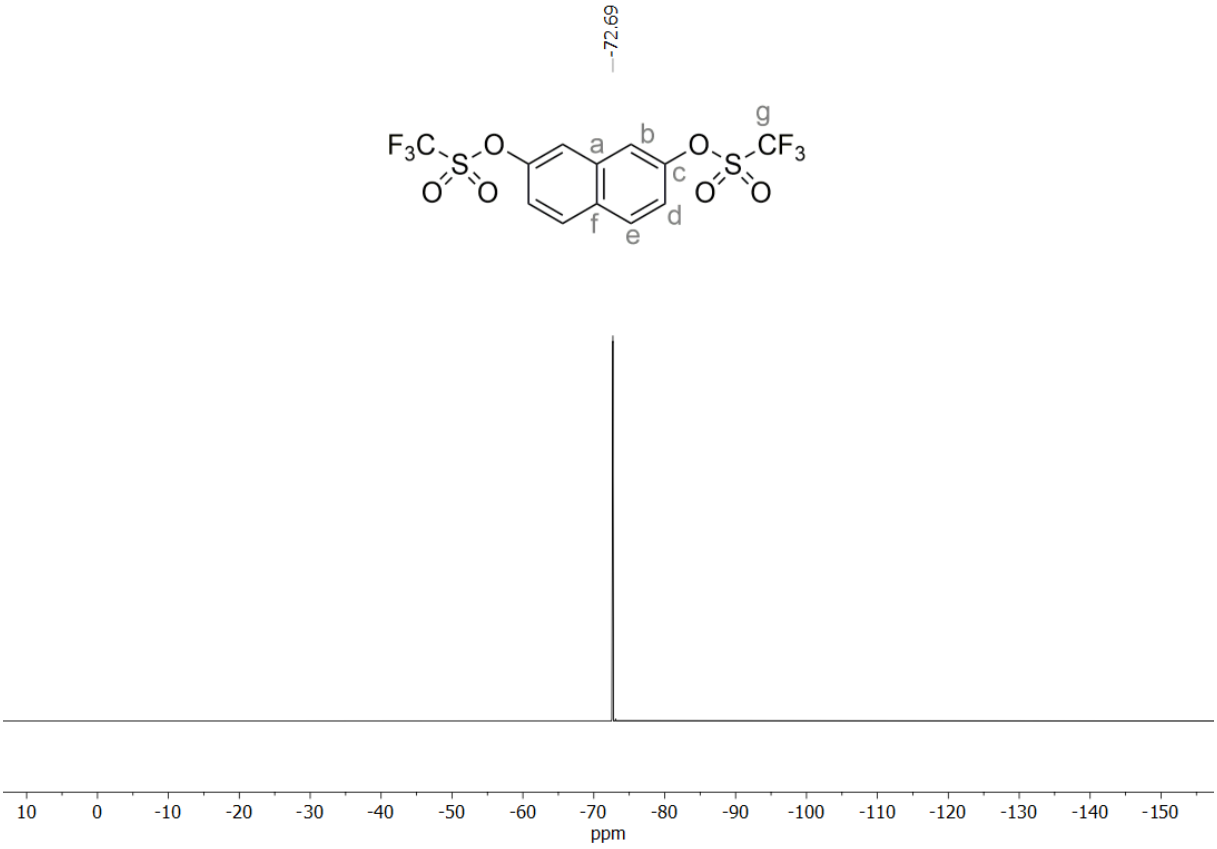

6.20. 2,7-Dimethylnaphthalene (21)

^{1}H NMR (601 MHz, $CDCl_3$)

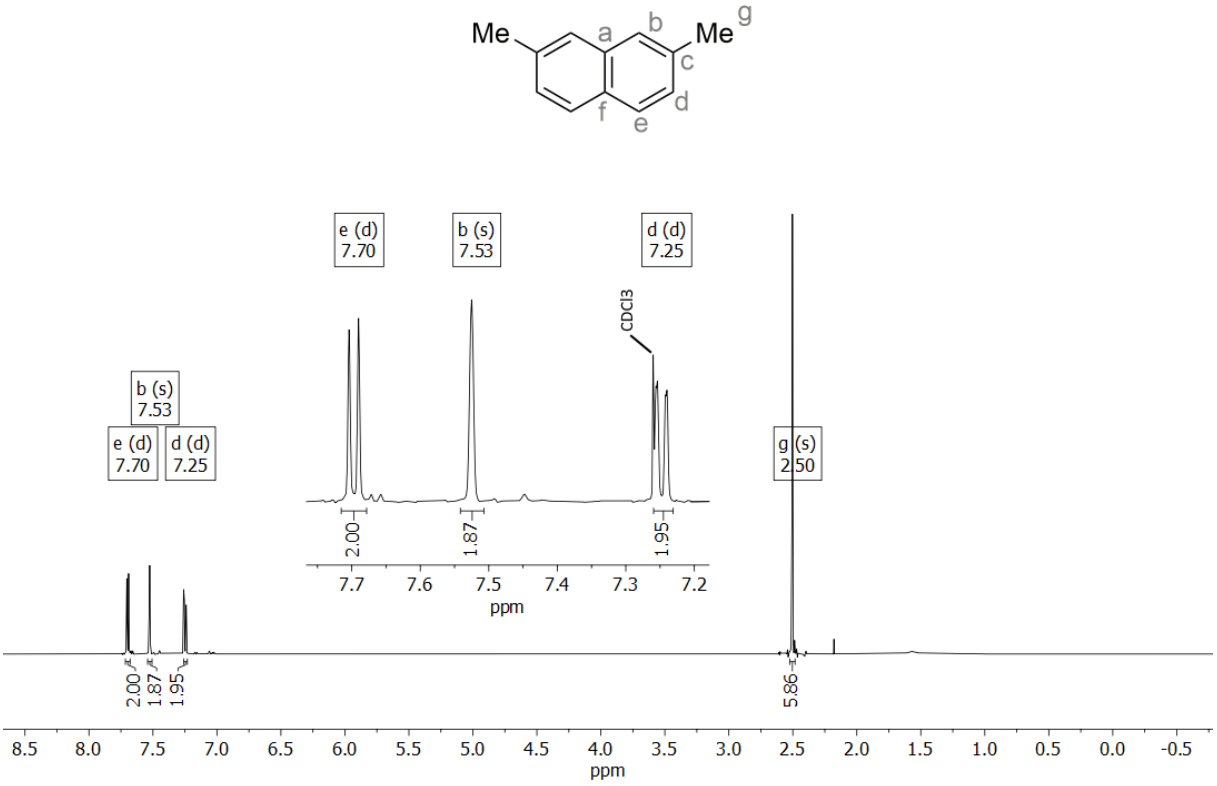

$^{13}C\{^{1}H\}$ NMR (151 MHz, $CDCl_3$)

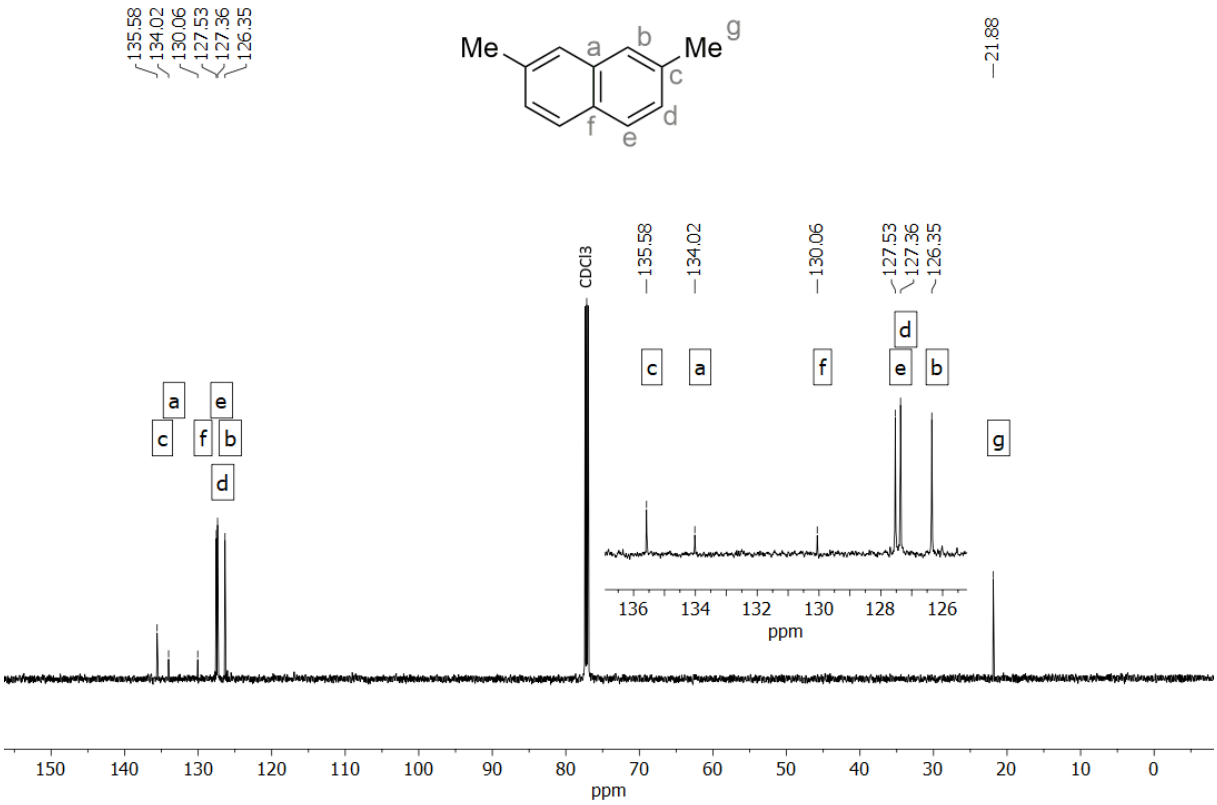

6.21. 2,7-bis(Bromomethyl)naphthalene (22)

^{1}H NMR (601 MHz, $CDCl_3$)

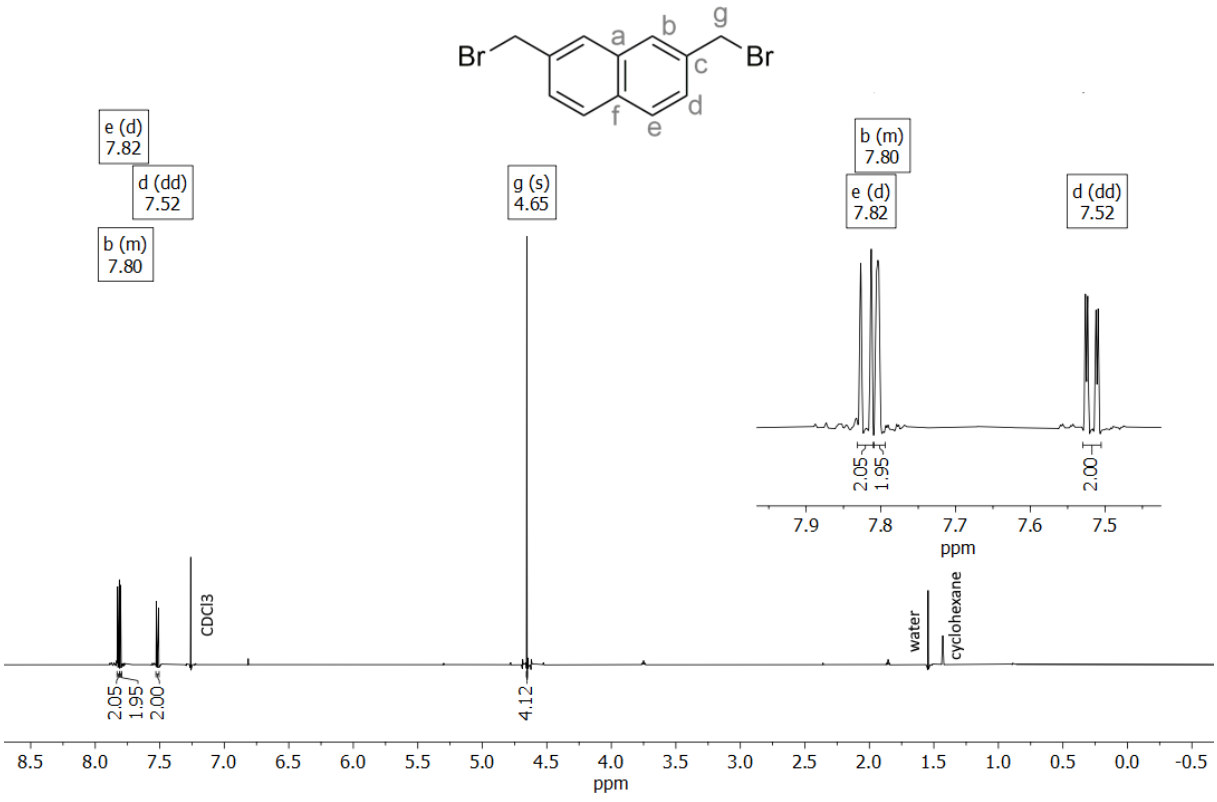

$^{13}C\{^{1}H\}$ NMR (151 MHz, $CDCl_3$)

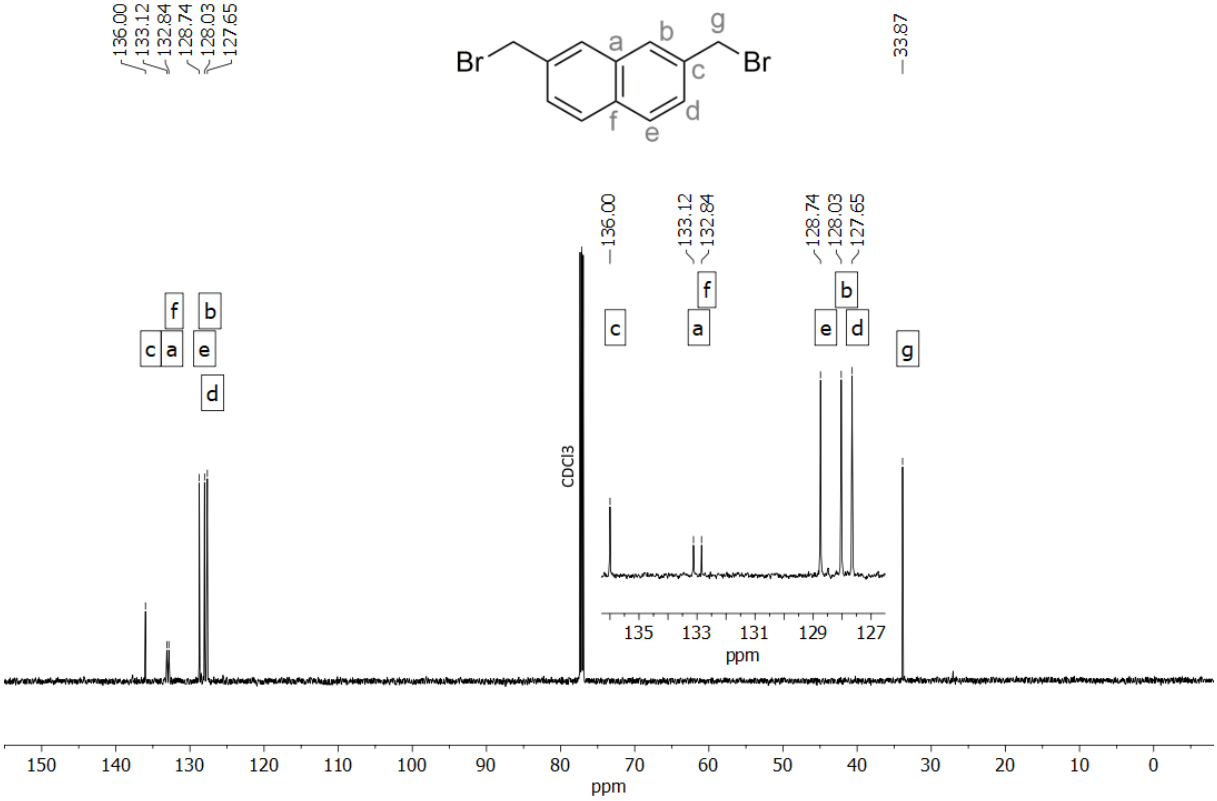

6.22. Naphthalene-2,7-bis(methylenetriphenylphosphonium) dibromide (23)

^{1}H NMR (601 MHz, DMSO-d_6)

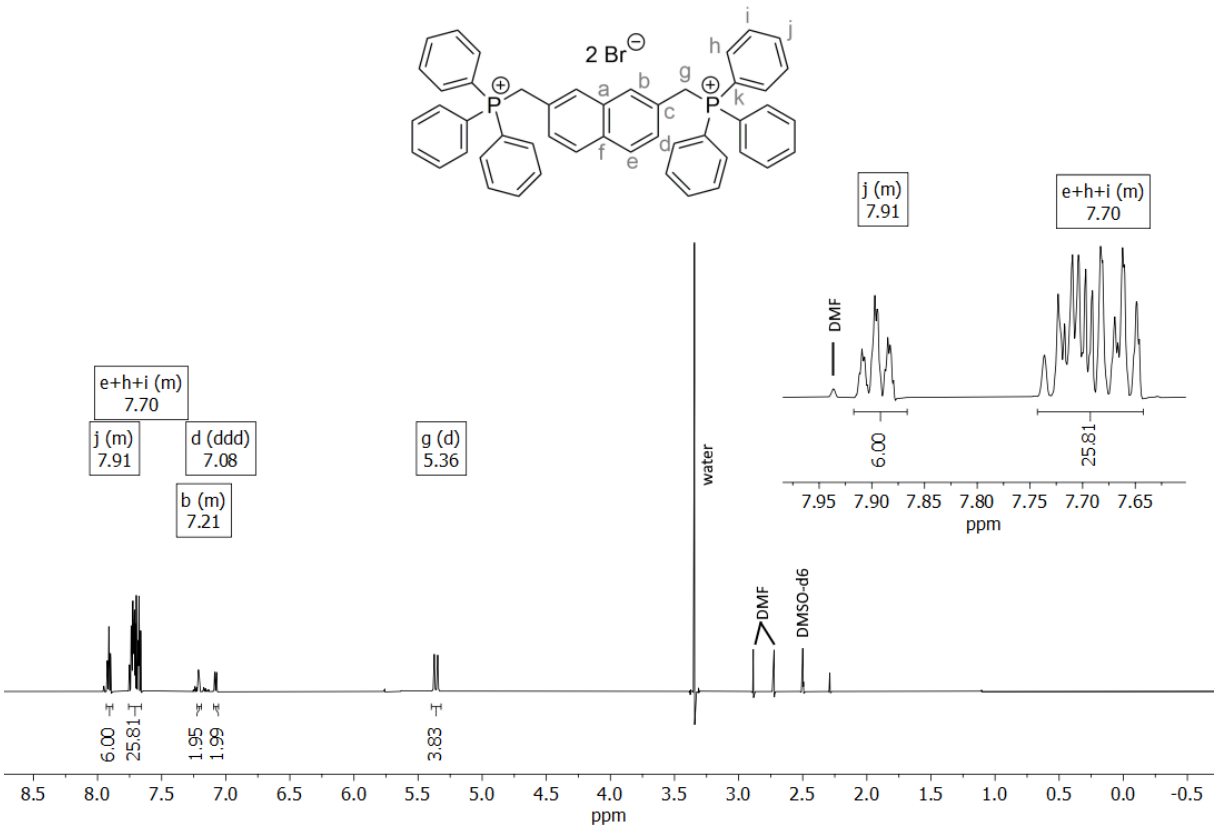

$^{13}C\{^{1}H\}$ NMR (151 MHz, DMSO-d_6)

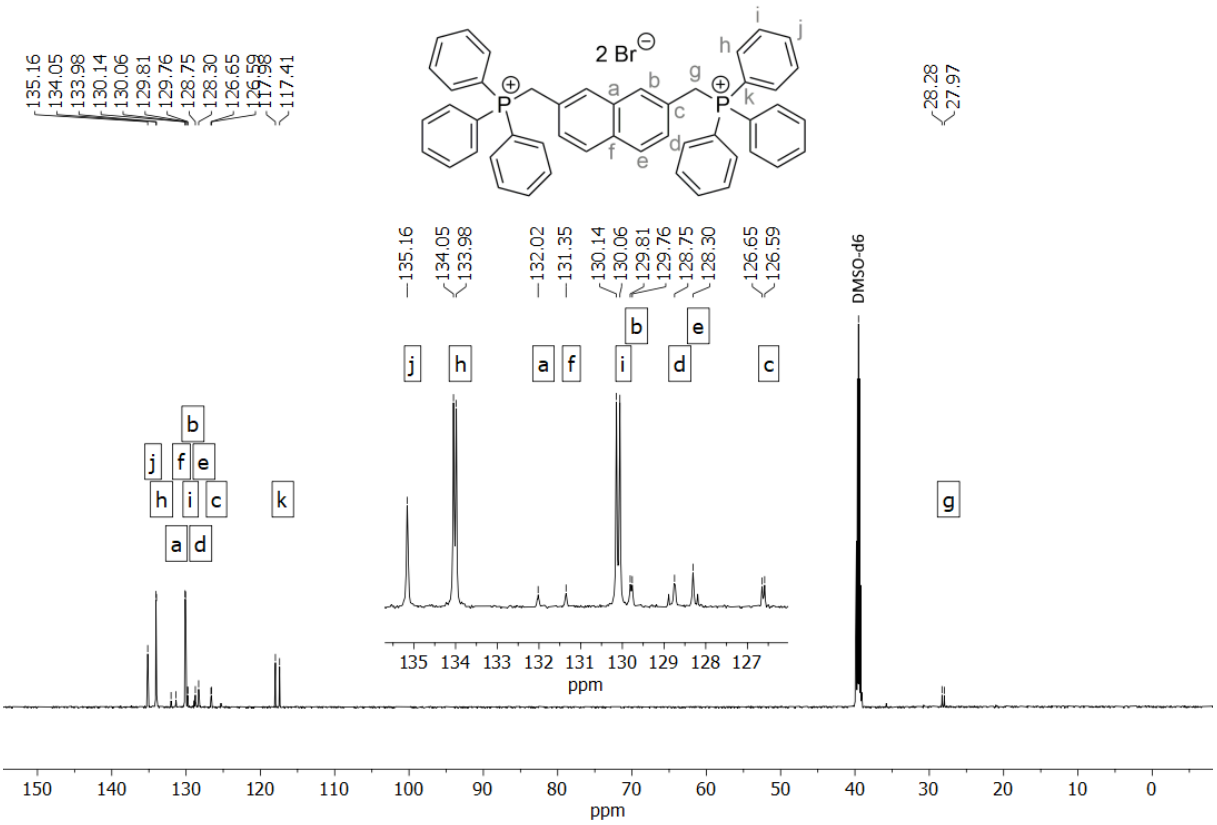

$^{31}P\{^{1}H\}$ NMR (243 MHz, DMSO-d_6)

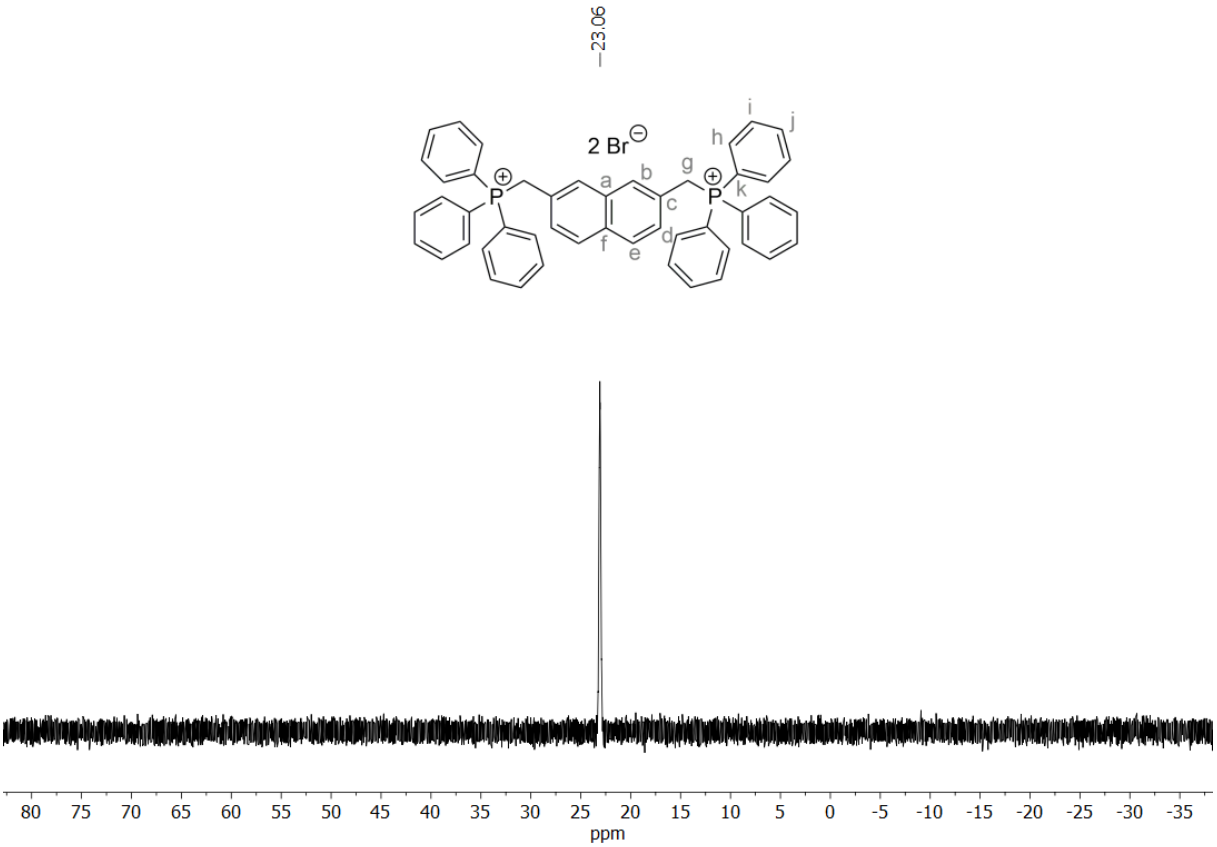

6.23. (*Z,Z*)-2,7-bis(2-(4-Bromophenyl)ethenyl)naphthalene (11)

^{1}H NMR (601 MHz, $CDCl_3$)

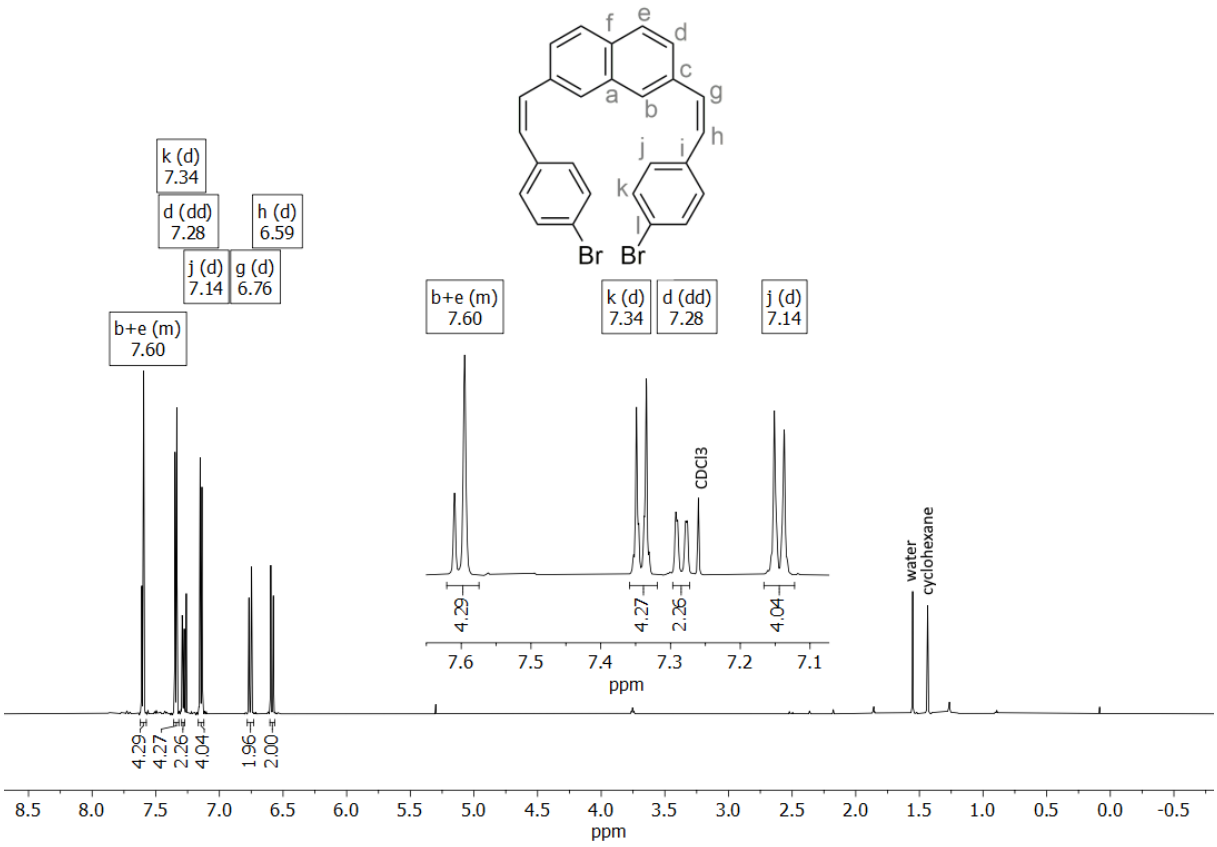

^{13}C{^{1}H} NMR (151 MHz, $CDCl_3$)

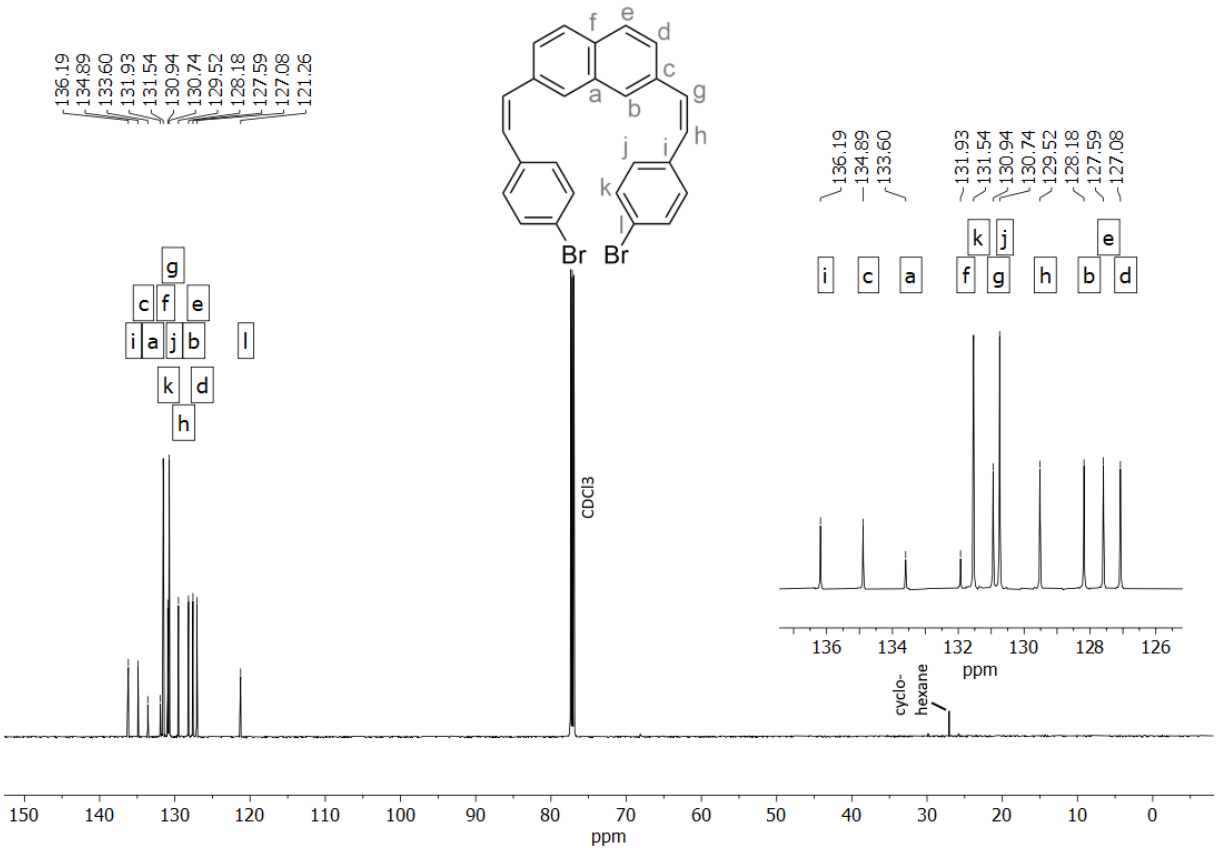

6.24. 2,15-Dibromohexahelicene (13)

^{1}H NMR (601 MHz, $CDCl_3$)

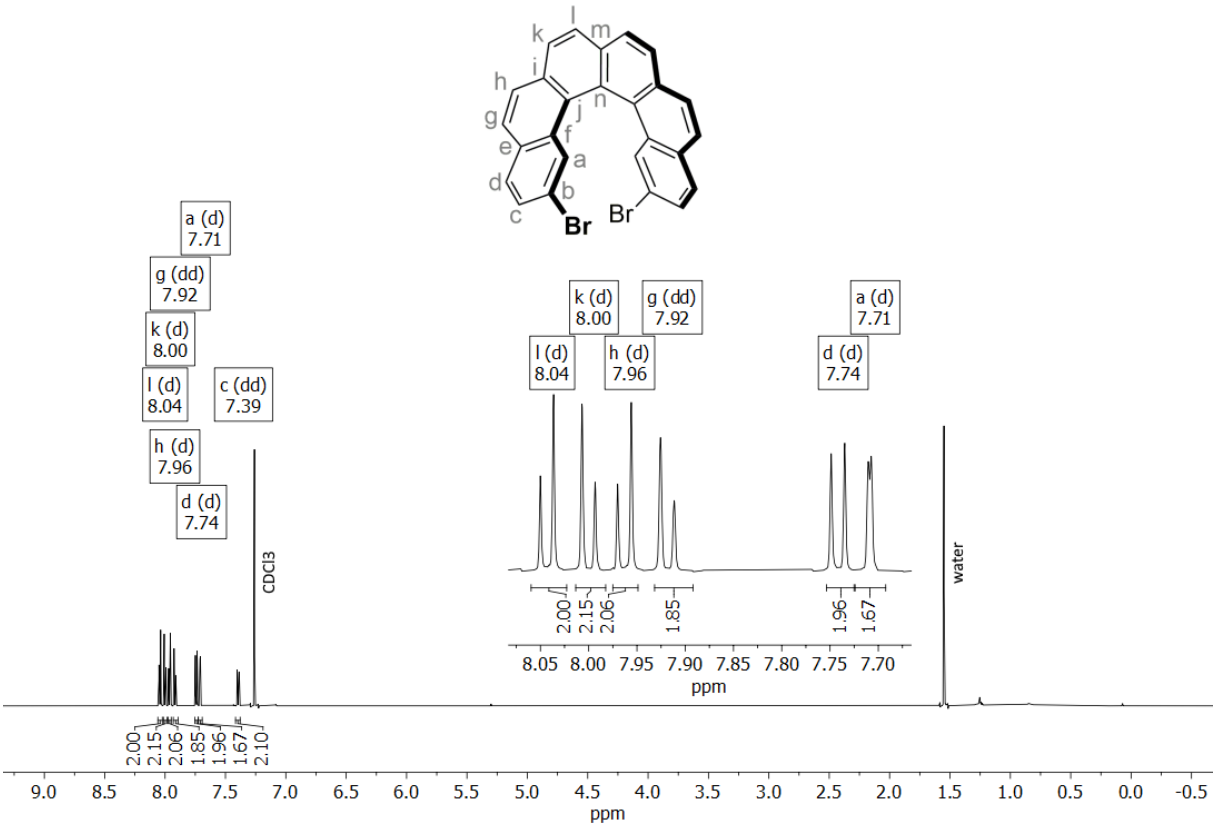

^{13}C{^{1}H} NMR (151 MHz, $CDCl_3$)

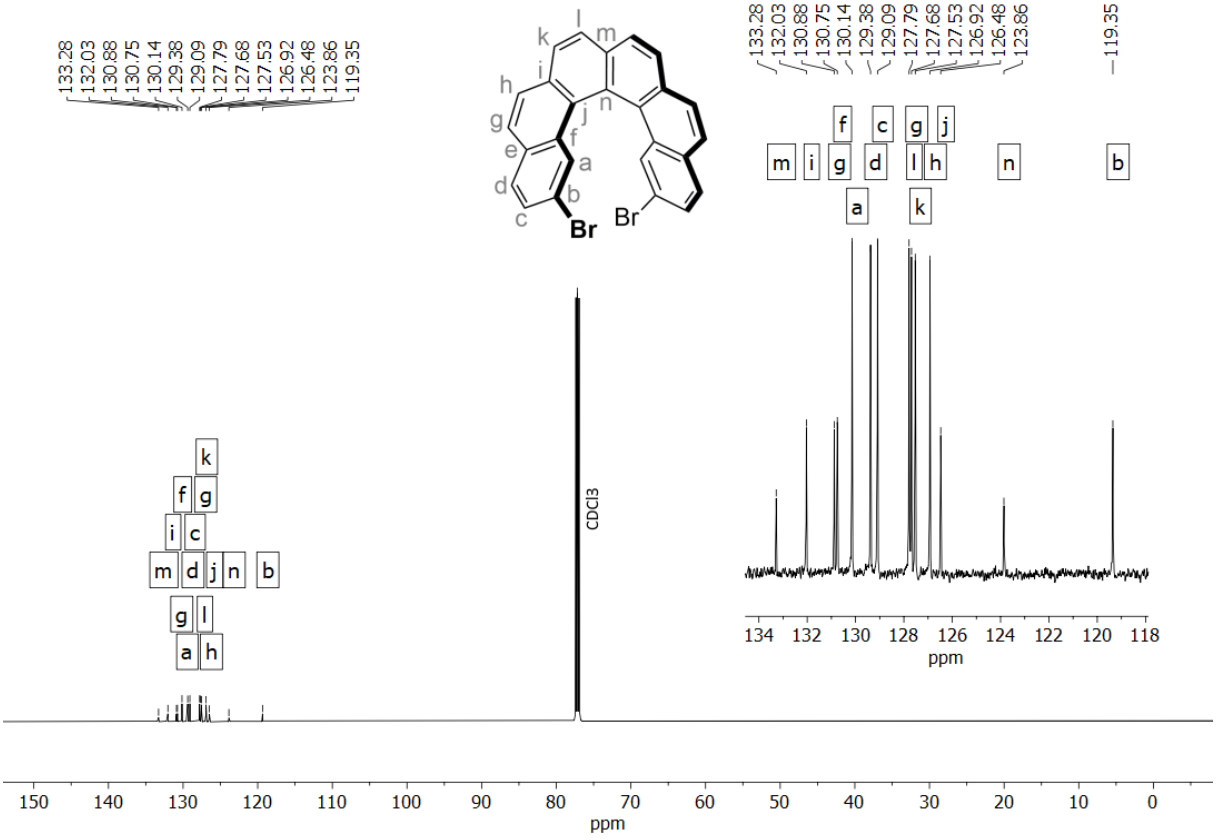

6.25. 2,15-Dimesitylhexahelicene (CC[6])

^{1}H NMR (601 MHz, $CDCl_3$)

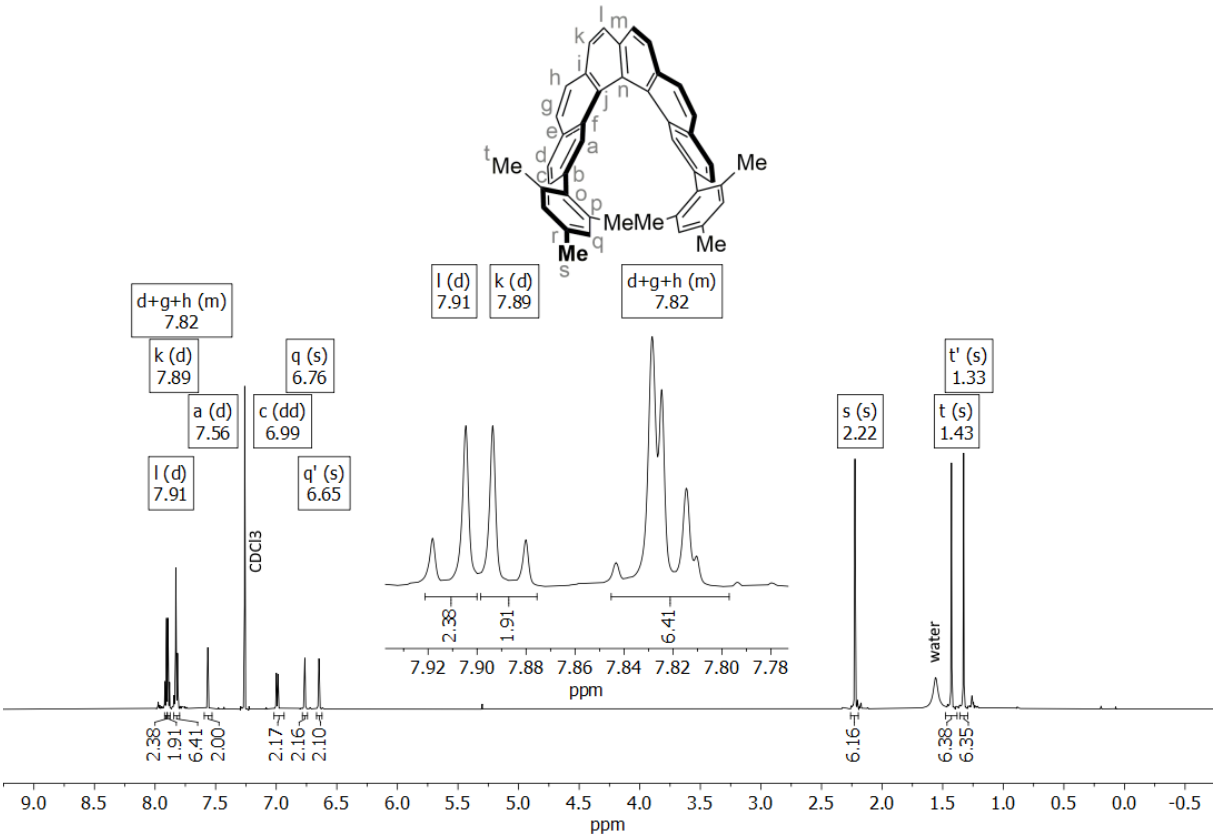

^{13}C{^{1}H} NMR (151 MHz, $CDCl_3$)

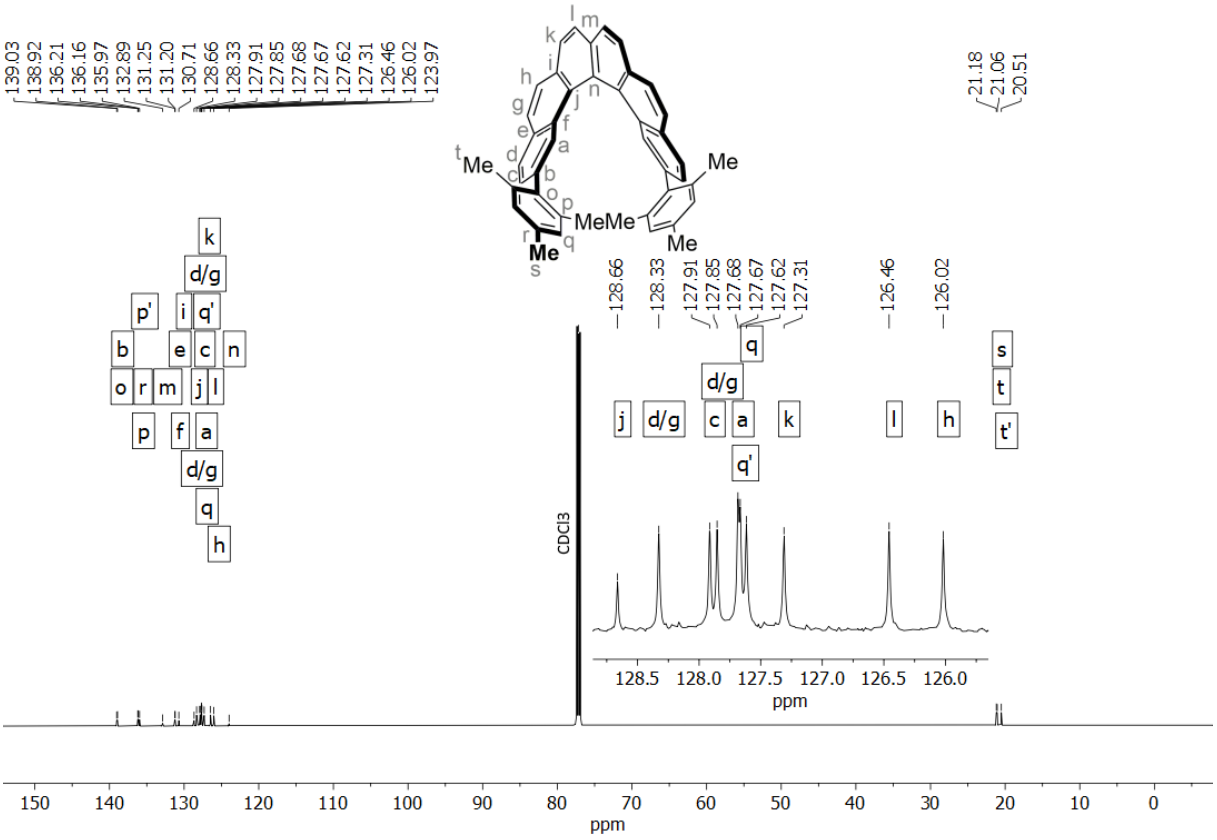

^{1}H NMR (601 MHz, C_6D_6 + trace of DCM). This solvent mixture allowed the best separation of the proton signals and sufficient solubility of the compound for ^{1}H NMR spectroscopy at the same time. The $^{13}C\{^{1}H\}$ NMR spectrum is not depicted due to the large overlap of the residual solvent signal of C_6D_6 and the signals of the compound.

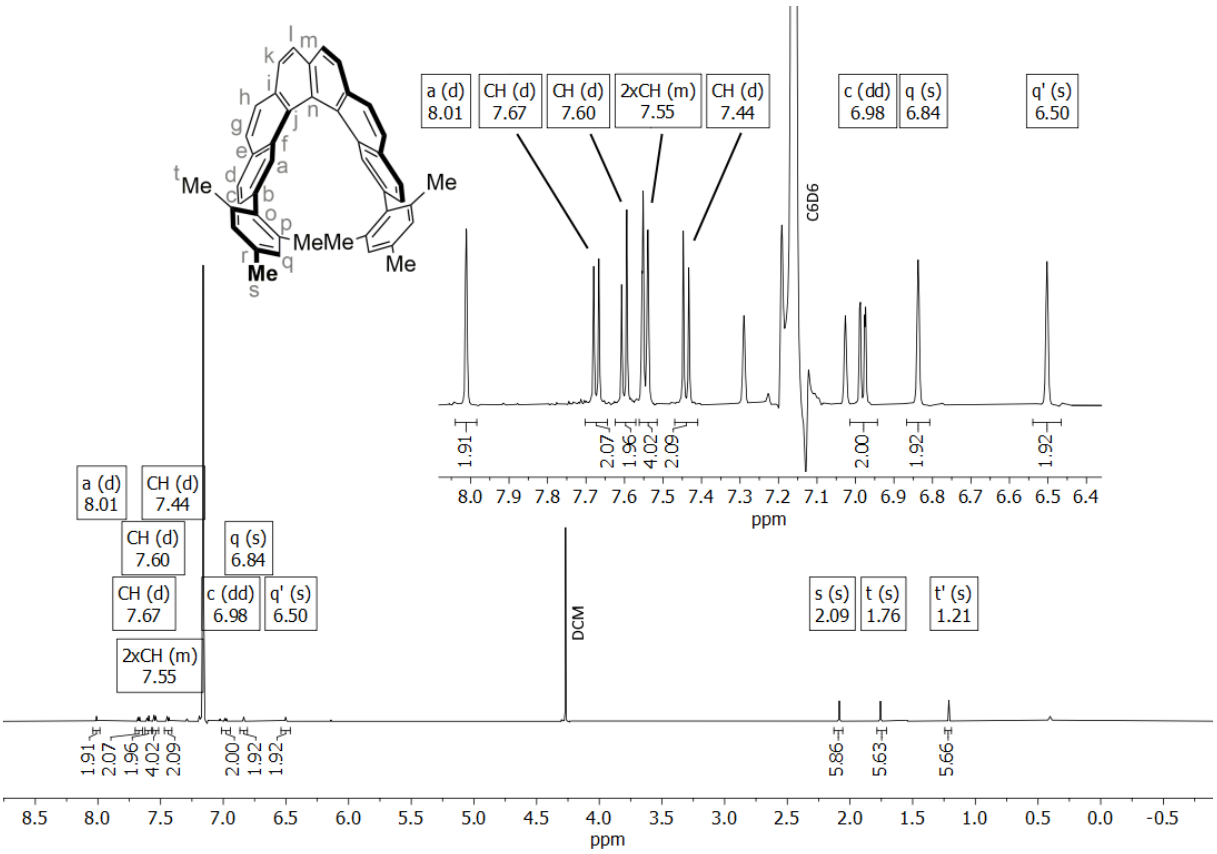

6.26. Temperature-Dependent ^{1}H NMR Measurements

Temperature-dependent ^{1}H NMR spectra of the investigated helicenes were measured in chloroform-d_1 (BN-helicenes, Fig. S28) or tetrachloroethane-d_2 (carbohelicenes, Fig. S29) to analyze the rotation of the mesityl-units around the Mes-helicene single bonds.

At 24 °C, both heterohelicenes showed one singlet for all aromatic protons and all *ortho*-methyl groups of the mesityl-substituents, respectively. Upon cooling to –30 °C (maximum cooling temperature of the probe head), the spectrum of **BN[5]** was nearly unchanged besides a small upfield shift of the N*H* resonance. The aromatic region of the ^{1}H NMR spectrum of **BN[6]** remained identical upon cooling, yet a broadening of the singlet that represents the *ortho*-methyl groups of the mesityl-substituents was found.

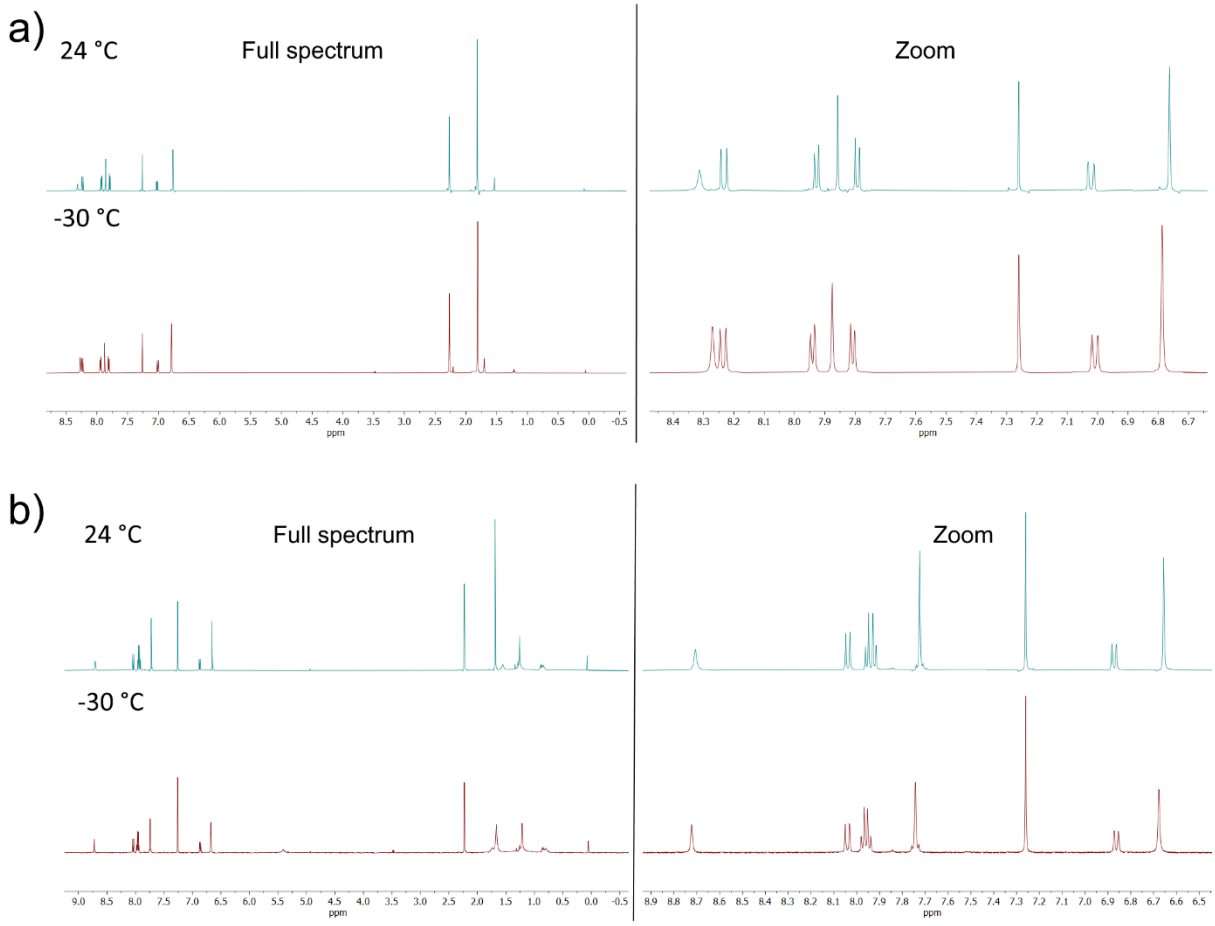

Fig. S28. Temperature-dependent ^{1}H NMR spectra of **BN[5]** (a) and **BN[6]** (b).

In contrast, both carbohelicenes showed two clearly separated proton signals for each aromatic proton and each *ortho*-methyl group of the mesityl-substituent at 24 °C. Coalescence does not occur for both **CC[5]** and **CC[6]** up to 80 °C (maximum heating temperature of the probe head), however, the signals of **CC[5]** clearly broadened and almost coalesced. The signals of **CC[6]** were only slightly broadened at 80 °C, which hints at a comparatively higher coalescence temperature.

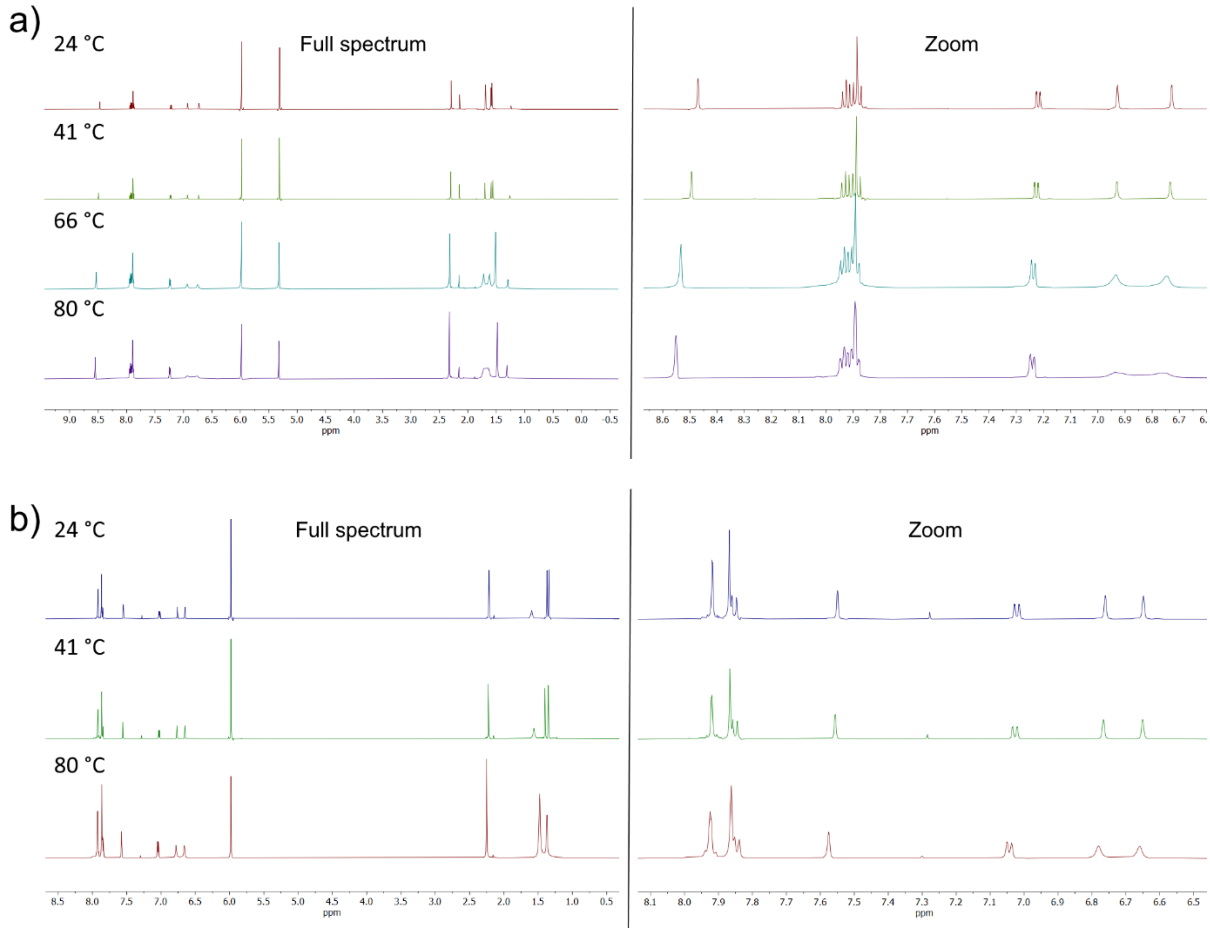

Fig. S29. Temperature-dependent ^{1}H NMR spectra of **CC[5]** (a) and **CC[6]** (b).

7. Calculations

7.1. Structure Optimizations

All calculations were run with Q-Chem 5.4 / 6.0[20] or Gaussian 09, Rev. B.01.[21] The structures were pre-optimized using a universal force field method (UFF).[22] Geometry optimizations of the ground states (S_0) and the first electronically excited singlet states (S_1) were carried out with Density Functional Theory (DFT)[23, 24] at the B3LYP[25-27] / cc-pVDZ[28] level of theory. The absence of imaginary frequencies confirmed that the obtained geometries were indeed energetic minima. The coordinates of the optimized structures are denoted in Table S49 – Table S53.

Table S49. Coordinates of the optimized structure of **BN[5]** (atom / x,y,z coordinates [Å]).

S_0 of **BN[5]**				S_1 of **BN[5]**			
C	0.08446200	1.41721800	4.24576400	C	0.00515300	1.42591700	4.27260600
C	0.16284900	0.71313400	3.00484000	C	0.13694100	0.72436000	3.01500200
C	-0.16284900	-0.71313400	3.00484000	C	-0.13694100	-0.72436000	3.01500200
C	-0.08446200	-1.41721800	4.24576400	C	-0.00515300	-1.42591700	4.27260600
C	0.01434400	-0.68167900	5.47094500	C	0.05276000	-0.70157400	5.47174800
C	-0.01434400	0.68167900	5.47094500	C	-0.05276000	0.70157400	5.47174800
C	0.68978900	1.44648400	1.87848100	C	0.68139900	1.44953000	1.92071500
C	0.81341700	2.86000900	1.93483600	C	0.77460600	2.89304500	1.96109100
C	0.49831500	3.53798000	3.14209500	C	0.39160000	3.56582100	3.15979600
C	0.19904400	2.83395800	4.28075700	C	0.05276000	2.86413500	4.28360100
C	-0.19904400	-2.83395800	4.28075700	C	-0.05276000	-2.86413500	4.28360100
C	-0.49831500	-3.53798000	3.14209500	C	-0.39160000	-3.56582100	3.15979600
C	-0.81341700	-2.86000900	1.93483600	C	-0.77460600	-2.89304500	1.96109100
C	-0.68978900	-1.44648400	1.87848100	C	-0.68139900	-1.44953000	1.92071500
N	1.18994000	0.80798900	0.75673500	N	1.18848900	0.82064200	0.79878000
B	1.82321300	1.43686600	-0.36946100	B	1.77038500	1.47055500	-0.35415700
C	-1.34548300	-3.58393700	0.80905000	C	-1.27295100	-3.61311400	0.84211500
C	-1.82321300	-2.96671800	-0.31183700	C	-1.73475600	-2.99481600	-0.30518600
B	-1.82321300	-1.43686600	-0.36946100	B	-1.77038500	-1.47055500	-0.35415700
N	-1.18994000	-0.80798900	0.75673500	N	-1.18848900	-0.82064200	0.79878000
C	2.49995100	0.54972800	-1.48926600	C	2.43477400	0.60143700	-1.48979900
C	-2.49995100	-0.54972800	-1.48926600	C	-2.43477400	-0.60143700	-1.48979900
C	2.10528500	0.66718400	-2.84577500	C	2.05364300	0.76810900	-2.85069200
C	2.73320000	-0.10896700	-3.83057600	C	2.66252300	-0.00023900	-3.85056500
C	3.76588400	-1.00001800	-3.52276100	C	3.66691300	-0.93127700	-3.56132400
C	4.16634200	-1.09739200	-2.18483800	C	4.05509500	-1.07981500	-2.22249400
C	3.55366700	-0.34851700	-1.17247600	C	3.45914800	-0.34465600	-1.19340300
C	-3.55366700	0.34851700	-1.17247600	C	-3.45914800	0.34465600	-1.19340300
C	-4.16634200	1.09739200	-2.18483800	C	-4.05509500	1.07981500	-2.22249400
C	-3.76588400	1.00001800	-3.52276100	C	-3.66691300	0.93127700	-3.56132400
C	-2.73320000	0.10896700	-3.83057600	C	-2.66252300	0.00023900	-3.85056500
C	-2.10528500	-0.66718400	-2.84577500	C	-2.05364300	-0.76810900	-2.85069200
C	1.00916800	1.62428400	-3.26628300	C	0.98042300	1.75645600	-3.25547100
C	-4.06335200	0.51106600	0.24753000	C	-3.95819000	0.56568100	0.22136200
C	-1.00916800	-1.62428400	-3.26628300	C	-0.98042300	-1.75645600	-3.25547100
C	4.06335200	-0.51106600	0.24753000	C	3.95819000	-0.56568100	0.22136200
C	4.42968400	-1.83626700	-4.59057400	C	4.31575900	-1.75337700	-4.64683600
C	-4.42968400	1.83626700	-4.59057400	C	-4.31575900	1.75337700	-4.64683600
H	0.03746000	-1.24026900	6.40952600	H	0.10984000	-1.24596800	6.41684300
H	-0.03746000	1.24026900	6.40952600	H	-0.10984000	1.24596800	6.41684300
H	0.58037200	4.62725100	3.16561100	H	0.43071400	4.65763200	3.17626200
H	0.06958500	3.34573600	5.23681900	H	-0.15891700	3.38239900	5.22199900
H	-0.06958500	-3.34573600	5.23681900	H	0.15891700	-3.38239900	5.22199900
H	-0.58037200	-4.62725100	3.16561100	H	-0.43071400	-4.65763200	3.17626200
H	1.16213400	-0.20524200	0.79304800	H	1.18537400	-0.19254300	0.84816700
H	-1.38041400	-4.67500800	0.91349100	H	-1.29597800	-4.70484800	0.94006700
H	-2.24417200	-3.59132200	-1.10461800	H	-2.13034000	-3.62752900	-1.10384400
H	-1.16213400	0.20524200	0.79304800	H	-1.18537400	0.19254300	0.84816700
H	2.40680500	-0.01006500	-4.87032600	H	2.34316800	0.13167400	-4.88862700
H	4.98513800	-1.77450200	-1.92128600	H	4.85203000	-1.78817200	-1.97532300
H	-4.98513800	1.77450200	-1.92128600	H	-4.85203000	1.78817200	-1.97532300
H	-2.40680500	0.01006500	-4.87032600	H	-2.34316800	-0.13167400	-4.88862700
H	0.10959900	1.52774200	-2.63905000	H	0.07733600	1.66489500	-2.63336500
H	0.70683200	1.44576300	-4.30893500	H	0.68222800	1.60589600	-4.30389600

H	1.33962300	2.67416000	-3.19458100	H	1.33216500	2.79705800	-3.15906900
H	-3.40817700	1.16190800	0.85283700	H	-3.28101000	1.21507800	0.80353800
H	-4.13203900	-0.45225500	0.77586900	H	-4.05355500	-0.37806100	0.77902400
H	-5.06281900	0.97164000	0.25409700	H	-4.94238600	1.05782500	0.21511600
H	-0.70683200	-1.44576300	-4.30893500	H	-0.68222800	-1.60589600	-4.30389600
H	-1.33962300	-2.67416000	-3.19458100	H	-1.33216500	-2.79705800	-3.15906900
H	-0.10959900	-1.52774200	-2.63905000	H	-0.07733600	-1.66489500	-2.63336500
H	5.06281900	-0.97164000	0.25409700	H	4.94238600	-1.05782500	0.21511600
H	3.40817700	-1.16190800	0.85283700	H	3.28101000	-1.21507800	0.80353800
H	4.13203900	0.45225500	0.77586900	H	4.05355500	0.37806100	0.77902400
H	5.52783100	-1.74687900	-4.54689700	H	5.41345500	-1.64702900	-4.62773900
H	4.10519700	-1.53749100	-5.59860100	H	3.96328500	-1.45731800	-5.64594000
H	4.18998400	-2.90668800	-4.46632700	H	4.09737600	-2.82767100	-4.51749300
H	-5.52783100	1.74687900	-4.54689700	H	-5.41345500	1.64702900	-4.62773900
H	-4.10519700	1.53749100	-5.59860100	H	-3.96328500	1.45731800	-5.64594000
H	-4.18998400	2.90668800	-4.46632700	H	-4.09737600	2.82767100	-4.51749300
C	1.34548300	3.58393700	0.80905000	C	1.27295100	3.61311400	0.84211500
C	1.82321300	2.96671800	-0.31183700	C	1.73475600	2.99481600	-0.30518600
H	2.24417200	3.59132200	-1.10461800	H	2.13034000	3.62752900	-1.10384400
H	1.38041400	4.67500800	0.91349100	H	1.29597800	4.70484800	0.94006700

Table S50. Coordinates of the optimized structure of **CC[5]** (atom / x,y,z coordinates [Å]).

S_0 of **CC[5]**				S_1 of **CC[5]**			
C	-4.27118600	0.44612000	-1.33459700	C	-4.30133700	-0.38292200	1.36376500
C	-3.02890200	0.34203100	-0.64181000	C	-3.03177700	-0.33558700	0.64354200
C	-3.02883000	-0.34235600	0.64193600	C	-3.03177900	0.33558500	-0.64352400
C	-4.27107300	-0.44658800	1.33478800	C	-4.30134100	0.38292000	-1.36374200
C	-5.49700700	-0.16554300	0.66313700	C	-5.51588500	0.13401500	-0.68271200
C	-5.49705800	0.16494800	-0.66288600	C	-5.51588300	-0.13401400	0.68274000
C	-1.88678700	1.03939100	-1.23543700	C	-1.91109500	-1.03391700	1.23269200
C	-1.97201900	1.49557000	-2.59072700	C	-1.96981900	-1.42847900	2.62603700
C	-3.18699200	1.33272700	-3.32804300	C	-3.16125800	-1.19336300	3.36743900
C	-4.30971400	0.88540100	-2.69821400	C	-4.30161500	-0.72956100	2.73878100
C	-4.30948300	-0.88588500	2.69839500	C	-4.30162300	0.72955500	-2.73875900
C	-3.18667000	-1.33307600	3.32816900	C	-3.16126800	1.19335400	-3.36742200
C	-1.97171800	-1.49575400	2.59079700	C	-1.96982500	1.42847000	-2.62602400
C	-1.88661400	-1.03958100	1.23550300	C	-1.91109700	1.03391200	-1.23267900
C	-0.74460900	1.43727500	-0.48770400	C	-0.77192500	-1.45462600	0.49273800
C	0.28732200	2.19246800	-1.03431800	C	0.28289700	-2.17354300	1.06879700
C	-0.88519800	-2.20769200	3.15853000	C	-0.87604300	2.10632300	-3.20500200
C	0.21772100	-2.54951100	2.40586900	C	0.23198400	2.47414600	-2.45126000
C	0.28763900	-2.19236600	1.03426500	C	0.28289500	2.17353700	-1.06879300
C	-0.74442400	-1.43734000	0.48770100	C	-0.77192300	1.45462100	-0.49272900
C	1.43859800	2.66546700	-0.19909300	C	1.43617400	-2.64393600	0.24152800
C	1.43892600	-2.66527500	0.19901200	C	1.43617600	2.64393500	-0.24153000
C	2.74438800	2.17353700	-0.44215500	C	2.74366700	-2.15764300	0.49712000
C	3.80774600	2.64582400	0.33602800	C	3.80977500	-2.62590000	-0.27885600
C	3.62494400	3.59772100	1.34718900	C	3.63172000	-3.56965200	-1.29872000
C	2.33078100	4.07811300	1.56401800	C	2.33730100	-4.04382000	-1.52910200
C	1.23376800	3.63173600	0.81194600	C	1.23603500	-3.59971200	-0.78323000
C	1.23409800	-3.63133400	-0.81222700	C	1.23605500	3.59977500	0.78317100
C	2.33113000	-4.07765600	-1.56430600	C	2.33732600	4.04388700	1.52903400
C	3.62531400	-3.59740900	-1.34730000	C	3.63173100	3.56966300	1.29869800
C	3.80811500	-2.64570600	-0.33595400	C	3.80976800	2.62584400	0.27889100
C	2.74474300	-2.17347700	0.44224000	C	2.74365700	2.15758200	-0.49707500
C	3.01491700	1.14217100	-1.51520500	C	3.01469300	-1.12945800	1.57341600
C	-0.13337500	-4.21635100	-1.09205800	C	-0.12858800	4.18399900	1.07788100
C	3.01532900	-1.14235900	1.51552100	C	3.01465200	1.12931600	-1.57330100
C	-0.13368400	4.21690700	1.09155500	C	-0.12862400	-4.18386900	-1.07799900
C	4.79334900	4.07766100	2.17485600	C	4.80441200	-4.04655900	-2.12139900
C	4.79375200	-4.07729200	-2.17494900	C	4.80443600	4.04659900	2.12134200
H	-6.43404400	-0.28502500	1.21210300	H	-6.45492500	0.21934800	-1.23370300
H	-6.43413400	0.28433600	-1.21180500	H	-6.45492100	-0.21934600	1.23373300
H	-3.21842700	1.65577500	-4.37138900	H	-3.18612000	-1.46359900	4.42595300
H	-5.27021200	0.86191100	-3.21885900	H	-5.23957400	-0.65085800	3.29445500
H	-5.26995900	-0.86253500	3.21908700	H	-5.23958400	0.65085200	-3.29443000
H	-3.21801700	-1.65614500	4.37151200	H	-3.18613200	1.46358600	-4.42593600
H	4.81190100	2.25484800	0.14507000	H	4.81320900	-2.23674100	-0.08055200
H	2.16408400	4.83192300	2.33912000	H	2.17448600	-4.79220800	-2.31020400
H	2.16442300	-4.83131000	-2.33955800	H	2.17452400	4.79232400	2.31009300

H	4.81228400	-2.25482700	-0.14486700	H	4.81319100	2.23663600	0.08062700
H	2.30809700	0.30042800	-1.46199900	H	2.27575600	-0.31466300	1.55699800
H	4.03210800	0.73581600	-1.41777700	H	4.01208900	-0.68486800	1.44291800
H	2.92433900	1.56844800	-2.52802400	H	2.97973800	-1.57121400	2.58305800
H	-0.78883300	-3.50141000	-1.61633500	H	-0.77285500	3.47451200	1.62299600
H	-0.65511100	-4.49677600	-0.16407700	H	-0.66632100	4.45121400	0.15548400
H	-0.04947300	-5.11231300	-1.72485300	H	-0.03630100	5.08800000	1.69806200
H	4.03223300	-0.73539500	1.41763800	H	4.01209200	0.68480700	-1.44285600
H	2.92564500	-1.56911200	2.52822600	H	2.97956400	1.57096900	-2.58298200
H	2.30799500	-0.30100800	1.46310000	H	2.27577400	0.31447100	-1.55673000
H	-0.04980100	5.11277000	1.72449100	H	-0.03635500	-5.08786500	-1.69819000
H	-0.78936600	3.50198100	1.61556700	H	-0.77283700	-3.47434400	-1.62313000
H	-0.65517000	4.49753400	0.16349100	H	-0.66640400	-4.45107200	-0.15562600
H	5.62153900	4.42845900	1.53691200	H	5.62552800	-4.40769400	-1.48005700
H	5.19583900	3.26649500	2.80594200	H	5.21608600	-3.23051500	-2.74018400
H	4.50507300	4.90519700	2.84012800	H	4.51796400	-4.86559000	-2.79779200
H	4.50535900	-4.90435200	-2.84076100	H	4.51792700	4.86544500	2.79793300
H	5.62166500	-4.42874400	-1.53700200	H	5.62541300	4.40801100	1.47997700
H	5.19668700	-3.26590900	-2.80547100	H	5.21632600	3.23049900	2.73990600
C	-0.88563800	2.20765900	-3.15850700	C	-0.87603500	-2.10633400	3.20501000
C	0.21728200	2.54962600	-2.40589500	C	0.23199000	-2.47415600	2.45126300
H	-0.96078100	-2.52896400	4.20059300	H	-0.93309800	2.38024700	-4.26177000
H	1.02331800	-3.13857900	2.84897200	H	1.04559300	3.03650000	-2.91197400
H	-0.68698200	-1.17428400	-0.56695700	H	-0.72697400	1.23290000	0.57220400
H	1.02276800	3.13881700	-2.84904000	H	1.04560100	-3.03650900	2.91197300
H	-0.96130800	2.52893400	-4.20056200	H	-0.93308600	-2.38026200	4.26177600
H	-0.68703600	1.17420200	0.56694300	H	-0.72698000	-1.23290300	-0.57219400

Table S51. Coordinates of the optimized structure of **BN[6]** (atom / x,y,z coordinates [Å]).

S_0 of **BN[6]**				S_1 of **BN[6]**			
C	0.82398000	4.91399600	0.92677800	C	0.86620700	4.95635300	0.87636900
C	1.59324400	4.24149400	1.83535700	C	1.66623100	4.26928800	1.77869500
C	1.42097800	2.83611100	2.03044600	C	1.50466800	2.88145600	1.97945300
C	0.51824700	2.11524000	1.18658900	C	0.55209100	2.14961300	1.16256600
C	-0.52127600	2.11602600	-1.18669400	C	-0.55753900	2.14806700	-1.16532900
C	-1.42529500	2.83627600	-2.02972200	C	-1.51039900	2.87590800	-1.98508100
C	-1.60129700	4.24083200	-1.83201800	C	-1.67823600	4.26330200	-1.78403400
C	-0.83416800	4.91360400	-0.92184600	C	-0.88392000	4.95277300	-0.87938100
C	-0.00429800	4.20568700	0.00190000	C	-0.00749400	4.26212000	-0.00113400
C	-0.00251200	2.78223800	0.00060600	C	-0.00460600	2.80832000	-0.00156000
C	-0.04976800	0.83627300	-1.67088300	C	-0.11176500	0.86844500	-1.66743600
C	-0.67537100	0.21658300	-2.78104700	C	-0.80007400	0.22281700	-2.74966400
C	0.05014500	0.83345200	1.66864000	C	0.10977100	0.87037000	1.66632600
C	0.67843800	0.21280700	2.77672500	C	0.80098600	0.22726700	2.74822800
C	0.19313700	-1.05369200	3.26244200	C	0.36344300	-1.05066500	3.21695800
C	-0.91134100	-1.67272600	2.74601600	C	-0.74427100	-1.69849200	2.71590600
B	-1.68268200	-0.98362900	1.61734700	B	-1.57571300	-1.00038400	1.64426800
N	-1.07232700	0.22600200	1.14481100	N	-1.01381000	0.25374900	1.18760600
N	1.07338400	0.23015000	-1.14705600	N	1.01304200	0.25619600	-1.18753700
B	1.68681700	-0.97728700	-1.62108100	B	1.57913800	-0.99699000	-1.64166200
C	0.91886800	-1.66522600	-2.75276400	C	0.75005400	-1.69878000	-2.71337400
C	-0.18626500	-1.04747400	-3.26929500	C	-0.35853800	-1.05480400	-3.21643100
C	-2.06696700	2.18055500	-3.11894700	C	-2.20596800	2.19622100	-3.02167200
C	-1.73199500	0.89361000	-3.45180200	C	-1.88891700	0.89971500	-3.36723300
C	2.06514100	2.17973400	3.11781500	C	2.20432400	2.20388200	3.01501400
C	1.73390600	0.89113400	3.44802200	C	1.88989100	0.90751000	3.36257300
C	-3.07316300	-1.43961700	1.01497600	C	-2.97283300	-1.46100500	1.07121200
C	3.07676800	-1.43215900	-1.01675500	C	2.97729200	-1.45279000	-1.06822700
C	-3.18902300	-2.60192300	0.21606300	C	-3.11619900	-2.67148600	0.34410300
C	-4.44070400	-2.98887100	-0.28476600	C	-4.37467000	-3.05898900	-0.13627800
C	-5.60235200	-2.26078200	-0.01071900	C	-5.52050100	-2.29037000	0.08953400
C	-5.48405500	-1.11841500	0.79088500	C	-5.37756400	-1.10150900	0.81802600
C	-4.24956400	-0.69917100	1.30107500	C	-4.13640400	-0.67612400	1.30284400
C	4.24926300	-0.68728800	-1.29175600	C	4.13510900	-0.66241900	-1.29264200
C	5.48614200	-1.10897900	-0.78054500	C	5.38100500	-1.08833500	-0.81146800
C	5.60512700	-2.25580500	0.00921400	C	5.52896800	-2.28059300	-0.09557600
C	4.44249000	-2.99220700	0.27231700	C	4.38413400	-3.05840900	0.12308100
C	3.19405700	-2.60440400	-0.22696800	C	3.12650600	-2.67185800	-0.35070400
C	-4.20331300	0.53902100	2.17512200	C	-4.07559100	0.61270300	2.09946600
C	6.93858700	-2.69440600	0.56628800	C	6.87358600	-2.72419000	0.42725800

C	4.20584400	0.55901200	-2.15460900	C	4.07269000	0.63353700	-2.07766500
C	-1.97234100	-3.43558400	-0.12358400	C	-1.92067500	-3.54575700	0.03867000
C	-6.94730900	-2.69124900	-0.54636900	C	-6.87489000	-2.72820100	-0.41272800
C	1.97740400	-3.44368400	0.09833000	C	1.93321800	-3.55223700	-0.05429800
H	0.85780100	6.00436400	0.86499600	H	0.91878000	6.04480700	0.80646100
H	2.28148800	4.77861100	2.49187500	H	2.38381300	4.80936300	2.40096700
H	-2.29057000	4.77741600	-2.48789400	H	-2.39669000	4.80066500	-2.40766200
H	-0.87076200	6.00376800	-0.85808800	H	-0.94208700	6.04090200	-0.80833800
H	-1.23179100	-2.61807500	3.19393300	H	-1.02063200	-2.66128300	3.15462000
H	-1.51764600	0.73111500	0.38511300	H	-1.49064500	0.76073700	0.44641400
H	1.51663200	0.73438200	-0.38560300	H	1.48687600	0.76494000	-0.44550800
H	1.24216200	-2.60860600	-3.20277200	H	1.02939200	-2.66129600	-3.15077900
H	-0.73723300	-1.48283600	-4.11150000	H	-0.94704000	-1.49888800	-4.02778700
H	-2.80439900	2.73508300	-3.70312800	H	-2.98457100	2.73560800	-3.56668300
H	-2.22276600	0.39122800	-4.28880700	H	-2.42869400	0.39388900	-4.17070400
H	2.80155400	2.73493100	3.70264400	H	2.98306300	2.74520200	3.55791600
H	2.22673000	0.38820800	4.28349500	H	2.43226800	0.40363300	4.16558700
H	-4.50851400	-3.88755600	-0.90550300	H	-4.46135500	-3.99058900	-0.70351300
H	-6.38148900	-0.53901100	1.03047000	H	-6.26342100	-0.49124400	1.02044900
H	6.38274800	-0.52589200	-1.01258200	H	6.26431900	-0.47372300	-1.00980800
H	4.51108100	-3.89849800	0.88246400	H	4.47544400	-3.99698400	0.67866300
H	-5.21655400	0.86306100	2.45623300	H	-5.08443100	0.94472900	2.38694000
H	-3.71722100	1.38831700	1.66587400	H	-3.61540000	1.43497400	1.52564200
H	-3.63603400	0.36231000	3.10339300	H	-3.48244700	0.49810400	3.02052400
H	7.76369100	-2.08504000	0.16800300	H	7.67986700	-2.05485300	0.09219900
H	7.14882300	-3.74948700	0.32383600	H	7.11807900	-3.74556000	0.09043500
H	6.96069300	-2.60837800	1.66664400	H	6.88751500	-2.73998900	1.53088400
H	3.62861200	0.39653900	-3.07917300	H	3.46678400	0.53227800	-2.99174400
H	5.21948300	0.87632500	-2.44205900	H	5.08017100	0.96067600	-2.37547200
H	3.73326100	1.40840100	-1.63270000	H	3.62750200	1.45430000	-1.48970400
H	-1.44088600	-3.76931500	0.78247900	H	-1.35857400	-3.80547400	0.94930200
H	-1.24537700	-2.86616300	-0.72604200	H	-1.21188100	-3.03520700	-0.63501800
H	-2.25048500	-4.33218400	-0.69792000	H	-2.22792300	-4.48359200	-0.44831200
H	-6.86132000	-3.58227100	-1.18616900	H	-6.79794000	-3.60450500	-1.07350100
H	-7.41734800	-1.89141100	-1.14338200	H	-7.37556900	-1.92175500	-0.97405100
H	-7.64694700	-2.93226600	0.27231600	H	-7.54297700	-2.99789500	0.42377400
H	2.25297800	-4.33964200	0.67488600	H	2.24086600	-4.48517400	0.44169800
H	1.45717400	-3.77866200	-0.81380900	H	1.38331300	-3.82132400	-0.96975200
H	1.24162400	-2.87752700	0.69304500	H	1.21373000	-3.04192200	0.60788000
H	0.74639700	-1.48987200	4.10272400	H	0.95400700	-1.49220800	4.02824500

Table S52. Coordinates of the optimized structure of **CC[6]** (atom / x,y,z coordinates [Å]).

S_0 of **CC[6]**				S_1 of **CC[6]**			
C	-0.66269400	4.96933100	-1.06388500	C	-0.71395700	4.98344700	-1.02174100
C	-1.27342000	4.28646000	-2.08029800	C	-1.34184900	4.28659200	-2.04451900
C	-1.06937700	2.88055500	-2.22719800	C	-1.12448400	2.89210400	-2.21048200
C	-0.30819200	2.16884500	-1.25905700	C	-0.30065500	2.18042600	-1.25171400
C	0.30507700	2.17894400	1.25106300	C	0.29902900	2.18687600	1.24676600
C	1.06586400	2.89839700	2.21384800	C	1.12322700	2.90283600	2.20204000
C	1.27278200	4.30254100	2.05443300	C	1.34279300	4.29603300	2.02837300
C	0.66429700	4.97747400	1.03144300	C	0.71628400	4.98805200	1.00147400
C	0.00040200	4.26620400	-0.01321100	C	0.00078400	4.30034300	-0.00829700
C	-0.00069800	2.83777400	-0.00695400	C	-0.00020300	2.83610300	-0.00430700
C	-0.24531800	0.88891200	1.65824800	C	-0.24936700	0.90713900	1.66404000
C	0.24369900	0.26707100	2.85025400	C	0.29638300	0.25098200	2.82665200
C	0.23992100	0.87461200	-1.65535400	C	0.24604500	0.89780600	-1.66229400
C	-0.25405600	0.24116800	-2.83912900	C	-0.30173000	0.23562900	-2.82056500
C	0.30155800	-0.99799300	-3.24694500	C	0.23166800	-1.01693700	-3.21279700
C	1.37273100	-1.55759000	-2.57865800	C	1.32492500	-1.57133500	-2.56665200
C	1.94470200	-0.89564000	-1.46174700	C	1.94046300	-0.88976100	-1.48611200
C	1.35444900	0.27788400	-1.00780500	C	1.37554200	0.30789100	-1.04360900
C	-1.35758200	0.28585000	1.01261800	C	-1.37849700	0.31456000	1.04721900
C	-1.95045100	-0.88260900	1.47606300	C	-1.94462700	-0.88040800	1.49531500
C	-1.38465500	-1.53234400	2.60325000	C	-1.33152100	-1.55604000	2.58098700
C	-0.31564700	-0.96658700	3.26970600	C	-0.23889000	-0.99868700	3.22559600
C	1.56523300	2.22945300	3.37993100	C	1.66052200	2.20948300	3.31547600
C	1.21671700	0.94000100	3.65766500	C	1.30243500	0.90311500	3.59472900
C	-1.57251600	2.20111100	-3.38559200	C	-1.66359600	2.19318000	-3.31954000
C	-1.22784400	0.90796000	-3.65079500	C	-1.30765000	0.88468000	-3.59146700
C	3.20433500	-1.41804300	-0.83354300	C	3.20269600	-1.41466400	-0.87229700

C	-3.20513800	-1.41255400	0.84442800	C	-3.20476900	-1.40869900	0.88019300
C	3.16572300	-2.48569400	0.08791000	C	3.18209300	-2.55529200	-0.03953600
C	4.36563400	-2.95249800	0.64484300	C	4.38421400	-3.02327400	0.51075200
C	5.60347500	-2.39492100	0.31249700	C	5.60879300	-2.39893100	0.25755600
C	5.62073800	-1.34080300	-0.60977000	C	5.60915800	-1.27290700	-0.57552600
C	4.44760600	-0.84175000	-1.18758500	C	4.43369400	-0.76780900	-1.14254200
C	-4.44783200	-0.82431200	1.16719200	C	-4.43452600	-0.76173900	1.13939000
C	-5.61745100	-1.33206400	0.58229300	C	-5.60956800	-1.27228000	0.56854600
C	-5.59234300	-2.40422000	-0.31408400	C	-5.60472800	-2.40106200	-0.25564700
C	-4.35002800	-2.97604900	-0.61662200	C	-4.37626900	-3.02881400	-0.49807900
C	-3.15865300	-2.50304500	-0.05449800	C	-3.17985600	-2.55775800	0.05392300
C	4.53102700	0.29363800	-2.18341300	C	4.50792900	0.44272500	-2.04697100
C	-6.85848100	-2.93215800	-0.94603700	C	-6.87653600	-2.92877700	-0.87572600
C	-4.54340200	0.33282500	2.13671200	C	-4.51648300	0.45490200	2.03497900
C	1.85783700	-3.12754200	0.48697700	C	1.88957900	-3.26632500	0.28796500
C	6.88629600	-2.90200300	0.92765800	C	6.89557400	-2.91448500	0.85651100
C	-1.84687800	-3.15630800	-0.42088500	C	-1.88431900	-3.26937300	-0.25979300
H	-0.70415300	6.06023100	-1.01720200	H	-0.78529100	6.07254100	-0.97003200
H	-1.84932600	4.81537600	-2.84341500	H	-1.94796900	4.81542300	-2.78357800
H	1.84878500	4.83717100	2.81348800	H	1.94935900	4.82808700	2.76474500
H	0.70773900	6.06784100	0.97513300	H	0.78912600	6.07674500	0.94375100
H	2.22371200	2.78559600	4.05177500	H	2.35622000	2.73912500	3.97134300
H	1.60823500	0.43258800	4.54267700	H	1.72824400	0.38512100	4.45706400
H	-2.23121800	2.75193700	-4.06158500	H	-2.35900000	2.72007100	-3.97792800
H	-1.62294200	0.39235100	-4.52945100	H	-1.73488600	0.36231300	-4.45045000
H	4.32663300	-3.77888500	1.36070000	H	4.35743200	-3.90269000	1.16091600
H	6.57829900	-0.89265000	-0.89228900	H	6.55659000	-0.77204000	-0.79722300
H	-6.57667500	-0.87397900	0.84083500	H	-6.55829000	-0.77127900	0.78235600
H	-4.30431800	-3.81873200	-1.31337600	H	-4.34557000	-3.91374500	-1.14114300
H	5.57864100	0.53126500	-2.41989300	H	5.55375100	0.69130300	-2.28043000
H	4.05570500	1.21060000	-1.79822200	H	4.04885000	1.33128300	-1.58334500
H	4.01348000	0.04756200	-3.12451200	H	3.97375100	0.27479500	-2.99546300
H	-7.75278900	-2.45206400	-0.52151800	H	-7.76365100	-2.41134000	-0.48106700
H	-6.95723500	-4.02081300	-0.80067600	H	-7.00011600	-4.00770100	-0.68483700
H	-6.86734000	-2.75182600	-2.03491300	H	-6.87212900	-2.79524400	-1.97147100
H	-4.02950300	0.11151600	3.08583400	H	-3.97811100	0.29942100	2.98311600
H	-5.59378700	0.56906000	2.36216700	H	-5.56376800	0.69628200	2.26955400
H	-4.07252200	1.24430800	1.73330800	H	-4.06710600	1.34396800	1.56267200
H	1.35912200	-3.60464100	-0.37258900	H	1.43328400	-3.72313800	-0.60529000
H	1.14922800	-2.38755400	0.89026000	H	1.14204600	-2.57339600	0.70433700
H	2.01736500	-3.90044800	1.25335500	H	2.05900500	-4.06764400	1.02238600
H	6.71295900	-3.79650800	1.54436300	H	6.72621800	-3.81576300	1.46427300
H	7.35120600	-2.13619600	1.57231500	H	7.36873400	-2.15629800	1.50351400
H	7.62788400	-3.16270800	0.15423100	H	7.62901100	-3.16919800	0.07282800
H	-1.99846900	-3.95096000	-1.16636300	H	-2.04868300	-4.08010100	-0.98497200
H	-1.35696600	-3.60791400	0.45718500	H	-1.43006700	-3.71342700	0.64082700
H	-1.13428400	-2.42774800	-0.83793600	H	-1.13725800	-2.57923700	-0.68176400
H	-0.10373300	-1.48346100	-4.13860500	H	-0.20838500	-1.52366200	-4.07566100
H	1.81603400	-2.49111600	-2.93275600	H	1.74707000	-2.51594600	-2.91610900
H	1.80272200	0.78218200	-0.15355400	H	1.85070000	0.82745100	-0.21234900
H	-1.83070600	-2.46114400	2.96618700	H	-1.75487300	-2.49826100	2.93539900
H	0.08536500	-1.44262400	4.16835300	H	0.19942000	-1.50069000	4.09209200
H	-1.80183500	0.78068300	0.15088900	H	-1.85216400	0.82959000	0.21233100

Table S53. Coordinates of the optimized structure of **BN[5]-(CN)$_2$** (atom / x,y,z coordinates [Å]).

S_0 of **BN[5]-(CN)$_2$**				S_1 of **BN[5]-(CN)$_2$**			
C	-4.34298200	0.65764700	-1.25703700	C	4.38896100	-0.56496000	-1.28476300
C	-3.10150500	0.44210600	-0.58268300	C	3.12854800	-0.39849100	-0.60271800
C	-3.10145600	-0.44249100	0.58258300	C	3.10848300	0.49754200	0.56789800
C	-4.34289900	-0.65812900	1.25696400	C	4.36168800	0.71525600	1.25411400
C	-5.56746000	-0.26495000	0.62848800	C	5.57343200	0.36035100	0.63104500
C	-5.56749700	0.26439500	-0.62851900	C	5.58632600	-0.15861000	-0.65830700
C	-1.98211900	1.23646600	-1.02745400	C	2.04713200	-1.22275600	-1.02553600
C	-2.05155900	1.94838000	-2.25533400	C	2.11519200	-1.95801600	-2.25470400
C	-3.25505400	1.92902300	-3.01253300	C	3.31513800	-1.88165700	-3.02942900
C	-4.38458100	1.34739000	-2.50097600	C	4.42145500	-1.24400500	-2.54581200
C	-4.38442900	-1.34790100	2.50089000	C	4.36125600	1.39651300	2.51698500
C	-3.25485100	-1.92946200	3.01241500	C	3.23776400	2.00364200	2.99174100
C	-2.05136200	-1.94869900	2.25520300	C	2.03767200	2.04573300	2.20476200
C	-1.98198700	-1.23675200	1.02733400	C	2.00346000	1.28478200	0.98338900

N	-0.86048100	1.43435600	-0.24310900	N	0.91547800	-1.42474500	-0.23822400
B	0.24626700	2.30859300	-0.51905400	B	-0.16738800	-2.33240500	-0.50745300
C	-0.95964500	-2.77336100	2.67418200	C	0.96236600	2.86263000	2.58535000
C	0.16104300	-2.98713100	1.90325200	C	-0.18955500	3.04616100	1.79358200
B	0.24652600	-2.30861200	0.51897600	B	-0.23239000	2.29734700	0.48463500
N	-0.86031300	-1.43449600	0.24301300	N	0.86370500	1.44157800	0.18332700
C	1.34445100	2.54937400	0.58337600	C	-1.27800600	-2.55189600	0.60301200
C	1.34484000	-2.54917900	-0.58337900	C	-1.39645000	2.49664700	-0.59962500
C	2.69802000	2.18938600	0.36736000	C	-2.64429200	-2.26156000	0.36376200
C	3.64918300	2.42089000	1.37064200	C	-3.59912900	-2.47353000	1.37185000
C	3.31196000	3.02276300	2.58698400	C	-3.25191100	-2.98963800	2.62274800
C	1.97562500	3.38992400	2.78705400	C	-1.90420800	-3.29703200	2.84731000
C	0.99401700	3.16253400	1.81553700	C	-0.92280100	-3.08833000	1.87034400
C	0.99465700	-3.16250800	-1.81553100	C	-1.14215000	3.22507300	-1.79028200
C	1.97641000	-3.38975400	-2.78693300	C	-2.17464800	3.39891800	-2.70355900
C	3.31264800	-3.02229500	-2.58675500	C	-3.50244900	2.87471600	-2.48894400
C	3.64962600	-2.42027500	-1.37041900	C	-3.75891400	2.18221000	-1.31074200
C	2.69831200	-2.18891000	-0.36724700	C	-2.75447800	1.99287700	-0.35763100
C	3.15150500	1.56585200	-0.93523100	C	-3.12543100	-1.75191500	-0.97829200
C	-0.42618000	-3.60781900	-2.10832600	C	0.21821500	3.82114000	-2.06510200
C	3.15153100	-1.56521200	0.93535900	C	-3.06202000	1.30536400	0.92526200
C	-0.42695800	3.60746500	2.10824700	C	0.50659700	-3.47734800	2.19641100
C	4.35690400	3.29873600	3.64091800	C	-4.28683500	-3.22496700	3.69672700
C	4.35775100	-3.29811900	-3.64057000	C	-4.54696000	3.10535800	-3.52919600
H	-6.50577900	-0.47080200	1.14807100	H	6.51045500	0.56864700	1.15238100
H	-6.50584700	0.47020500	-1.14806200	H	6.53251000	-0.33179300	-1.17555400
H	-3.28191700	2.46051600	-3.96618400	H	3.35067200	-2.41420300	-3.98313100
H	-5.34059500	1.42931100	-3.02178700	H	5.36714700	-1.27819500	-3.09197700
H	-5.34042700	-1.42989200	3.02172000	H	5.30013200	1.45362000	3.07329700
H	-3.28165700	-2.46098000	3.96605300	H	3.24974100	2.53608100	3.94574200
H	-0.88083600	0.97845900	0.66322700	H	0.95879300	-0.98163500	0.67398700
H	-1.06798500	-3.28145800	3.63791200	H	1.05208500	3.39965600	3.53481300
C	1.15641400	-3.89490800	2.38982600	C	-1.23404700	3.91069800	2.21943800
H	-0.88066000	-0.97854700	-0.66329500	H	0.90213300	0.93207700	-0.69303100
H	4.68693500	2.12422100	1.19230200	H	-4.64867300	-2.24108300	1.16501200
H	1.68935800	3.87145200	3.72716600	H	-1.60805700	-3.72034200	3.81223900
H	1.69034500	-3.87141700	-3.72703900	H	-1.98899500	3.95579400	-3.62504500
H	4.68729800	-2.12338200	-1.19199400	H	-4.75828200	1.78971600	-1.12019300
H	2.45892400	0.78773600	-1.29179800	H	-2.42032700	-1.03826700	-1.43341400
H	4.14102900	1.09833600	-0.82681500	H	-4.10684200	-1.26049700	-0.88708400
H	3.23290000	2.32676300	-1.72868200	H	-3.23711900	-2.58225600	-1.69437700
H	-1.08929700	-2.76057600	-2.35597600	H	0.97494500	3.03927000	-2.22336000
H	-0.88079400	-4.12969100	-1.25111900	H	0.55729100	4.42508800	-1.21054800
H	-0.45129600	-4.29467300	-2.96722200	H	0.19783800	4.46164300	-2.95771000
H	4.14096000	-1.09747600	0.82701900	H	-4.06151600	0.85453900	0.91959800
H	3.23301800	-2.32606400	1.72885800	H	-3.00894200	2.04191100	1.74734900
H	2.45873500	-0.78723600	1.29181800	H	-2.31649000	0.52769900	1.15399200
H	-0.45231300	4.29427600	2.96716900	H	0.53856500	-4.15467600	3.06284600
H	-1.08987300	2.76003800	2.35581600	H	1.13070800	-2.60295400	2.44886100
H	-0.88164500	4.12925200	1.25102800	H	0.99612600	-3.98599800	1.35186900
H	4.68440000	4.35283800	3.60627500	H	-4.32308400	-4.28787200	3.98956700
H	5.25024500	2.67220100	3.49867600	H	-5.29356200	-2.93582800	3.35972300
H	3.96694600	3.11459200	4.65461700	H	-4.05744700	-2.64912400	4.60943700
H	4.68541500	-4.35216600	-3.60587500	H	-4.67488000	4.18707700	-3.71084400
H	5.25097400	-2.67143400	-3.49824500	H	-5.51612800	2.67424800	-3.24934600
H	3.96787100	-3.11405500	-4.65431400	H	-4.22781800	2.66934200	-4.49249700
C	-0.95991300	2.77313600	-2.67432100	C	1.05627500	-2.80693900	-2.64620100
C	0.16072600	2.98707200	-1.90336400	C	-0.07804000	-3.03525600	-1.86371600
C	1.15596200	3.89499800	-2.38992700	C	-1.05716800	-3.95766500	-2.33680200
H	-1.06832100	3.28125300	-3.63803200	H	1.17150700	-3.33544500	-3.59853700
N	1.97174600	-4.63029000	2.78212000	N	-2.13908900	4.58896800	2.52152600
N	1.97119800	4.63048800	-2.78221700	N	-1.87815100	-4.69539700	-2.72179900

7.2. Transition States and Racemization Barrier

The structures of the transition states that occur during racemization were calculated with Q-Chem (jobtype: ts). The presence of a transition state was verified in all cases by a single imaginary frequency in the vibration spectrum. All

transition states showed largely-distorted, non-planar structures with C_s-symmetry and almost parallelly aligned mesityl-substituents. The overall impact of the BN-units was negligible (Fig. S30).

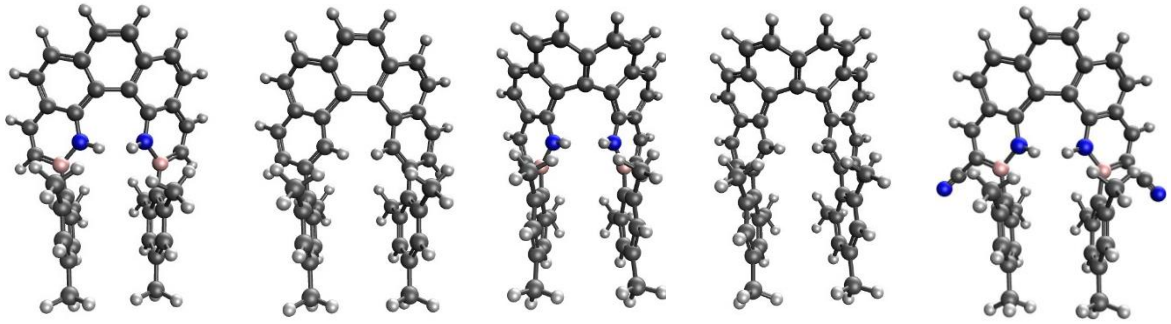

Fig. S30. Structures of the transition states of **BN[5]**, **CC[5]**, **BN[6]**, **CC[6]** and **BN[5]-(CN)$_2$**.

As the racemization barriers were determined experimentally by ECD in hydrocarbon solvent, we also performed the calculation of the transition states in consideration of the conductor-like polarizable continuum model (CPCM) with *n*-hexane as solvent (dielectric constant: 1.89). Comparing the energies of the optimized structures in S_0 with those of the transition states then allowed a calculation of the Gibbs' free activation energies of enantiomerization ($\Delta G^{\ddagger}(T)$) in solution. Table S54 shows that the BN-helicenes should racemize significantly more slowly than the carbohelicenes. Although the energy difference was calculated too high, this was in qualitative agreement with the experimental results ($\Delta G^{\ddagger}$(25 °C) = 25.7 kcal mol^{-1} for **BN[5]** and 24.3 kcal mol^{-1} for **CC[5]**). Moreover, the slightly decreased configurational stability upon the installment of two cyano-moieties ($\Delta G^{\ddagger}$(25 °C) = 25.0 kcal mol^{-1} for **BN[5]-(CN)$_2$**) was also mirrored by the calculations.

The elevating effect of BN-substitution on the racemization barriers was also found in the hexahelicenes, which indicates that *N-H* interactions play an important role with respect to the racemization rates.

Table S54. Calculated Gibbs' free energies of activation ($\Delta G^{\ddagger}$(T)) for the racemizations, using CPCM with *n*-hexane as solvent.

Compound	**BN[5]**	**CC[5]**	**BN[6]**	**CC[6]**	**BN[5]-(CN)$_2$**
ΔG [kcal mol^{-1}]	28.3	24.2	50.2	46.3	27.7

7.3. Nucleus-Independent Chemical Shifts (NICS)

NICS(0) values (in-plane nucleus-independent chemical shifts) were calculated with Q-Chem (jobtype: nmr) at the MP2[29] / cc-pVDZ level of theory, using the optimized structures from the respective S_0-calculations as inputs.

7.4. Natural Transition Orbitals (NTOs)

Natural transition orbitals (NTOs)[30] were calculated with Q-Chem (jobtype: sp, 40 roots). Fig. S31 shows visualizations (iso value: 0.025) of the NTOs that contribute most to the S_1 states, out of which fluorescence occurs. Also shown are the excitation energies and the respective oscillator strengths *f*. All transitions were symmetry-allowed due to a symmetry change upon excitation (C_2 → C_s or vice versa), except for HONTO → LUNTO and HONTO–1 → LUNTO+1 of **CC[5]**. Note that for **BN[5]-(CN)$_2$**, the S_2 state was calculated at a very similar wavelength (414 nm) to the S_1 state with a much higher oscillator strength of *f* = 0.0996 and 98.3% contribution of the HONTO (149) → LUNTO (150) transition. Therefore, this state is most likely responsible for the lowest-energy absorption and fluorescence characteristics.

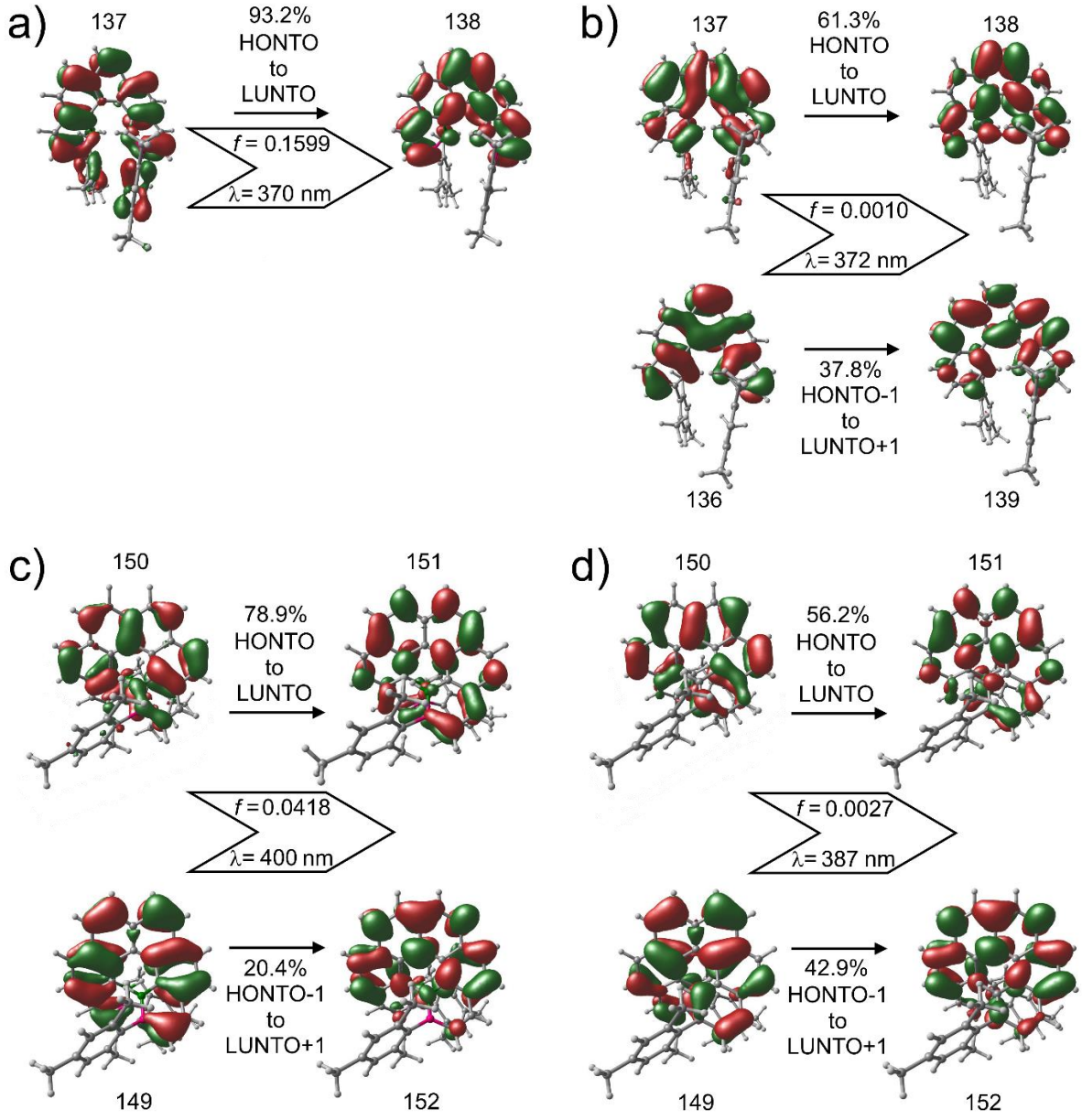

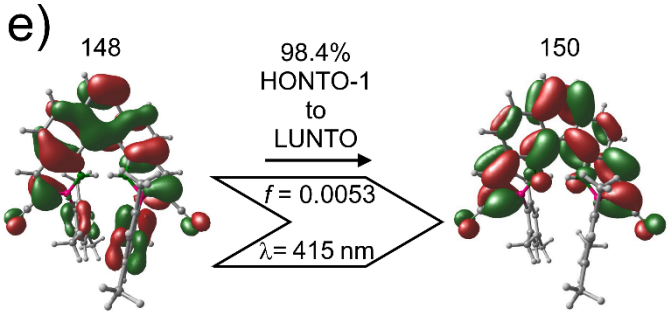

Fig. S31. NTO visualizations for **BN[5]** (a), **CC[5]** (b), **BN[6]** (c), **CC[6]** (d) and **BN[5]-(CN)$_2$** (e).

7.5. Electronic Circular Dichroism (ECD)

ECD spectra of the helicenes in *(M)*-configuration were calculated with Gaussian 09 (jobtype: td). Table S55 lists all wavelengths and rotatory strengths of the 50 lowest-energy states. Fig. S32 compares calculated and measured ECD spectra (second eluted enantiomer from (CSP)-HPLC). In all cases, negative CE was found at the highest wavelengths both in theory and in experiment. Therefore, the absolute configuration of the initially eluted helicenes was always (*P*), while it was (*M*) for the second fractions.

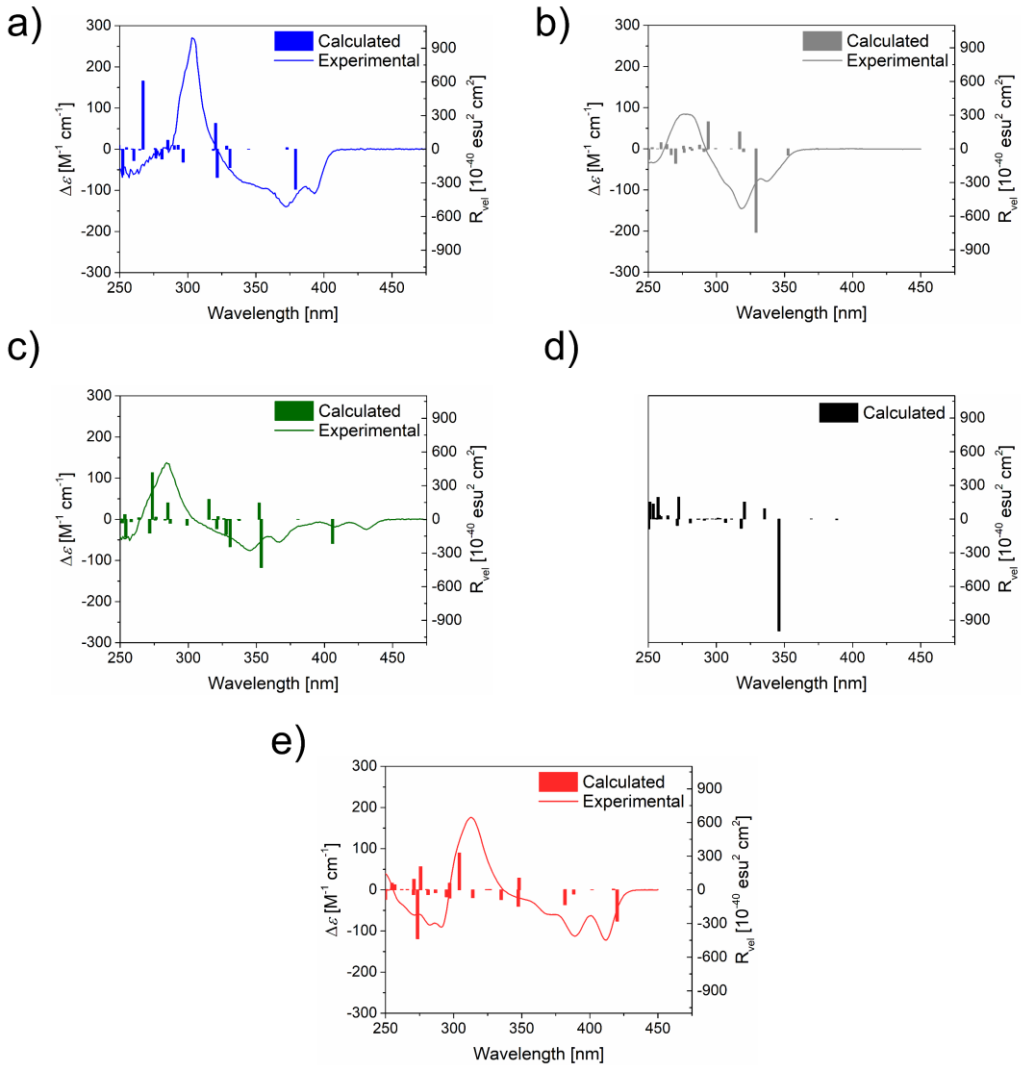

Fig. S32. Calculated Cotton bands of **BN[5]** (a), **CC[5]** (b), **BN[6]** (c), **CC[6]** (d) and **BN[5]-(CN)$_2$** (e) in (*M*)-configuration and experimentally obtained ECD spectra of the second eluted fractions from (CSP)-HPLC.

Table S55. Calculated rotatory strengths for the 50 lowest-energy states.

State	BN[5]		BN[6]		CC[5]		CC[6]		BN[5]-$(CN)_2$	
	λ [nm]	R_{vel} [10^{-40} $esu^2\,cm^2$]	λ [nm]	R_{vel} [10^{-40} $esu^2\,cm^2$]	λ [nm]	R_{vel} [10^{-40} $esu^2\,cm^2$]	λ [nm]	R_{vel} [10^{-40} $esu^2\,cm^2$]	λ [nm]	R_{vel} [10^{-40} $esu^2\,cm^2$]
1	379.24	-356	405.98	-216	373.87	3	388.35	-6	420.17	-279
2	372.96	14	380.50	1	352.57	-58	369.67	2	417.34	6
3	344.68	1	353.56	-430	329.15	-746	345.92	-997	401.69	1
4	331.01	-164	352.01	145	319.96	-26	335.36	93	388.25	-38
5	328.61	27	337.37	-10	317.08	152	320.59	151	381.87	2
6	321.69	-253	336.83	1	310.86	1	318.28	-82	381.75	-133
7	320.45	230	330.67	-244	299.44	5	311.19	1	348.02	105
8	318.80	-10	328.41	-6	293.99	241	311.14	-1	347.52	-149
9	296.62	-115	327.77	-134	293.01	-6	306.82	-30	334.92	-87
10	292.92	36	326.10	7	290.89	-24	302.73	3	326.73	5
11	290.19	32	321.85	25	290.17	1	301.26	7	324.20	2
12	286.53	-2	320.85	-85	287.68	33	300.63	0	314.13	-71
13	285.33	79	319.27	1	282.16	-15	299.54	-1	304.19	330
14	281.08	-87	318.32	-4	280.77	15	297.06	2	297.21	-75
15	276.67	-79	315.08	178	276.41	-31	293.22	2	297.06	60
16	276.05	9	299.16	-52	275.89	23	291.19	-12	294.75	-63
17	267.25	607	286.82	-37	270.06	-131	287.25	-2	286.68	-27
18	264.78	-6	285.06	148	266.77	-54	286.48	-3	281.20	-44
19	260.47	-101	283.01	-7	263.49	38	280.91	-35	280.39	4
20	259.29	2	276.22	20	259.38	54	272.36	195	279.10	0
21	255.06	14	275.78	-8	256.80	-1	271.34	-58	275.72	206
22	255.02	2	273.62	417	252.85	11	264.52	4	273.60	-436
23	252.31	-228	271.60	-124	250.28	-96	264.36	28	270.91	95
24	251.77	-4	263.75	15	247.31	118	259.34	21	270.53	-44
25	249.53	33	258.08	-23	246.45	-44	258.26	32	266.08	4
26	247.23	-4	254.07	-162	244.49	20	257.18	194	261.85	3
27	244.92	-66	253.46	43	241.70	-24	256.41	-2	256.80	46
28	244.23	-37	251.51	-33	241.40	-90	255.93	8	254.70	61
29	243.90	-2	250.71	3	239.94	-146	253.75	134	254.60	15
30	241.23	-1	250.60	-13	239.75	47	251.22	150	252.49	-2
31	237.83	-3	248.50	12	236.41	1	250.32	-89	251.80	-4
32	236.54	-8	248.16	-8	234.22	68	249.26	4	250.37	3
33	235.86	16	246.63	120	234.04	-20	247.74	6	249.89	-86
34	232.11	-102	243.31	1	232.35	42	244.94	77	246.80	-101
35	230.06	-5	240.51	37	231.79	-20	244.42	-64	246.79	8
36	229.48	14	238.76	41	230.32	-6	242.82	133	243.86	10
37	228.48	1	237.94	42	229.61	6	241.07	-4	239.88	21
38	227.05	43	236.84	19	228.81	121	240.51	-27	235.89	14
39	227.00	-54	236.72	1	227.36	-10	240.13	11	235.72	-7
40	226.48	47	236.31	35	224.90	116	239.67	-22	233.76	32
41	225.07	-1	235.74	47	224.84	78	237.91	-4	232.40	1
42	224.65	-48	232.58	-19	224.14	76	234.64	32	232.38	7
43	223.58	29	231.59	-49	223.08	17	234.35	-24	231.44	-3
44	223.19	-3	231.06	-17	221.27	82	233.09	-18	231.11	39
45	221.12	-5	227.39	-3	220.52	35	231.80	-31	231.02	-18
46	220.71	80	226.72	-22	219.98	-13	230.71	-82	229.55	15
47	220.24	-6	226.14	41	219.34	-26	230.12	-7	227.45	204
48	219.19	-3	226.03	-19	219.24	82	229.07	-99	225.86	-18
49	217.93	0	225.78	13	218.76	118	228.02	48	224.33	20
50	216.96	-26	225.68	11	217.21	-36	226.02	-3	221.87	2

7.6. Absorption and Luminescence Dissymmetry Factors

The dissymmetry factors g_{abs} and g_{lum} can be calculated using the theoretically obtained transition dipole moments, according to the simplified equation which is valid for most small organic molecules:

$$g_{abs\,/\,lum} \approx 4 \times |m| \times \cos(\theta) / |\mu|.$$

Here, |μ| and |m| are the electric and magnetic transition dipole moments for a particular transition, while θ is the angle between both. Table S56 shows the calculated transition dipole moments, angles and dissymmetry factors for the lowest-energy excitation and emission.

Table S56. Calculated transition dipole moments, angles and dissymmetry factors for the $S_0 \rightarrow S_1$ and $S_1 \rightarrow S_0$ transitions.

	$S_0 \rightarrow S_1$ transition				$S_1 \rightarrow S_0$ transition				
	|μ| [10^{-20} esu cm]	|m| [10^{-20} erg G^{-1}]	|θ| [°]	$\lvert g_{abs}\rvert$	|μ| [10^{-20} esu cm]	|m| [10^{-20} erg G^{-1}]	|θ| [°]	$\lvert g_{lum}\rvert$	$\frac{\lvert g_{lum}\rvert}{\lvert g_{abs}\rvert}$
BN[5]	334	2.61	114	0.0130	405	2.75	112	0.0103	0.79
CC[5]	32.6	0.08	0	0.0095	51.0	0.11	0	0.0085	0.89
BN[6]	195	1.59	134	0.0224	213	1.73	135	0.0229	1.02
CC[6]	51.7	0.37	106	0.0078	36.9	0.25	102	0.0058	0.74
BN[5]-$(CN)_2$	323	2.12	114	0.0107	77.2	0.44	111	0.0081	0.76

7.7. Validation of Dissymmetry Factors

Several recent studies that report the chiroptical properties of helicenes have made use of the long-range corrected hybrid functional CAM-B3LYP.[31-34] This method proved particularly useful for the accurate reproduction of the experimental dissymmetry factors g_{abs} and g_{lum}.

We were interested whether the unusually high experimental g_{lum} value of **BN[6]** was reproducible by using the same theoretical approach. The required calculations were performed by Prof. A. J. Mota from the Department of Inorganic Chemistry from the University of Granada. Using Gaussian 16, Rev. C.02,[35] the S_0 geometry of **BN[6]** was optimized at the B3LYP[26]-D3BJ[36] / 6-311+G(d,p) level of theory, including a Polarizable Continuum Model with DCM. Starting from this input geometry, the vertical transition was calculated with TD-DFT at the CAM-B3LYP[37]-D3BJ / 6-311+G(d,p) level of theory, which allowed to calculate the theoretical g_{abs} value. The same level of theory was applied to compute the optimized geometry in S_1 and the $S_1 \rightarrow S_0$ transition, also enabling the calculation of the theoretical g_{lum} value (Table **S57**).

Table S57. Calculated transition dipole moments, angles and dissymmetry factors for the $S_0 \rightarrow S_1$ and $S_1 \rightarrow S_0$ transitions of **BN[6]**. Levels of theory: a) B3LYP / cc-pVDZ, gas phase; b) CAM-B3LYP-D3BJ / 6-311+G(d,p), PCM with DCM.

	$S_0 \rightarrow S_1$ transition					$S_1 \rightarrow S_0$ transition				
	λ	|μ| [10^{-20} esu cm]	|m| [10^{-20} erg G^{-1}]	|θ| [°]	$\lvert g_{abs}\rvert$	λ	|μ| [10^{-20} esu cm]	|m| [10^{-20} erg G^{-1}]	|θ| [°]	$\lvert g_{lum}\rvert$
a)	406	195	1.59	134	0.0224	438	213	1.73	135	0.0229
b)	354	231	2.11	126	0.0213	392	311	2.38	121	0.0156

While the CAM-B3LYP method expectedly gave an overestimated excitation energy,[38] the $|g_{abs}|$ value was similar to the results obtained with B3LYP. With respect to the $S_1 \rightarrow S_0$ transition, CAM-B3LYP yields a reduced $|g_{lum}|$ value for two reasons: Firstly, the electric term |μ| undergoes a higher percentage-wise increase for $S_1 \rightarrow S_0$ than for $S_0 \rightarrow S_1$. Secondly, the angle θ for the $S_1 \rightarrow S_0$ transition is smaller than for the excitation. However, the theoretical $|g_{lum}|$ value (15.6×10^{-3}) agrees very well with the experimental value ($|g_{lum}| = 13.3 \times 10^{-3}$), as the deviation between experiment and calculation is only 17%. This confirms both the high quality of this theoretical approach and the accuracy of our experimental results.

8. References

1. O. V. Dolomanov, L. J. Bourhis, R. J. Gildea, J. A. K. Howard and H. Puschmann, OLEX2: A Complete Structure Solution, Refinement and Analysis Program, *J. Appl. Cryst.*, 2009, **42**, 339-341.
2. G. M. Sheldrick, SHELXT - Integrated Space-Group and Crystal-Structure Determination, *Acta Cryst.*, 2015, **A71**, 3-8.
3. G. M. Sheldrick, Crystal Structure Refinement with SHELXL, *Acta Cryst.*, 2008, **A64**, 112-122.
4. A. W. Baggett, M. Vasiliu, B. Li, D. A. Dixon and S.-Y. Liu, Late-Stage Functionalization of 1,2-Dihydro-1,2-azaborines via Regioselective Iridium-Catalyzed C–H Borylation: The Development of a New N,N-Bidentate Ligand Scaffold, *J. Am. Chem. Soc.*, 2015, **137**, 5536-5541.
5. Apparent singlet. Due to the broadening of the N-H resonance, the ^{3}J and ^{4}J couplings to C-H are not visible.
6. Y. Appiarius, T. Stauch, E. Lork, P. Rusch, N. C. Bigall and A. Staubitz, From a 1,2-Azaborinine to Large BN-PAHs via Electrophilic Cyclization: Synthesis, Characterization and Promising Optical Properties, *Org. Chem. Front.*, 2021, **8**, 10-17.
7. B. Wrackmeyer, Carbon-13 NMR spectroscopy of boron compounds, *Prog. Nucl. Magn. Reson. Spectrosc.*, 1979, **12**, 227-259.
8. B. Wrackmeyer, Organoboranes and tetraorganoborates studied by 11B and 13C NMR spectroscopy and DFT calculations, *Z. Naturforsch. B*, 2015, **70**, 421-424.
9. The ^{11}B nucleus (I = 3/2) has a quadrupolar moment and is located in an unsymmetrical environment. Therefore, a rapid ^{11}B spin relaxation occurs. This leads to extremely broadened ^{13}C resonances with low intensities, impeding their observation.
10. M. Di Giovannantonio, O. Deniz, J. I. Urgel, R. Widmer, T. Dienel, S. Stolz, C. Sánchez-Sánchez, M. Muntwiler, T. Dumslaff, R. Berger, A. Narita, X. Feng, K. Müllen, P. Ruffieux and R. Fasel, On-Surface Growth Dynamics of Graphene Nanoribbons: The Role of Halogen Functionalization, *ACS Nano*, 2018, **12**, 74-81.
11. S. Luliński and J. Serwatowski, Regiospecific Metalation of Oligobromobenzenes, *J. Org. Chem.*, 2003, **68**, 5384-5387.
12. V. Diemer, F. R. Leroux and F. Colobert, Efficient and Complementary Methods Offering Access to Synthetically Valuable 1,2-Dibromobenzenes, *Eur. J. Org. Chem.*, 2011, **2011**, 327-340.
13. L. D. M. Nicholls, M. Marx, T. Hartung, E. González-Fernández, C. Golz and M. Alcarazo, TADDOL-Derived Cationic Phosphonites: Toward an Effective Enantioselective Synthesis of [6]Helicenes via Au-Catalyzed Alkyne Hydroarylation, *ACS Catal.*, 2018, **8**, 6079-6085.
14. S. Jhulki, A. K. Mishra, T. J. Chow and J. N. Moorthy, Helicenes as All-in-One Organic Materials for Application in OLEDs: Synthesis and Diverse Applications of Carbo- and Aza[5]helical Diamines, *Chem. Eur. J.*, 2016, **22**, 9375-9386.
15. C. Schaack, E. Sidler, N. Trapp and F. Diederich, Helical Threads: Enantiomerically Pure Carbo[6]Helicene Oligomers, *Chem. Eur. J.*, 2017, **23**, 14153-14157.
16. W. Baker, F. Glockling and J. F. W. McOmie, 243. Eight- and higher-membered ring compounds. Part V. Di-(naphthalene-2 : 7-dimethylene) and its conversion into coronene, *J. Chem. Soc.*, 1951, 1118-1121.
17. T. R. Schulte, J. J. Holstein and G. H. Clever, Chiral Self-Discrimination and Guest Recognition in Helicene-Based Coordination Cages, *Angew. Chem. Int. Ed.*, 2019, **58**, 5562-5566.
18. K. Mori, T. Murase and M. Fujita, One-Step Synthesis of [16]Helicene, *Angew. Chem. Int. Ed.*, 2015, **54**, 6847-6851.
19. D. Göbel, S. Míguez-Lago, M. J. Ruedas-Rama, A. Orte, A. G. Campaña and M. Juríček, Circularly Polarized Luminescence of [6]Helicenes through Excited-State Intramolecular Proton Transfer, *Helv. Chim. Acta*, 2022, **105**, e202100221.
20. E. Epifanovsky, A. T. B. Gilbert, X. Feng, J. Lee, Y. Mao, N. Mardirossian, P. Pokhilko, A. F. White, M. P. Coons, A. L. Dempwolff, Z. Gan, D. Hait, P. R. Horn, L. D. Jacobson, I. Kaliman, J. Kussmann, A. W. Lange, K. U. Lao, D. S. Levine, J. Liu, S. C. McKenzie, A. F. Morrison, K. D. Nanda, F. Plasser, D. R. Rehn, M. L. Vidal, Z.-Q. You, Y. Zhu, B. Alam, B. J. Albrecht, A. Aldossary, E. Alguire, J. H. Andersen, V. Athavale, D. Barton, K. Begam, A. Behn, N. Bellonzi, Y. A. Bernard, E. J. Berquist, H. G. A. Burton, A. Carreras, K. Carter-Fenk, R. Chakraborty, A. D. Chien, K. D. Closser, V. Cofer-Shabica, S. Dasgupta, M. de Wergifosse, J. Deng, M. Diedenhofen, H. Do, S. Ehlert, P.-T. Fang, S. Fatehi, Q. Feng, T. Friedhoff, J. Gayvert, Q. Ge, G. Gidofalvi, M. Goldey, J. Gomes, C. E. González-Espinoza, S. Gulania, A. O. Gunina, M. W. D. Hanson-Heine, P. H. P. Harbach, A. Hauser, M. F. Herbst, M. Hernández Vera, M. Hodecker, Z.

C. Holden, S. Houck, X. Huang, K. Hui, B. C. Huynh, M. Ivanov, Á. Jász, H. Ji, H. Jiang, B. Kaduk, S. Kähler, K. Khistyaev, J. Kim, G. Kis, P. Klunzinger, Z. Koczor-Benda, J. H. Koh, D. Kosenkov, L. Koulias, T. Kowalczyk, C. M. Krauter, K. Kue, A. Kunitsa, T. Kus, I. Ladjánszki, A. Landau, K. V. Lawler, D. Lefrancois, S. Lehtola, R. R. Li, Y.-P. Li, J. Liang, M. Liebenthal, H.-H. Lin, Y.-S. Lin, F. Liu, K.-Y. Liu, M. Loipersberger, A. Luenser, A. Manjanath, P. Manohar, E. Mansoor, S. F. Manzer, S.-P. Mao, A. V. Marenich, T. Markovich, S. Mason, S. A. Maurer, P. F. McLaughlin, M. F. S. J. Menger, J.-M. Mewes, S. A. Mewes, P. Morgante, J. W. Mullinax, K. J. Oosterbaan, G. Paran, A. C. Paul, S. K. Paul, F. Pavošević, Z. Pei, S. Prager, E. I. Proynov, Á. Rák, E. Ramos-Cordoba, B. Rana, A. E. Rask, A. Rettig, R. M. Richard, F. Rob, E. Rossomme, T. Scheele, M. Scheurer, M. Schneider, N. Sergueev, S. M. Sharada, W. Skomorowski, D. W. Small, C. J. Stein, Y.-C. Su, E. J. Sundstrom, Z. Tao, J. Thirman, G. J. Tornai, T. Tsuchimochi, N. M. Tubman, S. P. Veccham, O. Vydrov, J. Wenzel, J. Witte, A. Yamada, K. Yao, S. Yeganeh, S. R. Yost, A. Zech, I. Y. Zhang, X. Zhang, Y. Zhang, D. Zuev, A. Aspuru-Guzik, A. T. Bell, N. A. Besley, K. B. Bravaya, B. R. Brooks, D. Casanova, J.-D. Chai, S. Coriani, C. J. Cramer, G. Cserey, A. E. DePrince, III, R. A. DiStasio, Jr., A. Dreuw, B. D. Dunietz, T. R. Furlani, W. A. Goddard, III, S. Hammes-Schiffer, T. Head-Gordon, W. J. Hehre, C.-P. Hsu, T.-C. Jagau, Y. Jung, A. Klamt, J. Kong, D. S. Lambrecht, W. Liang, N. J. Mayhall, C. W. McCurdy, J. B. Neaton, C. Ochsenfeld, J. A. Parkhill, R. Peverati, V. A. Rassolov, Y. Shao, L. V. Slipchenko, T. Stauch, R. P. Steele, J. E. Subotnik, A. J. W. Thom, A. Tkatchenko, D. G. Truhlar, T. Van Voorhis, T. A. Wesolowski, K. B. Whaley, H. L. Woodcock, III, P. M. Zimmerman, S. Faraji, P. M. W. Gill, M. Head-Gordon, J. M. Herbert and A. I. Krylov, Software for the frontiers of quantum chemistry: An overview of developments in the Q-Chem 5 package, *J. Chem. Phys.*, 2021, **155**.

21. M. J. Frisch, G. W. Trucks, H. B. Schlegel, G. E. Scuseria, M. A. Robb, J. R. Cheeseman, G. Scalmani, V. Barone, B. Mennucci, G. A. Petersson, H. Nakatsuji, M. Caricato, X. Li, H. P. Hratchian, A. F. Izmaylov, J. Bloino, G. Zheng, J. L. Sonnenberg, M. Hada, M. Ehara, K. Toyota, R. Fukuda, J. Hasegawa, M. Ishida, T. Nakajima, Y. Honda, O. Kitao, H. Nakai, T. Vreven, J. A. Montgomery, J. E. Peralta, F. Ogliaro, M. Bearpark, J. J. Heyd, E. Brothers, K. N. Kudin, V. N. Staroverov, R. Kobayashi, J. Normand, K. Raghavachari, A. Rendell, J. C. Burant, S. S. Iyengar, J. Tomasi, M. Cossi, N. Rega, J. M. Millam, M. Klene, J. E. Knox, J. B. Cross, V. Bakken, C. Adamo, J. Jaramillo, R. Gomperts, R. E. Stratmann, O. Yazyev, A. J. Austin, R. Cammi, C. Pomelli, J. W. Ochterski, R. L. Martin, K. Morokuma, V. G. Zakrzewski, G. A. Voth, P. Salvador, J. J. Dannenberg, S. Dapprich, A. D. Daniels, Ö. Farkas, J. B. Foresman, J. V. Ortiz, J. Cioslowski and D. J. Fox, Gaussian 09, Rev. B.01, Wallingford CT, 2010.

22. A. K. Rappe, C. J. Casewit, K. S. Colwell, W. A. Goddard and W. M. Skiff, UFF, A Full Periodic Table Force Field for Molecular Mechanics and Molecular Dynamics Simulations, *J. Am. Chem. Soc.*, 1992, **114**, 10024-10035.

23. P. Hohenberg and W. Kohn, Inhomogeneous Electron Gas, *Phys. Rev. B*, 1964, **136**, 864-871.

24. W. Kohn and L. J. Sham, Self-Consistent Equations Including Exchange and Correlation Effects, *Phys. Rev. A*, 1965, **140**, 1133-1138.

25. A. D. Becke, Density-Functional Exchange-Energy Approximation with Correct Asymptotic Behavior, *Phys. Rev. A*, 1988, **38**, 3098-3100.

26. A. D. Becke, A New Mixing of Hartree–Fock and Local Density-Functional Theories, *J. Chem. Phys.*, 1993, **98**, 1372-1377.

27. C. Lee, W. Yang and R. G. Parr, Development of the Colle-Salvetti Correlation-Energy Formula into a Functional of the Electron Density, *Phys. Rev. B*, 1988, **37**, 785-789.

28. T. H. Dunning Jr., Gaussian Basis Sets for Use in Correlated Molecular Calculations. I. The Atoms Boron Through Neon and Hydrogen, *J. Chem. Phys.*, 1989, **90**, 1007-1023.

29. C. Møller and M. S. Plesset, Note on an Approximation Treatment for Many-Electron Systems, *Phys. Rev.*, 1934, **46**, 618-622.

30. R. L. Martin, Natural transition orbitals, *J. Chem. Phys.*, 2003, **118**, 4775-4777.

31. C. A. Guido, F. Zinna and G. Pescitelli, CPL calculations of [7]helicenes with alleged exceptional emission dissymmetry values, *J. Mat. Chem. C*, 2023, **11**, 10474-10482.

32. M. A. Medel, C. M. Cruz, D. Miguel, V. Blanco, S. P. Morcillo and A. G. Campaña, Chiral Distorted Hexa-peri-hexabenzocoronenes Bearing a Nonagon-Embedded Carbohelicene, *Angew. Chem. Int. Ed.*, 2021, **60**, 22051-22056.

33. K. Dhbaibi, L. Abella, S. Meunier-Della-Gatta, T. Roisnel, N. Vanthuyne, B. Jamoussi, G. Pieters, B. Racine, E. Quesnel, J. Autschbach, J. Crassous and L. Favereau, Achieving high circularly polarized luminescence with push–pull helicenic systems: from rationalized design to top-emission CP-OLED applications, *Chem. Sci.*, 2021, **12**, 5522-5533.

34. S. Abbate, G. Longhi, F. Lebon, E. Castiglioni, S. Superchi, L. Pisani, F. Fontana, F. Torricelli, T. Caronna, C. Villani, R. Sabia, M. Tommasini, A. Lucotti, D. Mendola, A. Mele and D. A. Lightner, Helical Sense-Responsive and Substituent-Sensitive Features in Vibrational and Electronic Circular Dichroism, in

Circularly Polarized Luminescence, and in Raman Spectra of Some Simple Optically Active Hexahelicenes, *J. Phys. Chem. C*, 2014, **118**, 1682-1695.

35. M. J. Frisch, G. W. Trucks, H. B. Schlegel, G. E. Scuseria, M. A. Robb, J. R. Cheeseman, G. Scalmani, V. Barone, G. A. Petersson, H. Nakatsuji, X. Li, M. Caricato, A. V. Marenich, J. Bloino, B. G. Janesko, R. Gomperts, B. Mennucci, H. P. Hratchian, J. V. Ortiz, A. F. Izmaylov, J. L. Sonnenberg, Williams, F. Ding, F. Lipparini, F. Egidi, J. Goings, B. Peng, A. Petrone, T. Henderson, D. Ranasinghe, V. G. Zakrzewski, J. Gao, N. Rega, G. Zheng, W. Liang, M. Hada, M. Ehara, K. Toyota, R. Fukuda, J. Hasegawa, M. Ishida, T. Nakajima, Y. Honda, O. Kitao, H. Nakai, T. Vreven, K. Throssell, J. A. Montgomery Jr., J. E. Peralta, F. Ogliaro, M. J. Bearpark, J. J. Heyd, E. N. Brothers, K. N. Kudin, V. N. Staroverov, T. A. Keith, R. Kobayashi, J. Normand, K. Raghavachari, A. P. Rendell, J. C. Burant, S. S. Iyengar, J. Tomasi, M. Cossi, J. M. Millam, M. Klene, C. Adamo, R. Cammi, J. W. Ochterski, R. L. Martin, K. Morokuma, O. Farkas, J. B. Foresman and D. J. Fox, Gaussian 16, Rev. C.02, Wallingford CT, 2016.

36. S. Grimme, S. Ehrlich and L. Goerigk, Effect of the damping function in dispersion corrected density functional theory, *J. Comput. Chem.*, 2011, **32**, 1456-1465.

37. T. Yanai, D. P. Tew and N. C. Handy, A new hybrid exchange–correlation functional using the Coulomb-attenuating method (CAM-B3LYP), *Chem. Phys. Lett.*, 2004, **393**, 51-57.

38. D. Jacquemin, V. Wathelet, E. A. Perpète and C. Adamo, Extensive TD-DFT Benchmark: Singlet-Excited States of Organic Molecules, *J. Chem. Theory Comput.*, 2009, **5**, 2420-2435.